



THE UNIVERSITY OF  
**WAIKATO**  
*Te Whare Wānanga o Waikato*

**Research Commons**

<http://waikato.researchgateway.ac.nz/>

## **Research Commons at the University of Waikato**

### **Copyright Statement:**

The digital copy of this thesis is protected by the Copyright Act 1994 (New Zealand).

The thesis may be consulted by you, provided you comply with the provisions of the Act and the following conditions of use:

- Any use you make of these documents or images must be for research or private study purposes only, and you may not make them available to any other person.
- Authors control the copyright of their thesis. You will recognise the author's right to be identified as the author of the thesis, and due acknowledgement will be made to the author where appropriate.
- You will obtain the author's permission before publishing any material from the thesis.

# **Erosion and Sedimentation Processes at Northern Waihi Beach**

A thesis submitted in partial fulfilment  
of the requirements for the Degree

of

**Master of Science**  
In Earth and Ocean Sciences

at

**The University of Waikato**

by

**Alison Louise Bear**



THE UNIVERSITY OF  
**WAIKATO**  
*Te Whare Wānanga o Waikato*

2009

# ABSTRACT

---

The northern sector of Waihi Beach is an example of chronic erosive tendency. The sediment deficit along the area of beach fronting the seawall means that there is often no beach at high tide. This existing situation, and the various remedial options suggested, has created an emotive issue for beach residents. Accordingly, the current study was undertaken to identify and evaluate the fundamental coastal processes impacting upon the erosion at northern Waihi Beach.

Methods used to investigate this problem included: beach profiling and shallow water hydrographic surveying; mapping of sediments and the distribution of bedforms on the inner shelf using side-scan sonar, identification of nearshore sediment transport pathways from sediment textural analyses; collection and analysis of nearshore wave and current data; and numerical modelling of wave refraction and sediment transport processes.

A side-scan sonar survey, ground-truthed by surficial sediment analyses and underwater video and diver observations, indicated that the shallow inshore zone is characterised by a relatively featureless seabed dominated by fine sands. Large shore-normal sand ridges ( $\eta=0.4\text{--}2.5$  m,  $\lambda=300\text{--}1400$ ), with crests oriented northeast to southwest were identified between 15-30 m water depth offshore northern Waihi Beach. These very pronounced features consist of coarse megarippled ( $\eta\approx 0.12$  m,  $\lambda\approx 1$  m) sediment.

Sediment textural analyses revealed that offshore sediments vary from fine to coarse sand, showing a seaward-coarsening progression. Beach sediments consist of predominantly fine sands, with a slight inferred fining in grain size that occurs towards the northern end of the beach. This is possibly a result of lower wave energy when subject to swell and sea waves from the north, due to sheltering in the lee of Rapitiotio Point.

80 days of wave and current data were collected offshore northern Waihi Beach, during two separate deployments in Nov/Dec 2007 and May/June 2008. The summer deployment was characterised by waves from a northeast-east origin ( $H_s=1.09\text{m}$ ;  $T_s=7.13\text{s}$ ). Similar conditions were exhibited during the winter deployment ( $H_s=0.95\text{m}$ ;  $T_s=6.79\text{s}$ ). Observed relationships between wind direction and near-bed current direction, combined with calculated sediment entrainment rates, enabled predictions of the frequency of shoreward sediment transport by bottom currents to be made. Onshore currents, associated with winds from the southwest, prevailed during the deployment period. However, observed current velocities alone were generally incapable of inducing sediment motion. Analysis suggests that wave properties are likely to govern the frequency of sediment transport in the nearshore, as their presence is required to lift sediment into suspension for dispersal by ambient background currents. Onshore movement of sediment was estimated to be  $\sim 11,800$  m<sup>3</sup>/year or 2.6 m<sup>3</sup>/m.

Monochromatic wave statistics measured during the field study were used to calibrate a numerical wave refraction model. The wave refraction influence of Mayor Island was found to be the major feature influencing the distribution of wave energy along the shoreline, which is likely to contribute to localised accelerated beach erosion and dune setback. Wave energy focusing at northern Waihi Beach is maximised by swell waves, resulting in greater wave heights along eroding sectors of the beach.

Potential sediment transport rates were investigated. Results suggest the littoral drift direction was bi-directional at northern Waihi Beach, although net littoral drift was southeasterly during the study period. An estimated net loss of 46,200 m<sup>3</sup>/year or 10.3 m<sup>3</sup>/m was predicted for northern Waihi Beach during the present study. Longer-term drift patterns were examined using a five year record of wave data collected offshore Pukehina by Environment Bay of Plenty from 2003-2008. Similar patterns but with lower magnitudes of sediment transport were obtained, with net annual drift rates estimated to range from 1,300-58,000 m<sup>3</sup>/year.

A conceptual model of nearshore sediment dynamics is proposed for Waihi Beach to identify the major factors contributing to long-term erosion in the northern sector. Approximately 115,000 m<sup>3</sup> of sediment was estimated to be moving within the defined northern Waihi Beach littoral cell during the study period. The derived sediment budget produced a net deficit of sediment of approximately 36,000 m<sup>3</sup>/year or -8 m<sup>3</sup>/year during the year commencing November 2007. The net southeasterly littoral drift was determined the major contributor to the net erosion rate during the study period, with alongshore transport rates exceeding available supply to the beach from diabathic movement of sediment onshore.

Several aspects of the erosion problem at northern Waihi Beach are recommended to be researched further to identify what coastal management options are required.

# ACKNOWLEDGMENTS

---

There have been many people who have helped in the completion of this thesis, which I am indebted to. First, and foremost, I would like to thank my supervisor Professor Terry Healy for initiating the project and giving me both intellectual and moral support throughout my thesis. Your constructive criticism and wealth of knowledge in all areas was valued.

This project has been funded by Environment Bay of Plenty, and the financial support received has been fully appreciated. Particular thanks to Shane Iremonger for his enthusiasm and data provided for this thesis.

Field work was a large and most enjoyable part of this study, thanks to the many people who have helped in the field. A very big thank you must go to Dirk Immenga for his experience and technical knowledge in fieldwork, your interest and support for my project was greatly appreciated. Special thanks also to Chris, Craig, Dave, Pauline, Elodie and Bryna for your company and help on numerous occasions in the field.

Thanks to the outstanding contribution by Gegar Presetya, who has had a tremendous input into the numerical modelling content of this study, thanks for your time and ideas. To Glen, Dave and Adrian, your assistance using ArcGIS and help with numerous questions have been invaluable. Special thanks also to Willem de Lange for his input and suggestions regarding the hydrodynamics analysis.

And finally to mum and dad, thanks for all the unconditional support and love you have given me throughout my university years.

# TABLE OF CONTENTS

---

ABSTRACT.....	i
ACKNOWLEDGMENTS .....	iii
TABLE OF CONTENTS.....	iv
LIST OF FIGURES .....	viii
LIST OF TABLES .....	xii

## CHAPTER ONE: INTRODUCTION

1.0	PROBLEM BACKGROUND .....	1
1.1	STUDY LOCATION.....	3
1.2	HISTORY OF DEVELOPMENT AT WAIHI BEACH.....	4
1.3	AIMS AND OBJECTIVES .....	9
1.4	THESIS STRUCTURE.....	10
1.5	SUMMARY .....	12

## CHAPTER TWO: ENVIRONMENTAL SETTING GEOLOGY, SEDIMENTS AND HYDRODYNAMICS

2.0	INTRODUCTION.....	14
2.1	LOCAL GEOLOGY .....	14
2.1.1	<i>Tectonics</i> .....	16
2.1.2	<i>Geomorphology</i> .....	16
2.2	WAIHI BEACH SEDIMENT CHARACTERISTICS, SOURCES AND DISTRIBUTION.....	20
2.2.1	<i>Sediment Texture</i> .....	20
2.2.2	<i>Mineralogy</i> .....	21
2.2.3	<i>Sediment Sources and Distribution</i> .....	22
2.3	HYDRODYNAMICS OF THE BAY OF PLENTY AND IMPLICATIONS FOR COASTAL EROSION AT WAIHI BEACH.....	24
2.3.1	<i>Wind Climate</i> .....	24
2.3.2	<i>Wave Climate</i> .....	25
2.3.2.1	<i>Wave Refraction and Local Wave Focusing</i> .....	27
2.3.3	<i>Tides and Currents</i> .....	28
2.3.3.1	<i>Tides and Tidal Currents</i> .....	28
2.3.3.2	<i>Wind and Oceanic Currents</i> .....	29
2.3.4	<i>Storms and Cyclonic Activity</i> .....	30
2.3.4.1	<i>Storm Surge</i> .....	30
2.3.4.2	<i>Tropical Cyclones</i> .....	31
2.4	SUMMARY .....	32

## CHAPTER THREE: BEACH AND NEARSHORE MORPHOLOGY

3.0	INTRODUCTION.....	35
3.1	TOPOGRAPHIC AND HYDROGRAPHIC SURVEY OF WAIHI BEACH.....	36
3.1.1	<i>Dune and Sub-Aerial Beach Profiling</i> .....	36

3.1.2	<i>Surveying Method</i> .....	36
3.1.3	<i>Description of the Beach Profiles</i> .....	38
3.1.3.1	Island View (CCS49).....	40
3.1.3.2	The Loop (CCS50).....	42
3.1.3.3	Waihi Beach Stream (CCS53) .....	42
3.1.3.4	Waihi Beach North (CCS51) .....	43
3.1.3.5	The Surf Club (CCS52) .....	43
3.1.4	<i>Nearshore Profiling</i> .....	44
3.1.4.1	Field Programme.....	44
3.1.4.2	Description of Offshore Profiles.....	44
3.2	SIDE-SCAN SONAR IMAGERY .....	49
3.2.1	<i>Introduction</i> .....	49
3.2.2	<i>Side-Scan Sonar Operation</i> .....	49
3.2.3	<i>Survey Procedure</i> .....	51
3.2.4	<i>Side-Scan Sonar Image Processing</i> .....	52
3.2.5	<i>Discussion and Interpretation of the Sonagraph</i> .....	52
3.3	OFFSHORE BEDFORMS .....	60
3.3.1	<i>Introduction</i> .....	60
3.3.2	<i>Characteristics of Bedforms</i> .....	61
3.3.3	<i>Interpretation of Offshore Bedforms</i> .....	63
3.3.3.1	Bedform Generation and Distribution .....	64
3.4	SUMMARY .....	66

#### CHAPTER FOUR: SEDIMENT CHARACTERISTICS

4.0	INTRODUCTION.....	68
4.1	METHODS.....	68
4.1.1	<i>Sediment Sample Collection</i> .....	68
4.1.2	<i>Sediment Textural Analysis</i> .....	70
4.2	SEDIMENT ANALYSIS RESULTS.....	73
4.2.1	<i>Mean Grain Size</i> .....	75
4.2.1.1	Alongshore Variations .....	76
4.2.1.2	Cross-shore Variations.....	76
4.2.2	<i>Sorting</i> .....	78
4.2.3	<i>Mean Grain Size vs. Sorting</i> .....	79
4.2.4	<i>Skewness</i> .....	80
4.3	INFERENCE OF LITTORAL DRIFT.....	82
4.3.1	<i>SUNAMURA and HORIKAWA (1972) Model</i> .....	82
4.3.2	<i>MCLAREN (1981) Model</i> .....	84
4.3.3	<i>Waihi Model</i> .....	87
4.3.4	<i>Evaluation of Model Results</i> .....	89
4.4	SUMMARY .....	90

#### CHAPTER FIVE: NEARSHORE HYDRODYNAMICS AND SEDIMENT TRANSPORT

5.0	INTRODUCTION.....	92
5.1	WAVES.....	93
5.1.1	<i>Methods</i> .....	93
5.1.1.1	Data Collection .....	93

5.1.1.2	Data Analysis .....	96
5.1.2	<i>Results</i> .....	97
5.1.2.1	Monochromatic Wave Statistics .....	97
5.1.2.2	Wave Origin.....	102
5.2	CURRENTS .....	105
5.2.1	<i>Methods</i> .....	105
5.2.1.1	Data Collection .....	105
5.2.1.2	Data Analysis .....	105
5.2.2	<i>Results</i> .....	106
5.2.2.1	Current Characteristics .....	106
5.3	WIND.....	111
5.3.1	<i>Wind Characteristics</i> .....	111
5.3.2	<i>The Influence of Wind on Nearshore Current Generation</i> .....	115
5.4	SEDIMENT TRANSPORT AND INCIPIENT MOTION BY WAVES AND CURRENTS .....	118
5.4.1	<i>Introduction</i> .....	118
5.4.2	<i>Incipient Motion Induced by Waves</i> .....	118
5.4.3	<i>Incipient Motion Induced by Unidirectional Currents</i> .....	123
5.4.3.1	Threshold Velocity for Planar Beds.....	124
5.4.3.2	Threshold Velocities for Bedformed Areas .....	124
5.4.4	<i>Calculation of Diabathic Sediment Transport Rates</i> .....	128
5.4.5	<i>Results</i> .....	134
5.5	SUMMARY .....	137

## CHAPTER SIX: WAVE ENERGY FOCUSING AND NEARSHORE LITTORAL DRIFT

6.0	INTRODUCTION.....	140
6.1	WAVE REFRACTION MODELLING .....	141
6.1.1	<i>Introduction</i> .....	141
6.1.1.1	Wave Refraction Theory.....	141
6.1.1.2	Wave Energy Focusing .....	142
6.1.2	<i>Numerical Wave Propagation Model WBEND</i> .....	145
6.1.2.1	Introduction.....	145
6.1.2.2	Model Inputs and Outputs.....	146
6.1.2.3	Model Resolution.....	149
6.1.2.4	Model Calibration .....	150
6.1.2.5	Model Performance Statistics and Skill.....	151
6.1.2.6	Calibration Results.....	156
6.1.3	<i>WBEND Scenarios</i> .....	157
6.1.4	<i>Results</i> .....	158
6.1.5	<i>Discussion</i> .....	158
6.1.5.1	Influence of Mayor Island and Steel's Reef .....	158
6.1.5.2	Wave Direction Scenarios .....	162
6.1.5.3	Wave Period Scenarios .....	163
6.1.5.4	Storm Wave Scenarios.....	166
6.2	NEARSHORE LITTORAL DRIFT MODELLING AND SEDIMENT TRANSPORT BY WAVES.....	168
6.2.1	<i>Method</i> .....	168
6.2.2	<i>Results</i> .....	170



6.2.2.1	Littoral Drift during the Study Period .....	170
6.2.2.2	Longer-Term Littoral Drift .....	173
6.2.3	<i>Discussion of Littoral Drift Estimates</i> .....	174
6.3	SUMMARY .....	175

## CHAPTER SEVEN: SEDIMENT BUDGET FOR NORTHERN WAIHI BEACH

7.0	INTRODUCTION.....	178
7.1	THE SEDIMENT BUDGET CONCEPT .....	179
7.1.1	<i>Previous Application of Sediment Budgets in the Bay of Plenty</i> ...	180
7.2	THE NORTHERN WAIHI BEACH LITTORAL CELL.....	182
7.2.1	<i>Depth of Closure</i> .....	183
7.3	DIABATHIC TRANSPORT AT NORTHERN WAIHI BEACH.....	
7.4	SEDIMENT INPUTS INTO NORTHERN WAIHI BEACH (CREDITS) .....	188
7.5	SEDIMENT LOSS FROM NORTHERN WAIHI BEACH (DEBITS) .	191
7.6	INTEGRATED SEDIMENT BUDGET BALANCE .....	193
7.6.1	<i>Discussion of Sediment Budget Outcome</i> .....	194
7.7	SUMMARY .....	194

## CHAPTER EIGHT: SUMMARY, CONCLUSIONS AND RECOMMENDATIONS

8.0	INTRODUCTION.....	196
8.1	SUMMARY OF KEY FINDINGS .....	196
8.1.1	<i>Environmental Setting and Processes Influencing Erosion</i> .....	196
8.1.2	<i>Beach and Nearshore Morphology</i> .....	197
8.1.3	<i>Sediment Characteristics</i> .....	199
8.1.4	<i>Nearshore Hydrodynamics and Sediment Transport</i> .....	200
8.1.5	<i>Wave Energy Focusing and Nearshore Littoral Drift</i> .....	201
8.1.6	<i>Northern Waihi Beach Integrated Sediment Budget</i> .....	202
8.2	RECOMMENDATIONS AND SUGGESTIONS FOR FUTURE RESEARCH AT WAIHI BEACH.....	203
	REFERENCES.....	204

# LIST OF FIGURES

---

## CHAPTER ONE: INTRODUCTION

Figure 1.1: Severe erosion at northern Waihi Beach in 1974. Photograph taken by T.R. HEALY (1974).	2
Figure 1.2: The seawall in its present state at Waihi Beach showing the lack of beach at high tide. Photograph taken by the author 28/05/08	2
Figure 1.3: Location map of study area.	4
Figure 1.4: Close up of northern Waihi Beach showing the locations of Rapatiotio Point, Two Mile and Three Mile Creeks, the seawalls and the main areas of subdivision.	6
Figure 1.5: Proposed shoreline protection works for northern Waihi Beach by the WBOPDC. WBOPDC (2004).	8

## CHAPTER TWO: ENVIRONMENTAL SETTING

Figure 2.1: Waihi Beach shoreface and inner shelf morphology from digitized navy fair sheet soundings. HUME <i>et al.</i> (1995).	18
---	----

## CHAPTER THREE: BEACH AND NEARSHORE MORPHOLOGY

Figure 3.1: Locations of Environment Bay of Plenty benchmarks at northern Waihi Beach used for surveying in this study.	37
Figure 3.2: Beach profiles collected at northern Waihi Beach from September 2005 to June 2008.	39
Figure 3.3: Well-vegetated dunes at profile CCS49 at Island View. Photograph taken by T.R HEALY 23/08/06.	41
Figure 3.4: The rock revetment at CCS50 midway along The Loop. Photograph taken by the author 24/06/08.	41
Figure 3.5: Setting up the base station at CCS52 in front of the Waihi Beach Surf Club for beach and nearshore hydrographic surveying.	45
Figure 3.6: Nearshore profiles taken at northern Waihi Beach on the 24/06/08.	46
Figure 3.7: The side-scan sonar system. KLEIN ASSOCIATES INC (2008).	50
Figure 3.8: Sonagraph output illustrating the end of an elongated finger of megaripples in about 20 m water depth.	55
Figure 3.9: Side-scan sonagraph for offshore northern Waihi Beach.	57
Figure 3.10: Sediment facies map for offshore northern Waihi Beach.	58
Figure 3.11: The drop-camera attached to a cable and enclosed within a steel frame, with a diving weight belt attached.	62
Figure 3.12: Ripple classification based on ripple crest morphology. LARSON <i>et al.</i> (1997).	63
Figure 3.13: Megaripples with shell lag deposits at site 8 in 30 m water depth. Photographs taken by the author 28/05/08.	64

## CHAPTER FOUR: SEDIMENT CHARACTERISTICS

Figure 4.1: Location map of beach and offshore sediment samples.	69
Figure 4.2: Wentworth grain size scale classification table. FOLK (1968).	71

Figure 4.3: Longshore and cross-shore variation in mean grain size, sorting and skewness of swash, beach face, berm and dune samples at northern Waihi Beach.	74
Figure 4.4: Photograph of the sub-aerial beach at the northern end of Waihi Beach (facing north). Photograph taken by T.R. HEALY 25/04/05.	74
Figure 4.5: Mean grain size versus distance offshore at northern Waihi Beach determined from samples collected on the 28/05/08 and 03/12/08.	77
Figure 4.6: Bivariate analysis of mean grain size and sorting for northern Waihi Beach, using moment method parameters attained from RSA analyses.	80
Figure 4.7: Criterion for the inference of sediment transport direction according to the model SUNAMURA and HORIKAWA (1972). SUNAMURA and HORIKAWA (1972).	83
Figure 4.8: Inferred sediment transport directions along northern Waihi Beach as determined using the SUNAMURA and HORIKAWA (1972) model.	83
Figure 4.9: Inferred sediment transport directions along northern Waihi Beach as determined using the MCCLAREN (1981) model. (MCCLAREN, 1981).	86
Figure 4.10: Inferred sediment transport directions along northern Waihi Beach according to the Waihi model.	88

## CHAPTER FIVE: NEARSHORE HYDRODYNAMICS AND SEDIMENT TRANSPORT

Figure 5.1: S4 current meter mounted on stainless steel tripod.	93
Figure 5.2: Map of Waihi Beach showing positions of the three S4 and three ADV instruments used in the study.	94
Figure 5.3: Time series of significant wave height (upper) and period (lower) at WAI1, WAI2 and WAI3 during the summer S4 deployment (15/11/07 – 15/12/07) at northern Waihi Beach.	98
Figure 5.4: Time series of significant wave height (upper) and period (lower) at WAI1b and WAI3b during the winter S4 deployment (07/05/08 – 25/06/08) at northern Waihi Beach.	99
Figure 5.5: Wave rose plots for the summer deployment (15/11/07 – 15/12/07) at WAI1, WAI2 and WAI3.	101
Figure 5.6: Wave rose plots for the winter deployments at WAI1b (28/05/08 – 25/06/08) and WAI3b (07/05/08 – 04/06/08).	102
Figure 5.7: Joint distribution of significant wave height and period for both deployments at WAI1/WAI1b.	103
Figure 5.8: Mean current speeds recorded off Waihi Beach during the summer deployment (15/11/07 – 15/12/07) at WAI1, WAI2 and WAI3.	107
Figure 5.9: Summary plots of current speed and direction (relative to true north) at 1 m above the sea bed during the summer S4 deployment period (15/11/07 – 15/12/07).	108
Figure 5.10: Time series plots showing (a) significant wave heights ( $H_s$ ), (b) mean current speeds, and (c) water depths recorded off Waihi Beach during the winter deployment (07/05/08 – 25/06/08) at WAI1b and WAI3b.	110
Figure 5.11: Rose plot of wind direction and velocity (Tauranga Airport) corresponding to the summer S4 deployment (15/11/07 – 15/12/07).	112
Figure 5.12: Rose plot of wind direction and velocity (Tauranga Airport) corresponding to the winter S4 deployment (07/05/08 – 25/06/08).	113

Figure 5.13: Time series plot of significant wave height and wind direction at Waihi Beach over the summer deployment period (15/11/07–15/12/07).	114
Figure 5.14: Time series plot of significant wave height and wind direction at Waihi Beach over the winter deployment period (07/05/08–25/06/08).	114
Figure 5.15: Time series plot of current direction and wind direction over the winter S4 deployment (07/05/08 – 25/06/08).	115
Figure 5.16: Schematic of an upwelling circulation pattern in the friction dominated zone. NIEDORODA <i>et al.</i> (1985).	116
Figure 5.17: Time series plot current speed (cm/s) and wind speed (m/s) over the second half of the winter S4 deployment (28/05/08 – 25/06/08).	117
Figure 5.18: A diagram illustrating the orbital motions of waves in intermediate water depths where the orbits are elliptical but become flatter and smaller as the bottom is approached. OPEN UNIVERSITY (2002).	119
Figure 5.19: Near-bed orbital velocities ( $U_w$ ) at northern Waihi Beach during the summer S4 deployment, compared to the critical threshold velocity for sediment movement determined using the KOMAR and MILLER (1975) wave-orbital-speed theory.	122
Figure 5.20: Near-bed orbital velocities ( $U_w$ ) at northern Waihi Beach during the winter S4 deployment, compared to the critical threshold velocity for sediment movement determined using the KOMAR and MILLER (1975) wave-orbital-speed theory.	122
Figure 5.21: Near-bed orbital velocities ( $U_w$ ) at northern Waihi Beach during the short-term May ADV deployment, compared to the critical threshold velocity for sediment movement determined using the KOMAR and MILLER (1975) wave-orbital-speed theory.	123
Figure 5.22: Time series plot of current speed recorded at WAI1, WAI2 and WAI3 relative to the critical threshold velocity for sediment motion for each of the bedform types during the summer (2007) deployment.	126
Figure 5.23: Time series plot of current speed recorded at WAI1b and WAI3b relative to the critical threshold velocity for sediment motion for each of the bedform types during the winter (2008) deployment.	127
Figure 5.24: Time series plot of reference concentration ( $\bar{C}_{REF}$ ) during the summer deployment, determined from the formulae of Nielson (1986).	131
Figure 5.25: Time series plot of reference concentration ( $\bar{C}_{REF}$ ) during the winter deployment, determined from the formulae of Nielson (1986).	131
Figure 5.26: Suspended sediment flux integrated over time above the bed at a) WAI1, b) WAI2 and c) WAI3 during the summer deployment.	134
Figure 5.27: Suspended sediment flux integrated over time above the bed at WAI3b (days 128 -149) and WAI1b (days 149-177) during the winter deployment.	135

## CHAPTER SIX: WAVE ENERGY FOCUSING AND NEARSHORE LITTORAL DRIFT

Figure 6.1: Wave refraction occurs due to faster movement of waves in deep water than in shallower water. During a certain time interval, the wave crest at point B in deeper water moves farther than the crest at point A in shallower water, causing the wave crest to rotate and become more nearly parallel to the shore. KOMAR (1998).	143
--	-----

Figure 6.2: (a) The convergence or focusing of wave rays such as over a seafloor topographic high. (b) The divergence of wave rays such as over a topographic depression. KOMAR (1998).	144
Figure 6.3: Location map showing the position of EBOP's Pukehina wave buoy in relation to Waihi Beach and the S4 current meters deployed in the present study.	147
Figure 6.4: 50 m model grid of the Waihi Beach coastal sector generated and rotated 205° in SURFER.	148
Figure 6.5: The model grid. HUTT (1997).	149
Figure 6.6: Predicted model significant wave heights and direction against measured wave heights and direction at the S4 location WAI1b during the May/June 2008 deployment.	154
Figure 6.7: Predicted model significant wave heights and direction against measured wave heights and direction at the S4 location WAI3b during the May/June 2008 deployments.	155
Figure 6.8: Model simulation using mean wave conditions (Scenario 1: 1.04 m, 6.99 s, 62.5° True) as recorded by the S4 current meters during the field deployment.	159
Figure 6.9: Model simulation for a 1.04 m wave approaching from the NNE (Scenario 7). The location of Steel's Reef is shown.	161
Figure 6.10: Model simulation for a 1.04 m wave approaching from the NE (Scenario 5) illustrating the wide swath of wave sheltering extending south along Matakana Island and beyond the model grid boundary.	163
Figure 6.11: Sea wave (6 s period) simulation (Scenario 2), for a 1.04 m wave approaching Waihi Beach from the northeast.	165
Figure 6.12: Swell wave (11 s) simulation (Scenario 3), for a 1.04 m wave approaching Waihi Beach from the northeast.	165
Figure 6.13: Model simulation of a typical storm wave scenario approaching Waihi Beach from the ENE (Scenario 17: 3.5 m, 9.5 s, 72.5° True), illustrating active wave focusing near the surf club at the very northern end of Waihi Beach.	167
Figure 6.14: Spatial variation in nearshore sediment transport estimates along the northern sector of Waihi Beach over the study period.	171

## CHAPTER SEVEN: SEDIMENT BUDGET FOR NORTHERN WAIHI BEACH

Figure 7.1: Island View offshore profile (CCS49) with the Hallermeier inner limit (HIL) superimposed.	185
Figure 7.2: Schematic of the northern Waihi Beach littoral sector. Beach profile benchmarks used during this study are shown. Possible sediment transport pathways are specified, which are to be evaluated and compared against changes in the sand storage on the beach.	186
Figure 7.3: A) Showing the effect of an onshore wind producing an elevated still water level. The induced downwelling current facilitates diabathic transport of sediment offshore. B) Showing the effect of an offshore wind producing a reduced still water level. The induced upwelling current facilitates diabathic transport onshore. SCHWARTZ (2005).	188
Figure 7.4: Net annual credits and debits to the sediment budget along the northern Waihi Beach littoral cell.	193

# LIST OF TABLES

---

## CHAPTER TWO: ENVIRONMENTAL SETTING

Table 2.1: Light and heavy mineral assemblages for the Waihi Beach sand system. HARRAY and HEALY (1978); BRADSHAW <i>et al.</i> (1994).	22
---	----

## CHAPTER THREE: BEACH AND NEARSHORE MORPHOLOGY

Table 3.1: GPS Coordinates and elevations of frontal survey benchmarks at northern Waihi Beach. Northings and eastings are relative to the Bay of Plenty meridional circuit and elevation is above local Moturiki Datum.	37
Table 3.2: Summary of the sonar reflection types identified from the side-scan sonograph.	54
Table 3.3: Morphological classification of various bedforms adopted for this study. LARSON <i>et al.</i> (1997).	62
Table 3.4: Water depths and GPS co-ordinates of the eight locations where video imaging with the drop-camera was carried out.	63

## CHAPTER FOUR: SEDIMENT CHARACTERISTICS

Table 4.1: Sorting Classification. LARSEN <i>et al.</i> (1997).	72
Table 4.2: Skewness Classification. LARSEN <i>et al.</i> (1997).	72
Table 4.3: Kurtosis Classification. LARSEN <i>et al.</i> (1997).	72
Table 4.4: Summary of the range of moment textural characteristics for onshore sediments (dune, berm, beach face and lower swash) at northern Waihi Beach.	73
Table 4.5: Summary of the range of moment textural characteristics for offshore sediments (6, 15, 20, 25 and 30 m water depths) at northern Waihi Beach.	73

## CHAPTER FIVE: NEARSHORE HYDRODYNAMICS AND SEDIMENT TRANSPORT

Table 5.1: Deployment period and GPS location of all S4 and ADV wave and current meters used throughout the study.	95
Table 5.2: Monochromatic wave statistics measured in the nearshore at northern Waihi Beach for the summer (15/11/07 – 15/12/07) and winter (07/05/08 – 4/06/08 for WAI3b; 28/05/08 – 25/06/08 for WAI1b) deployments obtained from zero-down crossing analysis.	100
Table 5.3: Current statistics for northern Waihi Beach during the summer (15/11/07-15/12/07) and winter deployments (07/05/08-04/06/08 for WAI3b; 28/05/08-25/06/08 for WAI1b).	107
Table 5.4: Predicted rates of suspended-sediment flux at in 6 m depth off northern Waihi Beach.	136
Table 5.5: Estimates of diabathic transport along the 6 m contour within the northern Waihi Beach littoral cell.	137

## CHAPTER SIX: WAVE ENERGY FOCUSING AND NEARSHORE LITTORAL DRIFT

Table 6.1: Twenty different wave scenarios simulated in the WBEND model by using various combinations of wave height, wave period and wave approach angle.	158
Table 6.2: Net littoral drift volumes at five profiles along northern Waihi Beach simulated using the wave refraction model WBEND.	170
Table 6.3: Annual littoral drift volumes at five profiles along northern Waihi Beach predicted from the wave data collected offshore Pukehina Beach between 2003-2008. S. Iremonger, <i>pers comm.</i> 2008.	174

# CHAPTER ONE: INTRODUCTION

---

## 1.0 PROBLEM BACKGROUND

Erosion has been endemic along northern Waihi Beach since the major subdivision in the 1940s, where residential development took place on the dunes immediately behind the beach. An exceptionally bad sequence of erosion was experienced during the 1950s-70s (Figure 1.1). The Waihi Beach seawall was constructed in the late 1960s in an attempt to slow down erosion processes. The seawall has subsequently deteriorated and required continual replenishment of rip-rap boulders to hold the erosion. The condition of chronic sediment deficit along the beach fronting the seawall means there is usually no beach at high tide (Figure 1.2) and only a narrow beach at low tide. Thus, the amenity value of the beach is severely compromised.

The likely causes of erosion have been recognised:

- 1. Erosion is occurring as classic downdrift sediment starvation from the groin effect of Rapatiotio Point and insufficient diabathic sediment supply*

The ultimate cause of long term erosion at Waihi Beach is the excess of littoral drift potential over available sediment supply to the beach (HARRAY and HEALY, 1978). Littoral drift from the north is clearly not supplying sediment to Waihi Beach as the sands of Orokawa Beach are distinctly different (SCHOFFIELD, 1970; HARRAY and HEALY, 1978). The Rapatiotio Point headland at the northern end of the beach is thus inhibiting sediment supply to the littoral drift by providing a sheltering groin effect. If littoral drift is southeasterly in the long term, as is the overwhelming geomorphic evidence (HEALY *et al.*, 1977, HARRAY and HEALY, 1978), then erosion and dune recession at Waihi Beach will continue due to downdrift sediment starvation from the groin effect of Rapatiotio Point and insufficient diabathic sediment supply from the shoreface and inner shelf. Beach erosion is enhanced by streams discharging onto the beach and existing property protection works.





**Figure 1.1:** Severe erosion at northern Waihi Beach in 1974. Photograph taken by T.R. HEALY (1974).



**Figure 1.2:** The seawall in its present state at Waihi Beach showing the lack of beach at high tide. Photograph taken by the author 28/05/08.

- 2. Erosion is enhanced by episodes of wave energy focusing and resultant diabathic removal of beach sediment offshore.*

Sectors of beach subject to wave energy focusing typically exhibit localised higher breaking waves, resulting in greater wave set-up, run-up and surge, and are thus more erosion prone than adjacent regions (HEALY, 1987). This enhanced water level setup causes the frontal dune to be preferentially eroded, especially during storm events with strong onshore winds and associated nearshore downwelling currents removing sediment offshore. Sand may be expected to return to the beach during periods where wave conditions are suitable and offshore winds predominate.

In order to evaluate the coastal processes identified as factors contributing to beach erosion at northern Waihi Beach, the present study will undertake morphological and sedimentological surveys in conjunction with the collection of wind, wave and current data. This approach will ensure a thorough understanding of beach morphodynamics and sediment transport processes and patterns in the affected eroded sectors of beach.

## 1.1 STUDY LOCATION

Waihi Beach is located at the northern end of the 150 km long sandy coastline of the Bay of Plenty, 35 km northwest of Tauranga at the base of the Coromandel Peninsula (Figure 1.3). The 9 km long barrier beach faces northeast into the Pacific Ocean, and is bound by two significant outcrops of volcanic rock; Rapatiotio Point to the north and Bowentown Head at the southern end. Immediately southeast of Waihi Beach is the barrier island of Matakana, and the barrier beaches of Mount Maunganui and Papamoa. North of Waihi Beach, the coastline becomes rocky and cliffed with occasional pocket sandy beaches such as Orokawa, Whiritoa and Homunga Beaches.

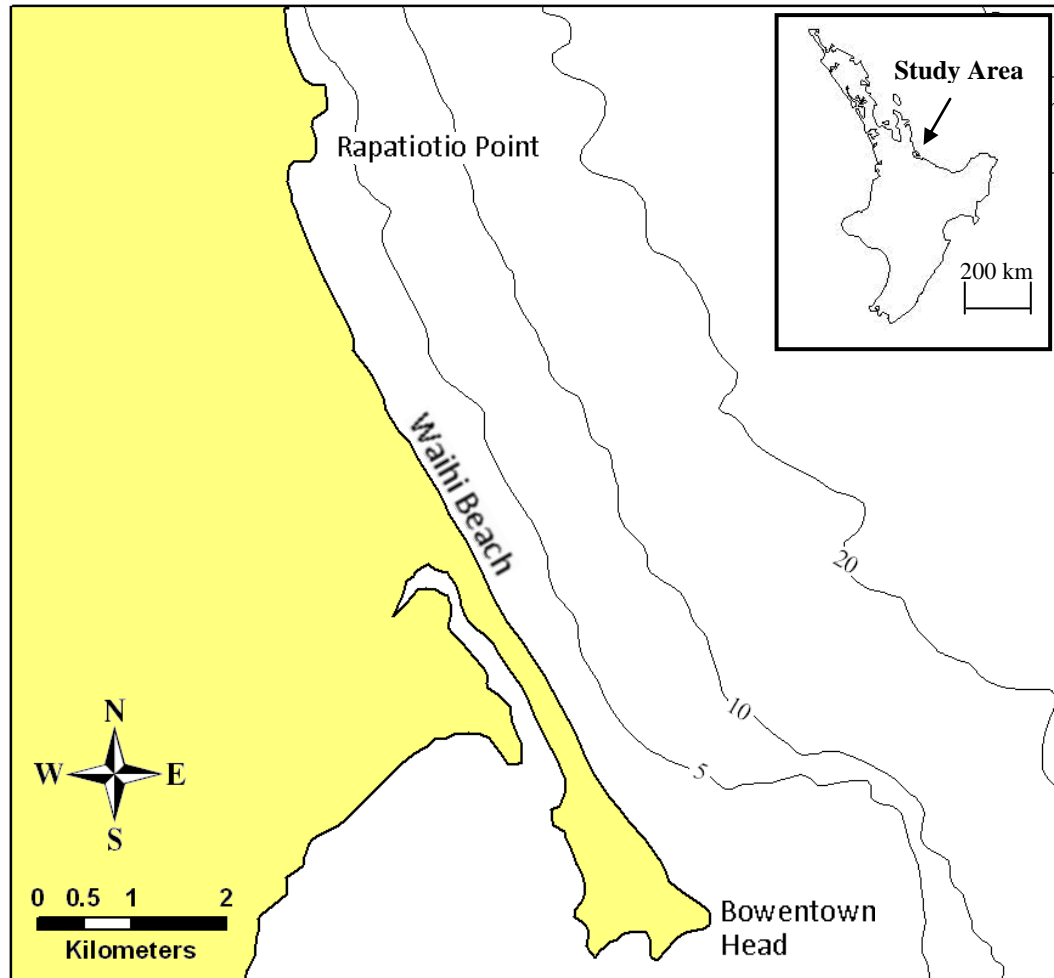


Figure 1.3: Location map of study area.

36 km offshore from Waihi Beach is Mayor Island, the major geomorphic feature impacting upon nearshore hydrodynamics by acting as a focal point for deepwater waves approaching the shelf. A shallow gradient inner shelf and shoreface rises to meet the coastline, punctuated by the Tertiary volcanic pinnacle of Steel's Reef near the 20 m isobath. Long-shore bar-trough topography and associated rip current channels are evident in the upper surf zone (STEPHENS *et al.*, 1999). The Waihi Beach nearshore and back beach are comprised totally of unconsolidated quartzo-feldspathic sands, typical of Bay of Plenty beaches (HEALY *et al.*, 1977).

## 1.2 HISTORY OF DEVELOPMENT AT WAIHI BEACH

Waihi Beach was originally developed as a health resort for miners and gold battery workers from Waihi. Although the goldmine in Waihi is well known, most

people are unaware that there was also gold at Rapatiotio Point at the northern end of Waihi Beach, known to residents at the time as “Mine Hill” (HANLEN, 1999). HANLEN (1999) claims that early mining reports tell of Sir James Hooten visiting the beach in 1870, where he panned gold in small quantities from the Waihi Stream, the Orokawa stream and Fraser’s Creek which flows into Homunga Bay just past Orokawa. Between 1894 and 1898 claims were pegged out and gold bearing lodes were uncovered. Old maps of Waihi Beach show that the Waihi Beach Mining Company had plans for a tramline from Pios point to the mine, but it never eventuated. In 1902 the road from Waihi to Waihi Beach was surveyed opening up public access to the beach area. Properties were eventually leased out in 1922, and the land subdivided into one tenth of acre lots in a bid to accommodate as many miners as possible (GIBB, 1997). In 1930 the local residents dug out Two Mile Creek and Three Mile Creek to drain the swampland further inshore and direct the water out to sea (HANLEN, 1999; BRUGMANS *et al.*, 2003).

Waihi Beach has been subject to several phases of subdivision. Coastal development commenced in 1948 with the subdivision of land along Shaw Road (Figure 1.4). Many of these initial beachfront properties were already too close to the eroding dunes, having been developed in a haphazard and unplanned manner (HARRAY, 1977). Serious erosion and flooding between 1951 and 1958 adversely affected beachfront properties, forcing at least six houses to be shifted back on their sections to avoid falling into the sea (WBOPDC, 2004). In spite of the obvious threat to existing coastal property further beachfront subdivision was established at Island View in 1957, closely followed by subdivision along the Loop between Two Mile and Three Mile Creeks in 1959. Final subdivision took place in 1975 at Glen Isla Place southeast of Three Mile Creek in 1975 (GIBB 1996, 1997). GIBB (1996) stated that all beachfront property along Waihi Beach is likely to be subject to adverse effects from erosion and flooding from the sea.

Severe coastal erosion and flooding in the 1950’s, 1960’s and 1970’s threatening beachfront development forced the community to implement a number of property protection schemes. In 1962 a vertical 140 m long timber seawall was constructed to protect nine threatened beachfront properties along Shaw Road. Timber training



**Figure 1.4:** Close up of northern Waihi Beach showing the locations of Rapatiotio Point, Two Mile and Three Mile Creeks, the seawalls and the main areas of subdivision.

groynes were also constructed at this time in an effort to confine Two Mile Creek and prevent mouth migration. In 1969 a steel and timber seawall was constructed along Shaw Road. The area between the dune and seawall was later backfilled

with quarry run (small rock), boulders and clay. The wall was fronted by 12 m long Meccaferi gabion groynes at 40 m spacing. This was followed in 1970 by completion of a similar seawall to protect The Loop, including training groynes for Three Mile Creek. In 1975 the Shaw Road seawall was further extended to the northwest and in 1983 a similar seawall was constructed to protect Glen Isla Place (GIBB, 1996; TONKIN & TAYLOR, 2004) (Figure 1.4).

According to GIBB (1996), the existing erosion protection structures along the Waihi Beach shoreline have exceeded their useful design life and are no longer providing sustainable protection of beachfront property and reserves. They are in a dilapidated and unsightly state as a result of years of severe wave storm damage. The timber and rail seawalls have been supplemented with large rock boulders and ad hoc erosion protection measures (TONKIN & TAYLOR, 2004), transforming the original approved scheme of a permeable timber seawall into a rubble mound revetment (GIBB, 1996). The rock revetment is poorly designed and constructed and is enhancing scour through wave reflection. There is significant and real risk to existing beachfront property owners from further property loss if the protection structures are destroyed by storm waves.

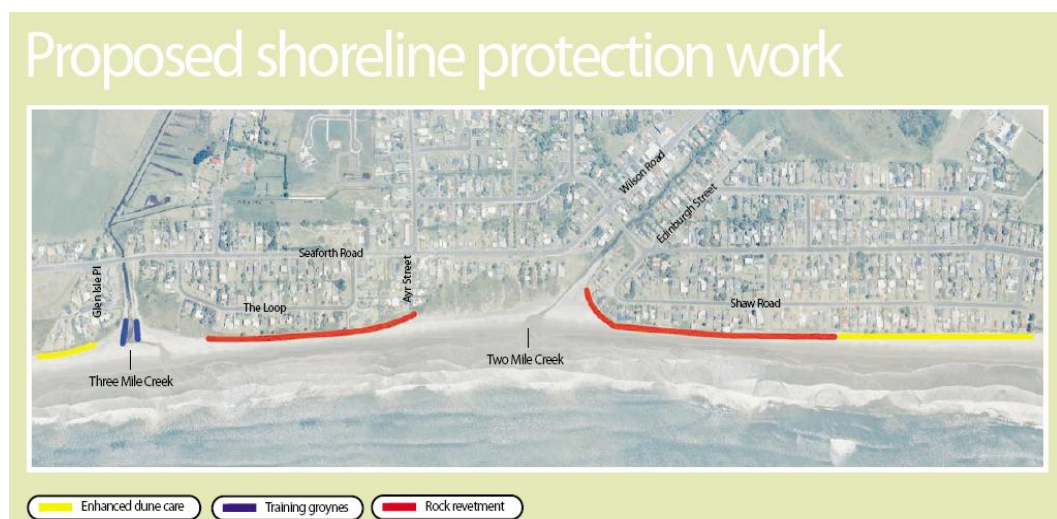
These historical structures implemented by previous local authorities prevent the natural recycling of sand between the dune and the littoral system and progressively lowers the beach profile. In a report assessing the environmental effects of erosion protection works along Waihi Beach prepared by TONKIN & TAYLOR (2004), it is stated that the required sand reservoir for an unprotected coastal area is estimated as  $400 \text{ m}^3 \cdot \text{m}^{-1}$  of beach. At the seawall this reservoir is certainly not available. Furthermore, impermeable structures such as rock revetments and seawalls inhibit groundwater flow and raise the water table in their immediate vicinity (PLANT and GRIGGS, 1992; STEELE, 1995; KOMAR, 1998). This increased water table elevation increases beach instability at the base of the seawall.

Since 1989 the Western Bay of Plenty District Council (WBOPDC) has been responsible for the administration of Waihi Beach. In response to community demand to repair the existing protection works, the Council undertook

comprehensive studies and significant public consultation to identify and investigate a range of potential options in order to create a more sustainable solution for the coastal hazard problems. In November 2004, after eight years of investigation and consultation the WBOPDC lodged Resource Consent applications under the Resource Management Act for three coastal protection measures along the Waihi Beach shoreline, between Coronation Park and Glen Isla Place. These measures are (TONKIN & TAYLOR, 2004) (Figure 1.5):

1. A rock revetment erosion protection structure extending approximately 1,050 m along the shoreline;
2. Enhanced dune care and beach replenishment, excavating sands from the foreshore area and using it to rebuild the existing frontal dunes for approximately 600 m; and
3. Training groynes to direct the flow from Three Mile Creek and relocate the mouth of the creek seaward of the frontal dunes.

The work was proposed to extend about 1,650 m along the most vulnerable stretch of the northern Waihi Beach shoreline and provide effective protection to beachfront property in a 1:50 year storm event (WBOPDC, 2004). Following a lengthy environment court hearing, consent to construct the rock revetment at Waihi Beach was approved by the Conservation Minister Steve Chadwick in May 2008. The consent was granted on the condition that “the rock seawall is not the



**Figure 1.5:** Proposed shoreline protection works for northern Waihi Beach by the WBOPDC. Source: WBOPDC (2004).

long term solution to coastal hazards at Waihi Beach”, and that by 2020 “the WBOPDC must undertake comprehensive investigations into the best ways to manage the long term effects of erosion. In doing this, it will be important that the Council works with the community to come up with a long term solution” (S. Chadwick, 5<sup>th</sup> May 2008, Press Release: New Zealand Government).

### 1.3 AIMS AND OBJECTIVES

The general aim of this research is to investigate nearshore sedimentation processes leading to, and impacting upon the erosion at Waihi Beach, particularly around the seawall at the southern end of Shaw Road and Two and Three Mile Creeks, and of the northern beach generally. The specific objectives are:

1. Estimate the amounts and likely origin of sediment in the littoral drift system, and predict net littoral drift direction and rates at different time scales based upon numerical modelling of sediment transport;
2. Produce new information on nearshore wave and current interaction with the beach and nearshore morphology in terms of sediment transport;
3. Determine the importance of wave energy focusing leading to localised enhanced dune retreat at the affected sector of the beach, and assess the role of Rapatiotio Point as a sheltering groin effect; and
4. Quantify a sediment budget for northern Waihi Beach.

Objective 1 involves sampling and sediment textural analysis along the beach and nearshore for trends of sediment texture to determine dominant sediment transport pathways. Littoral drift modelling is undertaken, based both upon the synoptic data collected and the long term wind and wave data, to obtain sediment transport directions and approximations of longshore drift. A side-scan sonar survey with



additional underwater video enables detailed assessment of bottom topography and bedforms, which are indicators of sediment transport pathways.

Objective 2 entails deployment of wave and current meters offshore from Waihi Beach to investigate nearshore hydrodynamics, which are fundamental to the characterisation of the coastal erosion at Waihi Beach. S4 and Acoustic Doppler Velocimeter (ADV) instruments placed at specific locations alongshore are used to investigate spatial variability in wave and current behaviour. Summer and winter field deployments enable seasonal variability to be assessed.

Objective 3 involves performing numerical wave refraction analysis using a 2-dimensional wave propagation model to identify the sea conditions which maximise wave energy concentrations along Waihi Beach. Recording current/wave meters deployed in strategic locations are used to calibrate the modelling, which simulates a variety of wave conditions.

An integrated sediment budget, Objective 4, is determined by calculating rates of longshore littoral drift and diabathic transport in the nearshore zone using collected wave, current and sediment textural data, and identifying the conditions promoting onshore and offshore transport at northern Waihi Beach. From calculations of source and sink volumes using obtained and existing data, an integrated sediment budget may be collated to identify net sediment transfer rates for the northern Waihi Beach littoral cell.

## 1.4 THESIS STRUCTURE

The thesis is structured as follows to achieve the outlined objectives:

Chapter 2 provides a synthesis of previous literature on the physical setting of the study site, describing the local geology and sediment characteristics of Waihi Beach. Hydrodynamic features which may influence coastal erosion and

sedimentation processes at Waihi Beach are also investigated to gain an understanding of the beach and nearshore dynamics.

Chapter 3 records an investigation of the beach and nearshore/shoreface morphology of northern Waihi Beach. Comparison of summer and winter beach profiles is used to assess the effects of spatial and temporal shoreline fluctuations. Nearshore morphology is described using hydrographic surveys. A side-scan sonar survey was undertaken to map the sediments and distribution of major geomorphic units on the inner shelf offshore northern Waihi Beach. Seabed morphology was subsequently ground-truthed by SCUBA diver observations, drop-camera video observations and sediment sampling.

Chapter 4 presents the methods and results of the sediment textural investigation. The spatial distribution of beach and nearshore sands are discussed and cross-shore profiles are presented. Three sediment textural transport models are applied to examine alongshore variations in sediment texture, and conclusions are drawn regarding the likely direction of littoral drift along Waihi Beach during the study period.

Chapter 5 describes the collection, analysis and results of the wave, current and wind data collected during 2007 and 2008. The hydrodynamic components are an essential requirement for undertaking numerical modelling simulations. Wave data recorded by S4 current meters deployed during the field study are used to calibrate the wave refraction model in Chapter 6. Measured wave and current information was combined with bathymetric and sediment data to determine thresholds for sediment entrainment, which is subsequently used to identify the likely periods and magnitudes of onshore-offshore sediment movement.

Chapter 6 describes the results of wave refraction simulations over the bathymetry offshore from Waihi Beach. The wave propagation model WBEND is introduced, and results of model calibration are presented. A variety of scenarios are used to investigate wave energy focusing at northern Waihi Beach due to refraction of waves by Mayor Island, Steel's Reef and the submarine topography. Potential littoral drift directions and rates of sediment transport simulated by WBEND over

both short-term and longer-term scales are discussed. From model predictions of littoral drift direction, an assessment of Rapatiotio Point inhibiting longshore sediment transport by providing a sheltering effect is made.

Chapter 7 integrates the sediment budget for northern Waihi Beach, calculating sediment inputs, outputs and transfers within the dune-beach-nearshore system. A conceptual model of the sediment transport dynamics is proposed for the northern Waihi Beach littoral cell, and the processes inducing significant sediment loss are identified.

Summaries of the major findings and final conclusions of this study are discussed in Chapter 8, followed by recommendations for further research of the beach erosion problem at northern Waihi Beach.

## 1.5 SUMMARY

Waihi Beach has a long and exhaustive history of coastal erosion and flooding problems. The primary cause of erosion at Waihi Beach is due to downdrift sediment starvation from the groin effect of Rapatiotio Point, and insufficient diabathic sediment supply to compensate the magnitude of sediment lost in the littoral drift. Erosion is also enhanced by episodes of wave energy focusing and resultant diabathic removal of sediment offshore.

The trend for shoreline retreat at northern Waihi Beach has been greatly worsened by the artificial formation of Two and Three Mile Creeks in the 1930s and the construction of seawalls at Shaw Road and the Loop between 1962 and 1980. These existing inadequate structures have severely constrained the natural functioning of the Waihi beach-dune system, and their effectiveness in providing sustainable protection of beachfront property is often the subject of heated debate and controversy. Having well exceeded their useful design life, the WBOPDC applied for resource consent for further coastal protection along the Waihi Beach

shoreline in 2004, including a rock revetment, enhanced dune care, and training groynes along Three Mile Creek.

This research examines the hydrodynamics and sedimentary morphodynamics at northern Waihi Beach, to gain a greater insight into shoreline dynamics and the coastal processes influencing erosion. Linking erosion and sedimentation processes to prevailing hydrodynamic conditions should enable a more complete scientific understanding of beach morphodynamics by identifying and evaluating the coastal processes contributing to beach erosion at northern Waihi Beach.

# **CHAPTER TWO: ENVIRONMENTAL SETTING GEOLOGY, SEDIMENTS AND HYDRODYNAMICS**

---

## **2.0 INTRODUCTION**

This chapter provides a general description of the physical environment of the study site in order to identify the major processes influencing the sediment budget at northern Waihi Beach. It has been compiled from many previous investigations concerning coastal erosion and sedimentation processes at Waihi Beach. It begins with the geologic evolution of the study area, providing insight into the geomorphic form and origin of the beach. Features of coastal and beach morphology are examined, along with sediment characteristics and supply. Previous studies of wind, wave and current (tidal, wind and oceanic) dynamics, tropical cyclones and storm surge along the East Coromandel-Western Bay of Plenty are reviewed and the implications for coastal erosion at Waihi Beach are discussed.

## **2.1 LOCAL GEOLOGY**

The geology of the region surrounding Waihi Beach is complex, resulting from periods of volcanism with associated faulting and tilting of the fault blocks (HARRAY, 1977). An understanding of the geologic evolution and geomorphology of coastal landforms is essential for a good interpretation of the processes in, and development of, Waihi Beach.

Waihi Beach is located at the northern end of the 150 km long sandy coastline of the Bay of Plenty. The 9 km long tombolo barrier system is situated between the relatively stable strong points of Bowentown Head at the southern end and the coastal terraces and volcanic hills of the Coromandel Ranges to the north (HARRAY, 1977; ABRAHAMSON, 1987). Immediately southeast of Waihi Beach is the Katikati ebb-tide delta of Tauranga Harbour, followed by the 24 km long Holocene barrier island of Matakana and the barrier beaches of Mount Maunganui

and Papamoa. North of Waihi Beach, the coastline becomes rocky and cliffed with occasional pocket sandy beaches, notably Orokawa, Whiritoa and Homunga Beaches.

The rocky headland to the north (Rapatiotio Point) and the Bowentown rhyolite dome to the south act to anchor both ends of the beach. These landforms along with sections of the ranges to the west of Waihi Beach are weathered remnants of Minden Rhyolitic Volcanics of late Miocene early Pliocene age. The Coromandel Ranges north of Waihi Beach and parts of the ranges to the west are a combination of Mid Miocene Beeson's Island Volcanics overlain by Minden Rhyolite. The Beeson's Island Volcanics include andesitic and dacite breccias, tuffs, dykes and lava flows, and are overlain by late Quaternary tephra (HARRAY, 1977; HARRAY and HEALY, 1978; ABRAHAMSON, 1987).

Following the Pliocene volcanism was a period of glacio-eustatic sea level fluctuation throughout the late Quaternary. During periods of low sea level, streams and rivers dissected the landscape to a base level that was about 100-150 m below the present day sea level removing large volumes of sediment offshore. The rivers adjusted to the higher base level associated with subsequent rises in sea level, resulting in flooding of the incised valleys into which both fluvial and marine sediments accumulated. Rapid shoreward migration of sediment occurred subsequent to sea level attaining its current position about 6,500 years ago. This landward movement of sediment formed the present coastline of the Bay of Plenty (HEALY *et al.*, 1977; HARRAY and HEALY, 1978).

Backing much of the beach is the Holocene-age frontal dune. A prominent second set of Holocene dunes lies 50 to 100 m inland of the present frontal dunes (HARRAY and HEALY, 1978), partially vegetated and sometimes modified by subdivision development (ABRAHAMSON, 1987). These sets of Holocene dunes converge in the lee of Bowentown Head to enclose the upper part of the Tauranga Harbour. The narrow barrier has advanced in front of remnant Pleistocene paleodunes further inland, which currently back 70% of the existing beach (HEALY *et al.*, 1977). A layer of Rotoehu Ash overlies these relict dunes. Low-

lying interdune regions are occupied by swamps and alluvial estuarine deposits of the Waihi Beach Formation (ABRAHAMSON, 1987).

### *2.1.1 Tectonics*

GIBB (1997) noted that a subsiding coast is likely to have a greater sensitivity to coastal erosion than an emerging coast. The Waihi coastline is situated within the back-arc region of the actively convergent Hikurangi subduction zone located along the plate margin between the Pacific and Australian Tectonic Plates, immediately northwest of the Taupo Volcanic Zone (BRADSHAW *et al.*, 1991; BRADSHAW *et al.*, 1994). The coast shows aspects of a typical collision coast, with widespread faulting producing a number of graben-like basins that act as “depo-centres for coastal and shelf sediments” (BRADSHAW *et al.*, 1994, p.76).

SHEPHERD *et al.* (1997) studied the geomorphological evolution of Matakana Island and estimated a maximum mean subsidence rate of about -0.1 m/1000 years for the last 125,000 years. The lack of uplifted late Quaternary shorelines around the study area suggests a trend of either tectonic down-drop in accord with Matakana Island, or stability (GIBB, 1997). ABRAHAMSON (1987) ascertained tectonic down-drop of Waihi Beach at similar rates to Matakana Island. At the Bowentown Yacht Club, for example, there is clear evidence of down-drop of at least 2 m based upon tephrachronology (HEALY, 1997).

### *2.1.2 Geomorphology*

Waihi Beach varies from a wide gently sloping beach in the north to a steep, short beach in the south (HEALY *et al.*, 1977). The dune crest level appears to increase in elevation to the south and reduce to the north where they have been partially destroyed or modified by human development (HARRAY, 1977; BRADSHAW *et al.*, 1991). There is historical evidence of former higher dunes at northern Waihi Beach, including observations by Mr Oliver Pipe who in the 1920's recalls vast dunes near the location of the present surf club “which seemed to be about 100 feet high” (HANLEN, 1999, p.26), although admits in reality it was probably about half of that. With prevailing westerlies there was a constant drift to the northern

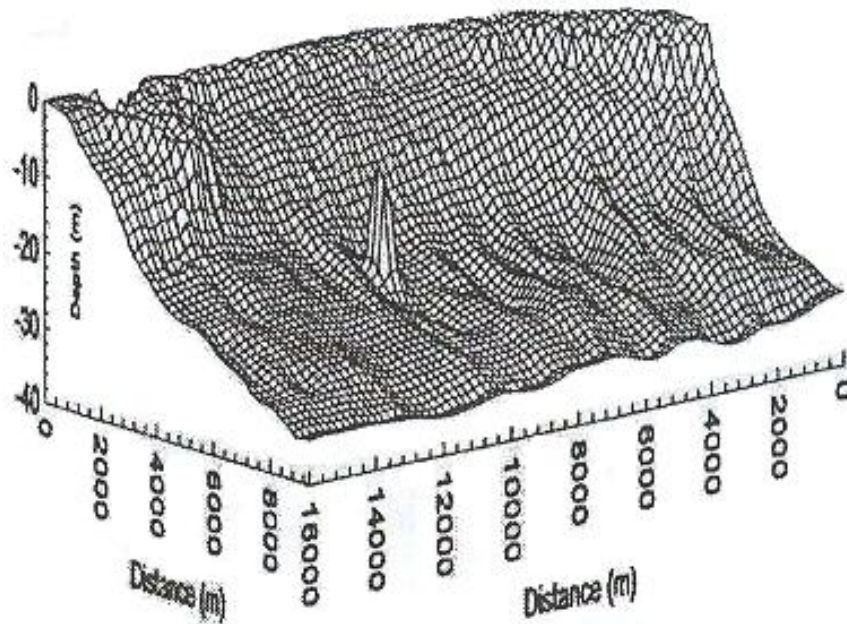
end of the beach, and as Pipe remembers “the sand drift in those days was terrific” (HANLEN, 1999, p.26). However, the build up of sand in the northern corner disappeared with the building of houses and the creation of lawns, which along with the spread of lupins helped to consolidate the dunes and anchor the drifting sand (HANLEN, 1999).

HEALY *et al.* (1977) classified Waihi Beach as a “long straight barrier beach”, the straightness being interrupted only by minor embayments carved into sectors of the dune face ranging from 800 to 2500 m in length and depths averaging 30 to 50 m (STEPHENS, 1996). These irregular but rhythmic large-scale features were first observed in the frontal dune at Waihi Beach by HARRAY (1977) and later described by HEALY (1987) and STEPHENS (1996) as “arcuate duneline embayments”. HARRAY (1977) observed four embayments along Waihi Beach during periods of erosion, and as many as six or more during accretional phases. Arcuate duneline embayments are erosional features (STEPHENS *et al.*, 1999) which appear to migrate up and down the beach. HEALY (1987) presents photographic evidence of the change in location of embayments in the longshore direction with time. He attributes these shifts to changing focal points of wave energy, producing embayment centres of erosion. HEALY (1987) observed dune cutback to be greater in specific locations along Waihi Beach, resulting in shallow embayments along the frontal dune line.

Waihi Beach is characterised by a reasonably flat intertidal and subtidal system. The morphology of the nearshore seabed is shown in Figure 2.1, and is comprised of the following topographic features (HUME and HICKS, 1993):

- The *upper shoreface* from the beach down to about 5 m to 8 m below Mean Sea Level (MSL)
- The *lower shoreface* from about 8 m to 20 m below MSL
- The *inner continental shelf* from 20 m to about 50 m below MSL





**Figure 2.1:** Waihi Beach shoreface and inner shelf morphology from digitized navy fair sheet soundings. The pinnacle on the inner shelf is Steel's Reef. Source: HUME *et al.* (1995).

The diabathic length of the upper shoreface is about 300 m in the south to 1000 m in the north of Waihi Beach (HUME and HICKS, 1993; BRUGMANS *et al.*, 2003). The upper shoreface is characterised by a subtle change in both seabed gradient and sediment composition. The boundary separating the upper and lower shoreface at ~5-8 m depth is thought by HUME and HICKS (1993) to represent the seaward limit of the “modern sand prism”, otherwise termed the inner closure depth, representing the day-to-day limit of exchange from surf related processes (HEALY, 1993). Similar depths have been described at Waihi Beach by HEALY (1993), who using data from HARRAY and HEALY (1978) suggested an inner limit of 5.7 m. DE LANGE and HEALY (1994) give a comparable inner limit of 5.5 m from the detailed data set available off the Tauranga Harbour entrance.

Long-shore bar-trough topography is also evident on the upper shoreface with strong rip currents associated with crescentic bar morphology (HOBAN, 1993; STEPHENS *et al.*, 1999). During the 1977 Bay of Plenty Coastal Erosion Survey (HEALY *et al.*, 1977) multiple offshore bars were found at central and southern Waihi Beach, with bars typically 150 m apart. Multiple bar formation at southern Waihi Beach was attributed to the presence of the Katikati ebb-tidal delta, but similar features at central Waihi Beach remained unaccounted for. From an

analysis of historical aerial photographs between 1948-1991 HOBAN (1993) found that two or three bars are evident at the southern end of Waihi Beach (Pio Shores) throughout the record. STEPHENS (1996) also observed up to three offshore bars at about 180 m, 250 m and 600 m offshore, and a mean bed slope of 1:58 between the beach berm and outer bar. Longshore bars with rip current channels can be seen migrating onshore and offshore in response to changes in the wave climate (HOBAN, 1993; BRUGMANS *et al.*, 2003). HEALY *et al.* (1977) noted that an absence of bars at northern Waihi Beach was associated with beach erosion.

HUME and HICKS (1993) and HUME *et al.* (1995) show the lower shoreface (at Katikati) to be convex-up and overlain by the Katikati inlet ebb-tide delta at the southern end of Waihi Beach. The delta extends offshore some 3 km to about 20 m depth, spanning 6 km alongshore, and stores approximately  $30 \times 10^6 \text{ m}^3$  of sand (HUME and HICKS, 1993; HICKS and HUME, 1996). Beyond this a gently sloping inner shelf extends to depths of around 40-50 m. The Tertiary volcanic bedrock reef known as Steel's Reef can be seen in Figure 2.1 piercing the inner shelf bathymetry approximately 4 km offshore from Waihi Beach.

A noticeable feature which characterises the inner continental shelf at Waihi Beach are large shore-normal coarse sand ridges described by Bradshaw *et al.* (1994) as "submarine dunes", which are welded on to the lower shoreface. The submarine dunes are slightly asymmetric to the northwest, have heights of 0.2 to 2.5 m (BRADSHAW *et al.*, 1994), are spaced about 250 to 1,300 m apart and are up to 2,000 m long (HUME and HICKS, 1993). They are interpreted to be relict deposits modified by present-day waves and currents. BRADSHAW *et al.* (1994) suggest that a predominant bottom current to the northwest of sufficient velocity to transport bedload sediments in 20 to 50 m water depth is implied by the asymmetry and strike of the submarine dunes. According to HUME and HICKS (1993), these shore-normal sand ridges play an important role in channelling sediment transport across the lower shoreface and inner shelf. From analysis of side-scan sonographs offshore from the Katikati inlet, they found that the megarippled troughs of the sand ridges apparently act as conduits for sand moving down from the upper shoreface or landwards from the inner shelf.

## 2.2 WAIHI BEACH SEDIMENT CHARACTERISTICS, SOURCES AND DISTRIBUTION

Sediment texture and mineral composition can be used to determine if a beach system is a renewable, partly renewable, or non-renewable resource (BRUGMANS *et al.*, 2003). Detailed analysis of the mineralogy and sedimentology of the Waihi Beach sand-body has been undertaken by HARRAY and HEALY (1978) and BRADSHAW *et al.* (1994). Sediment textures of the dune barrier and nearshore seabed have also been analysed by HOBAN (1993) and BEAMSLEY (1996).

### 2.2.1 *Sediment Texture*

Dune and beach sediments of the study area are mostly fine to medium sands. There is a progressive subtle fining of grain size northwards and an improvement in sorting from a “moderately well sorted medium sand” near Pio shores to a “well sorted fine sand” from Island View north (HARRAY and HEALY, 1978). Down the beach, sediment sorting is relatively poorer compared to the berm and dune sands (HARRAY and HEALY, 1978; HOBAN, 1993). Offshore, the beach out to about 5 m depth is characterised by moderately well sorted medium to fine sand. The lower shoreface consists of well sorted fine to very fine sand, and bottom morphology is dominated by small wave-generated ripples. At about 20 m water depth, there is an abrupt coarsening in sediment to poorly sorted gravelly coarse sand that extends down to about 50 m water depth. Sediments become muddier seaward of about the 50 m isobath (BRADSHAW *et al.*, 1994; HUME *et al.*, 1995; BEAMSLEY, 1996).

From side-scan sonar and SCUBA observations, DELL *et al.* (1985) and HUME and HICKS (1993) reported a sharp transition from the small wave-generated rippled fine sands to megarippled medium to coarse sands at depths of 20-40 m. The megaripples form abrupt contacts against the ripple fields, with fingers of megaripples or “submarine dunes” (BRADSHAW *et al.*, 1994) oriented obliquely through to shore normal. Coring by HUME and HICKS (1993) found that the fine sands and smaller wave-generated ripples overlie the coarser megaripple fields, as previously inferred by HARMS (1989) from side-scan sonographs. They note that

wave shoaling could be responsible for the movement of the fine sands and hence the covering or uncovering of the underlying megarippled facies. This transition from fine sands in the nearshore to higher proportions of coarse gravel between 20-40 m, indicating the boundary between shoreface and beach sediments, suggests a well-sorted system with limited exchange between offshore and inner shelf sediment bodies (HOBAN, 1993).

### 2.2.2 Mineralogy

Table 2.1 summarises the mineral composition of the sands along the Waihi Beach barrier system including the beach and nearshore seabed out to inner continental shelf. HARRAY and HEALY (1978) sampled the beach berm at three sites following erosion, minor accretion and accretion events in the mid 1970's. BRADSHAW *et al.* (1994) sampled the beach barrier, lower shoreface and inner shelf out to about 55 m depth at 35 sites. Approximately 94% of the beach sand is composed of light minerals of which quartz and feldspar make up about 60% (Table 2.1), and hence is commonly classified as "quartzo-feldspathic" (e.g. HUME and HICKS, 1993). The remaining 6% consists predominantly of heavy minerals hypersthene and hornblende. The beach sands are relatively homogenous in composition along the beach (HARRAY and HEALY, 1978). These sediments are generically related to the sediments of the shoreface and inner continental shelf. HUME and HICKS (1993) also found that the fine-grained felsic sands of the inner shelf overlay coarse-grained sand rich rock and shell fragments. BRADSHAW *et al.* (1994) identified glass-enriched sands that mantle the lower shoreface off Waihi Beach between 5 and 25 m water depth. It has been suggested that they may either be locally-derived sediments from larger infilled estuary systems that have been transported offshore during floods, or derived from the along-shelf dispersal of Tauranga shelf sands by periodic northerly-directed storm-generated currents discussed by BRADSHAW *et al.* (1991).

**Table 2.1:** Light and heavy mineral assemblages for the Waihi Beach sand system. All figures represent percentage of the total sample. \*Derived from HARRY and HEALY (1978). \*\*Derived from BRADSHAW *et al.* (1994).

Location	Light Minerals %						Heavy Minerals %					
	Plagioclase Feldspar	Quartz	Volcanic Glass	Rock Fragments	Shell Fragments	Total Lights	Hypersthene	Hornblende	Opagues	Cummingtonite	Augite	Total Heavies
Beach*	45	16	28	0	4	94	52	34	3	8	0	6
Upper Shoreface & Inner Shelf**	48	20	8	15	15	91	40	19	25	7	6	9
Lower Shoreface**	31	9	43	15	12	98	33	23	28	7		2

Frequent observation of Waihi Beach shows that there is quasi-permanent concentration of heavy minerals along the back beach, particularly at the northern end. Such lagged deposit of heavy minerals is a well-known indicator of beach erosion, because lighter minerals are preferentially removed by erosive phase waves leaving the finer heavy mineral as a lag. The presence of heavy mineral lag deposits is one line of evidence implying a condition of negative sediment budget from the study area.

### 2.2.3 Sediment Sources and Distribution

HARRY and HEALY (1978) identified the Waihi Beach mineral assemblage to be consistent with an ultimate origin from the erosion of the Quaternary tephra deposits of the Taupo Volcanic Zone. The sand was probably transported to the coast by the Tarawera, Rangitaiki and Kaituna Rivers south of Bowentown Head, where upon entering the littoral zone would have been transported northwest by a net longshore drift along the inner continental shelf.

HEALY *et al.* (1981) identified most beaches in the Coromandel as closed sedimentary systems, receiving little sediment from littoral drift or local river systems (BRADSHAW *et al.*, 1994). DELL *et al.* (1985) and BRADSHAW (1991) also

stated that the beaches in the eastern Coromandel are closed systems and renourishment is believed to be by diabathic sediment transport from the inner shelf. Immediately north of the study area are the isolated pocket bay-head barrier beaches of Orokawa, Homunga and Whiritoa. Textural analysis indicates that the sands of these beaches are relatively coarser (medium to coarse) than Waihi Beach (DELL *et al.*, 1985). HARRAY and HEALY (1978) found that these beaches were closed systems, also noting that the Waihi Beach beach sands were distinctly different from those at Orokawa Bay. Due to differences in sediment properties and the substantial headlands separating the beaches to the north of Waihi Beach, it would suggest that the Coromandel Ranges are not a supply source of sand to Waihi Beach.

BRADSHAW *et al.* (1991) found inner shelf-shoreface currents in the study area to be predominantly southerly during periods of calm offshore winds, producing a weak southerly-directed current regime, with strong northerly currents during storms. The authors suggest that the main source of sediment exchange for Waihi Beach is at the southern end through the Katikati ebb-tide delta system, or from offshore exchange with the continental shelf). The ebb-tide delta is composed of well sorted fine to very fine sand to about 20 m depth (HUME and HICKS, 1993) and is contiguous with the sands of Waihi Beach. Further south, the sand along Matakana Island follows a similar trend to Waihi Beach, becoming progressively finer and better sorted northwards (SHEPHERD *et al.*, 1997) inferring a net southeasterly littoral drift. GIBB (1997) considers the possibility that the Tauranga Harbour may be exporting sand through the Katikati Entrance, however, he summarises that the available evidence suggests the harbour is acting as a receiver of sand rather than a supplier of sand to the coast.

## 2.3 HYDRODYNAMICS OF THE BAY OF PLENTY AND IMPLICATIONS FOR COASTAL EROSION AT WAIHI BEACH

### 2.3.1 *Wind Climate*

Wind speed and direction are important mechanisms generating waves and currents. HEALY *et al.* (1977) noted the importance of winds, especially from the northeast, as a mechanism for producing high breaking wave conditions in the Bay of Plenty. HAY (1991) also suggests that localised wind climate is a critical parameter in the alteration of erosion and accretion patterns within the Bay of Plenty.

New Zealand's weather is largely determined by the general eastward progression of anticyclones and low pressure systems (QUALE, 1984). Although prevailing winds over northern New Zealand are typically low speed west to southwesterly, winds over the Bay of Plenty region are modified by local topography. The Waihi Beach coastline is sheltered by high country to the west, south and east, hence producing a sunny climate with considerably less wind than most other parts of the country (QUALE, 1984). However, the region also experiences infrequent gales mostly from the northeast or southwest (QUALE, 1984) causing humid conditions and often producing heavy rainfall.

PICKRILL and MITCHELL (1979) noted the quasi-cyclic nature of weather on the north east coast of New Zealand, with a fairly constant interval of 5-11 days between successive troughs of low pressure and associated cold fronts. These depressions are generally associated with unsettled weather and continuous strong onshore winds from the northeast, which generate local swell. Anticyclones between depressions typically produce offshore winds resulting in prolonged calm wave conditions (PICKRILL and MITCHELL, 1979). According to BRADSHAW *et al.* (1991) winds in the study area tend to blow from about 220° to 270°T, which is offshore along Waihi Beach. HARRAY (1977) and HOBAN (1993) also recorded southwesterly (230°) to northwesterly (290°) wind resultants at Waihi Beach.

QUALE (1984) noted that decaying tropical cyclones may also impinge upon the area. These subtropical low-pressure systems referred to as Tasman Depressions with an infrequent passage (10-20 per annum) are accompanied by high rainfall and strong onshore-directed east and northeast winds (BRADSHAW *et al.*, 1991). Decaying tropical cyclones affect the study area to a greater or lesser degree depending on their track southeast over New Zealand.

QUALE (1984) describes a seasonal variation in wind patterns with the highest frequencies occurring in spring and summer. He also noted that there is a marked diurnal variation in wind speed and direction, particularly in the summer when differential heating of the land and the sea causes afternoon onshore sea breezes and evening offshore winds. MACKY *et al.* (1995) and DE LANGE and GIBB (2000) state that during years with negative values of the Southern Oscillation Index (SOI) (associated with El Nino conditions), winds in the Bay of Plenty are generally offshore from the western quadrant. Positive SOI values (La Nina) on the other hand are characterised by more easterly onshore winds. DE LANGE and GIBB (2000) also note that during La Nina, the wind is generally contributing to positive storm surges and a general rise in mean sea level. There is a higher probability, therefore, of erosion and flooding from the sea occurring during La Nina dominant phases in the Bay of Plenty (DE LANGE and GIBB, 2000).

### 2.3.2 *Wave Climate*

The Bay of Plenty is described by PICKRILL and MITCHELL (1979) as a low wave energy zone due to sheltering by the New Zealand landmass from the prevailing deep-water waves approaching from the west and south. Waihi Beach therefore experiences reasonably low wave conditions for the majority of the year, with wave heights typically less than 1 m. However, the beach is susceptible to large wave forces and elevated water levels during onshore storms that often occur between April and August. During rare extreme events offshore wave heights of the order of 9 m with periods of 12 s (BRADSHAW *et al.*, 1994) can be experienced.



In the present study considerable variation in wave height was documented over both summer and winter S4 deployments, where periods of low energy are interrupted episodically by storms producing waves up to 3 m high. Similar patterns are noted by BRADSHAW *et al.* (1991) within the east Coromandel wave climate (including Waihi Beach), with wave heights in excess of 3 m. Wave and wind data from this study indicate high waves ( $H_s > 2$  m) occur during high north to northeasterly winds (Chapter 5).

HARRAY and HEALY (1978) obtained a significant breaking wave height of 0.6 m at Waihi Beach, and found that more than half (55%) of the significant wave heights recorded during their year-long study were less than 0.3 m. MACKY *et al.* (1995) provided measurements made from an ENDECO wave-track buoy deployed 8 km off the Katikati Entrance in 34 m water depth for a period of three years between 1991 and 1994. They recorded significant wave heights ( $H_s$ ) of less than 1 m for 70% of the time and a mean wave height of about 0.8 m. MACKY *et al.* (1995) noted that a slightly higher frequency of storm events with higher energy waves occurring in winter ( $H_s = 1.2$  m) compared to summer ( $H_s = 0.7$  m) results in a weak seasonality in the wave climate, a trend observed also by PICKRILL and MITCHELL (1979).

MACKY *et al.* (1995) concluded that because their wave data was collected during an El Nino climate phase it may not be representative of the long-term wave climate of this region. El Nino conditions are typically associated with southwesterly winds in the Bay of Plenty, which is offshore in the study area. In contrast, during a La Nina climate phase the wind tends to blow from the northeast quadrant resulting in higher wave events at Waihi Beach (MACKY *et al.*, 1995). HAY (1991) also suggests that stronger winds may possibly occur more frequently when the SOI is in its negative or La Nina phase. This suggests that persistent wave set-up will increase during La Nina periods and the rate of storm-induced erosion may also increase. New Zealand is now currently in a state of predominantly La Nina conditions since 1998, a pattern which may persist for 20 to 35 years (DE LANGE, 2000).

During three years of data collection, MACKY *et al.* (1995) observed 25 storm events with a maximum wave height of 6.7 m being recorded. They also observed that 66% of the 25 storms came from directions east of 60°T, and that the wave energy flux distribution had a pronounced peak in all years at 70-80°T (MACKY *et al.*, 1995). Similar results were obtained from S4 current meter data by HOBAN (1993) at Pio shores, who observed the dominant wave direction to be north to northeasterly.

PICKRILL and MITCHELL (1979) found that wave steepness on the northeast coast was variable, indicating the presence of both locally generated sea and ocean swell. These swell most likely originate from subtropical disturbances north of New Zealand, and can have a major influence on the erosion regime along the Bay of Plenty coastline (HAY, 1991). HARRAY and HEALY (1978) obtained a mean wave period of 11 s at Waihi Beach, with a range from 5 s during locally generated sea conditions, to 15 s at times of long period swell waves.

#### 2.3.2.1 Wave Refraction and Local Wave Focusing

HEALY *et al.* (1977) noted that refraction over the 20 km-wide continental shelf in the Bay of Plenty tends to modify the wave angle approach so that the waves become aligned near normal to the shoreline, with some refraction also occurring around offshore islands. Mayor Island and adjacent reefs and shoals offshore Waihi Beach have been found to provide a wave sheltering effect, particularly for long period waves (MACKY *et al.*, 1995). Observations in the wave data from other studies in the Bay of Plenty also indicate that refraction occurs near the coastline and wave focusing due to the irregularities in the inner shelf affects the direction and height of the incoming waves (e.g. HUME *et al.*, 1995). In the surf zone, the waves induce a longshore and cross-shore sediment transport. Consequently, wave refractive analyses have been shown to be an important element of coastal erosion and sedimentation processes along the Bay of Plenty coast (e.g. HEALY, 1987; HAY, 1991; PHIZACKLEA, 1993; HOBAN, 1993; BEAMSLEY, 1996; SAUNDERS, 1999; EASTON, 2002; SPIERS, 2005).

The formation of arcuate duneline embayments along Waihi Beach with erosion

in the embayment and accretion or no change on the horns is a local short-term erosion factor along the beach. In a study of aerial photographs from 1942 to 1977, HARRAY and HEALY (1978) recorded 42 m and 83 m of duneline retreat for embayments near Glen Isla Place and opposite Athenree, respectively. From wave refraction studies, STEPHENS (1996) found that the embayments were formed by enhanced sea level set-up from zones of wave convergence along the beach. The wave convergence was controlled by refraction of deep-water waves over the submarine dunes of the inner continental shelf and around Steel's Reef. STEPHENS (1996) also observed the formation of rip currents in the embayments that would interrupt any longshore drift, transporting littoral sands offshore. It is important to note that the Shaw Road area is also a favoured zone of the wave focusing (STEPHENS, 1996) and is one reason why there is a tendency for continual erosion at that critical sector.

### 2.3.3 *Tides and Currents*

#### 2.3.3.1 Tides and Tidal Currents

In the western Bay of Plenty, the astronomical tides are semidiurnal and the mean neap and mean spring tidal ranges for the open coast are 1.26 and 1.64 m respectively (HUME *et al.*, 1995). Tidal measurements recorded south of the study site at Mount Maunganui by HOBAN (1993) found tides to be microtidal with a tidal range between 0.8 m (neap) and 2.2 m (spring). Coastal erosion along Waihi Beach has a probability of occurring during high spring tides, especially if accompanied by onshore wave storms (GIBB, 1997). However, tides on New Zealand's east coast are more significantly influenced by monthly lunar (perogean-appogean) than bimonthly solar (spring-neap) cycles (TONKIN & TAYLOR, 2004).

While very strong currents run through the Katikati inlet at the southern end of Waihi Beach, peaking at over  $2 \text{ m.s}^{-1}$  on spring ebb tides (HUME and HERDENDORF, 1992); nearshore currents away from the delta are weak, with mean flows of  $0.05 \text{ m.s}^{-1}$  and a maximum of  $0.23 \text{ m.s}^{-1}$  (HICKS and HUME, 1997). Tidal currents have also been measured along the east Coromandel shelf by HARRIS *et*

*al.* (1983), who found average velocities of  $0.13 \text{ m.s}^{-1}$ . It is therefore thought that tidal currents at Waihi Beach are not strong enough to initiate sediment transport on the shelf, and are therefore of little significance to beach change (HOBAN, 1993). Thus, because waves and wave-induced currents are the dominant mechanism for sediment transport in the nearshore zone, Waihi Beach can be defined by the DAVIS and HAYES (1984) classification as a wave-dominated coastline.

### 2.3.3.2 Wind and Oceanic Currents

A strong but variable southeasterly directed geostrophic flow known as the East Auckland Current is present down the northeast coast of New Zealand (QUALE, 1984). The current is part of the western boundary current of the South Pacific subtropical gyre and is fed by the Tasman Front which is ultimately derived from the East Australian Current (HEATH, 1985). The East Australian Current is diverted around the northern tip of New Zealand near North Cape, and then flows southeast along the CONTINENTAL shelf passing through the Bay of Plenty (BRADSHAW *et al.*, 1991).

Inner shelf current patterns were studied along the East Coromandel Coast by BRADSHAW (1991) and BRADSHAW *et al.*, (1991) who found that the study area is dominated by two shore-parallel, near bottom currents. The first is a weak southerly-directed current resulting from offshore winds associated with passing anticyclones. It is noted to be part of the regional East Auckland Current flow, and with typical speeds of between  $0.1\text{--}0.2 \text{ m.s}^{-1}$ , they were considered not strong enough to generate sediment transport (BRADSHAW *et al.*, 1991). An opposite northward flowing current is derived from the infrequent passage of low pressure systems producing strong onshore winds. The northerly current was found to be generated by these onshore directed winds when they operated for considerable duration ( $>5$  hours) and high speeds ( $>12 \text{ m.s}^{-1}$ ). Current speeds of up to  $0.4 \text{ m.s}^{-1}$  were observed, which is sufficient to transport shelf sediments, with waves formed by the same onshore winds likely to intensify rates of sediment transport on the shoreface and nearshore (BRADSHAW *et al.*, 1991). BRADSHAW (1991) concludes that the interaction of waves with wind-driven currents is an important

mechanism for sediment transport over the inner shelf, with wave orbital motions entraining bottom sediments, and superimposed steady currents transporting them. Thus, waves determine when, and currents determine where, sediment is transported (BRADSHAW, 1991).

### 2.3.4 *Storms and Cyclonic Activity*

#### 2.3.4.1 Storm Surge

A storm surge results from the combined effects of barometric setup from low atmospheric pressure and wind set-up by strong winds blowing onshore that temporarily elevates the water level above MSL (PUGH, 2004). Water levels elevated under storm surge conditions not only pose an inundations hazard, but also allow larger waves to advance further up the beach profile due to increased wave run-up (HAY, 1991; BELL and GIBB, 2003) increasing flood damage potential and exacerbating coastal erosion, particularly of the frontal dune. DEAN and DALRYMPLE (1991) show that this is especially true on low gradient shorelines and in areas where the coast is fronted by a wide shallow region that maximises the wind stress effect (DE LANGE and GIBB, 2000; DEAN and DALRYMPLE, 2004), such as Waihi Beach. For Waihi Beach, HEALY (1993) calculated storm wave run-up levels of 4 m above MSL at the northern end and 5.4 m at the southern end. Similarly, GIBB (1994) estimated storm wave run-up levels of 4.5-5.5 m above Mean High Water Springs (MHWS).

Storm surges are generated in the Bay of Plenty by clockwise-revolving wind storms which may originate in either the mid-latitudes of the Tasman Sea (mid-latitude depression) or tropics (extra-tropical cyclone) (DE LANGE and GIBB, 2000). Internationally, New Zealand is not considered a region where storm surges are a major hazard compared to other countries (HEATH, 1979; DE LANGE and GIBB, 2000). Open-coast storm surge heights of up to 1 m above the predicted tide occur around the New Zealand shoreline, with a level of 0.9 m likely to represent a 100-year type surge event (TONKIN & TAYLOR, 2004). These surges have small amplitudes in comparison to the 2-3 m surges experienced in the Bay of Bengal, Gulf of Mexico, Gulf of Carpentaria, and other locations within the

tropics. Nevertheless, they have an important influence on coastal erosion and the subsequent sediment movement under storm conditions (HEATH, 1979; DE LANGE and GIBB, 2000).

#### 2.3.4.2 Tropical Cyclones

Tropical cyclones can produce major surges leading to coastal flooding and beach erosion. STURMAN and TAPPER (1996) define tropical cyclones as a non-frontal, synoptic-scale, cyclonic rotational low-pressure system of tropical origin, in which 10 minute mean winds of at least  $17.5 \text{ m.s}^{-1}$  occur, and the belt of maximum winds are in the vicinity of the systems centre. New Zealand commonly experiences 2-3 tropical cyclones per year (HARRIS, 1985).

For a tropical cyclone to develop, sea surface temperature must be at least  $26.5^{\circ}\text{C}$  and remain greater than  $20^{\circ}\text{C}$  to maintain intensity (HAY, 1991). Tropical cyclone activity in the Bay of Plenty is therefore predominant during the warmer months between November and March, although cyclonic events may occur at other times. Trajectories of these cyclones commonly move northwest to southeast, passing the Bay of Plenty approximately 300 km offshore (HARRIS, 1985).

The El Nino-Southern Oscillation (ENSO) fluctuations cause changes to the weather patterns of the Indian and Pacific Ocean, which subsequently alter the frequency of extra-tropical cyclones affecting New Zealand (DE LANGE, 2000). During La Nina, the wind is generally onshore from the northeast quadrant contributing to positive storm surges and a general rise in sea level. Higher mean sea levels during La Nina may also be attributed to raised water temperatures (DE LANGE, 2000). There is a higher probability, therefore, of erosion and flooding from the sea occurring during La Nina dominant phases in the Bay of Plenty, particularly as La Nina episodes provide a more suitable environment for extra-tropical cyclones to track south to New Zealand (DE LANGE and GIBB, 2000).

Wind direction also appears to have a major influence on the magnitude of storm surge in the Bay of Plenty. HAY (1991) found that for the data he analysed between 1873 and 1990, easterly winds were associated with the largest surge

(546 mm recorded at Moturiki Island), while winds from the north, northeast, southeast and south produced smaller surges.

Occasionally, tropical cyclones that produce high waves and storm surge coincide with high spring tides, further increasing the flooding risk for vulnerable low-lying coastal communities like that of Waihi Beach. Furthermore, associated with climate warming is the projected acceleration in sea-level rise and possible increases in the intensity of storms (BELL and GORING, 2003).

## 2.4 SUMMARY

The objective of this chapter was to review the physical environment at Waihi Beach and identify the dynamic features which may influence coastal erosion and sedimentation processes. Waihi Beach barrier is a Holocene landform situated on the leading edge of a tectonically active plate margin. Located at the northern end of the 150 km long sandy coastline of the Bay of Plenty, The 9 km long tombolo barrier system is bound by the Coromandel Ranges to the north and the Bowentown Rhyolite dome to the south. HEALY *et al.* (1977) classified Waihi Beach as a “long straight barrier beach”, varying from a wide gently sloping beach in the north where there is very little dune present, to a steep short beach with a pronounced dune in the south. Arcuate duneline embayments carved into sectors of the frontal dune face are a notable feature of the Waihi Beach coast, thought to be a result of wave focusing and the nearshore circulation system. The major morphological units which comprise the nearshore seabed at Waihi Beach are the upper shoreface, of which longshore bar-trough topography is evident; a convex-up lower shoreface, and a gentle inner continental shelf punctuated by Steel’s Reef. Large shore-normal megaripples composed of coarse sand occur on the lower shoreface and upper inner shelf. These are modified by present day large wave events and currents. Today, the megarippled troughs of the sand ridges may act as conduits for the cross-shore transport of fine sand, although this is not yet been proven.

Waihi Beach consists of quartzo-feldspathic fine to very fine sediments close to the shore, with coarser sediments found further offshore. The sediment character of the nearshore zone does not have significant alongshore variation. The most significant change is offshore where sedimentary distinctions can be associated with different morphological features. Waihi Beach has been identified as a closed sedimentary system, receiving little sediment from littoral drift or rivers. Available evidence suggests the main source of sediment exchange for Waihi Beach is through the Katikati ebb-tide delta system or from offshore exchange with the continental shelf.

The hydrodynamic parameters which may influence coastal erosion and sedimentation at Waihi Beach identified were:

- *Wind climate* within the Bay of Plenty is suggested to be a critical parameter of coastal erosion and accretion patterns within the region. Local topography influences wind direction and speeds at Waihi Beach, with surrounding mountain ranges provide a sheltering effect from predominant westerly winds. The region is however exposed to infrequent gales from the northeast and southwest.
- *Wave climate* within the Bay of Plenty region has been described as ‘low energy’ relative to the rest of the New Zealand coast. Wave steepness is variable, indicating a mixed swell and local sea environment, with a weak seasonal cycle. Bay of Plenty wave climate is largely influenced by the wind direction. During a La Nina climate phase the wind tends to blow from the northeast quadrant resulting in more wave events at Waihi Beach. It is suggested that waves at Waihi beach are influenced by wave refraction from Mayor Island and adjacent reefs and shoals. The importance of wave refraction causing increased wave energy (and hence erosion potential) at the shoreline at Waihi Beach is investigated in Chapter Six.
- *Tidal currents* at Waihi Beach are not strong enough to initiate sediment transport on the shelf, and are therefore of little significance to beach change. *Wind Currents* on the shoreface are weak and flow predominantly shore parallel, alternating between a southerly-directed current (0.1-0.2



m.s<sup>-1</sup>) during prevailing calm weather, and northerly-directed flow (up to 4 m.s<sup>-1</sup>) associated with passing low pressure systems producing strong onshore winds. Only the northwards flowing currents are considered sufficient to transport shelf sediments.

- *Storm surge and cyclone activity* have an important influence on coastal erosion and the subsequent sediment movement in the Bay of Plenty. Erosive events along the Waihi Beach coastline are expected during storm events, which increase wave steepness and raise the still water level. Elevated water levels under storm surge conditions will also increase wave run-up, increasing the potential for inshore inundation and inducing a greater probability of wave-induced erosion of the frontal dune. Tropical cyclones can produce major storm surge elevations resulting in coastal flooding and beach erosion. The Bay of Plenty is expected to experience positive storm surges and higher sea levels during La Nina phases than El Nino phases, because of predominant onshore winds and more suitable conditions for extra-tropical cyclones to track south to New Zealand.

# CHAPTER THREE: BEACH AND NEARSHORE MORPHOLOGY

---

## 3.0 INTRODUCTION

Exposed sandy beaches may be very dynamic, showing both short and long term trends in shape, accretion and erosion patterns. The overall morphology of a beach reflects the composition of its sediments and the physical forcing of waves, winds and currents (KOMAR, 1998; DEAN and DALRYMPLE, 2004). By measuring the dimensions of a beach repeatedly, the amounts of erosion or accretion can be determined over the period of the surveys as well as some indications of where the material may be going or coming from (DEAN and DALRYMPLE, 2004).

Hydrographic surveying of nearshore profiles may be used to assess trends or relationships in erosion and accretion patterns, while side-scan sonar images can identify wave-induced bedforms and sediment distributions. Bedforms are significant in that they are indicators of sediment transport by currents, which are induced by wave motion (TRENHAILE, 1997). Side-scan sonar was used in the present study to map sediments and the distribution of major geomorphic units offshore from northern Waihi Beach.

In this chapter, beach morphology is assessed by comparing beach and nearshore profile surveys undertaken across five selected transects along the beach on different occasions. The resulting cross-sections of the beach and nearshore are indicative of processes operating at the time of surveying, and provide excellent evidence of the magnitude and frequency of the cross-shore exchanges being experienced at northern Waihi Beach. Current shoreline trends are compared with earlier assessments by Environment Bay of Plenty (EBOP). Results from a side-scan sonar survey of the northern Waihi Beach nearshore zone are presented, providing valuable insights into sediment transport pathways and processes, and into the factors that shape the Waihi Beach shoreface.

## 3.1 TOPOGRAPHIC AND HYDROGRAPHIC SURVEY OF WAIHI BEACH

### 3.1.1 Dune and Sub-Aerial Beach Profiling

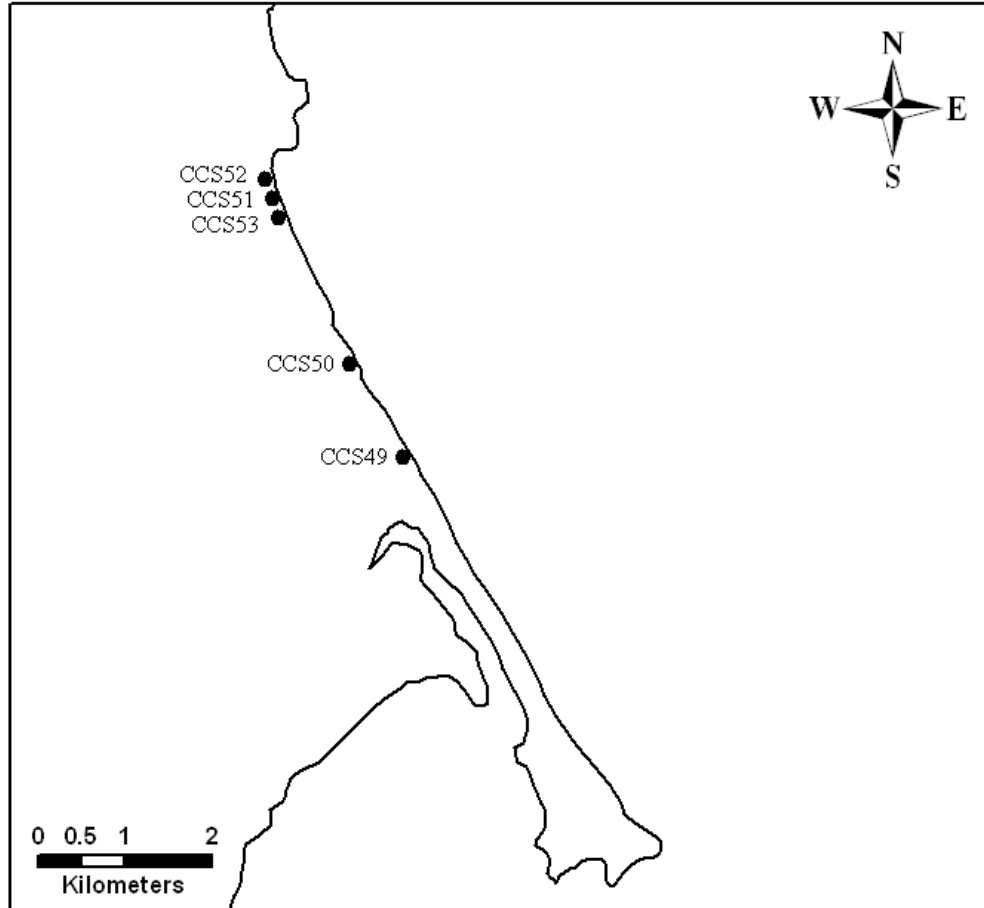
Dune and sub-aerial beach surveying was undertaken along northern Waihi Beach on the 14<sup>th</sup> January 2008 using the Total Station (Operated by Chris McKinnon, University of Waikato Field Technician), and again on the 23rd June 2008 in conjunction with nearshore profiling using Real Time Kinematic (RTK) satellite navigation and differential GPS (DGPS). Five topographic profiles were selected to be surveyed based on benchmark positions used in beach profiles undertaken by EBOP (IREMONGER, 2007), which were first profiled and described by HEALY *et al.* (1977) in the Bay of Plenty Coastal Erosion Survey (BOPCES). The use of existing survey benchmarks enables historical comparison of beach and nearshore profiles to be made. Historical beach profile data were also obtained from EBOP who undertake quarterly monitoring of BOPCES sites.

Figure 3.1 illustrates the locations where dune and beach profile surveys were undertaken. GPS coordinates and elevations of benchmarks are presented in Table 3.1. The second onshore survey was conducted in conjunction with an offshore survey.

### 3.1.2 Surveying Method

The beach profiles collected on 24<sup>th</sup> January 2008 were measured using a Total Station and a standard surveying rod with a triple prism attached. A Total Station is an electronic surveying instrument for measuring points in 3-dimensional space. Using a sophisticated angle measuring component, and laser beam emitting and mirror reflecting procedures, it determines the position of a target from a basic direction and the measured distance from the measuring point (HUANG *et al.*, 2002). These data points are recorded at regular intervals down the beach, from the frontal dune (or seawall) to the low water mark. The Total Station has been shown to generate high accuracy surveying output (e.g. HUANG *et al.*, 2002;

IREMONGER, 2007). Its telescope resolving power is 3 seconds, with a horizontal and vertical accuracy of 5 seconds for the angle measurement. For the distance measurement the accuracy is  $\pm 5$  mm.



**Figure 3.1:** Locations of Environment Bay of Plenty benchmarks at northern Waihi Beach used for surveying in this study. All benchmarks have been established from the original BOPCES survey sections. All benchmarks are surveyed to Moturiki Datum so each benchmark is at a known height above mean sea level.

**Table 3.1:** GPS Coordinates and elevations of frontal survey benchmarks at northern Waihi Beach. Northings and eastings are relative to the Bay of Plenty meridional circuit and elevation is above local Moturiki Datum.

Benchmark	Northing (m)	Easting (m)	Elevation above MSL (m)
CCS49 – ‘Island View’	736962	254943	5.950
CCS50 – ‘The Loop’	738010	254286	5.285
CCS51 – ‘North’	739882	253330	5.398
CCS52 – ‘Surf Club’	740086	253223	3.717
CCS53 – ‘Stream’	739595	253312	3.594

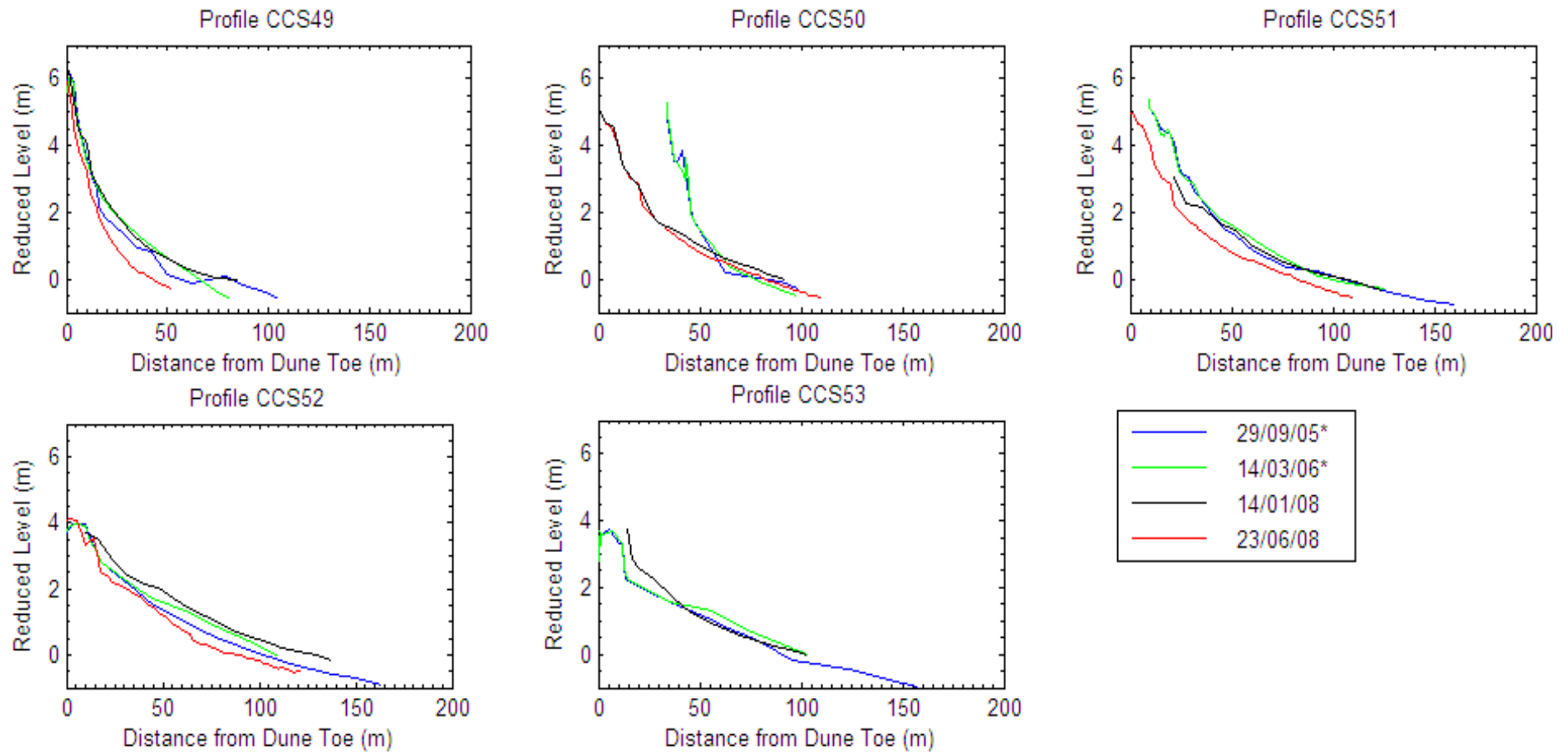
Onshore surveying was undertaken at or near low tide in order to maximise survey excursion distance and include as much nearshore bathymetry as possible. The survey was carried out to the limit of wading in an attempt to overlap the beach profile with the offshore survey, which was carried out at high tide.

### *3.1.3 Description of the Beach Profiles*

All beach profile sites have had their benchmark surveyed to Moturiki Datum so each benchmark is at a known height above mean sea level. Unfortunately, the benchmark at CCS53 has disappeared and so the location of its position was estimated based on GPS, which is accurate to within  $\pm 1-3$  m. Hence, the new benchmark location used in the present study may differ in position from the original established by the BOPCES (HEALY *et al.*, 1977). All beach profiles collected during summer (January 2008) and winter (June 2008) are shown in Figure 3.2. Two surveys taken by EBOP prior to the study period (September 2005 and March 2006) are also included to represent typical autumn and spring profiles. Due to difficulties locating the precise benchmark position of CCS53 and the uncertainty regarding how accurate the estimated position was in relation to the originally established position, profiling at this site was excluded from June 2008 onshore surveying. Likewise, CCS53 was not included in subsequent offshore profiling.

From observations in the present study and historical beach profile data from 2005 and 2006, the following site characteristics and associated changes between surveys are described to provide an understanding of shoreline fluctuations.

As previously mention by HEALY *et al.* (1977), the beach becomes increasingly narrower and steeper towards the southeast, with wide gently sloping gradients characteristic of profiles at the far northern end (Figure 3.2). Significantly higher dunes up to 6.3 m above MSL are observed at Island View, compared to the northern end of the beach (CCS52 and CCS53) where dunes are typically ~4 m, indicating greater sediment accumulation and availability for building the dunes towards the southern end of the study area.



**Figure 3.2:** Beach profiles collected at northern Waihi Beach from September 2005 to June 2008. Profiles obtained from Environment Bay of Plenty are marked \*.

#### 3.1.3.1 Island View (CCS49)

This site is located approximately half way along the Waihi Beach system, approximately 6 km north of the Bowentown Entrance. Figure 3.3 shows a beach with a well vegetated foredune. No berm is present (Figure 3.2), and there is also some evidence of cusp features present. The morphodynamic classification for this sector of beach according to the Wright Short model is longshore bar and trough (see Figure 3.6, section 3.1.4.1 Description of Offshore Profiles). A thick lag deposit of titanomagnetite is a characteristic feature of this part of the Waihi Beach coastline, and can be clearly seen fronting the dune in Figure 3.3.

The lowest beach profile elevation was the winter 2008 profile, with the greatest elevation of the berm and back beach observed in the summer 2008 profile. This change in profile geometry associated with changing seasons is brought about by a cyclical cut and fill, representing a cross-shore sediment transport and exchange between the offshore bar (KOMAR, 1998). Under higher wave conditions during the winter the berm is destroyed by the intensified wave swash. The sand removed from the berm is presumably moved offshore to form bars. The upper beach and berm begin to increase again with the return of lower wave energy conditions during summer. The envelope between the winter profile and the summer profile generally shows less than 1 m of vertical movement, progressively widening as the profile approaches MSL.

Despite the relatively minor fluctuations in dune height observed over the past three years, a report by ECO NOMOS (2003) (as cited in IREMONGER, 2007) suggested that duneline fluctuations at this location considerably exceed the scale of changes likely to be associated with storm cut and recovery. The larger fluctuations evident at this site are believed to reflect the additional influence of deep, arcuate duneline embayments (STEPHENS, 1996) and the adjacent Bowentown ebb tide delta at the southern end of the beach. This site has been classified by EBOP as being in a stable state for the last 18 years of the profiling record (IREMONGER, 2007).



**Figure 3.3:** Well-vegetated dunes at profile CCS49 at Island View. This photo also illustrates the longshore-bar-trough sequence typical of central to southern Waihi Beach. Photograph taken by T.R HEALY 23/08/06.



**Figure 3.4:** The rock revetment at CCS50, which is located midway along The Loop. Also note the remnants of the older timber wall. Photograph taken by the author 24/06/08.



### 3.1.3.2 The Loop (CCS50)

This site is located midway along The Loop, approximately 4 km from Rapatiotio Point. The site is in front of the residential development at The Loop and is equidistant between Two and Three Mile Creeks. This section of beach has a several metre high rock revetment present, along with the remnants of an older timber wall, as shown in the Figure 3.4. The beach profiles reflect the presence of this engineering works as a means of providing stability to the upper section of beach. The 2008 profiles show a change in the upper beach position (where the seawall is located) compared to the earlier profiles by EBOP, although this is most probably the result of a slightly different survey line being used. Considering the data of the present study separately from that of the Regional Council, and vice-versa, it can easily be seen that as a result of the revetment the “dune” position has remained stationary for the 5 and 7 month periods between surveys, respectively. However, upper and lower intertidal beach levels are relatively similar to those at CCS49.

There is some change in the vertical position of the mid to lower beach profile between seasons as a result of negligible sediment transfer from the upper beach to maintain the equilibrium beach profile. This movement means that during periods of lower beach elevation no dry beach is present during the upper portion of the tidal cycle. Shoreline change at CCS50 may also be attributed to the more complex processes operating at locations closer to the Two and Three Mile Creek outlets. As with CCS49, EBOP beach volume analysis indicates stability for this beach profile site (IREMONGER, 2007).

### 3.1.3.3 Waihi Beach Stream (CCS53)

This site is located at the southern boundary of the popular Waihi Beach at the northern extent on the eastern side of the small stream. This site’s origin is located within a dune care fenced area planted with native vegetation. The beach profiles in Figure 3.2 show a low angle beach with typically no berm feature present, with the exception of the March 2005 plot which does show evidence of sand accumulating in a berm shape approximately 50 m from the benchmark. Beach

volume analysis by EBOP suggests a pattern of accretion since 1997 (IREMONGER, 2007). Figure 3.2 shows a reasonably confined range of vertical movement between seasons.

#### 3.1.3.4 Waihi Beach North (CCS51)

A 5 m high frontal dune is present at this site which is vegetated by a mixture of exotic and native species. An incipient dune has also formed and is presently colonised by a dense cover of spinifex. The beach profiles in Figure 3.2 shows a tight grouping of representative profiles for this site. The winter profile however highlights that following periods of increased storm activity this section of beach can exhibit a marked negative vertical translation. Lower beach features are typically subtle at this site with no prominent berm development evident in the record. Combined analyses of beach volume and dune toe position records over the past 16 years by EBOP gives an overall state of stable for this beach profile site (IREMONGER, 2007).

#### 3.1.3.5 The Surf Club (CCS52)

This site is the northwestern most of the beach profile monitoring sites along Waihi Beach, positioned close to the surf club directly in front of the public toilets at The Esplanade. As with CCS53, the profile origin for this site is located in an area that has been fenced to deter human traffic and planted with a range of native species (Figure 3.5). The site was installed in 1998 as part of a monitoring programme focusing on an area where significant dune care work was to be undertaken by EBOP (IREMONGER, 2007). The last 70 years have seen these dunes removed by local residents, the consequent erosion leaving them standing at only about 1 m above MSL (BRUGMANS *et al.*, 2003). The dune care programme initiated by the Council has resulted in the redevelopment of these dunes which are currently around 4 m high above MSL.

Similar to CCS53 the beach exhibits a low angle with a wide high tide beach present. The frontal dune appears to have undergone minor changes in shape which can be attributed to the dune care work. As with CCS49, seasonal profile

shifts are evident, showing increased berm elevation during summer 2008. The following winter the beach face and berm are cut back just under 1 m. beach volume analysis by EBOP concluded that CCS52 has been in a stable state since 1997 (IREMONGER, 2007).

#### *3.1.4 Nearshore Profiling*

Detailed shallow hydrographic surveying was planned to be undertaken within the northern Waihi Beach nearshore. With sufficient bathymetric data, the creation of a digital terrain model was intended to allow for areas of sediment scour or accumulation to be identified. Unfortunately, persistent northeasterly to southeasterly winds and high swell created non-ideal surveying conditions for the most part of winter and spring 2008, which meant detailed profiling of the nearshore was not possible. Hydrographic surveying was therefore restricted to four offshore transects from benchmark locations CCS49 to CCS52 on only one occasion. Details of data acquisition in the field and the results obtained are presented in the following.

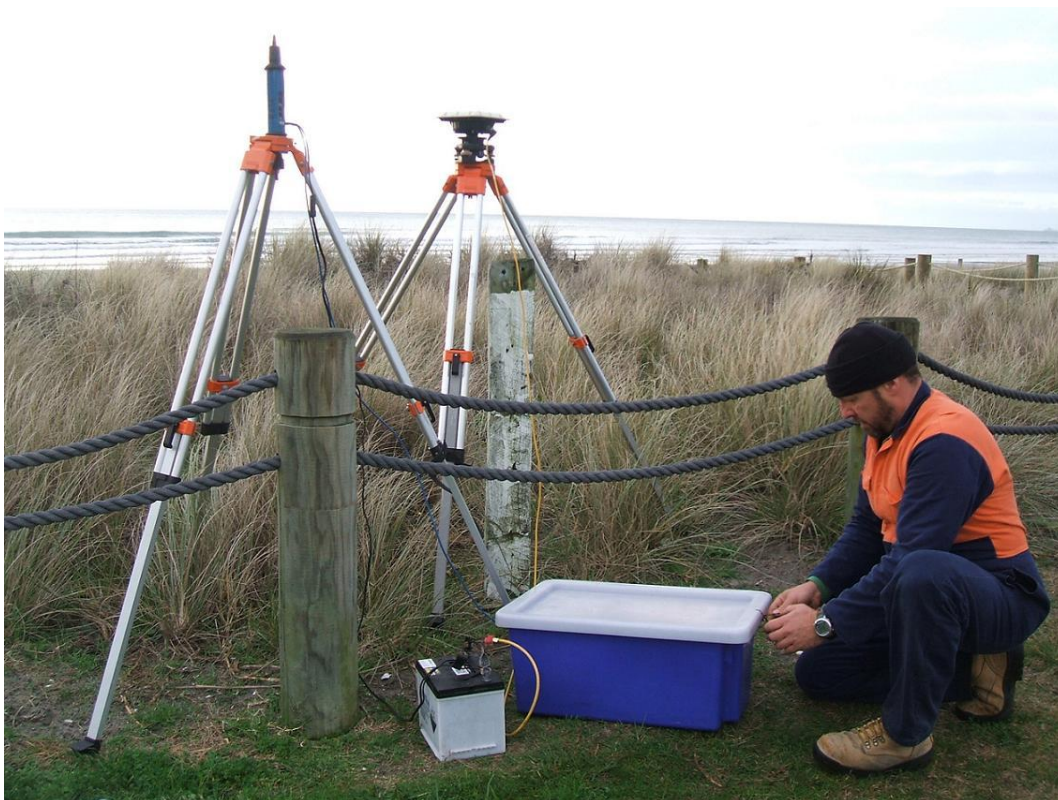
##### *3.1.4.1 Field Programme*

The University of Waikato vessel *Taitimu* was used for nearshore profiling, which was undertaken on 24/06/08 at high tide to allow the vessel to run landward of the nearshore bar in water depths of ~2 m. Beach profile surveys were measured the previous low tide so that surveys could be overlapped and connected, providing a continuous transect from the dune to ~10-12 m depth. Some small areas without data resulted in interpolated surfaces.

Position was recorded with each depth measurement using the GPS receiver on the boat, with real-time corrections from a second DGPS receiver fixed at a reference point, or base station, on shore. Benchmark CCS52 near the Surf Club was used as a permanent base station during all offshore surveys. The DGPS unit uses satellite data to calculate its position, and then records the difference between this with the known position. These corrections are recorded and transmitted to the GPS receiver on the boat, which applies these to its measurements (HURN,

1993). DGPS positions are accurate within 1 m (DIRK IMMENGA, *pers comm.* 2008).

One might assume there is a considerable degree of inaccuracy in the measured depths due to the combined effects of waves, tides, and other factors that may alter water levels. It is essential that these errors are corrected for. The heave compensation removes significant wave action from the survey data, and because the sounding depths are relative to the water level at the time of surveying, a tide gauge system is used to determine the water level associated with each profile. The water level is adjusted to Moturiki Datum so that the measured depths can be correlated with the beach profiles.



**Figure 3.5:** Setting up the base station at CCS52 in front of the Waihi Beach Surf Club for beach and nearshore hydrographic surveying.

#### 3.1.4.2 Description of Offshore Profiles

Nearshore profiles taken at northern Waihi Beach in June 2008 are presented in Figure 3.6. Typically, the nearshore zone at northern Waihi Beach is comprised of

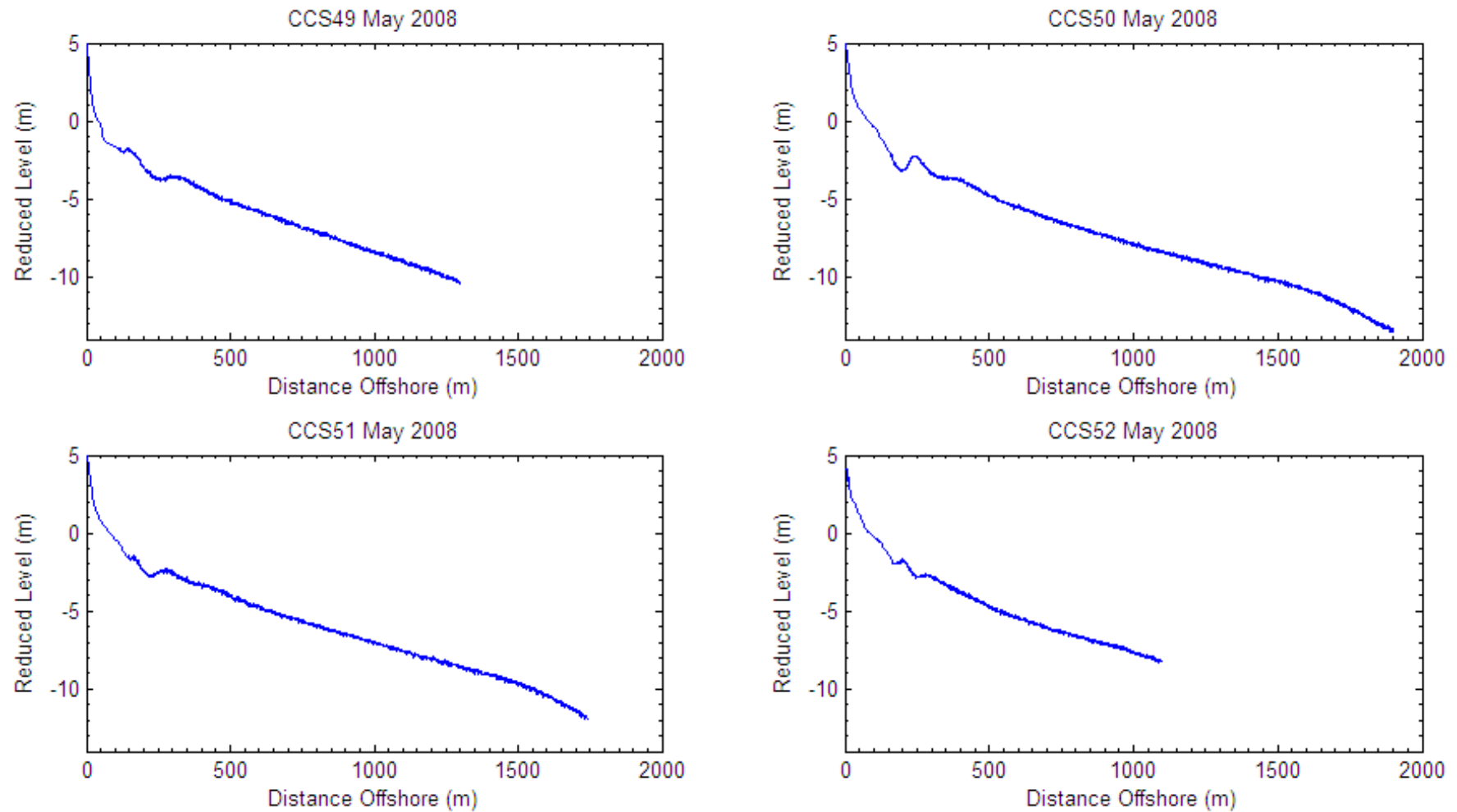


Figure 3.6: Nearshore profiles taken at northern Waihi Beach on the 24/06/08.

an offshore bar with an associated alongshore trough. In some cases a second offshore bar exists. Nearshore profiling at Waihi Beach by HEALY *et al.* (1977) and STEPHENS (1996), and at Pio Shores by HOBAN (1993) similarly indicated a multiple-barred beach system. KOMAR (1998) states that the number of bars on a beach depends mainly on the overall slope of the nearshore; the more gradual the slope the greater the number, with bars commonly absent on steep beaches. Multiple bar formation off Waihi Beach is therefore likely due to the very gentle gradient of the nearshore (Figure 3.6).

On a low sloping beach such as Waihi Beach, after waves have broken they may reform as they continue across the surf zone. These reformed waves may break a second (and perhaps third) time before they finally reach the shore. An outer bar may form in association with the initial zone of breaking, while inner bars develop where the reformed waves break, giving a multiple-bar system. A similar theory is that larger waves generate the outer bar, while subsequent lower waves pass over the outer bar with little effect to themselves or the bar and break closer to the shore, forming an inner bar (KOMAR, 1998). KING and WILLIAMS (1949) (as cited in KOMAR, 1998) found that the outer bar at Sidi Ferruch, North Africa, owed its position to the predominant break point of storm waves of great energy, while the inner bar depends on the predominant calm-weather waves.

The offshore profile for CCS49 shows a poorly defined longshore bar approximately 150 m offshore, followed by a trough and then another slightly larger outer bar. Beyond these features the seabed gradient is consistently around 1:200 out to a depth greater than 10 m. Both nearshore profiles of CCS51 and CCS52 display a similar bar-trough-bar sequence, although the nearshore bar peak is much less prominent at profile CCS51 than those of the other profiles. Little or no bar development is a common feature for sites in the Bay of Plenty which are located in the lee of rocky headlands (IREMONGER, 2007).

The offshore profile at CCS50 shows a definite longshore bar approximately 250 m from the shoreline, with a deep trough on its shoreward side. This indicates that sediment eroded from the beach face and berm fronting the seawall has shifted offshore and been deposited to form the nearshore bar. A poorly defined

secondary bar is also present at approximately 380 m offshore. Beyond these bar features is a characteristically flat nearshore zone. Seaward of ~1400 m the slope becomes mildly convex seaward, a feature also apparent at CCS51.

The nearshore slope off northern Waihi Beach decreases only slightly between 5 m and 14 m water depths (Figure 3.6). The gently sloping gradient of each profile and the position of the bar along each transect (350-400 m offshore) indicates a wide surf zone. This suggests that during the high wave energies typical of winter, the beach responds by shifting the breaker zone further offshore, thereby enhancing the dissipation of large waves before they reach the shoreline (KOMAR, 1998).

Location of sediment storage reflects the morphological state of the beach as well as the processes that operate (KOMAR, 1998). Sediment stored offshore generally indicates an erosional beach state, while onshore storage suggests accretionary calm conditions. Therefore, with the presence of longshore bars in conjunction with an apparent decrease in beach profile elevation compared to summer beach profiles (Figure 3.2), it is fair to suggest that profiles undertaken in June 2008 indicate a period of erosion at northern Waihi Beach, coinciding with periods of high wave energy (see wave analysis in Chapter 5).

## 3.1 SIDE-SCAN SONAR IMAGERY

### 3.1.1 Introduction

A side-scan sonar survey was undertaken to assist in the interpretation of surficial sediment patterns and identification of bedforms on the inner shelf. Alterations in sediment texture within the surveyed region may identify potential sediment sources and zones where wave orbital currents are initiating sediment transport at northern Waihi Beach.

### 3.1.2 Side-Scan Sonar Operation

Side-scan sonar is a system used to gather information on the morphological character of the seafloor by firing high frequency sound pulses and measuring the strength of the backscattered signals (KRUGER and HEALY, 2006). The side-scan sonar system consists of three main components (HEALY *et al.*, 1996; MORANG *et al.*, 1997):

1. Two opposing transducers contained in a “fish” which is towed behind the vessel;
2. A graphic chart recorder on board the vessel which is combined with a signal transmitter and processor; and
3. An electromechanical tow cable connecting and allowing the transfer of information between the two units.

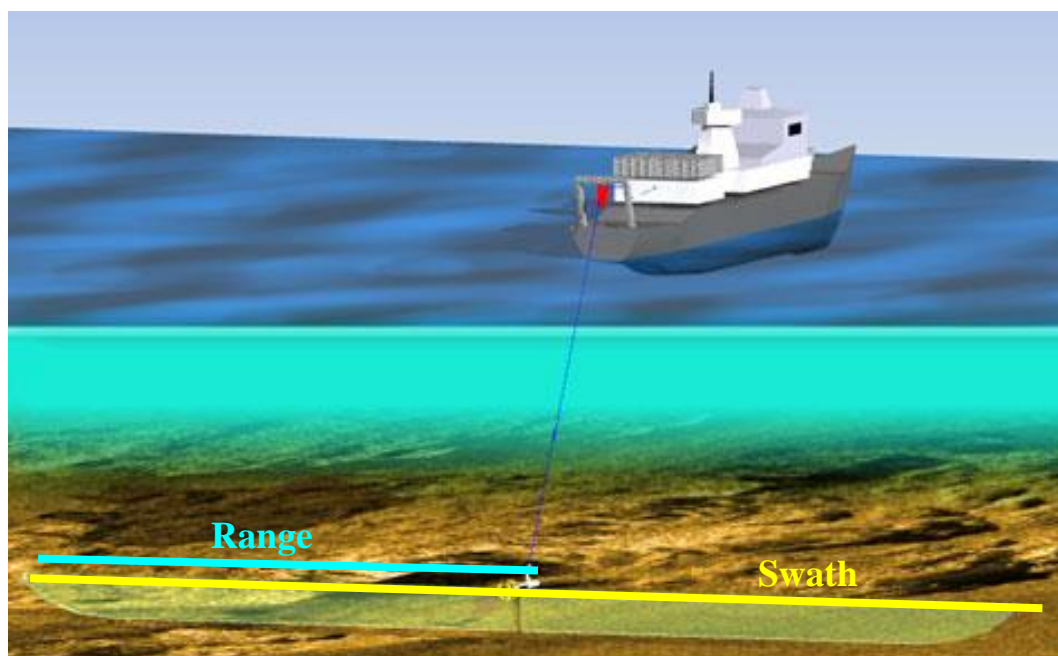
Deployed a certain height above the seabed, the transducer in the tow fish emits high frequency fan-shaped sound pulses perpendicular to the tow direction, which are reflected off the seafloor (Figure 3.7).

The intensity of the reflected signal is largely a function of the sediment properties and bottom roughness, and the angle of incidence of the sonar beam (MORANG *et al.*, 1997; KRUGER and HEALY, 2006). Coarser sediments and bedrock on the seabed tend to be highly reflective, producing a strong dark mark on the record.



Soft marine mud on the other hand absorbs part of the sound energy which mutes the reflected signal, and thus returns a weak lighter signal (MORANG *et al.*, 1997; KRUGER and HEALY, 2006). The strength of the reflection or backscatter is also related to seabed morphology, where a higher backscatter reflects a roughened seabed which could be due to sand waves, dunes and ripples. A more consistent backscatter pattern reflects a uniform, flat seabed. Side-scan sonar surveys provide an oblique photograph-like image of the seafloor called a sonagraph, which can be used to discern the distribution of surface sediments and morphological features (MORANG *et al.*, 1997; BARNHARDT *et al.*, 1998; VAN LANCKER *et al.*, 2004). However, side-scan sonar technology is still mostly limited to qualitative studies and is highly subjective (KRUGER and HEALY, 2006). Therefore, the collection of sediment samples, video transects, photographs and/or observations is often required to provide ground truthing for the survey (MORANG *et al.*, 1997; BARNHARDT *et al.*, 1998; KRUGER and HEALY, 2006).

The transducers are mounted in the tow fish and deployed behind the vessel in order to eliminate the effects of surface/vessel noise on the sonar and to obtain



**Figure 3.7:** The side-scan sonar system. The operating range of the side-scan sonar is determined by the distance that sound can travel from the transducer and return to the tow fish in a given time, with an assumed sound velocity of 1.5 km/s (the average speed that sound travels in water). The swath width is twice the operating range since the tow fish has a transducer on opposite sides. Source: KLEIN ASSOCIATES INC (2008).

better imaging geometry (MILLER *et al.*, 1997). Other factors which may affect the resolution of the sonagraph record include the vessel's travelling speed and wave activity. A fast vessel speed reduces the number of acoustic pulses or 'pings' that can be transmitted over a given distance, in some cases not allowing full ensonification to be achieved. A slow speed enhances sonagraph resolution by allowing more signals to be transmitted over a given distance and hence increasing the obtainable coverage (MORANG *et al.*, 1997; KLEIN ASSOCIATES INC, 2008). Increased wave activity in rough seas may also degrade the quality of the sonagraph by causing the tow fish to twitch and jerk (MORANG *et al.*, 1997).

### *3.2.3 Survey Procedure*

A side-scan sonar survey of northern Waihi Beach between Rapatiotio Point and Island View was conducted using a dual frequency Klein 595 side-scan sonar system. Surveying was undertaken using the University of Waikato's smaller vessel *Taitimu*. Vessel position fixing was achieved using GPS, and the sonar fish was towed at a constant speed of 4 knots and at distances of 5 m and 20 m behind the vessel depending on water depth. Fixes were adjusted to account for these layback distances.

Side-scan sonar mapping consisting of 20 runlines was undertaken in a 4.7 by 5.5 km area between 10 and 30 m water depth. An additional 5 runlines were also carried out between 6-7 m water depth off Orokawa Bay and around Rapatiotio Point, specifically for the purpose of identifying any features which may provide an indication of sediment exchange between Waihi Beach and the small pocket beach to the north. In deep water (15-30 m), side-scan swath lines were taken at 100 Hz, which provided swath coverage of up to 150 m either side of the vessel. In shallower water (<15 m) the frequency was increased to 500 Hz, allowing better resolution of wave-generated bedforms than would be achieved with a wider swath. The swath widths were slightly overlapping to ensure full coverage of the entire field site area. Survey runlines were carried out parallel to the shoreline to permit accurate detection and measurement of bedforms on the seafloor (HEALY *et al.*, 1996; HUME *et al.*, 2000).

All raw side-scan data are stored on CDs held within selective thesis volumes.

### *3.2.4 Side-Scan Sonar Image Processing*

Initial processing of the raw side-scan sonar data took place on an onboard system running the Klein software ISIS<sup>1</sup>, which may be used to compile runlines into an integrated side-scan sonar map. The ISIS system simultaneously receives acoustic data and positional information during surveying, from the Klein system and a GPS respectively. This allows for real-time positioning of a pixel of imagery known as geo-coding. Survey data collected by ISIS is then corrected for tow fish slant, boat speed and possible navigation errors, providing smooth track lines. The processed output file was imported into Delphmap<sup>2</sup>, which merges and mosaics multiple tracks together complete with accurate geographic co-ordinates. Once compiled, the image was then saved in GeoTiff image format, which is a tagged image file with navigational information included.

The GeoTiff (geo-referenced) image output from Delphmap was imported into ArcGIS and overlaid onto a shoreline map of the survey area (created from RNZN hydrographic charts) for image processing and detection of seafloor reflection patterns and features. Analysis of bedforms and sediment morphology were then identified from the created sonar image. In addition to the digitally created sonar image, an analog hardcopy printout from the Klein unit was also often referred to when defining obscure textural patterns because it has a higher resolution than the digitally created sonar image. All the different types of return patterns were subsequently identified and “ground-truthed” by offshore sediment sampling, SCUBA observations and drop-cam video analysis.

### *3.2.5 Discussion and Interpretation of the Sonagraph*

Table 3.2 depicts the different sonagraph outputs obtained from the side-scan sonagraph offshore northern Waihi Beach (Figure 3.9). Four major patterns were classified:

---

<sup>1</sup> ISIS © Sonar Software, Triton Elics International, Inc. 1991 - 1998

<sup>2</sup> Delphmap © Version 2.10, Triton Elics International, Inc. 1998.

1. *Flat to Lightly Rippled Fine Sand*

This pattern is characterised by a very weak return signal associated with fine grained sediments. The weak backscatter signal was commonly observed, particularly closer to the shore, displayed as a light grey tone on the sonograph record with a generally featureless surface (Table 3.2). Although the sonograph record suggested there were no bedforms corresponding to this facies, SCUBA ground truthing showed that small wave generated ripples ( $\lambda=5-10$  cm,  $\eta= 1-4$  cm) often occur in these regions. Ripples of this size are indistinguishable from flat surfaces on the side-scan sonar record because of the weak return signal and low resolution. (BRADSHAW *et al.*, 1994; BEAMSLEY, 1996).


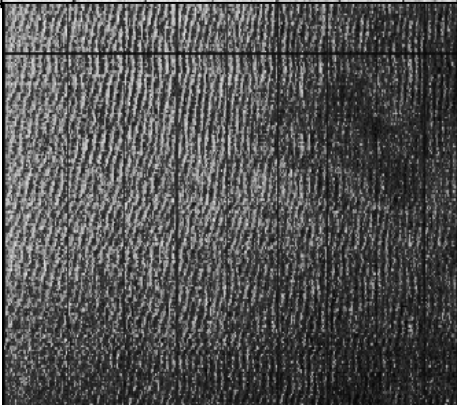

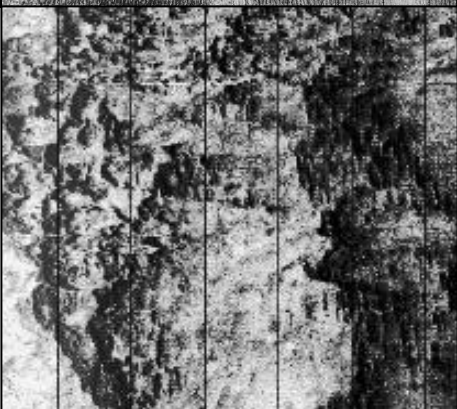
2. *Coarse Grained Megaripples*

This pattern is characterised by a strong black or dark grey coloured signal and rough textured sonograph facies (Table 3.2) generally associated with medium to coarse sediments, often with a high shell component. Megarippled facies run shore-parallel, and have heights ranging between 0.1-0.14 m and wavelengths of 0.5-1.5 m. It is understood that the orbital motions of large waves are responsible for the formation of these megarippled bedforms, and their existence is usually indicative of active sediment transport (BRADSHAW, 1991; HEALY *et al.*, 1996). They typically occur as elongated “fingers” oriented shore-normal (Figure 3.8). The boundary between fine featureless sand and megarippled coarse sands is characteristically very abrupt or sharp on one flank, with more diffuse contacts on the other.

3. *Combination of Coarse Grained Megaripples and Fine Featureless Sand*

Zones of coarse grained megaripples are also commonly observed combined with intervening fingers of fine featureless sand (Table 3.2). The fine sand typically appears to be transgressing over the coarse grain ripple bands, which seem to be topographically lower on the seabed than the fine sand. Similar features have been described in the Bay of Plenty inner shelf by HARMS (1989), BRADSHAW (1991), HUME and HICKS (1993), BRADSHAW *et al.* (1994), and HUME *et al.* (1995). HEALY *et al.* (1996), BARNHARDT *et al.*

**Table 3.2:** Summary of the sonar reflection types identified from the side-scan sonagraph.

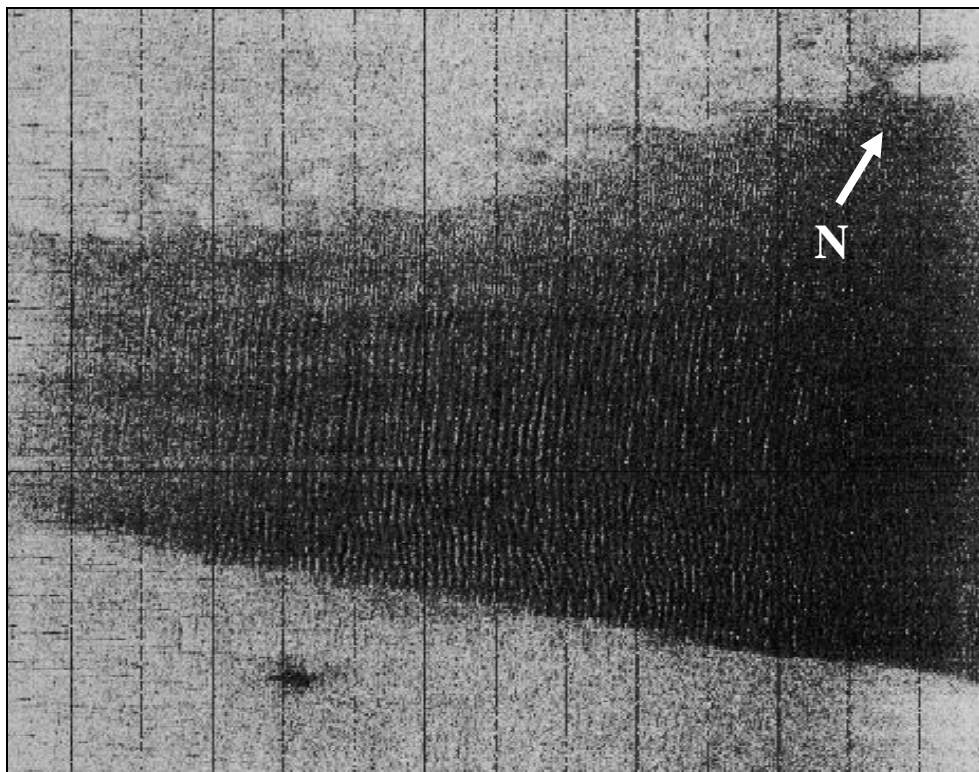
Sonar Reflection Type	Signal Description	Example Sonagraph Output
Flat to Lightly Rippled Fine Sand	Very light acoustic return tone. Associated with fine sand deposits and a general absence of seabed features. Small wave generated ripples ( $\lambda \approx 5-10$ cm; $\eta \approx 1-4$ cm) often exist that cannot be resolved by side-scan sonar	
Megaripples	Shore-parallel bedforms ( $\lambda \approx 0.5-1.5$ m; $\eta \approx 10-14$ cm). Reflected signal is strong (dark grey or black) corresponding to medium to coarse sediments, often with a large quantity of shell hash	
Coarse Megaripples and Fine Featureless Sand Combination (MR/FFS)	A combination of the two major feature patterns: extensive zones of dark coarse grain megaripples (often in topographic lows) overlain by fine featureless sand	
Bedrock	Strong reflection, displayed as a dark grey or black tone in the sonagraph. Has the appearance of a rough texture	

(1998) and SPIERS (2004) also describe this sonograph pattern of coarse grained ripples transgressed by fine featureless facies, and subsequently devised a combined facies pattern to describe it. Following their approach, a combined facies (MR/FFS) has been adopted in the present study to define these features which are typically too small to be detailed individually.

#### 4. *Bedrock*

Rocks are characterised by a strong reflectivity (dark grey to black tone) and a rough texture (Table 3.2). Strong, dark reflections define Steel's Reef in the sonograph record. Scattered bedrock was also observed directly offshore from Rapatiotio Point.

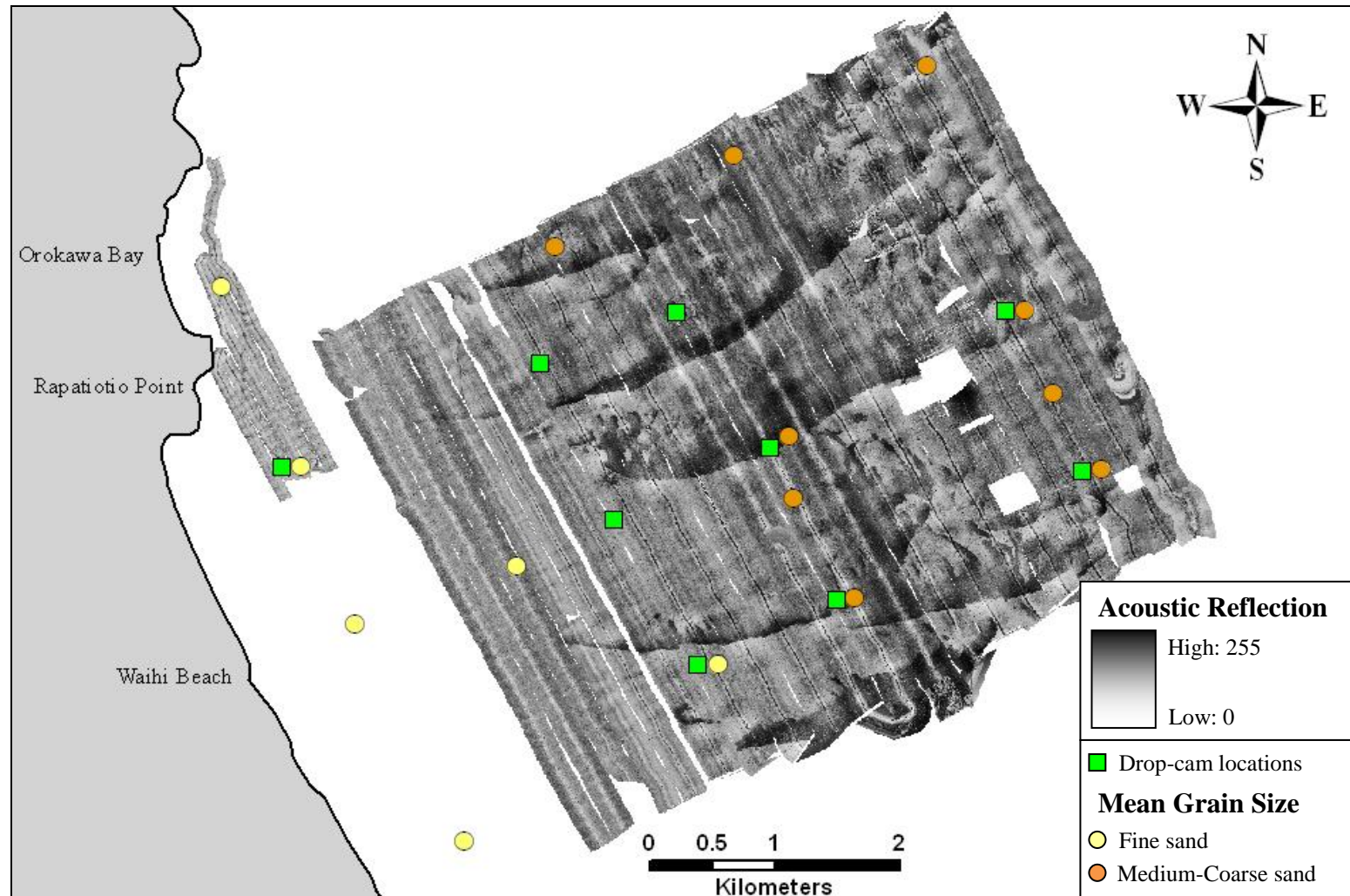
Following identification of the major sonograph facies patterns, a detailed sediment facies map of the surveyed area was created in ArcGIS (Figure 3.10), which clearly depicts the complex distribution of the different reflection types. Both the side-scan mosaic and facies map illustrate that the shallow inshore zone



**Figure 3.8:** Sonograph output illustrating the end of an elongated finger of megaripples in about 20 m water depth.

off northern Waihi Beach is dominated by fine featureless sands, with no identifiable bedforms out to depths of 10-15 m. The nearshore region off Orokawa Bay is also characterised by fine featureless sands, with some areas of bedrock confined to the base of Rapatiotio Point. Rocky reef was also detected on the southeastern boundary of the surveyed area indicating the presence of Steel's Reef. Unfortunately the reef is not well imaged on the side-scan sonograph (Figure 3.9) as this area corresponds to the start or end of the survey runlines, and the boats turning circle tends to degrade the quality of the returned image. Seaward of about 20 m depth the distribution of fine sands becomes patchy, with medium to coarse grained sands dominating out to the 30 m isobath (Figure 3.10).

Seaward of about 15 m depth the featureless topography is interrupted by large shore-normal shoreface-attached sand ridges. These very pronounced sand ridges are dominated by shore parallel megaripples of  $\lambda \approx 0.5-1.5$  m and are elongated in a shoreward direction, with increasing amplitude offshore (HUME *et al.*, 1995). They consist of coarse sediments and are often surrounded by the coarse megaripples and fine featureless sand (MR/FFS) combination facies, which are typically most dense on the northwestern side of each feature. Previous side-scan sonar surveys by BRADSHAW *et al.* (1994), HUME *et al.* (1995) and BEAMSLEY (1996) off Waihi Beach also indicates the presence of megaripples in similar localities, recording wavelengths as large as 2 m. BRADSHAW *et al.* (1994) suggests that the distribution of the megaripples in the shore-normal direction is controlled by the extent of the large sand ridges. HUME *et al.* (1995) compared side-scan sonar records and soundings from 1991 and 1995 and found that although the fine-sand distribution appeared to have changed markedly, the distribution of the megaripples and the aspects of the shore-normal sand ridges appeared to alter minimally. The minor changes identified between the two surveys could be explained by the redistribution of the finer sediments (HUME *et al.*, 1995).



**Figure 3.9:** Side-scan sonograph for offshore northern Waihi Beach, clearly showing the large shore-normal sand ridge features which characterise the inner shelf.



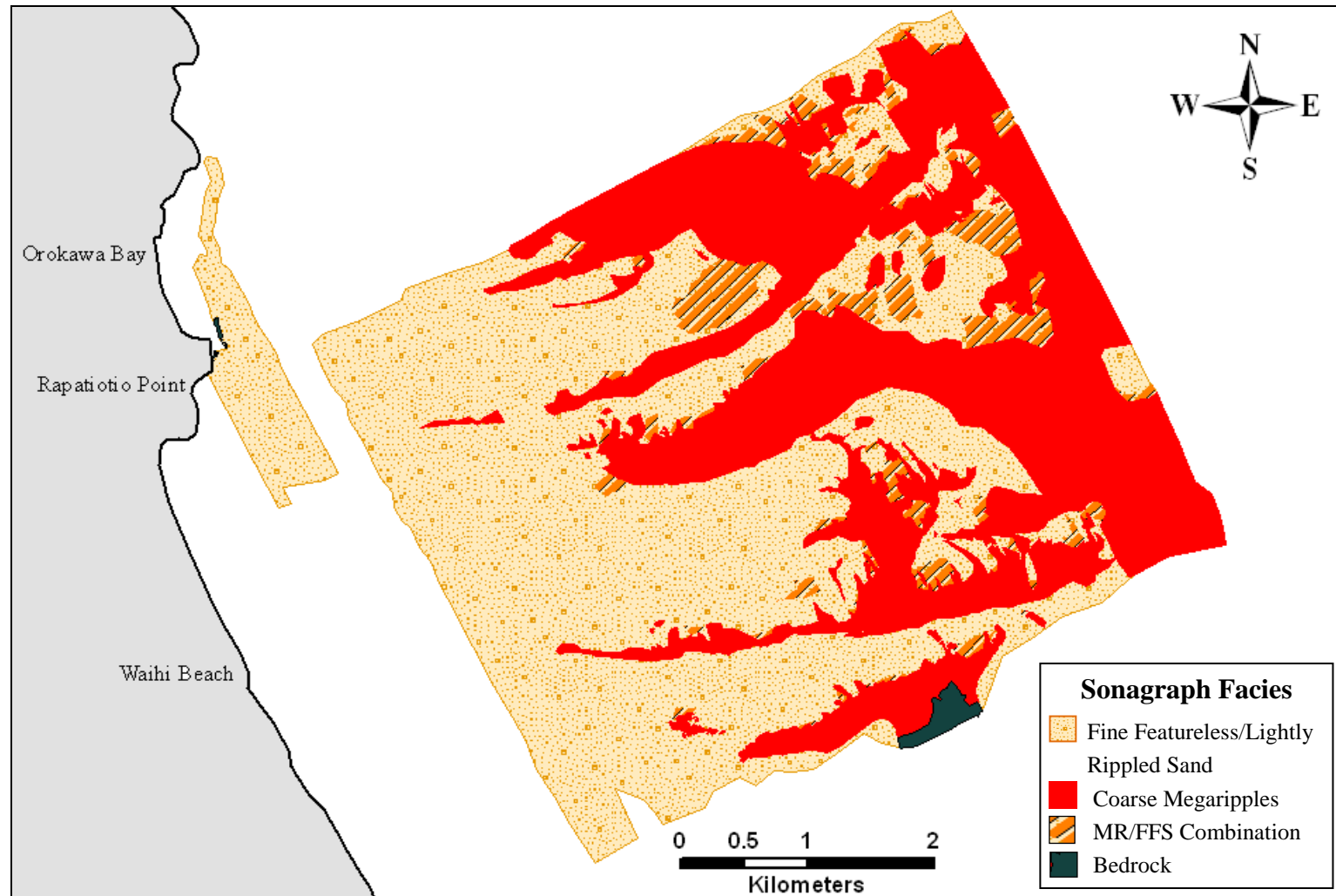


Figure 3.10: Sediment facies map for offshore northern Waihi Beach.

The elongated megarippled ‘fingers’ appear to have very sharply defined boundaries on the southeastern side, particularly at the shoreward extent of the finger. Along the northwestern edges a much more diffusive boundary typically exists, showing a gradual transition from coarser megaripples to lightly rippled and featureless sediment facies. The more diffusive contacts on the northwestern side may form as a result of the northwestward movement of the megarippled facies from the southeast, encroaching and gradually covering the finer flat to lightly rippled sediment facies. Coring by HUME and HICKS (1993) found that fine sand overlies the coarser megarippled sands. They note that wave shoaling could be responsible for the movement of the fine sands, and hence the covering or uncovering of the underlying megarippled facies.

Typically the coarse megaripple bands seem to occur in, or near, the trough axis of the shore-normal sand ridges (BEAMSLEY, 1996). Towards the southeast, there is a very abrupt transition in bottom topography to fine featureless or lightly rippled facies, thus creating the sharp boundary apparent in Figure 3.9. To the northwest, the megaripple facies progressively changes into flat to lightly rippled facies moving up the southeastern flank towards the crest of the shore-normal sand ridge. The decrease in sediment grain size and bedform magnitude associated with this transition from megaripple to lightly rippled facies also implies a decrease in energy; either less winnowing of fine material from the megarippled facies due to weak bottom currents acting on the sediments, or sediments reaching their limit of transportation and being deposited here (BEAMSLEY, 1996).

Elongated bands of coarse megaripples with well defined southeastern boundaries have been similarly observed at Waihi Beach by HUME and HICKS (1993), HUME *et al.* (1995) and BEAMSLEY (1996), and were also evident in several studies on the inner shelf off Tauranga Harbour and Mount Maunganui (HEALY, 1985; HARMS, 1989; FOSTER, 1991; SPIERS, 2004). FOSTER (1991) suggests that the sharpness of the boundary may be indicative of the age of the feature, with older features being degraded by the infiltration of finer sediments.

Confined areas of coarse grained megaripples and dense aggregations of MR/FFS combination facies are also randomly scattered amongst the dominant elongated

megaripple bands. It has been suggested by HARMS (1989), who also observed this feature, that the MR/FFS facies represent two separate and distinct layers in which the fine sediment transgresses over the surface of the coarse grained rippled features. The irregular patches of megarippled coarse sediments distributed on the fine sand cover suggest that winnowing processes could be operating to expose the underlying coarser bedforms. Previous wave refraction analyses in the Bay of Plenty have identified zones of wave focusing associated with bands of coarse megaripples, implying that high energy waves will winnow out finer material, producing depressed areas of coarser rippled sand (e.g. BRADSHAW, 1991; PHIZACKLEA, 1993; SPIERS, 2004).

### 3.3 OFFSHORE BEDFORMS

#### 3.3.1 *Introduction*

When sediment is moved by near bed currents, primarily induced by waves, the individual grains typically become organised into morphological elements called bedforms. Current-produced bedforms are diverse, occurring in a variety of shapes and scales depending on the characteristics of the material and its substrate. Although these small scale features typically have no immediate impact on the main flow patterns, they strongly influence the boundary layer structure and the turbulence intensity near the bed (NIELSON, 1992). Hence, they have a great influence on the sediment transport and bed morphology. Bedform orientations are useful indicators of flow pathways within the nearshore and inner shelf zones. Consequently, identification of bedform characteristics contributes to the understanding of sediment movement and delineation of sediment transport pathways (TRENHAILE, 1997).

Previous studies of inner shelf bed morphology in the western Bay of Plenty noted the presence of a range of bedforms including ripples, megaripples, sand waves and sand ridges (e.g. HARMS, 1989; BRADSHAW, 1991; FOSTER, 1991; HUME and HICKS, 1993; HUME *et al.*, 1995; BEAMSLEY, 1996; SPIERS, 2004). To observe

offshore bedforms at northern Waihi Beach, a video camera enclosed in a waterproof casing and attached to a steel frame and cable known as the drop-camera or the 'splash cam' (Figure 3.11) was used. A diving weight belt was attached to the frame so it would sit firmly upon the seafloor and not be moved about so much by the bottom currents. The dynamics and geometry of the bedforms at northern Waihi Beach will be discussed in detail together with their influence on sediment transport behaviours.

### 3.3.2 Characteristics of Bedforms

Bedforms were classified according to the system proposed by LARSEN *et al.* (1997). This system groups bedforms into four categories: ripples, dunes, planar beds and antidunes (Table 3.3):

- *Ripples* are small bedforms with a crest-to-crest spacing of 0.6 m or less, and heights typically around 0.03 m. Ripples may be further classified into five subgroups, which are illustrated in Figure 3.12.
- *Dunes* are bedforms with a crest-to-crest spacing of between 0.6 m and 1000 m. The term 'dune' replaces previously used terms in the literature such as 'megaripple' and 'sand wave'. Two types of dunes can be distinguished: two-dimensional and three-dimensional. A two-dimensional bedform is created due to the flow pattern of water being relatively unchanged and perpendicular to its overall direction, whereas a three-dimensional bedform is developed from near-bed eddies or variable vortices (LARSEN *et al.*, 1997).
- *Planar beds* are horizontal beds which do not have elevations or depressions larger than the maximum size of the exposed sediment (LARSEN *et al.*, 1997). Planar beds occur under two hydraulic conditions:
  1. The transition zone between the region of no movement and the initiation of dunes.
  2. The transition zone between ripples and antidunes, at mean flow velocities between 1-2 m.s<sup>-1</sup> (LARSEN *et al.*, 1997).

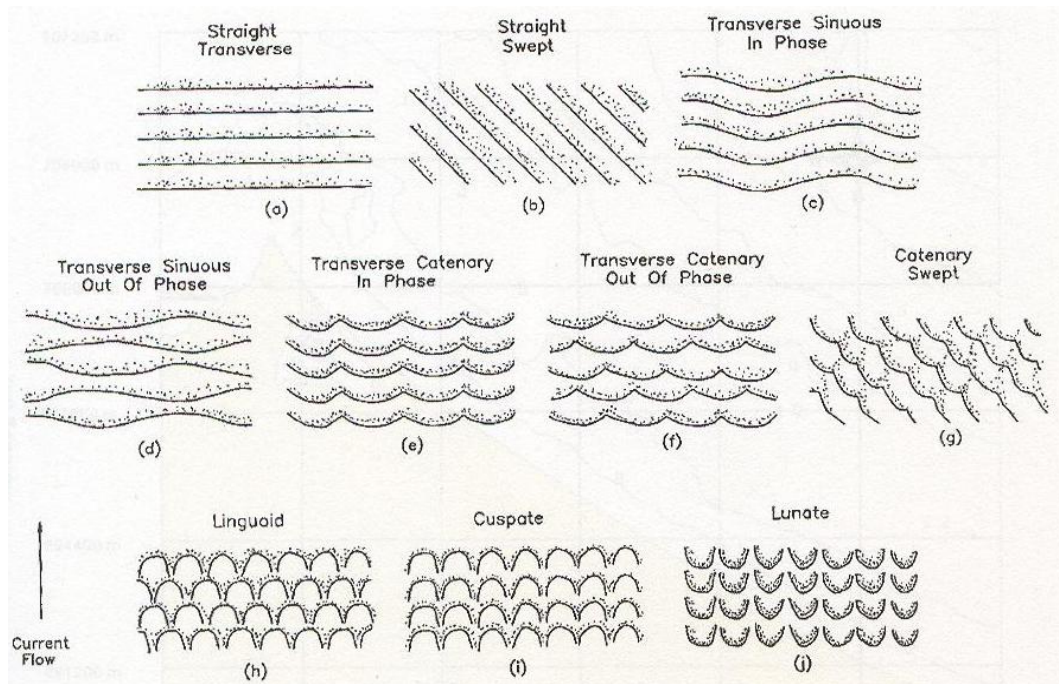


**Figure 3.11:** The drop-camera attached to a cable and enclosed within a steel frame, with a diving weight belt attached.

- *Antidunes* are morphological features (bedforms) that are in phase with water surface gravity waves. The height and wavelength of an antidune is dependent on the fluid and the characteristic of the bed material (LARSON *et al.*, 1997). These features are typically found in rivers where velocities may be greater than 2 m/s.

**Table 3.3:** Morphological classification of various bedforms adopted for this study. Source: LARSON *et al.* (1997).

	<b>Ripples</b>	<b>Dunes</b>	<b>Plane Bed</b>	<b>Antidunes</b>
<b>Crest-to-crest distance</b>	$\lambda < 0.6$ m	$0.6 \text{ m} \leq \lambda < 1000$ m	n/a	n/a
<b>Geometry</b>	1. Straight 2. Sinuous 3. Catenary 4. Linguoid 5. Lunate	1. Small ( $0.6 < \lambda < 5$ m) 2. Medium ( $5 < \lambda < 10$ m) 3. Large ( $10 < \lambda < 100$ m) 4. Very Large ( $\lambda > 100$ m)	n/a	n/a
<b>Typical flow velocity (m/s)</b>	0.1-0.97	0.32-2	>0.97	>1.7
<b>Detection</b>	Divers	Divers/sonographs/ echo-sounder	Divers/ sonographs	Divers/ sonographs



**Figure 3.12:** Ripple classification based on ripple crest morphology. Five types of ripple can be identified: straight (a-b); sinuous (c-d); catenary (e-g); linguoid (h) and lunate (j). Source: LARSON *et al.* (1997).

### 3.3.3 Interpretation of Offshore Bedforms

Video imaging was undertaken at nine locations offshore northern Waihi Beach to assess sediment characteristics, and the presence of bedforms and their associated size and orientation. The GPS co-ordinates where video imaging using the drop-camera was undertaken are presented in Table 3.4. The drop-cam sites are also noted on the side-scan sonograph in Figure 3.9

**Table 3.4:** Water depths and GPS co-ordinates of the nine locations where video imaging with the drop-camera was carried out. Northings and eastings are relative to the Bay of Plenty meridional circuit.

Video Location	Depth (m)	Northing (m)	Easting (m)
1	6	740257	254247
2	20	738578	257332
3	25	739285	258454
4	30	740135	259730
5	20	739915	256714
6	25	739803	257262
7	30	741087	259285
8	20	739915	256719
9	25	739945	257555

Figure 3.13 illustrates an example of megaripled bedforms recorded by the drop-cam offshore northern Waihi Beach.



**Figure 3.13:** Megaripples ( $\lambda=0.5$  m,  $\eta=12$  cm) with shell lag deposits at site 8 in 30 m water depth. This bedform type is commonly observed offshore northern Waihi Beach. Photograph taken by the author 28/05/08.

### 3.3.3.1 Bedform Generation and Distribution

Ripples and megaripples tend to form under oscillatory flow conditions (TRENHAILE, 1997). BRADSHAW (1991) suggests that the presence of ripples and megaripple bedforms on the east Coromandel coast shows that flows associated with wave orbital currents are important in reworking nearshore and inner shelf sediments in that region. A strong correlation between the wave orthogonal orientation and bedform alignment indicates the ripples observed at northern Waihi Beach are wave-generated features, with their formation a result of large wave-induced orbital motions associated with long period waves. BEAMSLEY (1996) provides further evidence to suggest wave orbital motions are responsible for the formation of the lightly rippled features, stating that these features tend to be confined to ~22 m depth, which corresponds to the outer limit of significant

wave shoaling processes as calculated by HUME and HICKS (1993). From the sediment facies map in Figure 3.10 it appears also that the lightly rippled features observed in the present study are similarly typically confined to depths shallower than approximately 22-24 m.

BRADSHAW (1991) identified extensive sand ridges on the east Coromandel shelf from sonagraph and echosounding traces, with ridge heights ranging between 1.5-7.5 m at depths of 20-30 m. Surveys along the coast revealed that ridges only formed where there was an abundance of fine sand. Although BRADSHAW (1991) was unsure whether the ridges were migratory or stationary, the formation of the ridges was thought to be due to coastally-trapped topographic waves, generated during cyclonic storm events. Hence, the occurrence of similar large scale bedform features in the nearshore zone at northern Waihi Beach indicates a complex environment formation.

Following a technique described by BLACK and HEALY (1983), the large shore-normal sand ridge heights were estimated from sonagraphs:

$$H = z \cdot \frac{s}{l} \quad 3.1$$

where  $H$  is the height of the object,  $z$  is the height of side scan tow fish above the seabed,  $s$  is the acoustic shadow length of the object(s) and  $l$  is horizontal distance of the object from the fish (BLACK and HEALY, 1983).

The sand ridges at northern Waihi Beach have heights between 0.4-2.5 m, and wavelengths of 300-1400 m. Crest lengths of the large shore-normal sand ridges ranged from 0.5-4 km, with crests oriented northeast to southwest between 15-30 m off northern Waihi Beach (Figure 3.9). Wave orbital velocity was identified as being the process responsible for the formation of the lightly rippled facies. However at greater depths, where the prominent sand ridges lie, unidirectional currents are more likely responsible for bedform formation. The orientation of the ridges thus indicates a net flow perpendicular to the crests towards the northwest, thereby suggesting a northwesterly directed alongshore sediment transport direction. BEAMSLEY (1996) similarly concluded that the asymmetrical nature of



the shore-normal sand ridges implies a northerly propagation of either the entire sand wave or the covering sediments.

A northwesterly directed current would preferentially carry finer sediment up the southeasterly facing side of the shore-normal sand ridges, depositing some sediment along the way. The strongest currents are likely to be experienced within the troughs of the sand ridges, where the megaripple facies dominate, with progressively decreasing current velocities heading up the southeastern flank of the sandwaves to where flat to lightly rippled facies are found (BEAMSLEY, 1996). BEAMSLEY (1996) proposes that the weakest currents are likely to be experienced on the northwestern flank of the sand ridges due to modification of the northerly directed current by topographic shadowing. He predicts an increase in sedimentation on the northwestern flank of the sand waves as a result of the topographical current shadowing.

The implication of the bedforms observed and discussed in this chapter for diabathic sediment transfer will be investigated in Chapter 5 (section 5.4.4 *Calculation of Diabathic Sediment Transport Rates*).

### 3.4 SUMMARY

Beach profile and nearshore hydrographic surveys were undertaken to examine the characteristics and behaviour of the beach and nearshore at northern Waihi Beach.

- Each of the sub-aerial beach profiles indicate a low angle beach with typically no berm feature present. The beach becomes increasingly narrower and steeper towards the southeast, with wide gently sloping gradients characteristic of profiles in the north.
- Measured summer profile elevations were typically higher than the subsequent winter profiles, with beach levels fluctuating up to 1-1.5 m between seasons. The observed lowering in profile elevation during winter

is indicative of cross-shore sediment transport and exchange with offshore bars, which were shown to be present at the time of winter profiling from hydrographic surveying undertaken in June 2008.

To examine nearshore morphology, an intensive side-scan sonar survey was undertaken in a 5.5 by 4.7 km area off northern Waihi Beach, as well as offshore sediment grab sampling, SCUBA diver and video observations. A detailed sediment facies map was produced and illustrates a complex distribution of sediment textures and bedforms on the inner shelf:

- The shallow inshore zone is dominated by fine featureless sands. Seaward of about 15 m depth, the featureless topography is interrupted by large sand ridges ( $\eta=0.4\text{--}2.5$  m,  $\lambda=300\text{--}1400$  m) which are elongated in a shore-normal direction. These very pronounced features are dominated by shore parallel coarse megaripples ( $\eta\approx 0.1\text{--}0.14$  m,  $\lambda\approx 0.5\text{--}1.5$  m), and are often surrounded by the coarse megaripples and fine featureless sand (MR/FFS) combination facies, which are typically concentrated on the northwestern side of each feature.
- A net current flow towards the northwest, and likewise a net northwesterly directed alongshore sediment transport, is implied by the asymmetry (oriented northeast to southwest) of the large sand ridges. Sharp well-defined southeastern boundaries and diffuse northwestern boundaries are noted for the majority of these features. The gradual transition from coarser megaripples to lightly rippled and featureless sediment facies typically observed along the northwestern edges is thought to form as a result of the northwesterly directed sediment transport.

# CHAPTER FOUR: SEDIMENT CHARACTERISTICS

---

## 4.0 INTRODUCTION

A beach is characterised by a particular sediment texture and composition, although a large amount of variability may exist across the beach and also alongshore. The distribution of sediments reflects the nature of the source material, and provides information about the energy of the environment and possible sediment transport pathways (LARSEN *et al.*, 1997; MORANG *et al.*, 1997; KOMAR, 1998). Transport of the beach sediment is likewise influenced by the sediment properties. Therefore, investigation of spatial changes in grain size parameters (mean grain size, sorting and skewness) may allow for the identification of net sediment transport pathways at northern Waihi Beach.

This chapter investigates the nature and distribution of beach and offshore sediments at northern Waihi Beach through examination of local sediment textural characteristics. The Rapid Sediment Analyser (RSA) was used to determine textural properties, from which sediment transport directions may be interpreted from various models. Three were examined here: the SUNAMURA and HORIKAWA (1972) model, the MCLAREN (1981) model, and the “Waihi” model.

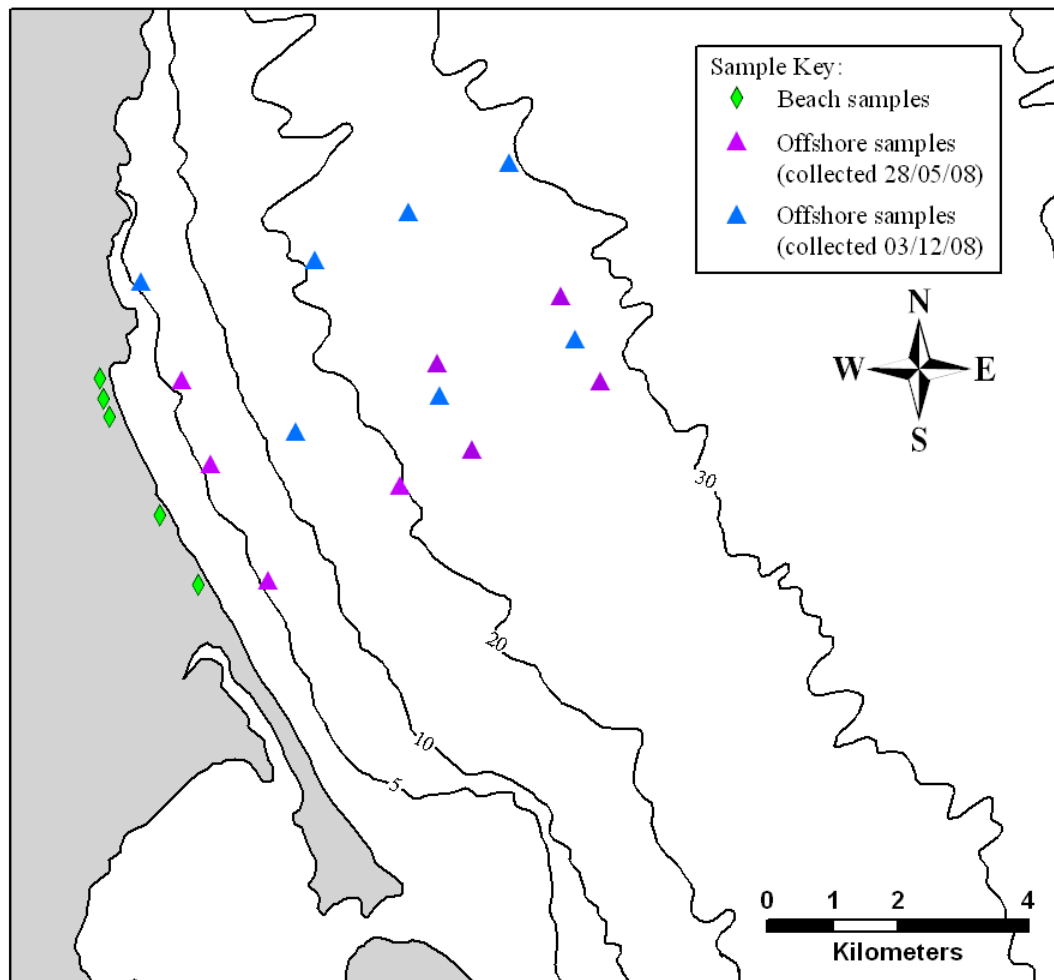
## 4.1 METHODS

### 4.1.1 *Sediment Sample Collection*

Surficial sediment samples were collected along 5 shore-normal transects previously marked by EBOP on the 24<sup>th</sup> January 2008 and the 3<sup>rd</sup> January 2009. Using a small shovel, samples were collected from the toe of the frontal dune, berm (or the upper beach when no prominent berm was present), mid-beach face, and lower swash zone on each of the 5 profiles. Initial offshore sampling took place on the 28<sup>th</sup> of May 2008, with additional samples collected on the 3<sup>rd</sup> of December 2008 following the side-scan sonar survey. The University of

Waikato's grab sampler was used to collect bottom sediments between 6 and 30 m water depth. Each sample consisted of approximately 500 g of surficial sediment.

Beach profiles and nearshore hydrographic surveying were undertaken in conjunction with January 2008 sample collection, so that during sediment textural analysis the samples can be spatially located and related to morphology and hydrodynamic zones (LARSEN *et al.*, 1997). A total of 40 onshore samples and 15 offshore samples were collected and analysed during the study period (Figure 4.1).



**Figure 4.1:** Location map of beach and offshore sediment samples. Green diamonds indicate beach samples collected by hand on 24/01/08 and 03/01/09. Purple triangles represent offshore samples collected prior to the side-scan sonar survey (28/05/08), and blue triangles represent the locations where offshore sediment samples were collected post-surveying (03/12/08). Offshore samples were obtained using the University of Waikato's grab sampler.

## 4.1.2 Sediment Textural Analysis

Sediment grain size analysis was carried out using the University of Waikato's Rapid Sediment Analyser (RSA). The RSA is a settling tube system with a fall distance of 1.612 m. It measures particle settling velocity, which is a function of the particle size, shape and density (KOMAR, 1998). The samples are released into the settling tube, where the rate of grain mass accumulation on a pan suspended at the bottom of the fall tube, and connected to an electronic balance, is measured by computer. The RSA operates semi-automatically, using Stoke's Law (Equation 4.1) to determine grain size and settling velocity by calculating the time it takes for a particular sediment particle to fall through a water column a known distance:

$$\omega = \frac{1}{18} \frac{(\rho_s - \rho_f)gD^2}{\mu} \quad 4.1$$

where  $\omega$  is settling velocity ( $\text{m}\cdot\text{s}^{-1}$ ),  $\rho_s$  is the density of the sediment ( $\text{kg}\cdot\text{m}^{-3}$ ),  $\rho_f$  is the density of fluid inside the RSA ( $\text{kg}\cdot\text{m}^{-3}$ ),  $g$  is gravitational acceleration ( $9.81 \text{ m}^{-1}\text{s}^{-2}$ ),  $D$  is the mean sediment diameter (m) and  $\mu$  is the viscosity of fluid ( $\text{m}^2\text{s}^{-1}$ ).

All sediment samples were initially prepared by washing through -1Ø and 4Ø sieves in order to remove any large shells and mud size particles, respectively. Sub-samples of approximately 20-30g were extracted from the initial samples and oven dried for 48 hours at 50° C. Each sub-sample was then passed through the RSA, with data collection occurring for 300 seconds after sample release. The RSA undertakes a size class distribution analysis using both the FOLK and WARD (1957) graphical method and the method of moments (DE LANGE *et al.*, 1997). The generally applied density of  $2,650 \text{ kg}\cdot\text{m}^{-3}$  for quartz was used as this is considered to be generally representative of Bay of Plenty beach sediments (PHIZACKLEA, 1993). However, the presence of shell fragments and/or titanomagnetite in large quantities for some samples may be a potential source of experimental error.

The RSA method was favoured over standard mechanical sieves because it permits faster processing of sand-sized sediment samples, and provides a more realistic measure of the hydraulic behaviour of the grains while being transported

by waves and currents compared to sieving (USACE, 2002). Sub-samples of 20-30g were selected to be analysed as it has been shown by DE LANGE *et al.* (1997) that the variability of settling tube results is least for samples of this size range. Results from the RSA are output as normal frequency and cumulative frequency curves, from which the mean grain size, sorting, skewness and kurtosis can be extracted. Mean grain size is based on the Wentworth Scale, shown in Figure 4.2 and the classes of sorting, skewness, and kurtosis are described in Tables 4.1–4.3.

Millimeters	$\mu\text{m}$	Phi ( $\phi$ )	Wentworth size class	
		-20		
4096		-12	Boulder (-8 to -12 $\phi$ )	
1024		-10		
256		-8	Pebble (-6 to -8 $\phi$ )	
64		-6		
16		-4	Pebble (-2 to -6 $\phi$ )	Gravel
4		-2		
3.36		-1.75		
2.83		-1.50	Gravel	
2.38		-1.25		
2.00		-1.00		
1.68		-0.75		
1.41		-0.50	Very coarse sand	
1.19		-0.25		
1.00		-0.00		
0.84		0.25		
0.71		0.50	Coarse sand	Sand
0.59		0.75		
1/2	500	1.00		
0.42	420	1.25		
0.35	350	1.50	Medium sand	
0.30	300	1.75		
1/4	250	2.00		
0.210	210	2.25		
0.177	177	2.50	Fine sand	
0.149	149	2.75		
1/8	125	3.00		
0.105	105	3.25		
0.088	88	3.50	Very fine sand	
0.074	74	3.75		
1/16	63	4.00		
0.0530	53	4.25		
0.0440	44	4.50	Coarse silt	
0.0370	37	4.75		
1/32	31	5	Medium silt	Mud
1/64	15.6	6	Fine silt	
1/128	7.8	7	Very fine silt	
1/256	3.9	8		
0.0020	2.0	9		
0.00098	0.98	10		
0.00049	0.49	11		
0.00024	0.24	12	Clay	
0.00012	0.12	13		
0.00006	0.06	14		

Figure 4.2: Wentworth grain size scale classification table. After FOLK (1968).

**Table 4.1:** Sorting Classification. Source: LARSEN *et al.* (1997).

Sorting Range ( $\phi$ )	Description of Sorting
< 0.35	Very well sorted
0.35 – 0.50	Well sorted
0.50 – 0.71	Moderately well sorted
0.71 – 1.00	Moderately sorted
1.00 – 2.00	Poorly sorted
2.00 – 4.00	Very poorly sorted
> 4.00	Extremely poorly sorted

**Table 4.2:** Skewness Classification. Source: LARSEN *et al.* (1997).

Skewness Range	Description of Skewness
< + 0.3	Very fine-skewed
+ 0.3 to + 0.1	Fine-skewed
+ 0.1 to - 0.1	Near symmetrical
- 0.1 to - 0.3	Coarse-skewed
> - 0.3	Very coarse-skewed

**Table 4.3:** Kurtosis Classification. Source: LARSEN *et al.* (1997).

Kurtosis Range	Description of Kurtosis
< 0.67	Very platykurtic
0.67 – 0.90	Platykurtic
0.90 – 1.11	Mesokurtic
1.11 – 1.50	Leptokurtic
1.5 – 3.00	Very leptokurtic
> 3.00	Extremely leptokurtic

Mean grain size gives an indication of the magnitude of the applied force required to move the grain. Sorting is the variation in grain sizes for a particular sample, whereas skewness and kurtosis indicate how closely the sample distribution approximates the normal Gaussian probability curve. A negative or coarse skewness indicates a dominance of larger grain sizes, whereas sediments that have excess fine material are said to be positively or finely skewed. Kurtosis is the degree of peakedness of the size distribution, with platykurtic distributions being flatter than normal distributions indicating deficits in the extremes, whilst

leptokurtic distributions are more peaked than the normal distribution curve, indicating an excess in the extremes (DYER, 1986; LARSEN *et al.*, 1997; KOMAR, 1998).

## 4.2 SEDIMENT ANALYSIS RESULTS

All the sediment textural statistics from RSA analyses are included in Appendix I. Tables 4.4 and 4.5 present a summary of the range of moment sediment characteristic parameters obtained from onshore and offshore samples from northern Waihi Beach during this study, respectively. The trends across the beach and along the coast for mean grain size, sorting and skewness are portrayed in Figure 4.3. Although kurtosis values were provided for each sample, these were not analysed as they appear to have been of limited use in most sedimentological studies.

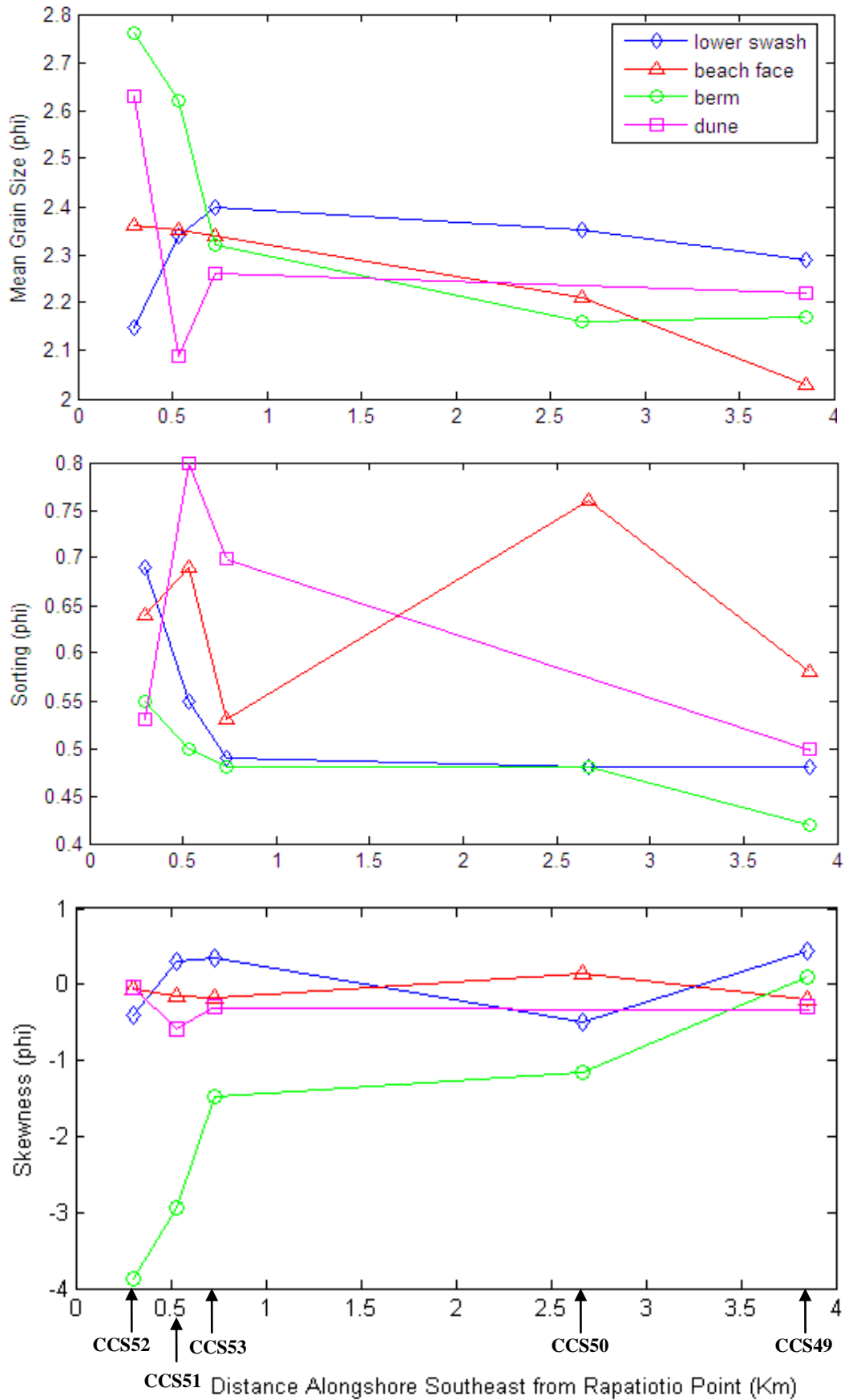
**Table 4.4:** Summary of the range of moment textural characteristics for onshore sediments (dune, berm, beach face and swash) at northern Waihi Beach. All units are in phi ( $\emptyset$ ). *fs* = fine sand.

Sample Location	Mean Grain Size ( $\emptyset$ )	Size Class	Sorting	Skewness	Kurtosis
CCS52	2.15 – 2.76	<i>fs</i>	0.53 – 0.69	-3.87 – -0.04	2.35 – 28.0
CCS51	2.34 – 2.79	<i>fs</i>	0.50 – 0.80	-2.94 – 0.31	2.31 – 23.0
CCS53	2.26 – 2.34	<i>fs</i>	0.48 – 0.70	-1.48 – 0.43	2.53 – 12.7
CCS50	2.16 – 2.35	<i>fs</i>	0.47 – 0.48	-1.15 – 0.14	2.29 – 12.7
CCS49	2.03 – 2.29	<i>fs</i>	0.42 – 0.58	-0.30 – 0.43	2.71 – 7.83

**Table 4.5:** Summary of the range of moment textural characteristics for offshore sediments (6, 15, 20, 25 and 30 m water depths) at northern Waihi Beach. All units are in phi ( $\emptyset$ ). *fs* = fine sand, *ms* = medium sand, *cs* = coarse sand.

Water Depth	Mean Grain Size ( $\emptyset$ )	Size Class	Sorting	Skewness	Kurtosis
6 m	2.32 – 2.74	<i>fs</i>	0.61 – 0.84	-1.07 – -0.41	1.02 – 4.32
15 m	2.57	<i>fs</i>	0.87	-0.76	4.84
20 m	1.49 – 2.32	<i>ms-fs</i>	0.58 – 1.31	-0.86 – 0.05	2.44 – 5.75
25 m	0.91 – 1.7	<i>cs-ms</i>	0.48 – 1.33	-0.18 – 1.96	1.89 – 8.09
30 m	0.71 – 1.45	<i>cs-ms</i>	0.55 – 0.72	0.75 – 1.66	4.18 – 7.76





**Figure 4.3:** Longshore and cross-shore variation in mean grain size, sorting and skewness of swash (blue), beach face (red), berm (purple) and dune (green) samples at northern Waihi Beach. Note that dune data is missing at CCS50 because of the seawall there is no dune present.

#### 4.2.1 Mean Grain Size

The mean is the most important and commonly used statistic to characterise the average grain size of a distribution (LARSEN *et al.*, 1997) because it is a simple comparative indicator of the weight force that must be balanced by an applied stress before transport by water or wind is possible (LEEDER, 1982). From the textural analysis it can be observed that all of the collected onshore samples consist of fine sands (2.03 – 2.79  $\phi$ ) (Table 4.4). These findings are similar to those noted by HEALY *et al.* (1977), HARRAY and HEALY (1978), BRADSHAW (1991) and FULTON (1991) who also observed that the sub-aerial beach in the northern sector of Waihi Beach consisted of fine sands, resulting in the formation of a relatively flat beach profile which typically lacks a well formed berm (Figure 4.4). Measured grain sizes offshore from Waihi Beach range from fine (2.74  $\phi$ ) to coarse sands (0.71  $\phi$ ) (Table 4.5). These results are in good agreement with mean grain sizes measured by BEAMSLEY (1996) off Waihi Beach, who found nearshore sands varied from fine (>2.95  $\phi$ ) to very coarse (-0.26  $\phi$ ).



**Figure 4.4:** Photograph of the sub-aerial beach at the northern end of Waihi Beach (facing north). Photograph taken by T.R. HEALY 25/04/05.

#### 4.2.1.1 Alongshore Variations

The mean grain sizes for the four morphological units sampled along northern Waihi Beach all tend to become marginally coarser towards the southern end of the study area (Figure 4.3). This alongshore pattern is in good agreement with HARRAY and HEALY (1978) who also observed a general trend of increase in grain size towards the southern (Bowentown) end of the beach, where higher energy conditions and a steeper beach slope prevail. Regions of coarser sands towards the south may also perhaps be associated with a zone of wave energy focusing, as finer grains tend to winnow out and move away from the high energy zones. Examination of wave focusing and the distribution of wave energy along the shoreline as a result of wave refraction will be explored using numerical simulation modelling in Chapter 6.

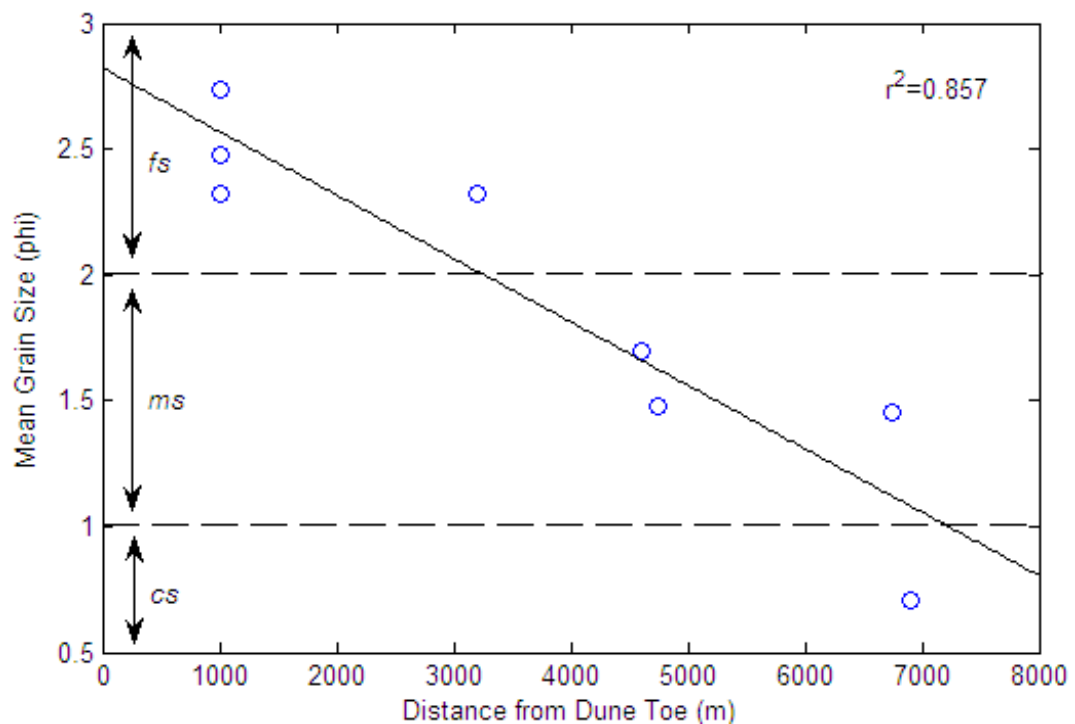
An alternative explanation may be that beach sands in the central and southern sectors of Waihi Beach are nourished from coarser offshore sediments by diabathic exchange. The slight inferred fining in grain size that occurs towards the northern end of Waihi Beach is possibly a result of lower wave energy at the shore when subject to swell and sea waves from the north to northwest, due to sheltering in the lee of Rapitiotio Point and associated shoals and wave refraction effects from Mayor Island.

#### 4.2.1.2 Cross-shore Variations

Conceptually, beach face and lower swash sediments should be coarser and more poorly sorted than berm and dune sediments, since these beach geomorphic units experience a higher level and greater fluctuations in wave energy. In contrast, the berm and dune are affected by more occasional processes such as storm surge, high tides and wave washover effects, with constant winnowing and sorting by wind. Although the pattern described above was detected along the CCS52 and CCS51 profiles, for the remaining three profiles this trend was inverted and the beach face and swash sediments were typically finer (Figure 4.3). This undulating change in grain size is related to local fluctuations in the hydrodynamic regime along northern Waihi Beach. Overall, however, there is very little cross-shore

variation in the grain sizes of collected onshore sediments, with all beach sediment samples classified as fine grained sands. There is a more definite variation in sediment size with distance offshore (Figure 4.5).

Although sediments collected from the northern Waihi Beach nearshore (~6-20 m water depth) were classified as moderately to moderately well sorted fine sands, seaward of the 25 m isobath there was a progression of coarse, poorly sorted gravelly sands. A plot of the inter-relationship between mean grain size and offshore distance (Figure 4.5) confirms that the mean grain size of the sediments becomes progressively coarser with distance offshore. The negative trend is supported by an  $r^2$  value of 0.757 which suggests that 75.7% of the variation in the samples is explained by the trend-line displayed. This trend may be occurring because finer grains are more easily uplifted and transported by the waves, producing a general movement of finer material onshore. Coarser sands remain offshore to form an “erosional-lag inner shelf deposit” (BRADSHAW *et al.*, 1994, p.93). These results are consistent with the results of DELL *et al.* (1985), HOBAN



**Figure 4.5:** Mean grain size versus distance offshore at northern Waihi Beach. Mean sediment grain sizes have been determined from samples collected on the 28/05/08 and 03/12/08.

(1993) and BRADSHAW *et al.* (1994). However, they are contrary to observations made by BRADSHAW (1991) of a seaward-fining progression to be typical of barrier spit beaches such as Waihi.

#### 4.2.2 *Sorting*

The sorting of a sediment sample refers to the range of sizes present. A numerical measure of the sorting is the standard deviation. “Poorly” sorted samples have a large standard deviation or a wide range of sediment sizes. Poorly sorted samples represent environments where weak sediment transport leaves a range of sediment sizes, and/or sediment input in which the normal sorting process has not had sufficient time to occur. “Well” sorted samples with grains of mostly similar sizes are usually characteristic of areas with more active sediment transport processes, selectively removing or winnowing out certain sediment sizes.

Sediments collected from the beach and nearshore at northern Waihi Beach were predominantly moderately well sorted and well sorted sands (Tables 4.4 and 4.5). These results are in agreement with HEALY *et al.* (1977), FULTON (1991) and BEAMSLEY (1996), who also found beach sediment to be generally well sorted along Waihi Beach. Sorting within the beach face and lower swash zone was found to be more irregular in sorting values than that of the berm (Figure 4.3), as is typical in such a turbulent and rapidly changing sedimentary environment (HARRAY and HEALY, 1978). The presence of shell fragments in swash samples would have also contributed to poorer sorting of those sediments.

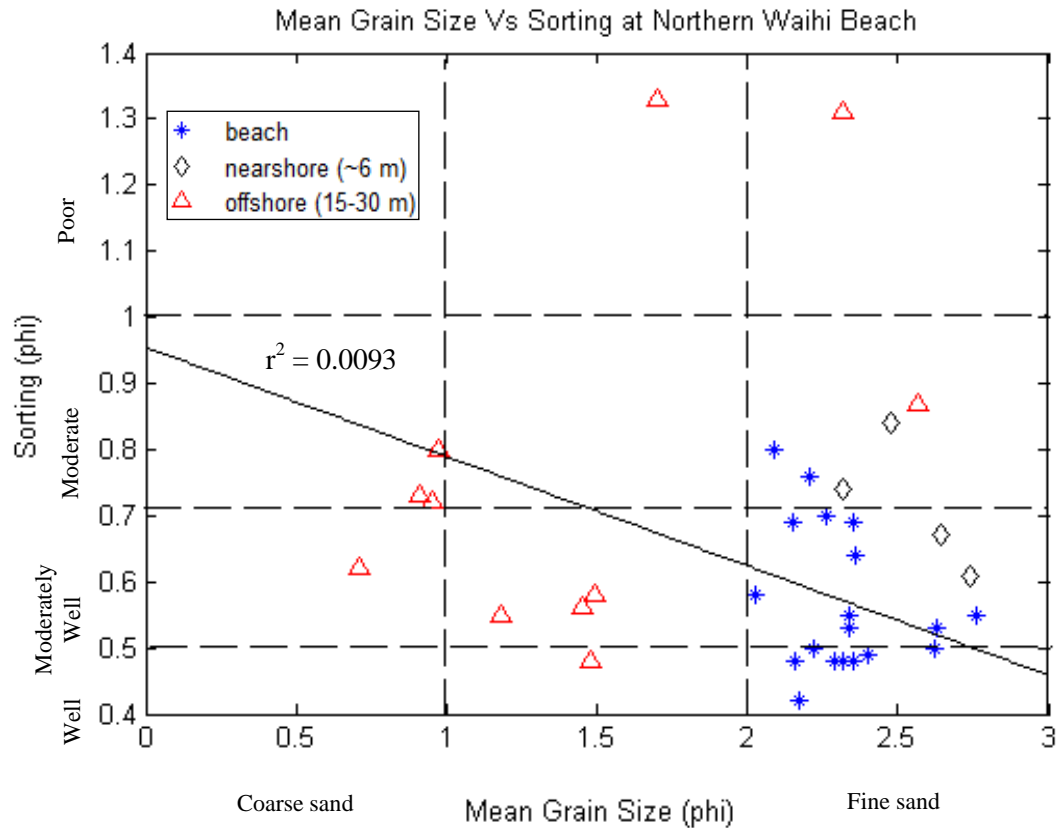
Sorting becomes relatively poorer seaward of 20 m. In particular, offshore samples taken at 20 m and 25 m on the CCS49 and CCS51 transects, respectively, revealed poorly sorted gravely sands. Sediment textural analysis by HOBAN (1993) at Pio Shores similarly revealed that the degree of sorting decreases offshore from the surf zone, observing the least well sorted sediments to be the coarse sands and gravels at the 30 m isobath. HOBAN (1993) notes that continual processes do not exist in this environment, with episodic events producing deposited sediment in a “dropped” nature (FOLK, 1980), thereby producing more poorly sorted sediments. BRADSHAW *et al.* (1994) and HUME *et al.* (1995) have also reported an abrupt

coarsening in sediment to poorly sorted gravely sands beyond the 20 m isobath. They note that patches of medium to fine sand overlie the coarse sands between 20-50 m water depth, which may explain the high standard deviation in grain sizes and hence poor sorting at these depths in the present study. Further, the sharp transition from moderately well sorted to poorly sorted sediments somewhere between 6 m and 20 m depth is indicative of the approximate seaward limit of active sediment transport under waves at the time of sampling (BEAMSLEY, 1996).

The spatial sorting of beach sediments may be an indicator of longshore sediment transport, with the degree of some sorting tending to increase in the direction of net littoral drift (HEALY *et al.*, 1977; HARRAY and HEALY, 1978; HEALY, 2007). For the beach (berm, beach face and swash) and dune there is a subtle improvement in sorting towards the south (Figure 4.3), implying that the littoral drift at the time of sampling was in a southerly direction. This trend is supported by FULTON (1991), however it is inconsistent with the results of other previous sediment textural investigations at Waihi Beach (e.g. HARRAY and HEALY, 1978) who have documented the opposite trend, stating that sorting of beach sediments tends to deteriorate towards the southern end.

#### 4.2.3 Mean Grain Size vs. Sorting

A bivariate scatterplot of mean grain size versus sorting for beach and offshore sediments was created to determine whether any inter-relationships between these two parameters existed (Figure 4.6). A very weak trend towards increased sorting with decreasing grain size is indicated, however the  $r^2$  value (0.0093) confirms that this trend is not significant, nor is it representative of the variation in the samples. The plot does confirm that the beach samples comprise predominantly fine, moderately to well sorted sands, and illustrates the seaward-coarsening progression and deterioration in sediment sorting with increasing depth.



**Figure 4.6:** Bivariate analysis of mean grain size and sorting for northern Waihi Beach, using moment method parameters attained from RSA analyses. Blue asterisks represent beach samples, black diamonds indicate nearshore samples from 6 m depth, and red triangles represent offshore samples taken between 15-30 m water depths. A regression analysis shows a weak negative trend as indicated by the low  $r^2$  value. 0.0093

#### 4.2.4 Skewness

Skewness provides a measure of the symmetry of sediment size distribution curves (LARSEN *et al.*, 1997). Coarsely skewed sediments have a dominance of coarse material with a tailing off of fines, whilst finely skewed sediments have a dominance of fine material with a tailing off of coarse sediments. Nearly symmetrically skewed sediments are an indication of a state of dynamic equilibrium with the wave and energy conditions present at time of sampling (BEAMSLEY, 1996).

Sands collected along the foreshore at northern Waihi Beach range from near symmetrical in the north, to fine and strongly finely skewed in the south (Figure 4.3). Hence, progressing southeast along the beach there is a marginal increase in the concentration of fine sediment in proportion to coarse sediment. These finely

skewed samples represent the fine component of transported sediment, since fine sediment is transported preferentially to coarse, possibly indicating that these materials are those that are being more actively transported. A significantly wide fluctuation in sediment skewness in berm samples is observed in Figure 4.3, with sands collected from the berm tending to be much more negatively skewed than those observed at other locations across the beach profile. The over-abundance of coarser sediment may be attributed to the deposition of coarser material by wave up-rush, and subsequent winnowing of finer fractions by wind (KOMAR, 1998).

According to DEAN and DALRYMPLE (2004), DUANE (1964) showed that a negative or coarse skewness indicates an erosive environment where the finer materials have been removed by the action of waves or currents. On the contrary, a depositional environment would likely have a positive or fine skewness. Applying this theory to Waihi Beach supports a southeasterly directed littoral drift (HEALY *et al.*, 1977; HARRAY and HEALY, 1978) by implying that sediment is eroded from the northern end where beach (berm) sediments were typically found to be coarsely skewed, and then transported and deposited in the south where beach sediments are predominantly finely skewed (Figure 4.3).

Like sorting, cross-shore skewness trends are more complex. Sands taken from onshore Waihi Beach ranged from near symmetrical to strongly finely skewed. Offshore, however, sediments obtained at depths of 6 m and 20 m were predominantly coarsely to strongly coarsely skewed. This trend is supported by findings from HOBAN (1993) and BEAMSLEY (1996) who also found samples offshore from the surf zone tended to be negatively skewed, indicating a scarcity of fine sands. This is likely to be a result of the winnowing of finer grain sizes by a strong energy environment associated with strong wave-orbital velocities and breaking waves. At greater depths (20-30 m) sediment becomes predominantly finely skewed again, implying that the lower energy levels of the deeper ocean allow finer grains to settle. The presence of fines at these depths is confirmed by the observations of ribbons of fine sand which transgress the coarser sands, as seen in the side-scan sonograph in Chapter 3 (section 3.2.5).



### 4.3 INFERENCE OF LITTORAL DRIFT

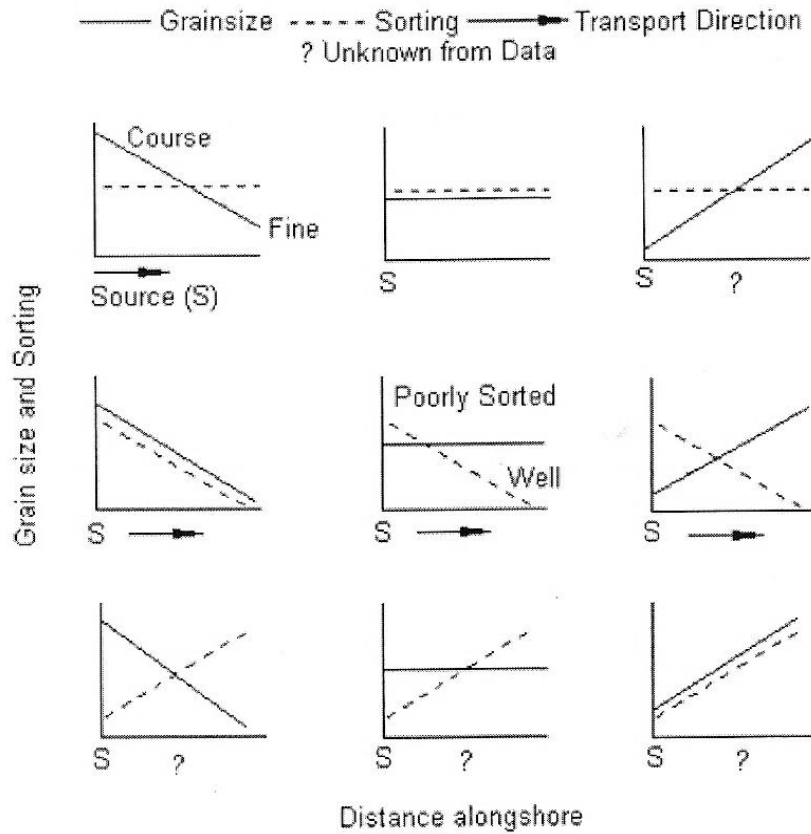
Littoral drift is the main mechanism by which sediment is supplied to a beach, and hence the direction of littoral drift is one of the major concerns in the study of erosion and sedimentation along sandy beaches. As the wave environment changes during the year, the sediment transport can change directions; however, at most coastlines there is a dominant direction of sediment transport (DEAN and DALRYMPLE, 2004). The analysis of spatial changes in grain size parameters (mean size, sorting and skewness) is one of the methods which can allow the identification of net sediment transport pathways. The following three littoral drift models have been employed using sediment textural trends from northern Waihi Beach to permit a reasonable inference for sediment transport.

The models are applied for the combined January 2008 and January 2009 beach face sample collections.

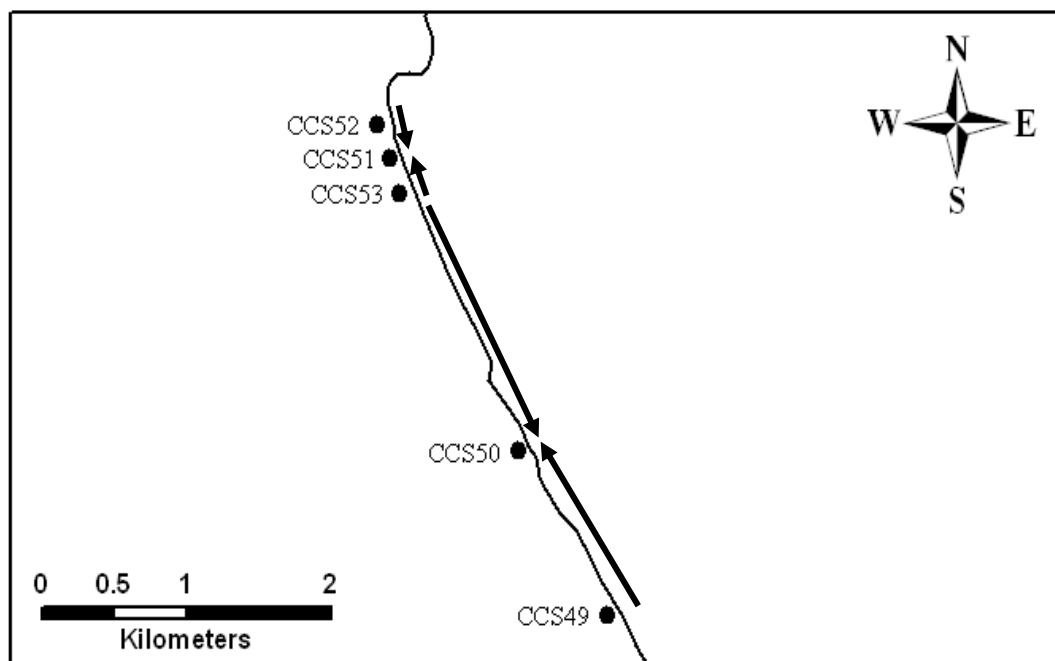
#### 4.3.1 *SUNAMURA and HORIKAWA (1972) Model*

SUNAMURA and HORIKAWA (1971; 1972) devised a model which uses spatial trends in sediment characteristics mean grain size and sorting to determine the direction of littoral drift. Figure 4.7 illustrates nine different combinations of trends in mean grain size and sorting that potentially may occur from sediment textural data, along with the inferred alongshore sediment transport directions for each. Using the spatial variation of mean grain size and sorting for each profile location (Figure 4.3), the inference criteria of SUNAMURA and HORIKAWA (1972) (Figure 4.7) were then applied to evaluate the direction of sediment movement at northern Waihi Beach. Figure 4.8 illustrates the littoral drift directions predicted at each benchmark location.

One limitation of the SUNAMURA and HORIKAWA (1972) model which should be taken into consideration is that the model assumes the beach has only one sediment source. This limitation is acceptable for Waihi Beach, as diabathic



**Figure 4.7:** Criterion for the inference of sediment transport direction according to the model SUNAMURA and HORIKAWA (1972). Certain combinations of grain size and sorting may indicate littoral drift direction. Source: SUNAMURA and HORIKAWA (1972).



**Figure 4.8:** Inferred sediment transport directions along northern Waihi Beach as determined using the SUNAMURA and HORIKAWA (1972) model. The model was applied to beach face samples collected in January 2008 and January 2009.

onshore sediment transfers are considered to be the single greatest contributor of material to the sediment budget (although this interpretation is not definitively proven). Waihi Beach has previously been identified as a closed sedimentary system, receiving little sediment from rivers or longshore littoral drift (HEALY *et al.*, 1981; BRADSHAW *et al.*, 1994; HUME *et al.*, 1995). The model also assumes a uniform mineralogy throughout the entire sample area. This limitation is not satisfied within the Waihi Beach coastal sector. Field observations confirm the presence of thick bands of titanomagnetite commonly accumulating at the northern end of the beach, compared to the southern end where the mineral is typically absent except as a lag deposit following erosive storm wave action. Hence, the determined sediment transport directions may have possible errors and should be considered cautiously. It is also important to note that drift trends inferred by the sediment textural model of SUNAMURA and HORIKAWA (1972) are likely to show the pre-sampling wave drift direction, and not net short-term trends.

According to the SUNAMURA and HORIKAWA (1972) model, littoral drift is bi-directional along Waihi Beach for the January 2008 and January 2009 samples analysed, with longshore currents converging at CCS50 (The Loop) and CCS51 (Figure 4.8).

#### 4.3.2 MCLAREN (1981) Model

A second model pertaining to the prediction of sediment transport from textural parameters is the 'MCLAREN model' (MCLAREN, 1981; MCLAREN and BOWLES, 1985). The MCLAREN (1981) model is similar to the SUNAMURA and HORIKAWA (1972) model, in that it uses spatial trends in sediment texture to determine sediment transport pathways along the coast. However, it also incorporates an additional characteristic – sediment skewness – into the assessment of littoral drift direction. According to this model, grain size distributions will change in response to erosion, transport and deposition, producing three possible scenarios (MCLAREN, 1981; MCLAREN and BOWLES, 1985):

- Case I: Complete Deposition

The deposited sediment should become finer, better sorted and more negatively skewed in the direction of transport.

- Case II: Partial Deposition

The sediment lag remaining after erosion should be coarser and more positively skewed than its source.

- Case III: Partial Deposition

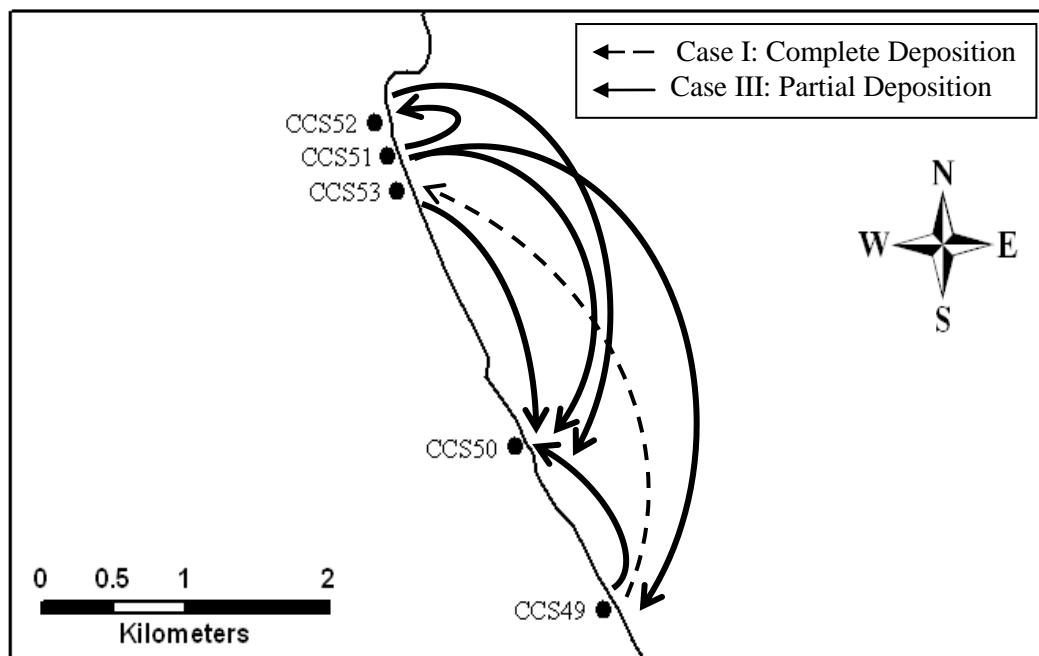
Sediment transport undergoes selective deposition due to decreasing energy of the transport process. The resulting deposit may be either finer or coarser than the source, with better sorting and a more positive skewness.

These three options, therefore, enable the inference of sediment transport directions from textural parameters. MASSELINK (1992) found that the model inferred transport directions contrary to the known littoral drift direction along the Rhone Delta Coast. MASSELINK (1992) suggested that the model was based on three critical assumptions that may be unjustified in the nearshore zone:

1. The model assumes uni-directional flow, whereas littoral drift can often be bi-directional;
2. The transported sediment is supposedly derived from only a single source. However, in reality, on a beach sediment may typically be derived from several sources, including local erosion of beaches, cliffs and dunes, and from fluvial and offshore sources.
3. The model assumes that net littoral drift is the primary factor influencing sediment characteristics along a coastline. It fails to consider other mechanisms which may also influence sediment characteristics of beach sands, including diabathic sediment transport, complex refraction processes and wave energy focusing, the latter two of which have previously been shown to be important at Waihi Beach (HEALY, 1987; STEPHENS, 1996).

Despite these apparent conflicts, the MCLAREN (1981) model was applied to northern Waihi Beach onshore samples (Figure 4.9; Appendix II). Because the

MCLAREN (1981) model has the same limitations as the SUNAMURA and HORIWAKA (1972) model, there may also be possible errors in predicted littoral drift directions.



**Figure 4.9:** Inferred sediment transport directions along northern Waihi Beach as determined using the MCCLAREN (1981) model. The model was applied to beach face samples collected in January 2008 and January 2009. Note that the source-deposit relationship indicating Case I deposition between CCS49 and CCS53 is rejected as complete deposition is unlikely to occur in such a high energy environment (MCCLAREN, 1981).

Results of the MCCLAREN (1981) model are illustrated in Figure 4.9, comparative assessment of sediment textural parameters is presented in Appendix II. Of eight possible source-deposit relationships, only one (CCS49 as a source for CCS53) indicates Case I deposition requiring total deposition of sediment in transport onto a beach face. Because beach face sediments undergo continuous movement through the action of breaking waves and swash, Case I is unlikely to occur in this environment and can be reasonably rejected (MCLAREN, 1981).

The remaining seven relationships are all Case III deposition, which is perfectly reasonable for beach face sedimentation (MCLAREN, 1981). Of these, five trend southeast and two trend northwest (Figure 4.9) which suggests that overall longshore transport of beach face sediments is taking place from northwest to southeast. As with the SUNAMURA and HORIKAWA (1972) model predictions,

benchmark CCS50 is again the location of converging littoral drift, thus implying this site is a potential sink for CCS49 to the southeast and all the sites to the northwest. Drift reversal between CCS51 and CCS52 towards the northwest may be due to the presence of rip currents, often observed at northern Waihi Beach (STEPHENS, 1996), and so sands are slightly finer and better sorted at this location. The complex trends are perhaps an indication of the local refraction patterns and zones of wave focusing, which will be modelled in Chapter 6.

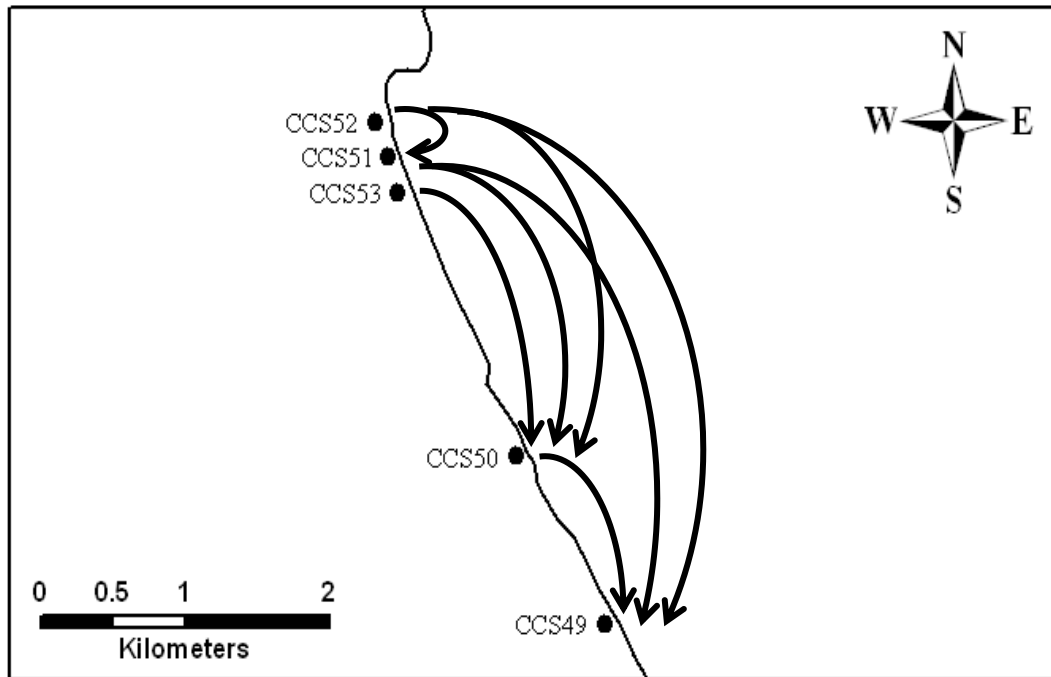
#### *4.3.3 “Waihi” Model*

As the previous two models have demonstrated, a fining of sediment grain size in a given alongshore direction can indicate the littoral drift direction; the logic being that finer particles are more easily uplifted and transported by waves and will therefore travel faster and further in the long-term. To make matters more complicated, however, all sand grains are not of equal specific gravity, nor spherical, and thus lighter and angular grains may move in preference to the heavier smaller grains (HEALY and DELL, 1982). This arises partly because of the intergranular dispersive stresses in an energetic system. HEALY and DELL (1982, p.7) state that “the dispersive stress increases as the square of the particle diameter and hence differential stress on the larger particles tends to force them to the surface where dispersive stress is minimised”. Once on the surface coarser particles can then be moved preferentially.

Both the SUNAMURA and HORIKAWA (1972) and the MCCLAREN (1981) models assume that beach sediments are composed of rounded quartz-predominant grains of equal density. However, HARRAY and HEALY (1978) and HEALY and DELL (1982) suggest that at Waihi Beach, coarser and more angular sands are preferentially entrained and transported by wave processes due to angular variability and variable density of the larger grains. The “Waihi” model, proposed by PHIZACKLEA (1993) based upon the findings of HARRAY (1977) and HARRAY and HEALY (1978) for Waihi Beach, is similar to the MCLAREN (1981) model except that it allows for the effect of grain shape and variation in mineralogy. According to this model, sediment transported from an updrift source should produce a deposit which is coarser, more poorly or better sorted, and be more

negatively skewed due to the addition of coarser sized grains. The resultant source sediment will become finer, better or poorly sorted and more positively skewed.

Results of the Waihi model are illustrated in Figure 4.10, comparative assessment of sediment textural parameters is presented in Appendix II.



**Figure 4.10:** Inferred sediment transport directions along northern Waihi Beach according to the Waihi model. The model was applied to beach face samples collected in January 2008 and January 2009.

The Waihi model predicts seven possible transport pathways, all of which indicate a net southeastward littoral drift direction (Figure 4.10). This is in good agreement with environmental indicators of littoral drift direction identified by HEALY *et al.*, (1977) and HARRY and HEALY (1978), including a wave resultant and onshore wind resultant directed  $4^\circ$  and  $12^\circ$  south of shore-normal, respectively. These results suggest that coarser and more poorly sorted sands are preferentially entrained by waves at Waihi Beach and are transported southeasterly, leaving a finer and better sorted deposit at the northern end of the beach. This theory is supported by the alongshore distribution in mean grain size for the present study, which showed onshore sediments display a southwards coarsening progression. The distribution in sediment sorting along Waihi Beach on the other hand showed the opposite trend, revealing a subtle improvement towards the south. However,

results from more comprehensive sediment textural investigations undertaken by HARRAY and HEALY (1978) of Waihi Beach sediments found that sorting of beach sands does in fact tend to deteriorate towards the southern end. PHIZACKLEA (1993) proposes that the Tauranga Harbour may possibly be the source of coarser, more poorly sorted sands towards the southern end of the beach.

#### *4.3.4 Evaluation of Model Results*

From results of the SUNAMURA and HORIKAWA (1972) sediment transport model (Figure 4.8), bi-directional sediment transport is indicated at CCS50 and CCS51. If converging littoral drift was present at these locations, and if littoral drift was significant over the long-term, there would be expected sediment accumulation near the Rapatiotio Point headland and noticeable accretion at The Loop (CCS50). However, there is no evidence to support a healthier sediment budget at either location, and in fact the beach fronting the seawall at The Loop has an extremely narrow profile indicative of a major sediment deficit. Therefore, sediment transport implications by the SUNAMURA and HORIKAWA (1972) model may be incorrect, otherwise littoral drift rates must be relatively small.

Sediment transport directions as determined by the MCCLAREN (1981) model were similar to that of the SUNAMURA and HORIKAWA (1972) model, predicting drift reversals at CCS49 and CC51 (Figure 4.9). However, with only two of the transport pathways identified indicating sediment transport towards the northwest, this model favours a more definite southeasterly drift along northern Waihi Beach.

The Waihi model predictions imply a very certain sediment transport direction towards the southeast (Figure 4.10), with no northwesterly component implied at any location along the study area. Geomorphic evidence is highly supportive of the model predictions. As well as wind and wave resultants implying a southeasterly littoral drift, the sand dunes are significantly higher at the central and southern sectors of Waihi Beach than at the northern end of the beach, indicative of major sediment flux from the north. Thus, this model and the theory of preferential entrainment of coarser particles (HEALY and DELL, 1982), is (as expected) very applicable to Waihi Beach.



To summarise, mean grain size and sorting textural models, based upon the beach sediment samples collected and analysed in this study, indicate overall net sediment transport is to the southeast from Rapatiotio Point towards central Waihi Beach (Island View). It is important to note, however, that because only five sampling sites were selected along the study area for sediment grain size analysis, the spatial accuracy of directional estimates from each model is limited. In order to make results more convincing, a greater density of alongshore beach sample locations, ideally every 500 m (providing ~9 samples), is necessary to make huge valid assumptions. Littoral drift direction and implications will be revisited in greater depth in Chapter 6, where the numerical model WBEND is employed to determine rates and magnitudes of sediment transport at northern Waihi Beach. The results of numerical littoral drift modelling will subsequently be used for the sediment budget in Chapter 7.

#### 4.4 SUMMARY

The beach and offshore sediments at northern Waihi Beach were analysed following the classification scheme of FOLK (1968) to identify the nature and distribution of nearshore sediments.

- All beach sediments obtained can be classified as near symmetrical to finely skewed, and moderately well to well sorted. Mean grain sizes of sampled beach sediments were fine grained sands.
- Nearshore sediment samples displayed a general coarsening and deterioration of sorting with distance offshore, with a noticeable coarsening of sediments seaward of about 20 m depth. These trends are associated with the presence of the large megarippled features identified in the side-scan sonar survey in Chapter 3.
- Alongshore trends in sediment sorting display a subtle improvement towards the southern end of the beach, implying an overall sediment transport to the southeast at the time of sampling.

Comparison of sediment grain size distributions over the nearshore region provided information about physical processes influencing sediment transport and deposition at northern Waihi Beach.

- Sediment grain size appears to remain relatively constant along northern Waihi Beach, but there is a slight trend for sand to become marginally coarser towards the southern end of the study site. This may be associated with a zone of wave energy focusing, where finer sand is preferentially removed and transported offshore. Alternatively, beach sands in the south may be nourished by coarser offshore sediments through diabathic onshore exchange.
- The slight inferred fining in sediment grain size at the far northern end may be due to Rapatiotio Point acting as a shelter to the influence of north and northwesterly generated waves, resulting in lower wave energy at the shoreline.

Using measured sediment textural characteristics, net littoral drift directions along northern Waihi Beach were identified by applying three sedimentological models.

- At northern Waihi Beach, collective geomorphic evidence indicates a net southeastward drift (HEALY *et al.*, 1977; HARRAY and HEALY, 1978). The Waihi model produced comparable results with a southeasterly drift, and the MCCLAREN (1981) model suggested an overall dominance to the southeast. The less complex SUNAMURA and HORIKAWA (1972) model implies that littoral drift is bi-directional at northern Waihi Beach, with currents converging at CCS50 and CCS51. However, because there is no obvious geomorphic manifestation of sediment accumulation evident at either of these locations, it must be assumed that littoral drift rates are relatively small, or that sediment transport implications by the SUNAMURA and HORIKAWA (1972) model are unjustified along Waihi Beach.

# CHAPTER FIVE: NEARSHORE HYDRODYNAMICS AND SEDIMENT TRANSPORT

---

## 5.0 INTRODUCTION

Results from previous beach and nearshore morphological studies in the Bay of Plenty (e.g. BRADSHAW, 1991; PHIZACKLEA, 1993; SAUNDERS, 1999; SPIERS, 2004) suggest that a combination of wave oscillatory and wind-induced currents transport and distribute sediments in the beach-nearshore system. In order to determine nearshore sediment transport patterns, information is required on the nearshore wave regime and local current patterns that operate within the nearshore zone. For the present study, three InterOcean S4 current meters were deployed offshore Waihi Beach over a total period of 80 days, encompassing a broad range of wave and current information.

In this chapter, a detailed assessment of nearshore hydrodynamics is made using measured wave and current data collected at six locations in the nearshore off northern Waihi Beach. Methods to collect and analyse the wave and current data are detailed, followed by results of monochromatic analysis. Wind speeds and direction are analysed to determine their importance in wave formation and patterns, and to evaluate the influence of winds on nearshore current generation offshore Waihi Beach. This information is then combined with bathymetric and sediment data to determine thresholds for sediment entrainment, which will subsequently be used to identify the likely periods and magnitudes of onshore-offshore sediment movement for the sediment budget in Chapter 7.

## 5.1 WAVES

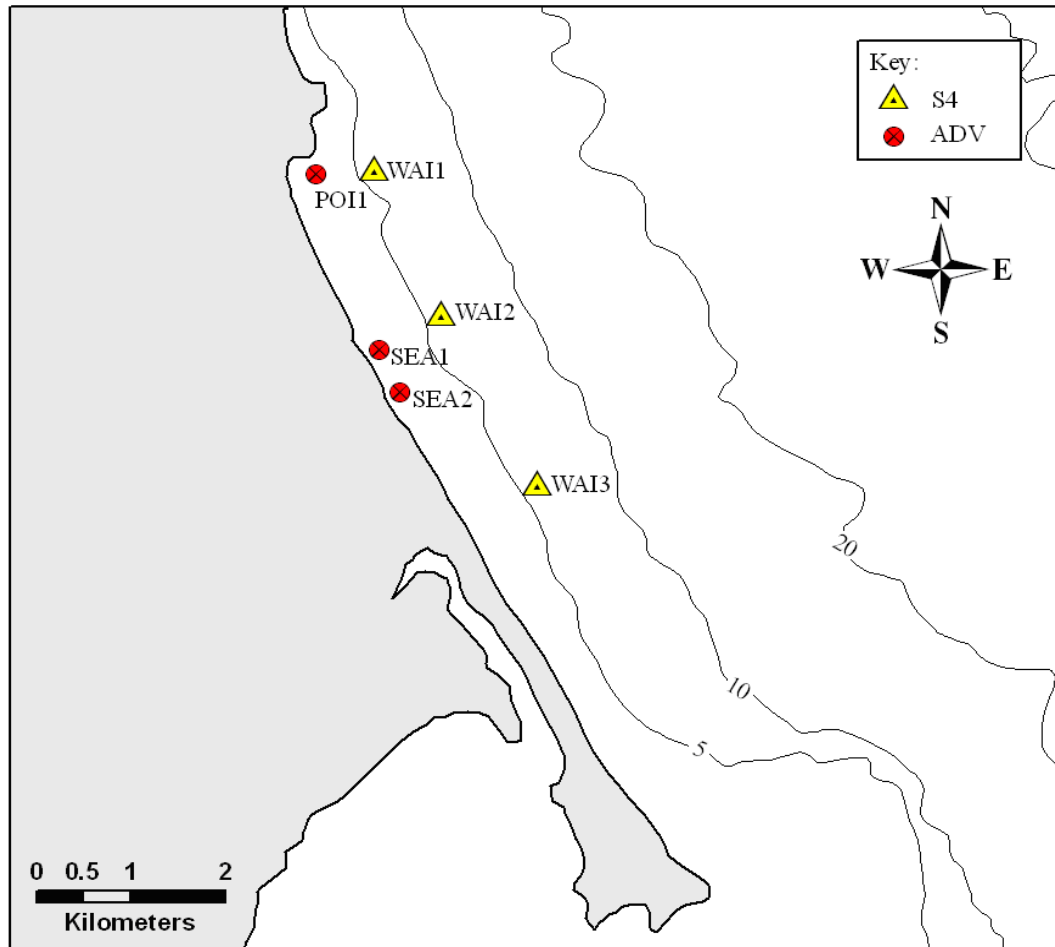
### 5.1.1 Methods

#### 5.1.1.1 Data Collection

Three InterOcean S4 current meters were deployed just beyond the surf zone at Waihi Beach in order to gain insight into the hydrodynamic processes occurring in the nearshore. The S4's were deployed in ~6 m water depth at low tide, mounted upon stainless steel tripod frames secured to the seafloor with weights added prior to deployment on the beach (Figure 5.1). These frames are designed to handle extreme breaking conditions, but also ensure that the S4's remain in a vertical position 1 m above the seabed. Figure 5.2 shows the positioning of the instruments. All S4's were programmed to sample at a rate of 2 Hz in the burst mode, recording wave and current information for 18 minutes every hour. They were programmed to record data simultaneously specifically for the purpose of calibrating the wave refraction model in Chapter 6. A total of two S4 deployments were conducted; a summer deployment from 15<sup>th</sup> November to 15<sup>th</sup> December 2007 and a winter deployment between 7<sup>th</sup> May and 25<sup>th</sup> June 2008 (Table 5.1).



**Figure 5.1:** S4 current meter mounted on stainless steel tripod.



**Figure 5.2:** Map of Waihi Beach showing positions of the three S4 and three Acoustic Doppler Velocimeter (ADV) instruments used in the study.

Three SonTek Triton Acoustic Doppler Velocimeter (ADV) instruments captured a brief snapshot of the wave regime from two short-term deployments in May and June 2008, in water depths of ~3.5-4 m with sensors 0.8 m above the bed. These instruments provide accurate current, pressure and level data while withstanding punishing conditions in the surf zone. One ADV was located in the lee of Rapatiotio Point (POI1), while the other two instruments recorded wave and current data in front of (SEA1) and adjacent to (SEA2) the seawall near Two Mile Creek (Figure 5.2). A similar setup to the S4 instruments was used, with the ADV's mounted upon small steel tripod frames, with sufficient weights added to inhibit movement or burial due to the turbulent nature of the surf zone. The burst mode setting for the ADV's involved recording wave information for 2 minutes every hour at 2 Hz. All three instruments remained in the surf zone for 23 hours between 11:00 o'clock on the 28<sup>th</sup> of May and 10:00 o'clock on the 29<sup>th</sup> of May 2008. A second deployment between 13:00 o'clock on the 24<sup>th</sup> of June to 10:00

o'clock on the 25<sup>th</sup> of June 2008 provided a further 21 hours of data. Both deployments coincided with the winter S4 deployment to enable comparisons between the data sets of the two instruments.

Table 5.1 summarises the positions and recording periods all of the wave and current meters used throughout the study.

**Table 5.1:** Deployment period and GPS location of all S4 and ADV wave and current meters used throughout the study. GPS locations are in NZ map grid.

Instrument	File Name	Deployment Period		GPS Location
		'Summer'	'Winter'	
S4	WAI1	15/11/07 –		E2771194
		15/12/07		N6418750
S4	WAI2	15/11/07 –		E2771913
		15/12/07		N6417165
S4	WAI3	15/11/07 –		E2772895
		15/12/07		N6415299
S4	WAI1b		28/05/08 –	E2771194
			25/06/08	N6418750
S4	WAI3b		07/05/08 –	E2772895
			25/06/08	N6415299
ADV	POI1	28/05/08 –		E2771379
		29/05/08		N6416786
ADV	SEA1	28/05/08 –	24/06/08 –	E2771851
		29/05/08	25/06/08	N6416314
ADV	SEA2	28/05/08 –	24/06/08 –	E2770753
		29/05/08	25/06/08	N6419013

The summer S4 deployment produced 30 days of wave and current information at all three S4 locations. However, due to non-ideal weather conditions the winter deployment which commenced on the 7<sup>th</sup> of May consisted of only one S4 at the southernmost location WAI3b. On the 28<sup>th</sup> of May a second S4 was successfully deployed at the far northern end (WAI1b) and the original S4 at WAI3b was replaced with a new instrument and battery. Unfortunately, the replacement S4 at WAI3b only recorded wave and current information for 8 days before suffering a power failure.

#### 5.1.1.2 Data Analysis

All of the burst measurements recorded by the S4 instruments were initially processed using the InterOcean Systems software package WAVE For Windows, an ocean wave analysis and display program designed specifically for describing the current and wave climate at a specific location. Characteristics such as significant wave height, wave period and spectral analysis parameters are calculated using the time series of pressure and the two components of particle kinematics data collected by an S4 directional wave instrument (INTEROCEAN SYSTEMS, INC., 1996). The WAVE program provides the user with a range of analysis and presentation options, and also allows processed statistics to be converted from S4B file format into S4 ASCII format.

Processing of the raw ADV burst data was initially undertaken using the SonTek software View Triton-Pro. This program predicts very accurately the first order wave statistics: wave height, the peak period, the mean direction and spreading. View Triton-Pro also provides the user with a complete set of the raw data in either ASCII or Matlab format for further custom processing. For this study, processed S4 and ADV data were saved as ASCII text files and then used for a range of Matlab scripts.

Prior to any comprehensive directional analysis, a magnetic variation of 21.5°E was added to both the raw S4 and ADV wave direction data to orientate the statistics relative to True North.

The analysis of wave data is typically approached through either determining monochromatic wave statistics or applying spectral wave analysis. For the purpose of this study, only monochromatic techniques were used to analyse the S4 and ADV wave data collected throughout the duration of the study. Monochromatic wave analysis typically focuses on determining the significant wave statistics of height ( $H_s$ ) and period ( $T_s$ ), defined by MUNK (1944) (as cited in the Shore Protection Manual, 1984) as the average of the largest one third of the waves measured over a given interval of time. These representative wave statistics can be extracted from raw wave data through the methods of zero up-crossing or

down-crossing analysis. This requires that data be adjusted to represent fluctuations about a mean water level of zero. For monochromatic waves, all the waves in a wave field are assumed to have the same period and height. However, this is not the case for real ocean waves.

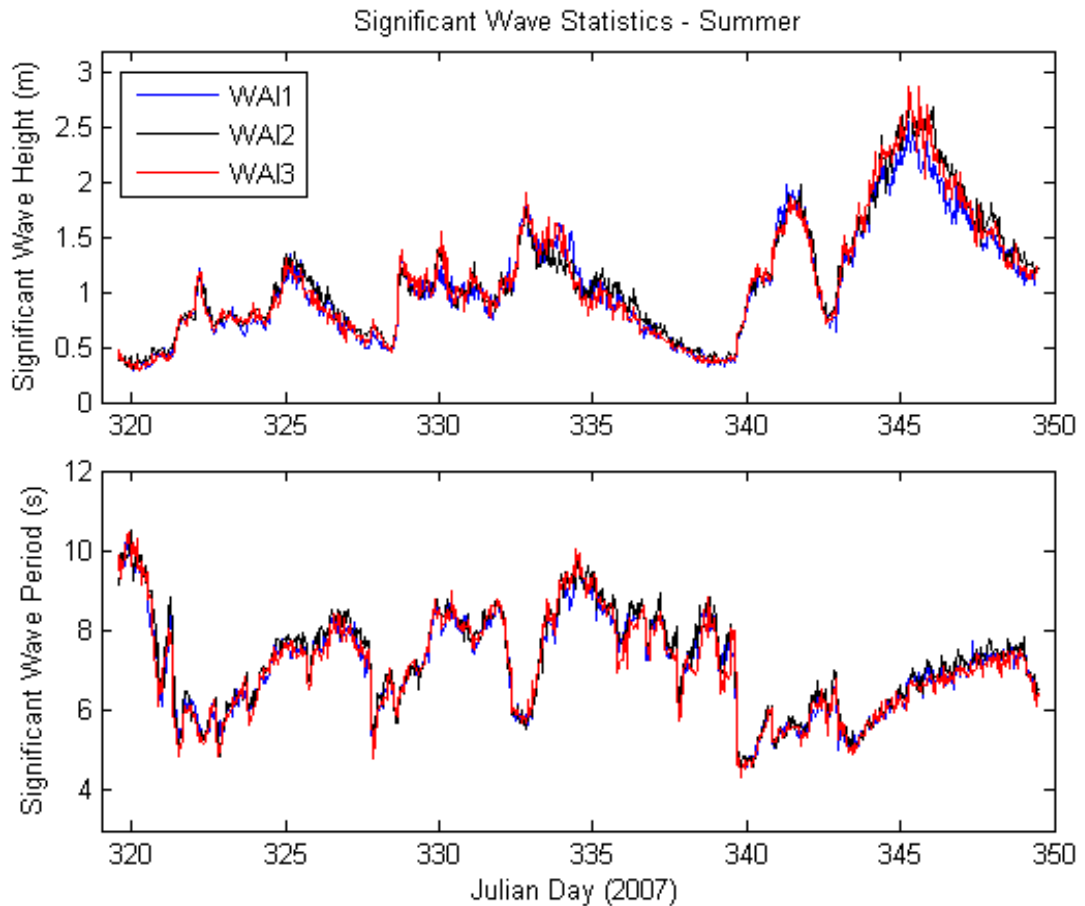
## 5.1.2 *Results*

### 5.1.2.1 Monochromatic Wave Statistics

Time series plots of significant wave height ( $H_s$ ) and period ( $T_s$ ) recorded over the summer and winter S4 deployment periods are depicted in Figures 5.3 and 5.4 respectively.  $H_s$  recorded during the summer deployment by the three S4s ranged from 0.29 m to 2.88 m, with a mean wave height of 1.09 m. The majority of waves (80%) recorded offshore had wave heights of less than 1.5 m, while only 6% of waves reached heights in excess of 2 m. If a storm event was to be defined as conditions in which  $H_s$  exceeded 2 m, then only one storm struck Waihi Beach between November 15<sup>th</sup> and December 15<sup>th</sup> near the end of the deployment period between Julian days 343-347 (Figure 5.3).

A much more energetic wave climate was observed over the longer winter deployment, with three major storm events being recorded. During the final and largest storm event, which began on day 167 and proceeded through to the end of the deployment, recorded  $H_{1/10}$  reached a maximum of 3.88 m at WAI1b. Between storms the sea significantly abated, with a particularly prolonged period of calm between days 150 to 167 (Figure 5.4). The mean significant wave height was 0.95 m, which is slightly below that of the summer deployment. The range in  $H_s$  spanned 0.13 m to 3.05 m indicating that wave heights were more variable during winter, although this may simply be due to the longer duration of the winter deployment period and cannot be attributed solely to seasonal influences. Much like the summer deployment, measured  $H_s$  during the winter period exceeded 1.5 m and 2m ~21% and ~7% of the time, respectively.

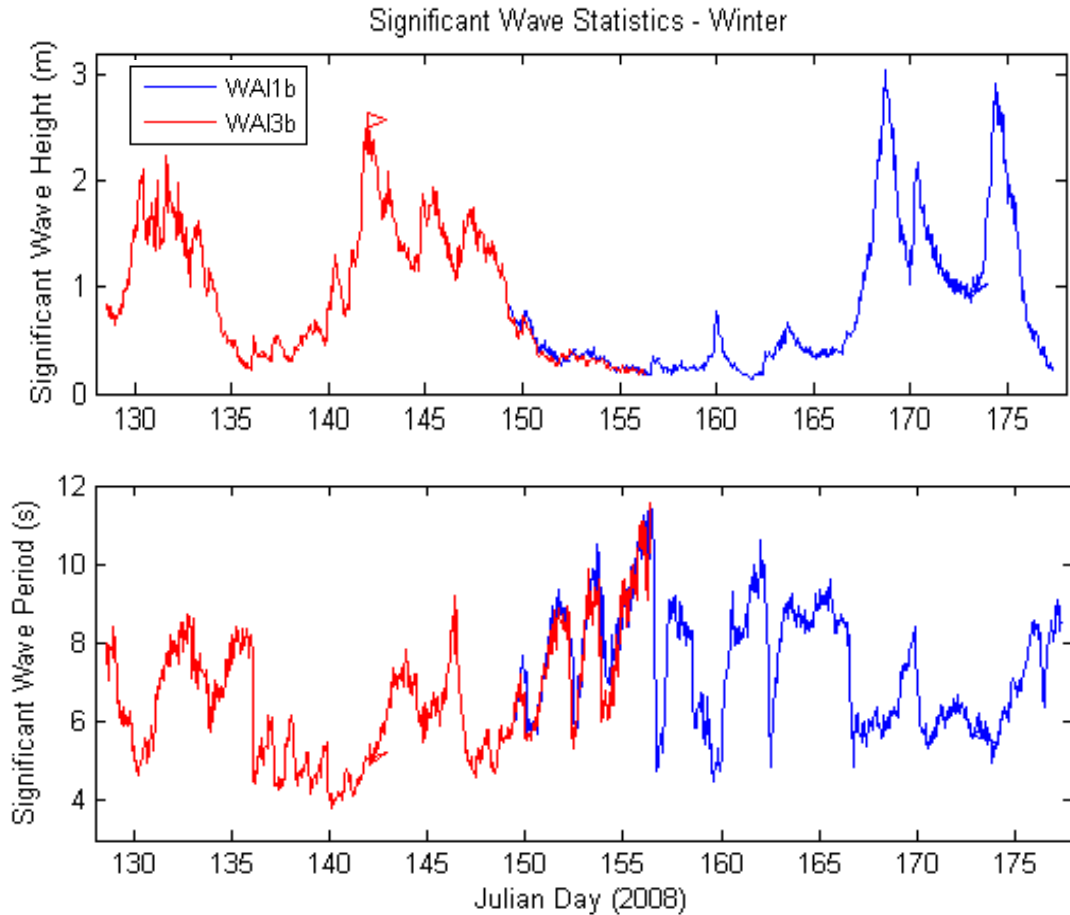




**Figure 5.3:** Time series of significant wave height (upper) and period (lower) at WAI1 (blue) WAI2 (black) and WAI3 (red) during the summer S4 deployment (15/11/07 – 15/12/07) at northern Waihi Beach.

These findings are considered above average for Waihi Beach when considering observations from previous investigations. HARRAY (1977) and HARRAY and HEALY (1978) report a significantly lower mean nearshore  $H_s$  of 0.6 m from a years worth of wave data, and found that at Waihi Beach waves less than 0.3 m in height occurred for 55% of the time. HOBAN (1993) similarly reports lower wave heights than those of the present study from an S4 deployment in 6 m water depth off Pio Shores. However, wave data obtained by HOBAN (1993) may not be typical of the long-term climate because they were obtained in strong El Nino conditions (1990-1994), when offshore winds persist and fewer storms occur.

For both the summer and winter periods in which the S4's were deployed, the average and extreme parameters at each location are given in Table 5.2. Significant wave heights recorded by the northernmost S4 current meter (WAI1)



**Figure 5.4:** Time series of significant wave height (upper) and period (lower) at WAI1b (blue) and WAI3b (red) during the winter S4 deployment (07/05/08 – 25/06/08)) at northern Waihi Beach.

are consistently smaller than at both the central (WAI2) and southern (WAI3) S4 locations (Table 5.2). A possible reason may be because the position of the S4 WAI1 is partly sheltered from the north to northwest by the Rapatiotio Point headland. Wave refraction from Mayor Island may also have caused a small reduction in wave heights recorded by WAI1 and focusing at the other S4 sites. The refraction influence of Mayor Island on alongshore variation in wave height will be examined in the wave refraction modelling in Chapter 6.

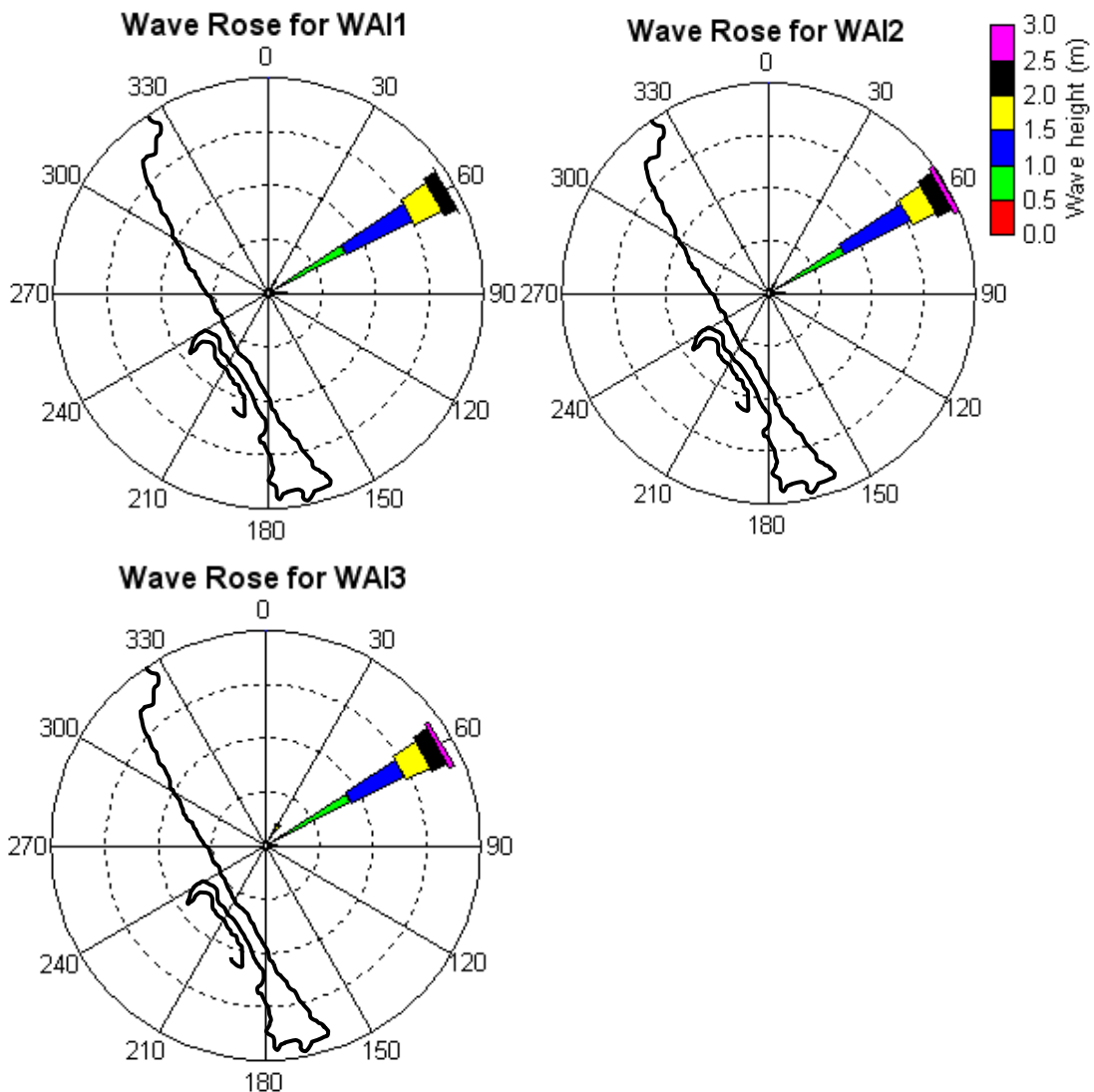
From Table 5.2, comparison between summer and winter deployments at northern Waihi Beach indicate that there are not notable differences in terms of mean significant wave period. Mean  $T_s$  were typically around 7 s during both seasons, with a maximum wave period of 10.49 s for summer and 11.42 s for winter. This slightly higher maximum wave period over the winter deployment indicates that

**Table 5.2:** Monochromatic wave statistics measured in the nearshore at northern Waihi Beach for the summer (15/11/07 – 15/12/07) and winter (07/05/08 – 4/06/08 for WAI3b; 28/05/08 – 25/06/08 for WAI1b) deployments obtained from zero-down crossing analysis.  $H_s$  = height of the highest 1/3 of waves;  $H_{1/10}$  = height of the highest 10% of waves;  $H_{max}$  = maximum wave height;  $T_s$  = period of the highest 1/3 of waves;  $T_p$  = peak period; Dir = mean direction.

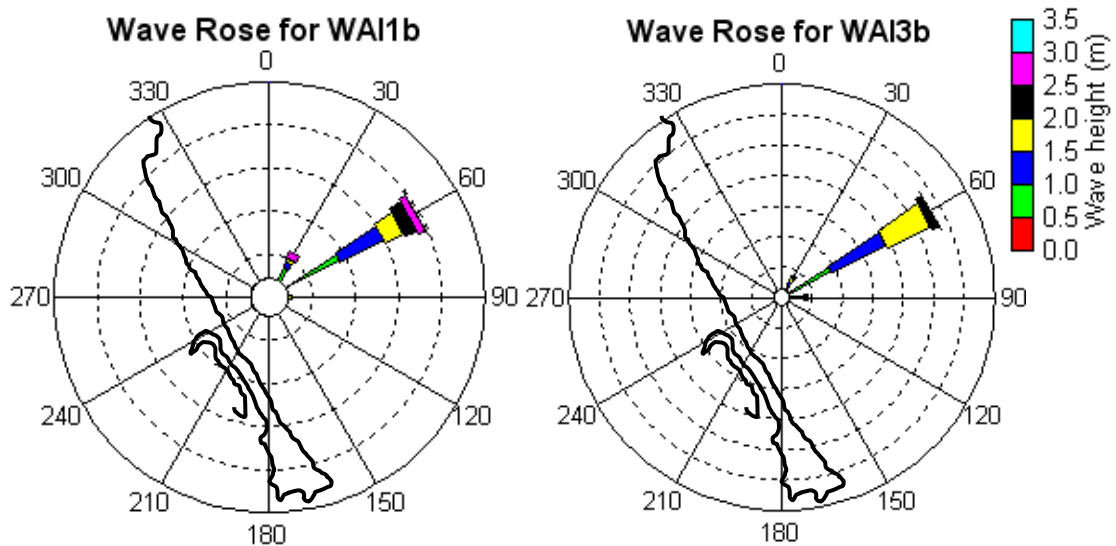
		Summer Deployment			Winter Deployment	
		WAI1	WAI2	WAI3	WAI1b	WAI3b
$H_s$ (m)	Min	0.29	0.31	0.28	0.13	0.23
	Max	2.55	2.70	2.88	3.05	2.63
	Mean	1.06	1.12	1.10	0.74	1.16
	Std Dev	0.38	0.42	0.44	0.54	0.40
$H_{1/10}$ (m)	Min	0.37	0.40	0.36	0.17	0.29
	Max	3.25	3.44	3.67	3.88	3.35
	Mean	1.36	1.43	1.40	0.94	1.48
	Std Dev	0.64	0.68	0.70	0.84	0.70
$H_{max}$ (m)	Min	0.45	0.49	0.43	0.21	0.36
	Max	4.09	4.34	4.63	4.91	4.32
	Mean	1.70	1.79	1.75	1.19	1.87
	Std Dev	0.81	0.87	0.89	1.06	0.89
$T_s$ (s)	Min	4.53	4.57	4.32	4.48	3.81
	Max	10.25	10.49	10.44	11.42	9.19
	Mean	7.10	7.22	7.07	7.47	6.10
	Std Dev	1.18	1.23	1.23	1.48	1.28
$T_p$ (s)	Min	3.51	3.98	3.13	3.11	3.02
	Max	13.93	16.13	15.17	17.21	17.81
	Mean	9.35	9.47	9.27	10.16	8.58
	Std Dev	1.60	1.65	1.80	2.242	3.39
Dir (°)	Mean	61.42	62.49	57.22	52.00	63.68
	Std Dev	9.37	9.06	9.82	33.68	11.72

the presence of intense local storm systems was responsible for generation of larger winter waves, particularly towards the end of the deployment. These results are consistent with findings by HOBAN (1993), who reported  $T_s$  offshore Pio Shores ranged between 3.5 and 13 s during a week-long deployment. However, measured mean and maximum wave periods in the present study are significantly lower than those observed by HARRAY (1977) and HARRAY and HEALY (1978), who report mean and maximum  $T_s$  of 11 s and 15 s respectively. The lower measured  $T_s$  values in the present study indicate the presence of locally generated sea waves in addition to the predominant swell, which is further discussed in section 5.1.2.2 *Wave Origin*.

Wave approach directions measured by S4 current meters for both summer and winter deployments are detailed by the rose plots in Figures 5.5 and 5.6 respectively. Both figures illustrate that wave approach at Waihi Beach was predominantly from the northeast-east during the monitoring period, the direction to which the study area is exposed to an unlimited fetch. The direction of approaching waves in the nearshore is severely restricted to a very narrow swell window, ranging between  $0^{\circ}$  and  $80^{\circ}$  (True) with a mean direction of  $60.3^{\circ}$  over summer and  $57.8^{\circ}$  over the winter deployment period. This directional spectrum clearly illustrates that wave refraction processes are modifying incoming swell waves and effectively concentrates waves into a narrow directional band. SILVESTER and HSU (1997) state that one of the key features of swell waves is the



**Figure 5.5:** Wave rose plots for the summer deployment (15/11/07 – 15/12/07) at WAI1, WAI2 and WAI3. Each frequency band denotes 20% of the total number of waves. The shoreline of Waihi Beach is superimposed.



**Figure 5.6:** Wave rose plots for the winter deployments at WAI1b (28/05/08 – 25/06/08) and WAI3b (07/05/08 – 04/06/08). Each frequency band denotes 10% of the total number of waves. The shoreline of Waihi Beach is superimposed.

constancy of their direction at points on a coast. The similarity between the two deployment periods suggests that direction is independent of seasonal change, despite the much longer winter deployment period.

#### 5.1.2.2 Wave Origin

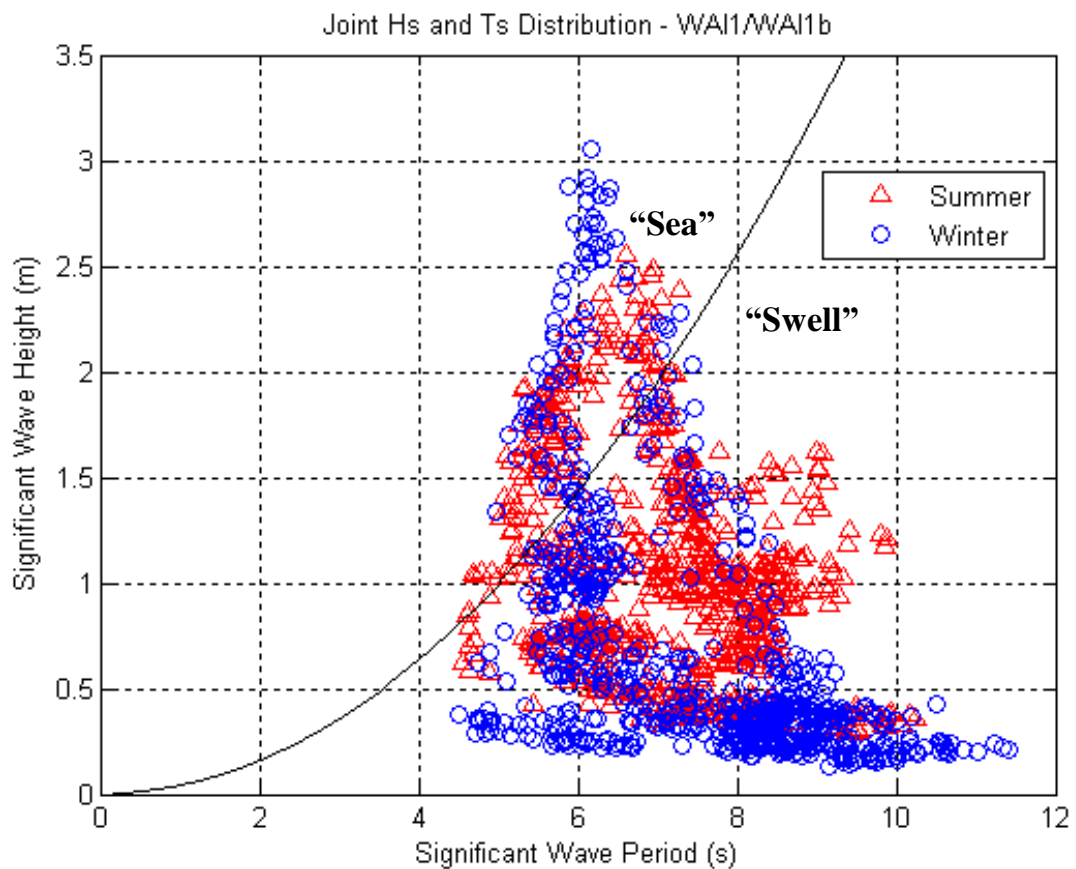
If a wave field may be defined by a combination of monochromatic waves, it is necessary to define the distribution of wave heights and wave periods present. DRAPER (1966a) suggested that a scatter diagram relating significant wave height and zero-crossing period would be an appropriate method of conveying this information. This form has been widely adopted and a number of joint probability distributions have been derived from it (DRAPER, 1966a).

The joint probability distribution can be used to make inferences about the origin of the measured waves (MACKY *et al.*, 1995), thereby allowing the relative importance of sea (locally generated) and swell waves to be assessed. The Shore Protection Manual (USACE, 1984) presents equations for significant wave height ( $H_s$ ) and significant wave period ( $T_s$ ) in a fully-arisen sea, which can be combined and used to differentiate between swell and sea waves:

$$\frac{H_s}{(gT_s)} = 0.00408 \quad 5.1$$

This function defines the maximum wave height for a given wave period above which wave breaking occurs, and can hence be regarded as a measure of wave steepness (MACKY *et al.*, 1995). Figure 5.7 illustrates joint  $H_s$  and  $T_s$  scatter distributions at WAI1 for both of the S4 deployments at that location. Equation 5.1 has been added to determine whether waves recorded were locally generated sea waves or swell waves generated some distance from the location of the S4's.

The critical wave steepness is exceeded on several occasions indicating the presence of sea waves, generally associated with larger wave heights. MACKY *et al.* (1995) reported similar findings from waves recorded in 34 m water depth off the Katikati inlet, and suggested that the measured waves lying above the line of



**Figure 5.7:** Joint distribution of significant wave height and period for both deployments at WAI1/WAI1b. Red triangles represent the summer deployment (15/11/07 – 15/12/07) and blue circles represent the winter deployment (28/05/08 – 25/06/08). The curved line marks the limit between sea and swell waves (USACE, 1984).

critical steepness were likely to have been generated within about 500 km of the wave buoy. From Figure 5.7 it appears that locally generated “seas” from storm systems within the Bay of Plenty were probably responsible for the waves above 2 m during both the summer and winter deployments.

For the majority of waves however, wave steepness was much less than 0.00408 indicating a swell dominated wave climate, where waves originate some distance from the S4 and have decayed significantly before reaching the instrument location. Alternatively, some of the waves below the critical limit may represent measurements of subsiding waves in a post storm period (MACKY *et al.*, 1995). Distantly-generated swell waves tend to be associated with lower wave heights compared to that of locally generated sea waves, as wave height has reduced due to wave energy dissipation (SILVESTER and HSU, 1997).

Sea waves tend to be steeper than swell waves, and therefore plot closer to the curve of limiting steepness. Hence, contoured joint probability distributions of real waves tend to be bimodal. This trend is represented in Figure 5.7, especially so in the winter data. One limb associated with above average wave heights and a wave period of 6-6.5 s extends vertically from the main cluster of data. A second limb extending horizontally is characterised by small wave heights with increasingly long periods up to ~11.5 s. A similar pattern was observed by DE LANGE (1990, 1991) and SPIERS (2005) from studies at Tauranga and Mount Maunganui, which suggests that the first limb probably represents locally generated seas, whereas the second limb is indicative of swell waves originating some distance away. DE LANGE (1991) concludes that the typical wave climate in the Bay of Plenty consists of a persistent long period swell with locally-generated sea superimposed, a trend which is also apparent in this data set.

In summary, the scatter distributions of  $H_s$  and  $T_s$  for WAI1 for both deployments demonstrate a dominance of swell waves, with a small but significant cluster of sea waves restricted to wave heights over 2 m. This is consistent with findings from HARRAY (1977), who reported that low swell waves are dominant at Waihi Beach.

## 5.2 CURRENTS

### 5.2.1 Methods

#### 5.2.1.1 Data Collection

Current measurements were obtained from the same S4 wave meters that were deployed 1 m above the seabed in ~6 m water depth at three positions along Waihi Beach (Figure 5.2 and Table 5.1). The same sampling regime was used with the burst mode recording for 18 minutes every hour at 2 Hz.

#### 5.2.1.2 Data Analysis

Current data were retrieved from the S4s and analysed using S4 Application Software (S4APP). This programme graphically resolves current velocities, directions and water depth, which can then be converted into ASCII format for further analysis using Matlab. Before any detailed analyses of current data could be undertaken, the raw orbital velocity and directional data output from the S4 were first converted into a more useful form. As with wave data, a magnetic variation of 21.5°E was added to the raw data to orientate the statistics relative to True North. The data were then converted to radians and resolved into N-S and E-W velocity components, as most analyses work more effectively if the data are in the form of velocity vectors. This conversion involves standard trigonometric relationships. The N-S and E-W components calculated from the measured variables “speed” and “direction” for each 18 minute burst were then extracted and the total number of values per burst (2160) averaged. The N-S and E-W velocity components were squared and summed, with the square root of the resulting values taken to determine the current speed at 1 m above the bed. Current direction was calculated using the Matlab function ‘atan2’.

A further problem encountered is that Matlab uses Cartesian conventions, so that 0° is along the x-axis and angles increase anticlockwise. However, all marine instruments including S4’s measure compass directions where 0° is along the y-



axis and angles increase clockwise. In order to correctly display the directional plots utilised for this analysis, it was necessary to convert the directional data from compass directions to Cartesian coordinates, then express the angles in radians instead of degrees and resolve N-S and E-W velocity vectors.

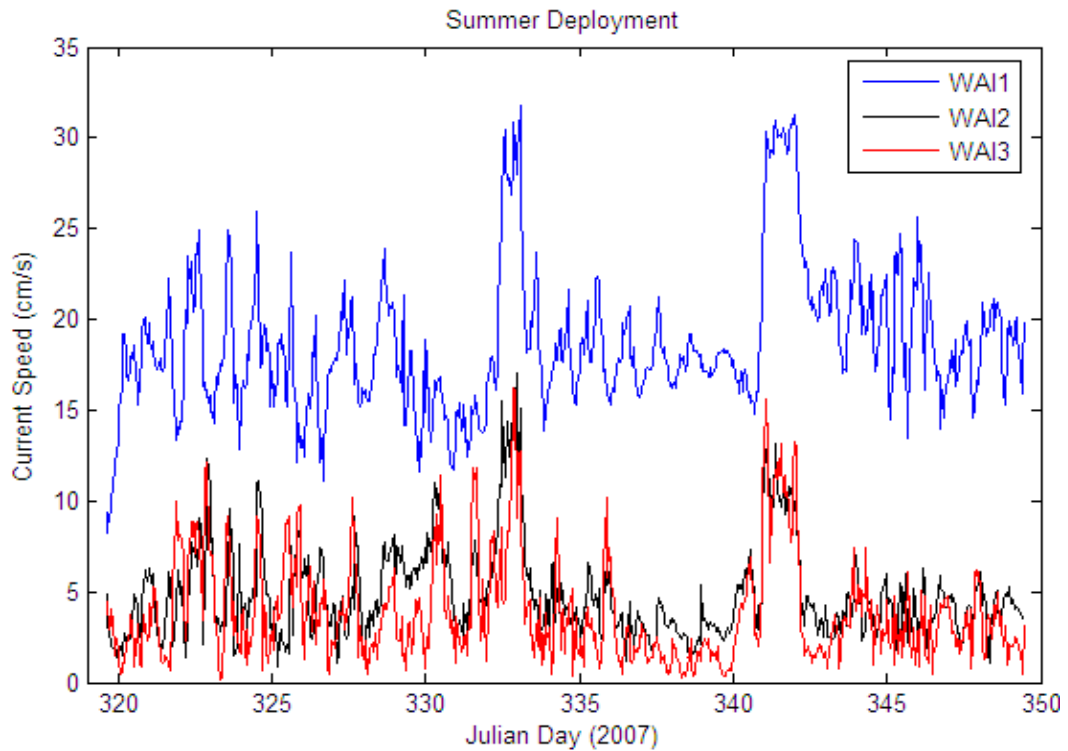
A comprehensive analysis using monochromatic techniques was undertaken using a series of Matlab scripts written by the author for the purpose of examining the behaviour of nearshore currents at northern Waihi Beach. General trends in current speed and direction observed over the deployment periods are described in the following section.

## 5.2.2 *Results*

### 5.2.2.1 Current Characteristics

During the summer deployment, current velocities in 6 m water depth range between 0.17 and 31.78 cm/s (Figure 5.8). The strongest currents were observed at WAI1 off Rapatiotio Point, with all measurements typically twice the speed of those recorded at the other two S4 locations. The mean current speed at WAI1 was 18.66 cm/s, compared to 4.86 cm/s and 3.87 cm/s at WAI2 and WAI3 respectively (Table 5.3). A reasonable explanation for this strong spatial variation in current speeds becomes apparent upon examination of current directions and alongshore distribution in measured wave heights.

Figure 5.9a illustrates that current directions measured at WAI1 were predominantly (> 70%) towards the northeast, which is offshore at Waihi Beach. In contrast, at WAI3 (Figure 5.9c) and similarly at WAI2, the predominant current directions recorded were alongshore (i.e. flow towards the northeast or southwest). Therefore, the significantly stronger offshore currents recorded at the far northern end of Waihi Beach may possibly be rip currents being picked up by the S4 WAI1 near Rapatiotio Point. Unfortunately, there is no conformational evidence which proves these strong offshore currents are in fact rips, although they have been previously reported at northern Waihi Beach by STEPHENS (1996).

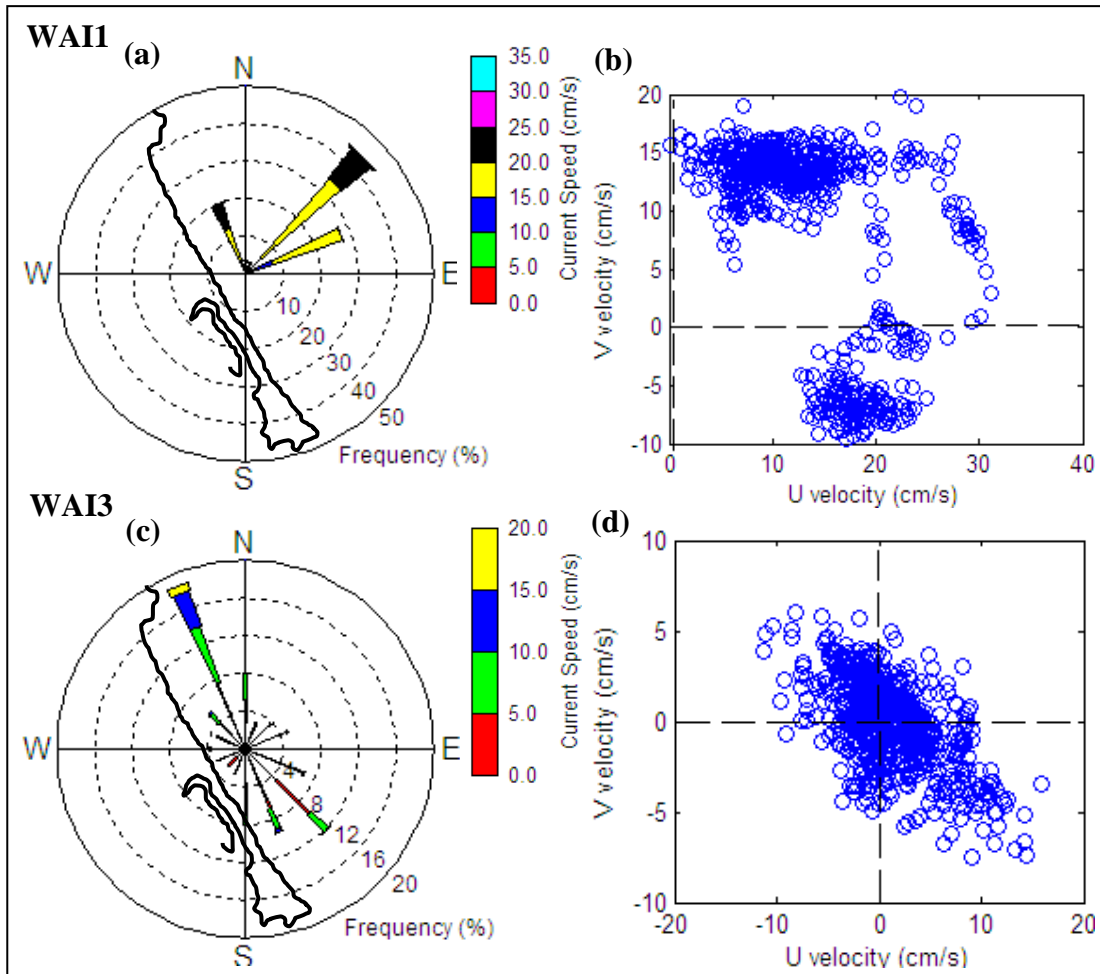


**Figure 5.8:** Mean current speeds recorded off northern Waihi Beach during the summer deployment (15/11/07 – 15/12/07) at WAI1 (blue), WAI2 (black) and WAI3 (red).

Where wave heights are greatest along the wave crest, the wave set-up is also greatest and horizontal pressure gradients are established between areas of higher and lower wave set-up. Water therefore tends to flow from positions of higher to lower wave height, generating longshore currents. Wave analysis in the previous section revealed that significant wave heights measured by the S4's at WAI2 and WAI3 during the summer deployment were consistently larger than those recorded by WAI1 off Rapatiotio Point. This implies that a pressure gradient exists between the S4 sites, and is likely to be generating a longshore current

**Table 5.3:** Current statistics for northern Waihi Beach during the summer (15/11/07-15/12/07) and winter deployments (07/05/08-04/06/08 for WAI3b; 28/05/08-25/06/08 for WAI1b). Currents were measured at 1 m above the seabed in 6 m water depth at the three S4 locations. \*Refers to the direction the currents are moving towards.

	Summer Deployment			Winter Deployment	
	WAI1	WAI2	WAI3	WAI1b	WAI3b
Mean Speed (cm/s)	18.66	4.86	3.87	6.05	11.15
Minimum Speed (cm/s)	8.28	0.89	0.17	0.17	1.28
Maximum Speed (cm/s)	31.78	17.03	16.24	37.98	45.82
Mean Direction (°)*	33.33	328.08	353.85	357.02	237.18



**Figure 5.9:** Summary plots of current speed and direction (True) at 1 m above the sea bed during the summer S4 deployment period (15/11/07 – 15/12/07). Rose plots of current direction and speed recorded at WAI1 (a) and WAI3 (c) have the Waihi Beach shoreline superimposed. N-S and E-W vector plot incorporating current direction and speed at WAI1 (b) and WAI3 (d). All plots show the direction towards which the currents flowed. Because the Waihi Beach coastline runs almost north-south, the E-W velocities are assumed to correspond to onshore-offshore.

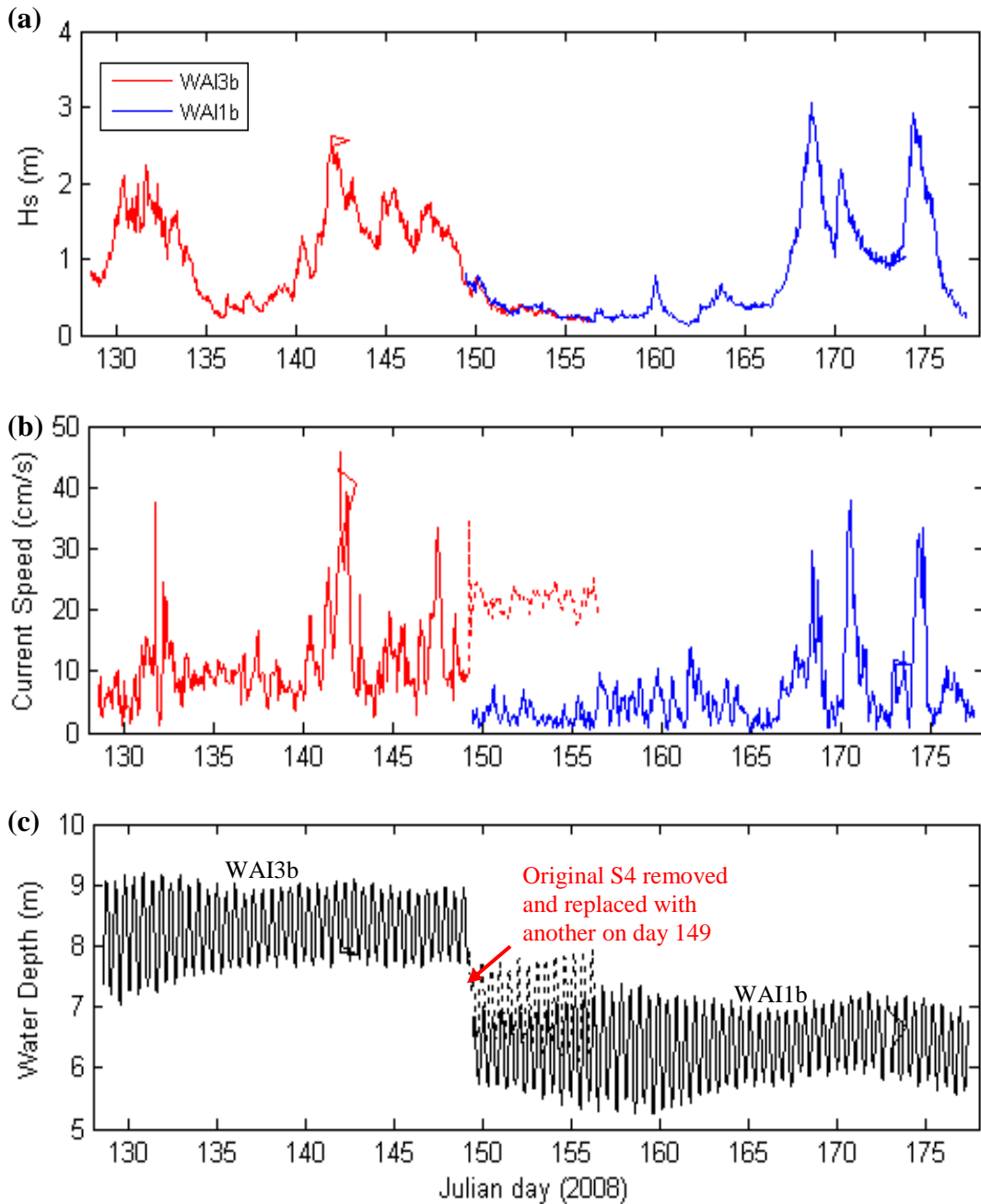
flowing towards the northwest. The persistent northwesterly directed currents, as recorded at WAI2 and WAI3 (Figure 5.9c), result in a piling up of water against the headland at the far northern end of the beach which is then forced offshore. Another possible explanation for the predominance of currents to the northeast at WAI1 could be a tidally driven phase eddy that spins up the southeastern side of Rapatiotio Point, such as those observed at West End Ohope Beach by SAUNDERS (1999) and at Cape Rodney by HUME *et al.* (2000). In situations where headlands protrude into strong tidal flows, the tidal current residuals associated with large phase eddies are strongly directed along the shoreface toward the tip of the headland (HUME *et al.*, 2000). This provides a mechanism to transport sand from the beach and shoreface flanking the headland towards the tip of the headland.

From here the sand is most likely lost offshore to deeper water or re-circulated by eddy flows back to the beach (HUME *et al.*, 2000). Further investigations into current patterns off Rapatiotio Point would be required to provide conformational evidence for the existence of an eddy.

The rose plot of current direction at WAI1 (Figure 5.9a) demonstrates that only a narrow band of current directions ( $306^{\circ}$ – $68^{\circ}$  True) were recorded at that location during the summer deployment, compared to a much more varied current regime at WAI3 (Figure 5.9c) and WAI2 over the same period. It is believed that the limited distribution of current directions recorded at WAI1 is likely to be a result of the sheltering effect caused by Rapatiotio Point, which appears to be the major factor controlling current directions at the northern end of the beach. Figure 5.9c shows that at WAI3, alongshore currents flowing towards the northwest are stronger and more persistent than those flowing southeast.

Directional changes in the bottom currents capable of entraining and transporting sediments are noticeable in the alongshore and onshore-offshore current velocity plot for WAI1 (Figure 5.9b). U currents show that during peak storm conditions current speeds may have been capable of transporting fine sand material offshore, exceeding the 18 cm/s threshold value suggested by BRADSHAW (1991) for the East Coromandel inner shelf. For the northeast coast of New Zealand, HARRIS *et al.* (1983) suggest that the threshold velocity for fine sand (0.2 mm) is 18 to 22 cm/s. At WAI3 (Figure 5.9d), where alongshore currents are predominant, both the northwest and southeast bottom currents observed are not strong enough to generate sediment transport (i.e. measured U velocities always  $<17$  cm/s), although they would be with superimposed wave orbital velocities.

Figure 5.10 illustrates mean current speeds measured by S4's WAI1b and WAI3b during the winter deployment period at Waihi Beach. In an attempt to identify the underlying causes for the trends observed, significant wave heights ( $H_s$ ) and water depth (demonstrating tidal variation) measured over the same time period have also been plotted to try and distinguish possible relationships between the data sets. Upon analysis of the depth data (Figure 5.10c) at WAI3b there appears to be



**Figure 5.10:** Time series plots showing (a) significant wave heights ( $H_s$ ) and (b) mean current speeds recorded off northern Waihi Beach during the winter deployment (07/05/08 – 25/06/08) at WAI1b (blue) and WAI3b (red). A time series of water depths is also provided (c) to illustrate the difference between the depths at the two instrument locations, and the influence of semi-diurnal tidal waves on measured current speeds. Note that the dotted lines indicate faulty data, which have therefore been eliminated from further analyses.

a decrease of 1-1.5 m in the measured water depths from day 149 onwards, coinciding with the date when the original S4 deployed at WAI3b was replaced by another with a full battery. Because the replacement S4 was deployed in the exact location and mounted upon the same frame as the previous instrument, the apparent “drop” in water depth observed is likely due to a malfunction in the S4

recording set-up. Consequently, it is believed that these unusual depth values may be the cause of the significantly higher current speeds observed at WAI3b between days 150 and 158 (indicated by the dotted line in Figure 5.10b), compared to that of WAI1b over the same period. Due to the uncertainty as to the reliability of this data, the final 8 days of current speed and direction information collected at WAI3b from the winter deployment have been eliminated from further analyses, leaving only the initial 21 days (days 128-149) of reliable data.

Nearshore current records during the winter deployment reached a maximum speed of 45.82 cm/s, with mean speeds of 6.05 cm/s at WAI1b and 11.15 cm/s at WAI3b (Table 5.3). The mean current direction at WAI1b was towards 357° and 237° at WAI3b, although analysis of the time series of directions showed that they were well dispersed. The difference in mean direction between WAI1 and WAI1b indicates that offshore currents did not play as big a role at this location during the winter deployment as they did during the summer, with alongshore currents persisting throughout the entire winter record. As with the summer deployment there is a great amount of variation in current speeds (Figure 5.10b). A comparison of wave heights and current speeds in Figure 5.10a and b shows excellent correlation. In general, as wave height increases there is a corresponding increase in current velocity that also displays great temporal variability, indicating that these currents are wave-generated. There also appears to be an underlying cyclical trend associated with the semi-diurnal tidal wave, particularly noticeable during the calm period between days 155-165, where the slight increase in current speeds can be associated with the increased water depths due to the spring tide.

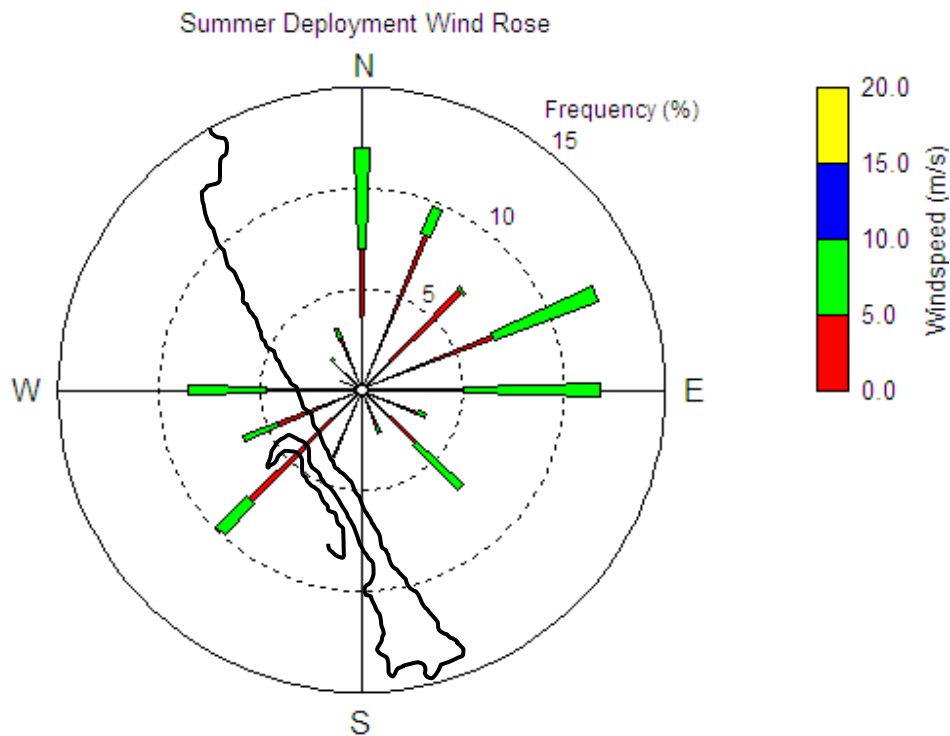
## 5.3 WIND

### 5.3.1 *Wind Characteristics*

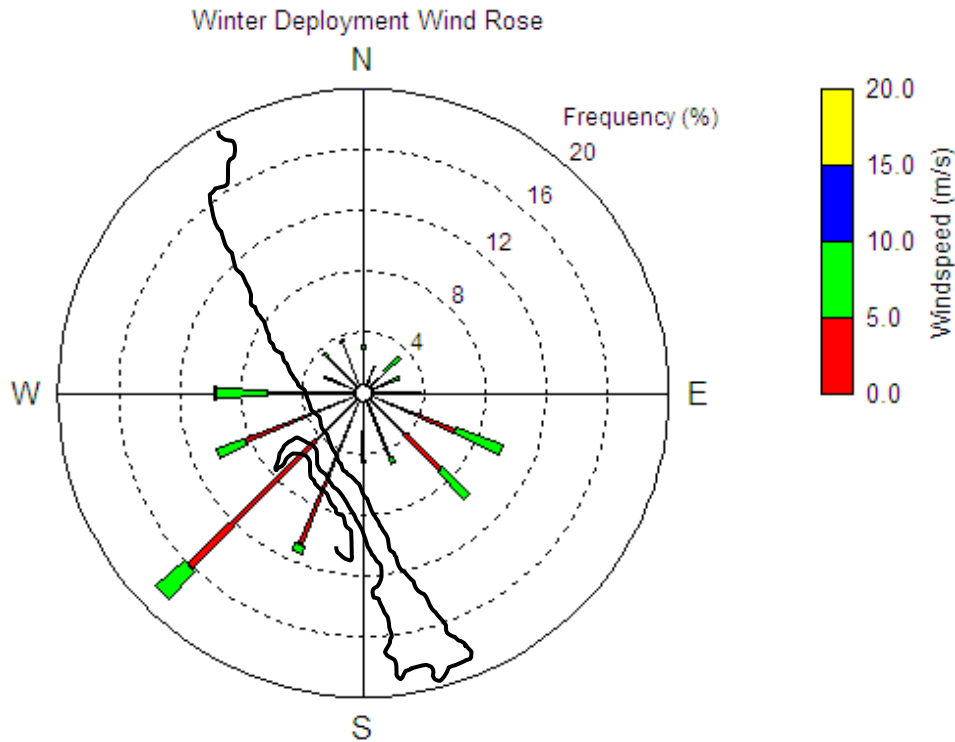
Wind records coinciding with both the S4 deployment periods were obtained from the NIWA Climate Database (CliFlo) for the Tauranga Airport (37.673°S, 176.196°E) site, approximately 35 km southeast of Waihi Beach. Measurements

were taken hourly, providing mean wind speeds and directions which are summarised in Figure 5.11 and 5.12 for the summer and winter deployment periods respectively. During the summer deployment period the wind direction appears to be well dispersed recording both onshore and offshore winds. North to east (onshore) airflows prevail for approximately 50% of the period analysed.

The hourly wind speeds were only slight to moderate during the summer deployment, with velocities generally less than 5 m/s (~70%) with a minimum of 0.5 m/s and a maximum of 8.8 m/s. The mean wind velocity recorded during this period was 3.84 m/s. In comparison to the summer deployment, wind direction data recorded during the winter deployment proved to be less variable, primarily from 110° to 270°. Winds from the southwest were most dominant, although only occurring for ~18% of the period analysed. Offshore winds occurred approximately 42% of the time. Wind speeds were generally low, with a range of 0.5-10.3 m/s and a mean velocity of 3.24 m/s. 85% of the wind speeds recorded were less than 5 m/s and wind speeds only exceed 10 m/s on two occasions. Southwesterly winds accounted for ~20% of the winds exceeding 5 m/s.



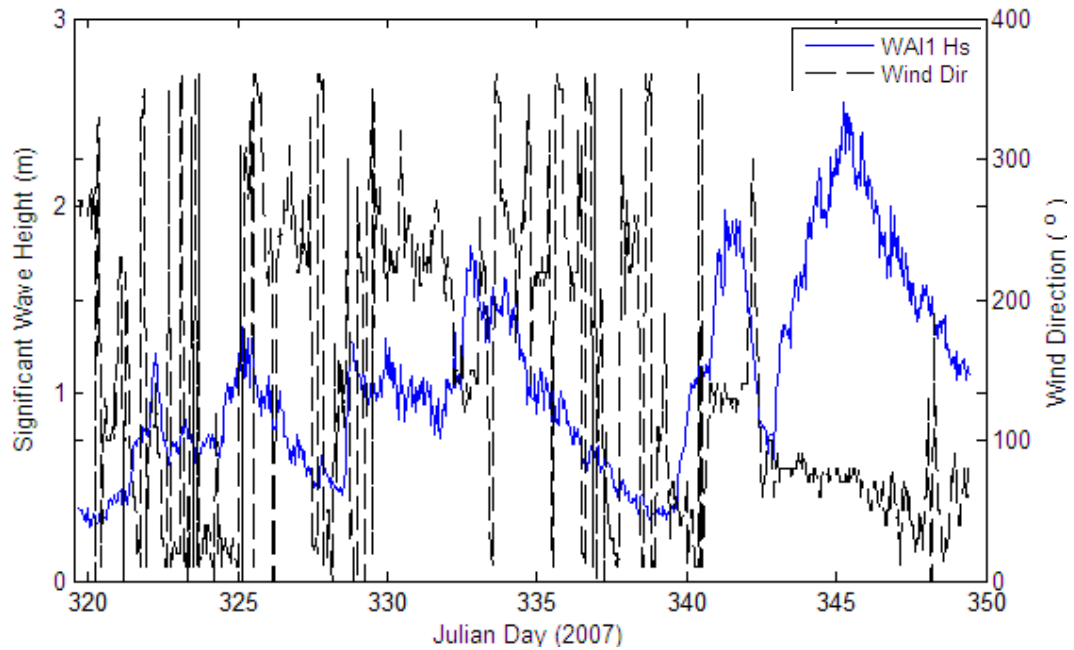
**Figure 5.11:** Rose plot of wind direction and velocity (Tauranga Airport) corresponding to the summer S4 deployment (15/11/07 – 15/12/07). The direction refers to the direction from which the wind came. The shoreline of Waihi Beach is superimposed.



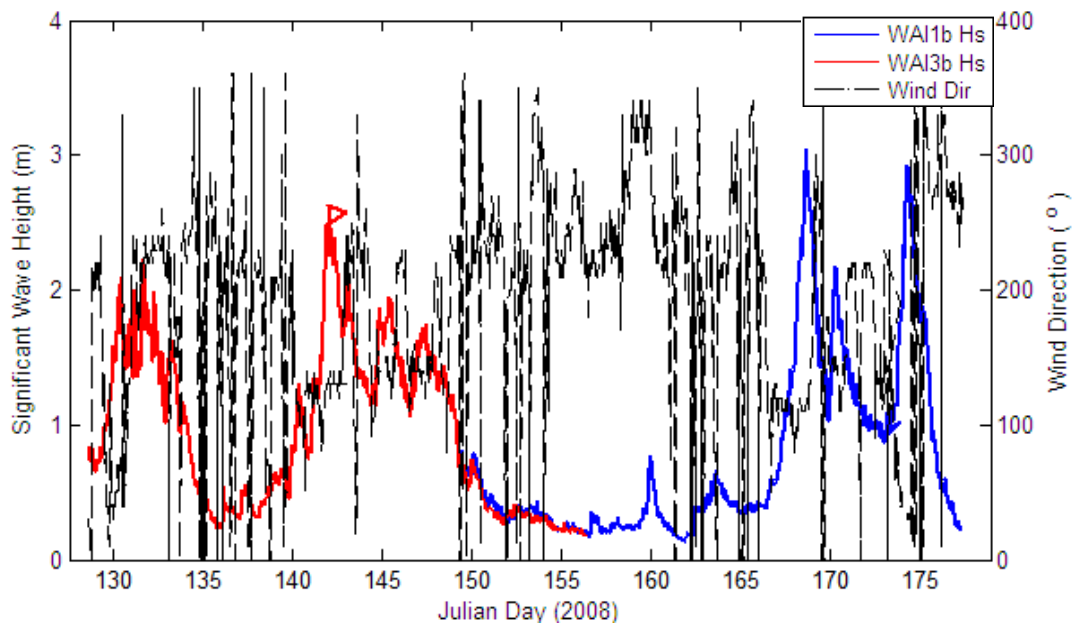
**Figure 5.12:** Rose plot of wind direction and velocity (Tauranga Airport) corresponding to the winter S4 deployment (07/05/08 – 25/06/08). The direction refers to the direction from which the wind came. The shoreline of Waihi Beach is superimposed.

There is a strong relationship between onshore and offshore winds and the generation of waves in the nearshore zone at Waihi Beach. Comparisons between  $H_s$  and wind direction for both the summer and winter S4 deployment periods (Figures 5.13 and 5.14) shows that the larger wave events are generally associated with strong onshore winds (east to northeasterly). This pattern is most obvious in the final and largest swell event of the summer deployment (Figure 5.14) with northeasterlies dominating from day 343 to the end of the deployment period. Swell events between days 323-325, 332-333, 339-340 (2007) and 140-142, 167-169 (2008) during the summer and winter deployments respectively, are also characterised by a pattern of northeasterly to southeasterly winds. In most cases after the peak  $H_s$  has been reached, west to northwesterlies dominate. The prolonged period of calm between days 151-159 of the winter deployment period is typified by offshore winds, which vary from southwesterly through to northwesterly.





**Figure 5.13:** Time series plot of significant wave height ( $H_s$ ) and wind direction at northern Waihi Beach over the summer S4 deployment period (15/11/07 – 15/12/07).  $H_s$  values represent those recorded at WAI1 (blue) and wind direction (black) is from the Tauranga Airport.

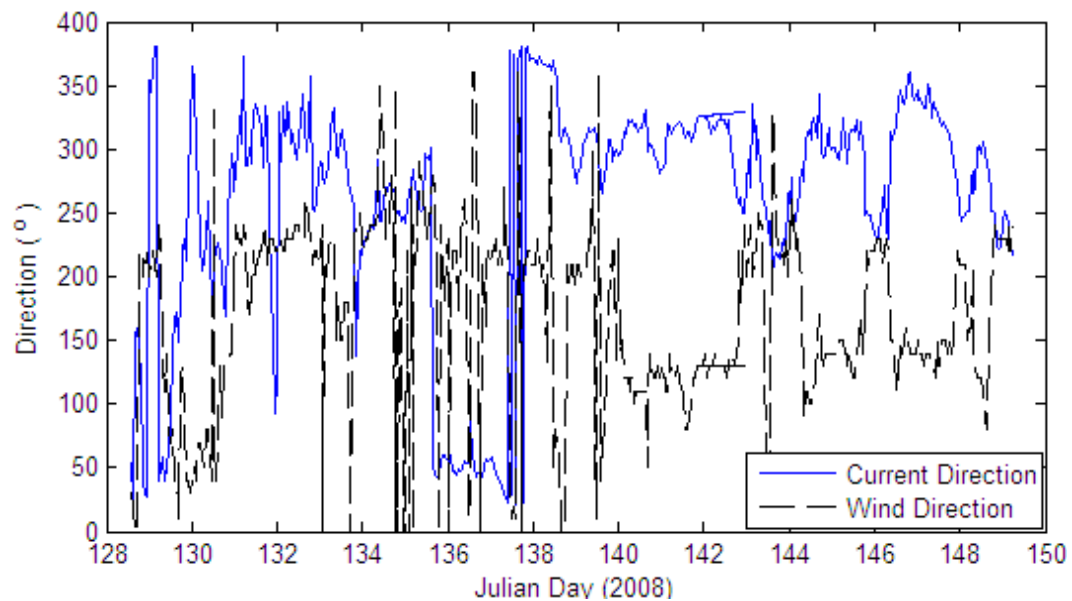


**Figure 5.14:** Time series plot of significant wave height ( $H_s$ ) and wind direction at northern Waihi Beach over the winter S4 deployment period (07/05/08 – 25/06/08).  $H_s$  values represent those recorded at WAI1b (blue) and WAI3b (red) and wind direction (black) is from the Tauranga Airport.

5.3.2 *The Influence of Wind on Nearshore Current Generation*

Direction and velocity data obtained for both winds and currents throughout the S4 deployment periods were examined to determine the role of wind on currents in the area. Comparison between the nearshore currents at WAI1 and the corresponding wind record suggest that wind direction does not have any apparent effect upon current direction at that location, although variation in current velocity does slightly resemble similar oscillations in wind speed. This is consistent with the idea that the strong offshore currents recorded at WAI1 during the summer deployment were likely due to a rip current fed by long-shore directed currents within the surf zone.

Comparison of wind and current records for the remaining S4 locations during both summer and winter revealed that the near-bed current typically counteracts the approaching wind direction. For example, the time series of current and wind direction over the first half of the winter deployment (Figure 5.15) shows that offshore-directed winds blowing from the southwest are associated with ~southwesterly onshore currents. Offshore winds forcing onshore currents are

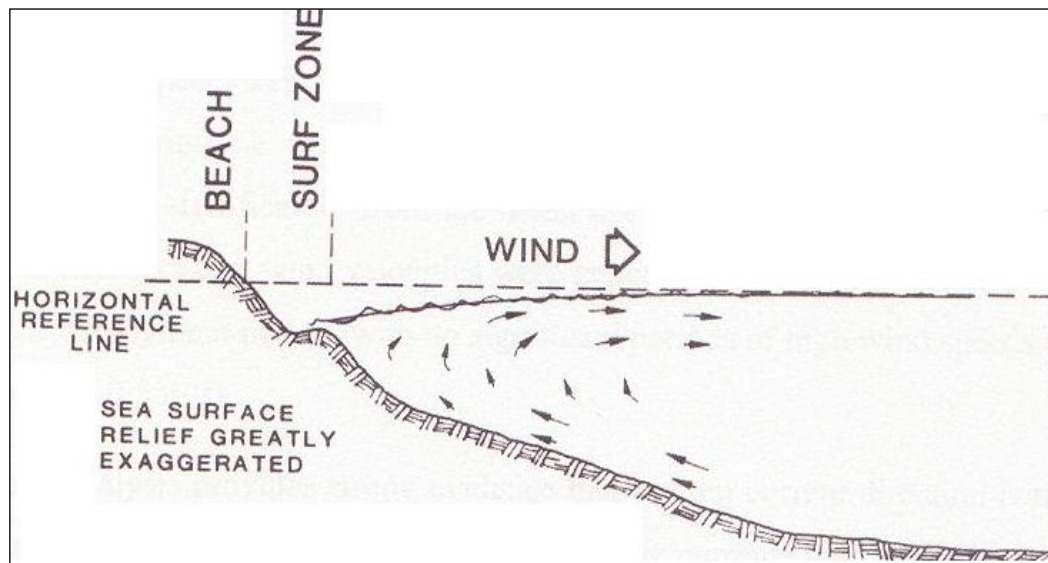


**Figure 5.15:** Time series plot of current direction and wind direction over the winter S4 deployment (07/05/08 – 25/06/08). Current direction data represent those recorded over the first half of the winter deployment at WAI3b (blue) and wind direction (black) is from the Tauranga Airport. Current direction refers to the direction the current is travelling toward, whereas wind direction relates to the direction from which the wind came.

indicative of coastal upwelling (Figure 5.16) (NIEDORODA *et al.*, 1985). An upwelling circulation occurs when offshore wind stresses drive surface waters in a similar direction. In the friction dominated zone, where Coriolis force has a limited effect, the result is localised set down of the sea level and a compensating onshore directed near bed current (NIEDORODA *et al.*, 1985; WRIGHT, 1995).

A second major trend observed throughout both summer and winter deployment records is that periods of onshore ~east to east-southeasterly winds correspond with north to northwesterly alongshore currents. However, current direction was maintained in a northwesterly direction during the southwesterly wind burst earlier in the record (Julian days 131 – 134) despite changes in wind approach, suggesting that there may be other factors influencing current circulation in the area. Observed wind and current patterns at all S4 locations (excluding WAI1) appear to alternate between these two identified trends. This is particularly noticeable in Figure 5.15 from Julian 139.5 onwards.

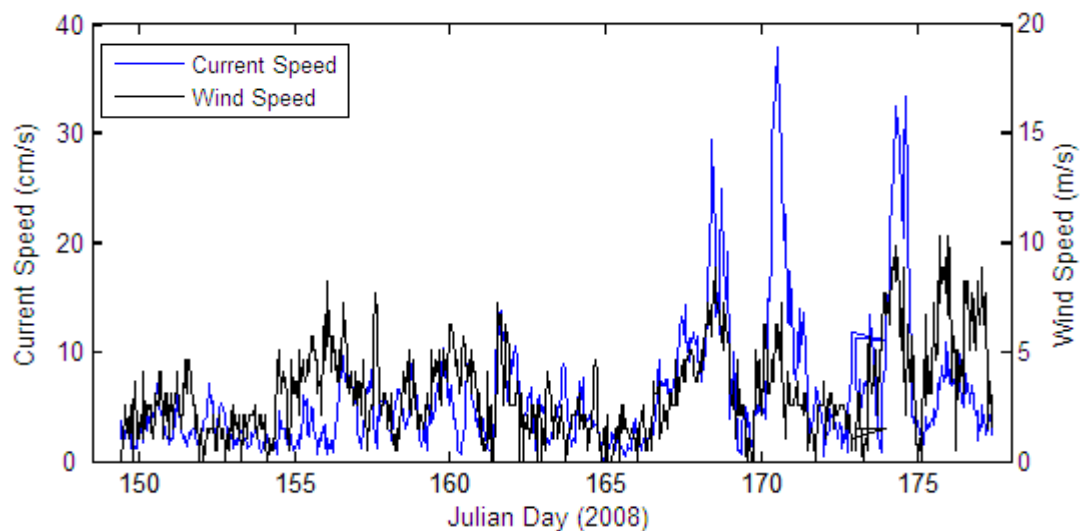
Figure 5.17 indicates that oscillations in wind speed coincide with current speed oscillations, with current velocity typically increasing during periods of increased wind speeds. The absence of a lag suggests that wind speed has an almost



**Figure 5.16:** Schematic of an upwelling circulation pattern in the friction dominated zone. Source: NIEDORODA *et al.* (1985). Note that an offshore wind results in localised set down of the sea level and a compensating onshore-directed bottom current (NIEDORODA *et al.*, 1985).

immediate effect on current magnitude near the seabed. However, the fastest wind speeds recorded during the winter period do not occur in concordance with the greatest current velocities, i.e. the magnitude of change is not so well correlated. For example, it can be seen in Figure 5.17 that the three major peaks in current velocity near the end of the winter deployment reveal speeds of a much higher magnitude ( $>30$  cm/s) than the remainder of the record; and yet the corresponding increase in wind speeds, although typically greater than the mean velocity, are only slightly higher than the rest of the time series associated with slower currents. This may be a result of generally low wind velocities, with no significant periods of high wind speeds recorded during either deployment. Furthermore, the data were collected from Tauranga and thus may not be an accurate representation of the wind conditions experienced at Waihi Beach during the deployment period.

Alongshore directed north to northwest currents are associated with the strongest current velocities recorded throughout the deployment period. By contrast, onshore currents (west to southwest) were observed to be relatively weak. Analysis suggests that west to southwest airstreams, which were observed to be dominant during the winter deployment, will tend to generate only weak onshore directed currents. Hence, alongshore currents associated with strong onshore east to east-southeasterly winds demonstrate the greatest potential for sediment transport at northern Waihi Beach.



**Figure 5.17:** Time series plot current speed (cm/s) (blue; measured at WAI1b 1 m above the seabed) and wind speed (m/s) (black; from the Tauranga Airport) over the second half of the winter S4 deployment (28/05/08 – 25/06/08). Current speed has been plotted in cm/s to enable good visual comparison between the two data sets.

## 5.4 SEDIMENT TRANSPORT AND INCIPIENT MOTION BY WAVES AND CURRENTS

### 5.4.1 Introduction

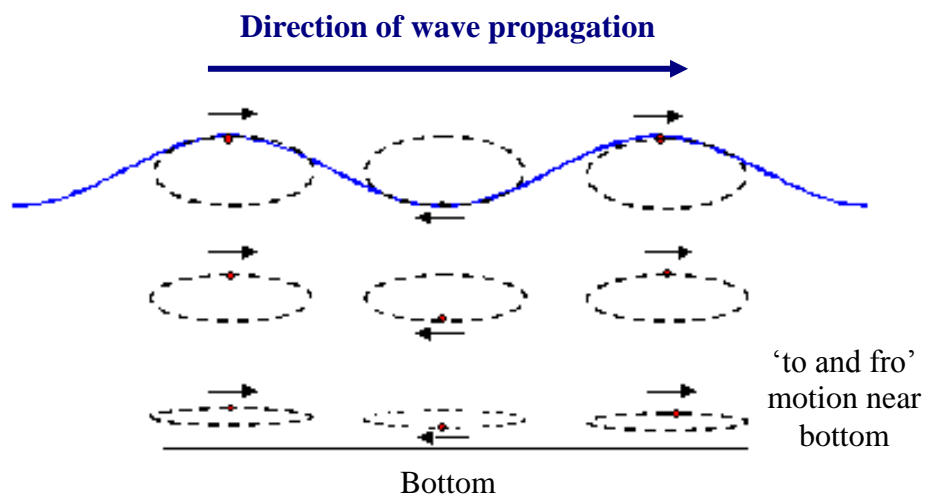
The study of initiation of sediment motion under steady flows and under waves and predictions of critical threshold velocities are of practical importance in sediment transport calculations. The ‘critical threshold’ for sediment movement refers to the velocity when water is flowing over a bed of unconsolidated sediment at which the shear stress acting on these sediment particles will be sufficient to dislodge them from the bed; causing incipient motion to occur (MILLER *et al.*, 1977; DYER, 1986; BEHESHTI and ATAIE-ASHTIANI, 2008; BOHLING, *in press*). Once critical sediment transport rates are known, assumptions as to whether certain conditions will be periods of accretion or erosion can be determined.

The circumstances necessary to initiate sediment motion are a function of the sediment size and density, the fluid density and viscosity, and the flow conditions (average velocity or intensity of turbulent stresses) (MILLER *et al.*, 1977; NIELSON, 1992). Therefore, a combination of the sediment characteristics determined from RSA textural analyses (Chapter 4) along with wave and current data collected during the S4 and ADV deployments were required to calculate critical threshold values for wave orbital velocities and near-bed currents at each instrument location.

### 5.4.2 Incipient Motion Induced by Waves

Waves are the dominant entrainment mechanism for sediment, producing oscillatory and rapidly varying currents. Surface waves produce an oscillatory motion in the water, the water particles following circular paths if the water is deep, and elliptical paths in the case of waves in intermediate and shallow water (Figure 5.18). Near the bottom, the elliptical motion is reduced to a to-and-fro horizontal movement (KOMAR, 1998). As the near-bed wave orbital velocity is

gradually increased over the bed of sediment, there comes a stage when a few sediment particles start to move. This moment is generally known as the initial motion of sediment under waves (YOU, 2000) and largely determines the extent of sediment transport in the nearshore zone. As sediment motion is initiated, the sediment is thrown off the bottom and entrained by mean flows. The majority of sediment transport occurs close to the seabed (VINCENT *et al.*, 1982; VINCENT and DOWNING, 1994), predominantly during storm conditions which induce large waves and stronger bottom currents (VINCENT *et al.*, 1982).



**Figure 5.18:** A diagram illustrating the orbital motions of waves in intermediate water depths where the orbits are elliptical, but become flatter and smaller as the bottom is approached. Adapted from OPEN UNIVERSITY (2002).

The threshold velocity for sediments due to near-bed wave orbital velocities is evaluated using relationships derived by KOMAR and MILLER (1975). Studies of initial motion of sediment in oscillatory flow using these methods have previously been applied in studies by SAUNDERS (1999) and SPIERS (2004). Threshold values are compared with predicted near-bed wave orbital velocities ( $U_w$ ), taken to be the maximum velocity at which a given water particle moves, in order to determine the frequency for which the threshold is exceeded. The wave orbital velocities are calculated using the data obtained during both S4 and ADV deployments.

KOMAR and MILLER (1975) concluded that for sediment grain diameters less than 0.5 mm (medium sands and finer), the threshold under waves is best related by the following equation:

$$\frac{\rho U_w^2}{(\rho_s - \rho)gD} = a'' \left( \frac{d_o}{D} \right)^{1/2} \quad 5.2$$

where  $U_w$  is the near-bottom orbital velocity,  $d_o$  is the orbital diameter of the wave motion ( $d_o = U_w T / 2\pi$ ),  $D$  is the grain diameter,  $\rho_s$  is the sediment density which is assumed to be quartz ( $2,650 \text{ kg.m}^{-3}$ ), and  $\rho$  is the density of water ( $1,025 \text{ kg.m}^{-3}$ ). For  $a''$ , the empirical proportionality coefficient, a value of 0.21 is recommended (KOMAR and MILLER, 1975).

Because KOMAR and MILLER's (1975) theory assumes that the bed is flat, this means that the form drag and skin friction parameters are not considered. According to KOMAR and MILLER (1975), the application of this technique can be further simplified given that the threshold for a given grain size and density can be specified by a single combination of wave period and orbital velocity. The longer the wave period the lower the shear stress, meaning that a greater orbital velocity is required to exceed critical threshold and initiate movement (KOMAR and MILLER, 1975; KOMAR, 1976), resulting in less erosion. This implies that different wave periods have differing threshold velocities, given a constant wave size. One limitation of this method, however, is that it assumes the waves to be sinusoidal in shape and therefore very stable, but in reality the orbital motions of sea waves are typically irregular (KOMAR, 1976).

The point at which sediment motion is initiated was investigated by GREEN (1999), who tested three different methodologies and found that KOMAR and MILLER's (1975) wave-orbital-speed theory provided the best predictions of the onset of sediment motion when waves were characterised by significant wave height ( $H_s$ ) and mean spectral period ( $\bar{T}$ ). Assuming linear Airy-wave theory, these two parameters are combined and the corresponding maximum horizontal orbital velocity at the bed calculated by:

$$U_w = \frac{\pi H_s \cosh(kh)}{\bar{T} \sinh(kh) \cosh(k(z_p + h))} \quad 5.3$$

where  $z_p$  is the height of the pressure sensor above the bed and  $k$  is the wave number, defined by KOMAR (1998) as:

$$k = \frac{2\pi}{L} \quad 5.4$$

with wave length ( $L$ ) calculated by:

$$L = \frac{g}{2\pi} T^2 \tanh\left(\frac{2\pi h}{L}\right) \quad 5.5$$

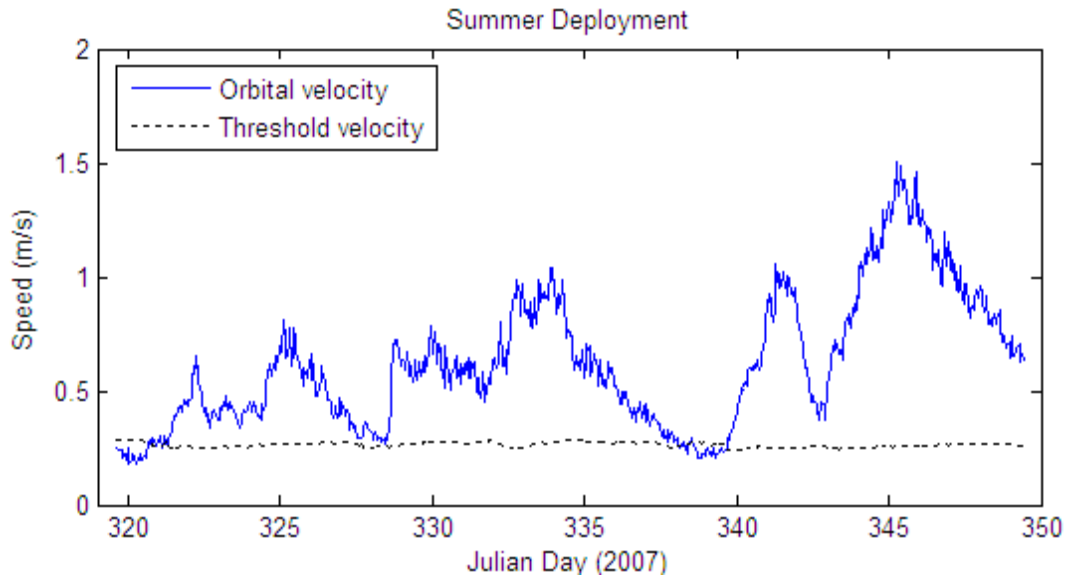
This relationship is difficult to solve directly in that it contains the wave length on both sides of the equation. KOMAR (1998) shows that in shallow water this equation can be simplified to:

$$L = T\sqrt{gh} \quad 5.6$$

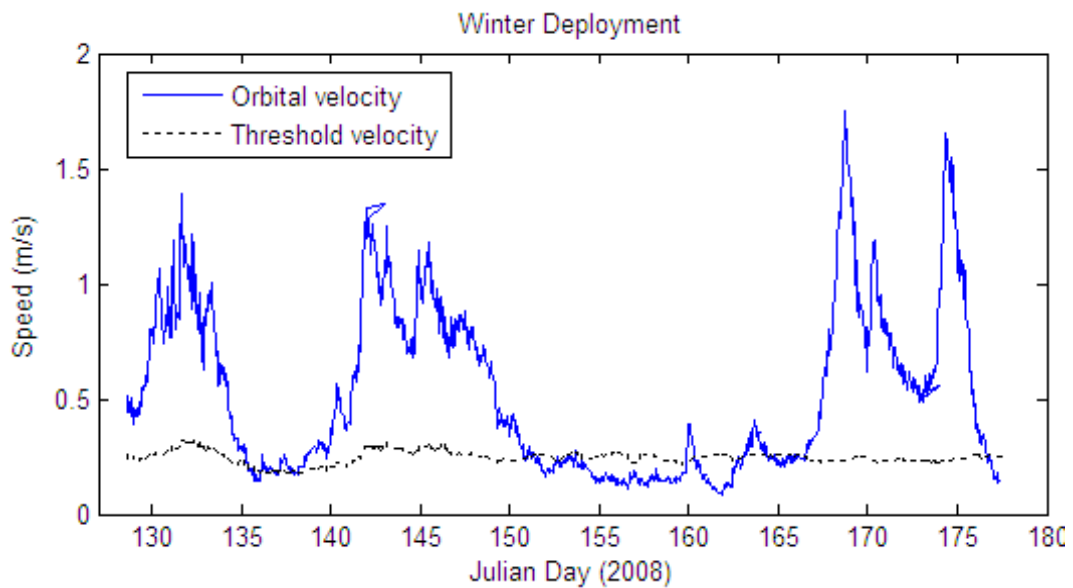
Following the methodology of SAUNDERS (1999) and SPIERS (2004), time series data of near-bed orbital velocities using  $H_s$  and  $\bar{T}$  at 6 m depth were evaluated to determine how often they exceeded the critical threshold velocity. This was undertaken using averaged wave data from the S4 sites for each separate deployment.

Figure 5.19 indicates that during the summer deployment period sediments at 6 m water depth were constantly agitated by waves, with the wave orbital velocity ( $U_w$ ) exceeding the sediment threshold 96% of the time due to a consistent swell. Similarly, during the winter period (Figure 5.20), the critical threshold velocity was commonly exceeded (86% of the deployment period). It is mainly during the period of prolonged calm weather and sea conditions between Julian days 151-163 that  $U_w$  dropped below the threshold for sediment motion. Overall, these results indicate that sediments at this depth are generally mobile.





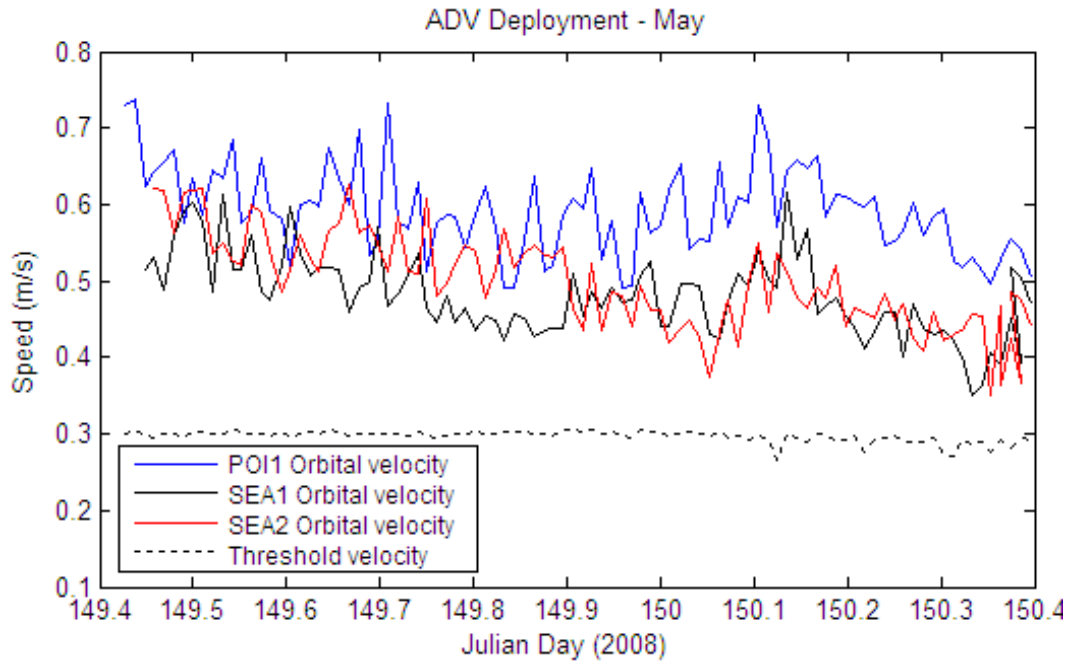
**Figure 5.19:** Near-bed orbital velocities ( $U_w$ ) at northern Waihi Beach during the summer S4 deployment, compared to the critical threshold velocity for sediment movement determined using the KOMAR and MILLER (1975) wave-orbital-speed theory.  $H_s$  and  $\bar{T}$  were used to calculate near-bed orbital velocities using linear Airy-wave theory. The time series of orbital velocities and critical threshold velocities shown represent the average values of the data from all three S4's deployed during the summer period.



**Figure 5.20:** Near-bed orbital velocities ( $U_w$ ) at northern Waihi Beach during the winter S4 deployment, compared to the critical threshold velocity for sediment movement determined using the KOMAR and MILLER (1975) wave-orbital-speed theory.  $H_s$  and  $\bar{T}$  were used to calculate near-bed orbital velocities using linear Airy-wave theory. The time series of orbital velocities and critical threshold velocities shown represent the average values of the data from the two S4's deployed during the winter period.

KOMAR and MILLER's (1975) theory was also applied to ADV wave data collected at each of three ADV locations in 3.5-4 m water depths. As expected,

threshold values were always exceeded by a large amount indicating constant agitation of sediment by waves within the surf zone. These results also show that even the very calm conditions recorded during each of the ADV deployments (i.e. mean  $H_s=0.73$  m and 0.29 m for May and June deployments respectively) were still capable of entraining sediment for transport by currents (Figure 5.21).



**Figure 5.21:** Near-bed orbital velocities ( $U_w$ ) at northern Waihi Beach during the short-term May ADV deployment, compared to the critical threshold velocity for sediment movement determined using the KOMAR and MILLER (1975) wave-orbital-speed theory.  $H_s$  and  $\bar{T}$  were used to calculate near-bed orbital velocities using linear Airy-wave theory. The three time series of orbital velocities represent the wave collected data from ADV's POI1 (blue), SEA1 (black) and SEA2 (red).

#### 5.4.3 Incipient Motion Induced by Unidirectional Currents

Once sediment movement has been initiated by waves, the sediment may be transported by a combination of wave or current induced flows. The threshold velocity of non-cohesive sediment movement by the action of unidirectional currents alone, without any wave orbital motion effects, was calculated for planar beds using a method derived by MILLER *et al.* (1977). The critical threshold of sediment motion for bedforms is evaluated following a method outlined by BLACK (1983) for Whangarei Harbour sediment transport, which accounts for the surface roughness of the seabed. These methods, which have been previously

adopted in studies by BRADSHAW (1991), PHIZACKLEA (1993), SAUNDERS (1999), LONGDILL (2004) and SPIERS (2004), are described below and then applied to S4 and ADV current measurements.

#### 5.4.3.1 Threshold Velocity for Planar Beds

The threshold velocity at 1 m above the bed, for quartz-density material, over a planar bed is given by (MILLER *et al.*, 1977):

$$u_{1cr} = 122.6D^{0.29} \quad 5.7$$

where  $D$  is the sediment grain size (m). A sediment of grain size 0.18 mm was used to determine this value. The grain size used is based on the mean grain diameter for offshore sediments collected at 6 m depth (Chapter 4). This formula gives a critical threshold value of 0.38 m/s at a reference point 1 m above the bed.

#### 5.4.3.2 Threshold Velocities for Bedformed Areas

A method derived by BLACK (1983) was used to determine the threshold velocity over bedformed areas. An initial requirement is determining the critical skin friction velocity ( $u'_{*cr}$ ), which is taken from the MILLER *et al.* (1977) threshold curve derived for quartz grains ( $\rho_s = 2,650 \text{ kg.m}^{-3}$  and  $\rho = 1,000 \text{ kg.m}^{-3}$ ) using a known grain diameter (Figure 3 in MILLER *et al.*, 1977). Sediment samples collected at the S4 sites during May 2008 were used, providing mean grain sizes of 0.18 mm corresponding to a  $u'_{*cr}$  value of 0.013 m/s. Sediment threshold velocities are also affected by the presence of bedforms. A rippled bed separates the flow and creates near-bed eddies that enhance sediment suspension by increasing the intensity of vortices downcurrent from the crests and increasing the skin friction (KOMAR, 1976; BRADSHAW, 1991; PHIZACKLEA, 1993). The surface roughness term ( $z_0$ ) describes this effect over 2-dimensional bedforms:

$$z_0 = \frac{\eta^2}{2\lambda} \quad 5.8$$

where  $\eta$  refers to the height of the bedform (m) and  $\lambda$  is the bedform wavelength (m). Results from the side-scan sonar survey (Chapter 3) indicate that three dominant bedform types can be observed at northern Waihi Beach. This is confirmed by previous data collected over the inner shelf by BEAMSLEY (1996). Firstly is the flat or ‘planar’ bed, and is accounted for by the formulae of MILLER *et al.* (1977). The remaining bedform types include lightly rippled ( $\eta \approx 0.02$  m and  $\lambda \approx 0.1$  m) and coarse grained megaripples ( $\eta \approx 0.12$  m and  $\lambda \approx 1$  m). These two bedforms are included in the calculation of threshold velocity by using the formulae of BLACK (1983) and yield  $z_0$  values of 0.0020 and 0.0078 for lightly rippled and coarse grain rippled beds, respectively.

Incorporating the values obtained for surface roughness, the critical form drag factor  $c''$  can then be determined from:

$$\frac{c''}{\sqrt{8}} = 3.3 \log_{10} \left( \frac{h}{2z_0} \right) - 2.3 \quad 5.9$$

where  $h$  is the water depth (m). Given that the current data collected by the S4’s was in ~6 m water depth, this produces a value of  $c'' = 23.1$  for lightly rippled beds and  $c'' = 17.6$  for coarse grained megaripples. The terms determined for critical skin friction velocity ( $u'_{*cr}$ ), surface roughness ( $z_0$ ) and the critical form drag ( $c''$ ) are integrated into the critical friction velocity term, given by:

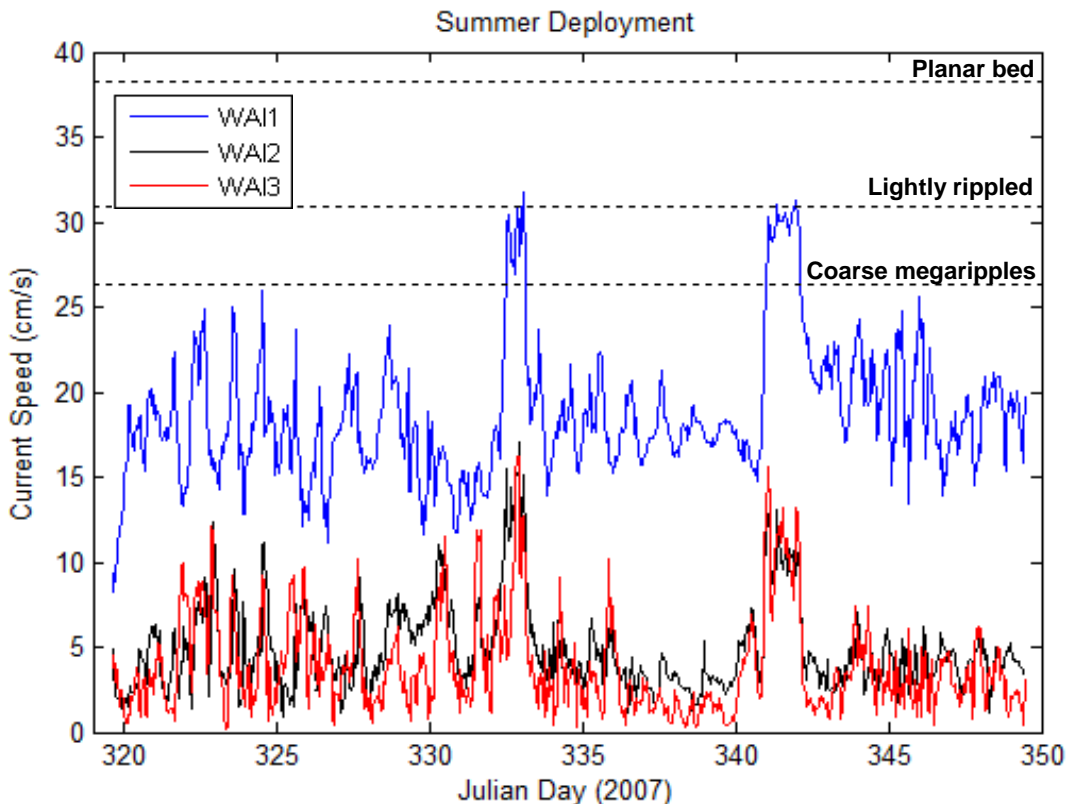
$$u_{*cr} = \frac{u'_{*cr}}{\left\{ 1 - \left[ \frac{5.75}{c''} \log_{10} \left( \frac{0.37h}{z_0} \right) \right]^2 \right\}^{0.5}} \quad 5.10$$

In order to allow for comparisons between critical threshold velocities and the measured current speeds, the position of the S4’s at 1 m above the seafloor must be accounted for. The following equation defines the critical threshold velocity at 1 m above the seabed ( $u_{1cr}$ ):

$$u_{1cr} = 5.75u_{*cr} \log_{10} \left( \frac{1}{z_0} \right) \quad 5.11$$

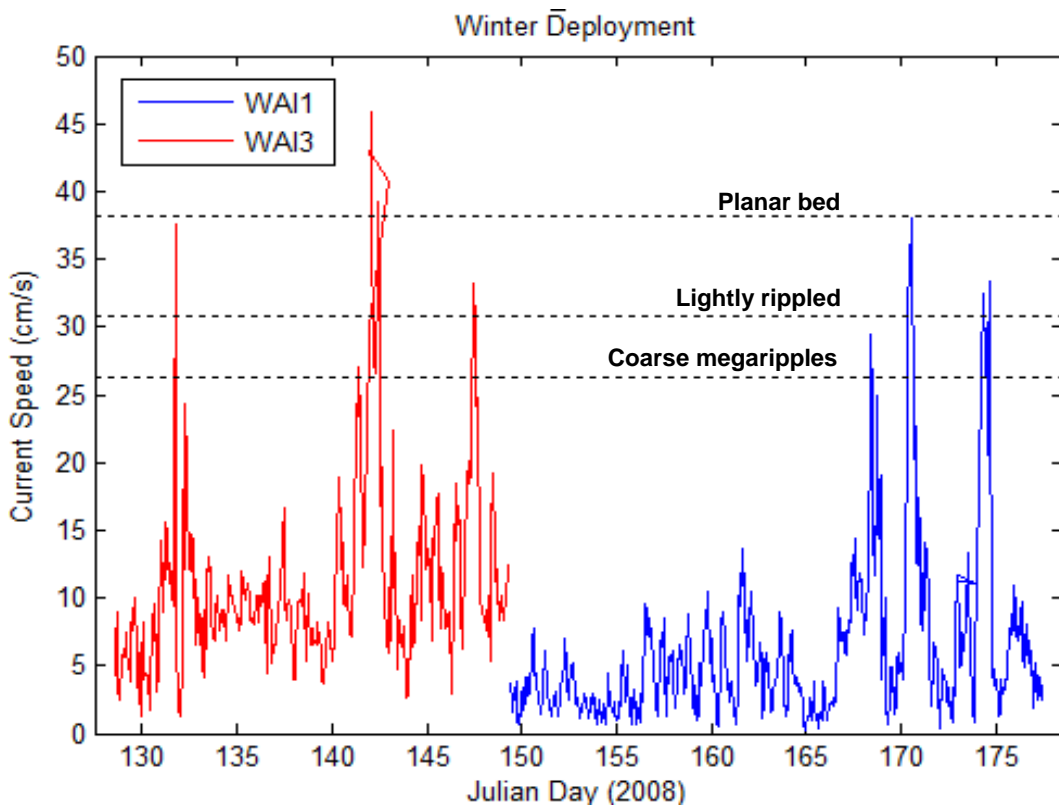
Using this method the critical threshold value for lightly rippled bedform type is 0.31 m/s and 0.26 m/s for coarse grained megaripples.

The critical threshold values derived from the formulae of MILLER *et al.* (1977) and BLACK (1983) are plotted against the current speed at 1 m above the bed (Figures 5.22 and 5.23) for both the summer and winter S4 deployments. During the summer deployment, there were no currents which exceeded the critical threshold value for planar beds of 38 cm/s (Figure 5.22) necessary for sediment transport. Measured current velocities from the winter deployment are predicted to exceed threshold on only one occasion over planar beds (Figure 5.23). However, this accounts for just 0.5% of the entire winter deployment. At the location of S4's WAI2 and WAI3, current speeds recorded during the summer



**Figure 5.22:** Time series plot of current speed (cm/s) recorded at WAI1 (blue), WAI2 (black) and WAI3 (red) relative to the critical threshold velocity for sediment motion (cm/s) for each of the bedform types during the summer (2007) deployment. Threshold values are determined for planar beds using the method of MILLER *et al.* (1977). Thresholds for lightly rippled and coarse grain megaripples are derived using the formulae of BLACK (1983). All plots are for currents recorded at 1 m above the bed in 6 m water depth.

deployment are not capable of initiating sediment entrainment over rippled beds. Only the strong seaward flowing currents measured at WAI1 were strong enough to initiate transport of sediment during the summer deployment. During the 1 month period, the predicted threshold value for the lightly rippled sediment facies was only exceeded <0.2% of the time. As a result of the more variable current regime during the winter deployment, threshold values were exceeded more often than in summer. However, because of the longer duration of the winter deployment, the proportion of current velocities measured that were strong enough to entrain sediments over lightly rippled bedforms corresponds to just 1.7%. The threshold for megaripples was more commonly exceeded over both deployments: ~2% of the time during the summer and ~3% of the time during the winter period. However, according to the side-scan sonograph (Chapter 3) coarse grained megaripples occur to a much lesser extent in the nearshore than the featureless and lightly rippled bed types, which dominate out to ~25 m depth.



**Figure 5.23:** Time series plot of current speed (cm/s) recorded at WAI1b (blue) and WAI3b (red) relative to the critical threshold velocity for sediment motion (cm/s) for each of the bedform types during the winter (2008) deployment. Threshold values are determined for planar beds using the method of MILLER *et al.* (1977). Thresholds for lightly rippled and coarse grain megaripples are derived using the formulae of BLACK (1983). All plots are for currents recorded at 1 m above the bed in 6 m water depth.

The MILLER *et al.* (1977) theory was also applied to ADV current data collected at three locations in 3.5-4 m water depth (Figure 5.2). However, during both overnight deployments the current velocities observed were well below the threshold values, indicating that even at these shallower depths ambient background currents are incapable of initiating sediment movement.

This analysis suggests that between water depths of 3.5-6 m, the role of currents in initiating sediment entrainment is insignificant for the current velocities observed. Sediment transport is therefore likely to be dependent upon the ability of waves to initiate sediment motion; mean currents can then transport the bed sediment entrained and suspended by stronger wave orbital currents (BELL *et al.*, 1997). However, this method does not incorporate the important influence of wave-induced currents on the threshold speed for sediment movement. These findings are in good agreement with the results of other inner shelf sediment transport investigations (including, but not limited to: HARMS, 1989; MATHEW, 1997; BELL *et al.*, 1997; SAUNDERS, 1999; SPIERS, 2004). These studies indicate that, in general, nearshore current velocities are insufficient to initiate sediment movement and require wave motion to initiate entrainment. It can therefore be concluded that wave properties are likely to govern the frequency of sediment transport at northern Waihi Beach in 6 m water depth (and shallower), as they are required to initiate and maintain particle entrainment. The role of nearshore bottom currents is to define where the entrained sediment is transported to.

#### *5.4.4 Calculation of Diabathic Sediment Transport Rates*

The net sediment transport on the shoreface is normally attributed to the combination of residual currents and suspended sediments. The exceedance of sediment entrainment threshold values is not necessarily associated with large sediment transport rates, although it is likely to be determined by the magnitude of near-bed velocities and water depth (HARMS, 1989). In an attempt to determine how wave induced near-bed orbital velocities affect the amount of suspended sediment made available for transport by mean currents, the sediment reference

concentration was predicted. The ‘reference concentration’ ( $\bar{C}_{REF}$ ) is defined by GREEN and BLACK (1999) as the concentration of suspended load near the bed.

The reference concentration under waves was determined using the method of NIELSEN (1986), which has been applied in previous morphological studies by GREEN and BLACK (1999), SAUNDERS (1999) and SPIERS (2004). The reference concentration on a flat bed is given by:

$$\bar{C}_{REF} = 0.005\rho_s\theta'^3 \quad 5.12$$

where  $\theta'$  is the dimensionless, time-averaged skin friction, which is based upon the ratio between stabilizing and stirring forces acting on individual particles (GREEN and BLACK, 1999) and is expressed as:

$$\theta' = \frac{0.5\rho f'_w U_w^2}{(\rho_s - \rho)gD} \quad 5.13$$

It is recommended by GREEN and BLACK (1999) that an expression of  $U_3$  should be used in place of  $U_w$ . However, upon comparison of both methods to sediment transport calculations at West End Ohope Beach, SAUNDERS (1999) concluded that  $U_3$  may underestimate the near-bed orbital velocity. Therefore, the near-bed orbital velocity calculated previously (section 5.4.2 *Incipient Motion Induced by Waves*) is used in the present study.  $f'_w$  is the wave friction factor, defined by GREEN and BLACK (1999) (after SWART, 1974) as:

$$f'_w = \exp \left[ 5.213 \left( \frac{2.5D}{A_w} \right)^{0.194} - 5.977 \right] \quad 5.14$$

where  $A_w$  is the wave-induced water semi-excursion at the bed, given as:

$$A_w = \frac{U_w}{2\pi/T} \quad 5.15$$



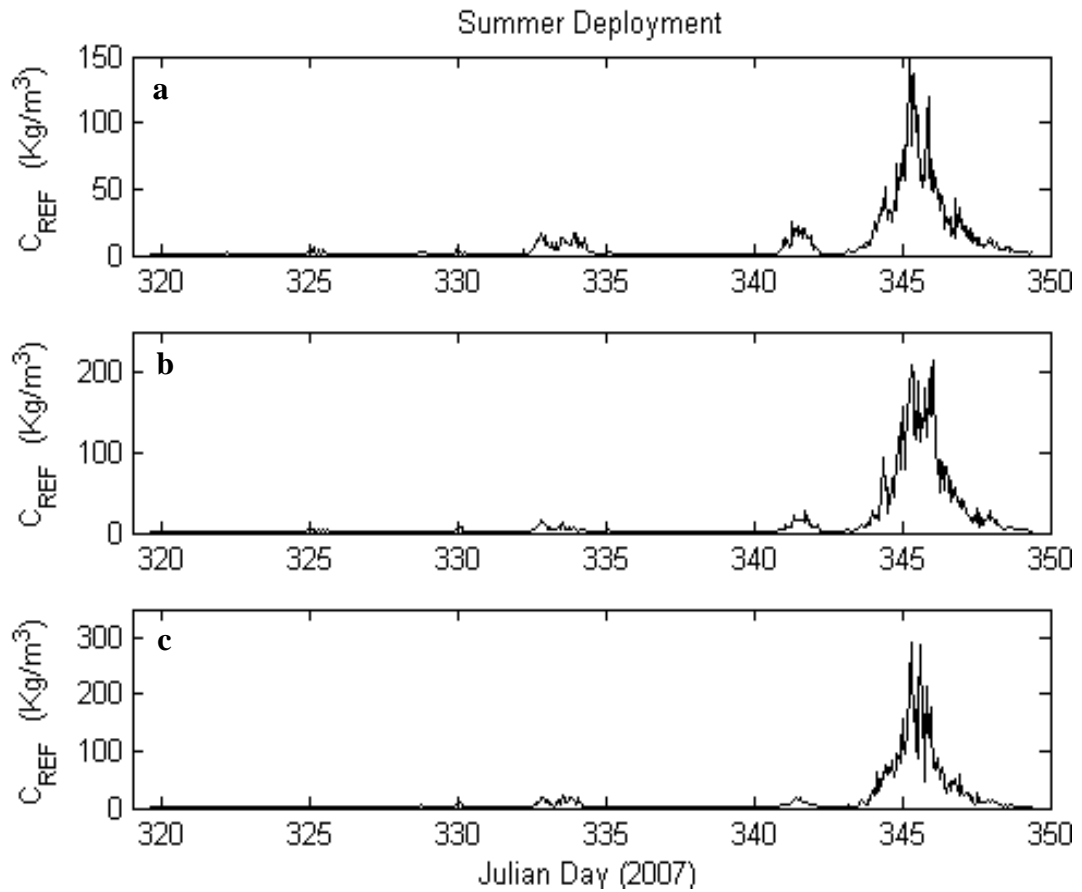
For rippled beds, a correction is made to account for the contraction of streamlines and consequent flow accelerations at ripple crests:

$$\theta' = \frac{0.5\rho f_w' U_w^2}{(\rho_s - \rho)gD(1 - \pi\eta/\lambda)^2} \quad 5.16$$

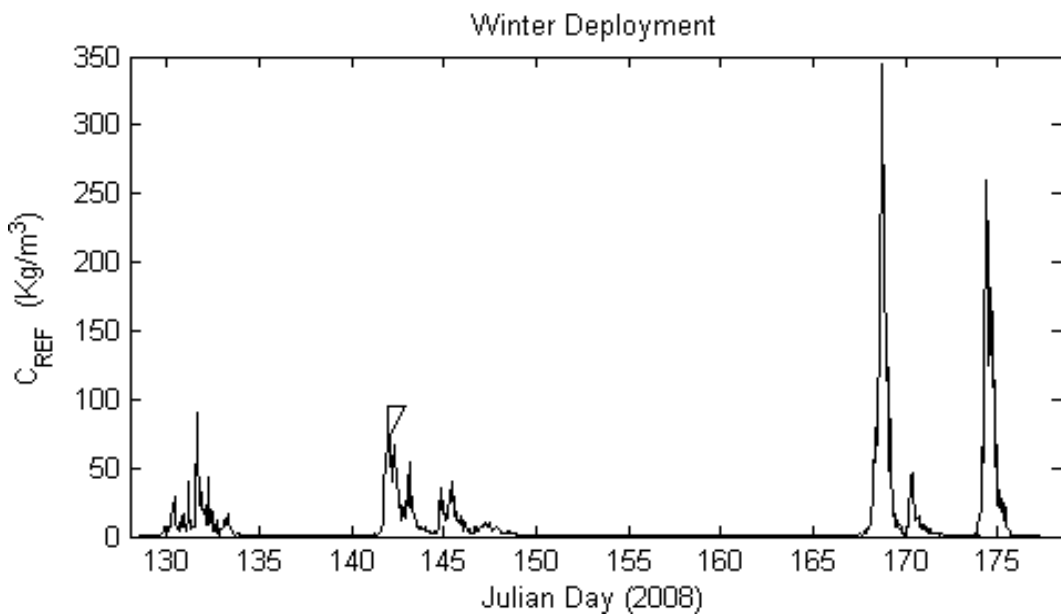
However, studies in the Bay of Plenty by SAUNDERS (1999), using a sediment grain size similar to that of this study, indicate that the correction of flow over ripples within the friction factor resulted in unrealistic amplification of the reference concentration. According to BLACK *et al.* (1998), estimates of the skin friction factor often assume a flat bed despite the presence of small wave-generated ripples. Therefore, the skin friction factor over flat beds will be used for transport calculations in this study.

Figures 5.24 and 5.25 show time series of the predicted reference concentrations ( $\bar{C}_{REF}$ ) at each S4 location during the summer and winter deployments at northern Waihi Beach. Only the periods of the wave record in which wave orbital velocities exceeded the initial motion threshold were included for sediment transport estimates. Values of  $\bar{C}_{REF}$  vary significantly within and between each of the S4 locations, with predicted values ranging between 0.18 kg/m<sup>3</sup> and 345 kg/m<sup>3</sup>. Figures 5.24 and 5.25 illustrate relatively constant levels of suspension near the bed at 6 m, with a small number of periods of significantly high sediment concentration, corresponding to the larger wave events (>1.5 m), superimposed on top of this trend. These episodic events which punctuate the record were often three orders of magnitude greater than the background reference concentration.

Predicted  $\bar{C}_{REF}$  values between the two deployments were reasonably similar, both demonstrating exponential increases in suspended sediment concentration during storm events. There did however appear to be some variation between S4 locations (Figure 5.24).  $\bar{C}_{REF}$  values for WAI1 were significantly lower than those of WAI2 and WAI3, for example, reflecting the wave sheltering influence of Rapatiotio Point shielding wave heights and hence wave orbital velocities.



**Figure 5.24:** Time series plot of reference concentration ( $\bar{C}_{REF}$ ) during the summer deployment, determined from the formulae of NIELSON (1986). The reference concentration values for each instrument are displayed as: a) WAI1, b) WAI2 and c) WAI3.



**Figure 5.25:** Time series plot of reference concentration ( $\bar{C}_{REF}$ ) during the winter deployment, determined from the formulae of NIELSON (1986). The reference concentration values from Julian days 128-149 and 149-177 represent the estimates for WAI3b and WAI1b respectively.

The predicted reference concentration values were compared against a study undertaken at Mount Maunganui Beach by SPIERS (2004), at sites in 8, 11 and 15 m water depths, and under comparable wave conditions to that experienced at Waihi Beach during the study period. Values of  $\bar{C}_{REF}$  in the present study compare fairly well with those predicted and observed by SPIERS (2004) at 8 m depth ( $\sim 0.14\text{-}250 \text{ kg/m}^3$ ). However, at the greater depths of 11 m and 15 m,  $\bar{C}_{REF}$  values were often at least one order of magnitude less than those predicted at Waihi Beach in 6 m depth. This illustrates the effect of depth on sediment transport potential, as the frequency in which sediment is entrained and also the concentration of suspended sediment is greatly reduced when water depth is increased. This observation is supported by a study in the Mangawhai-Pakiri embayment by BLACK *et al.* (1998), who reported that mobility in this area was highly dependent on water depth and wave height variation. The effect of wave height on the reference concentration at Waihi Beach is also pronounced. The suspended sediment concentration under small waves of  $\sim 1 \text{ m}$  is  $\sim 1.03 \text{ kg/m}^3$ . Under 1.5 m and 2.5 m high waves,  $\bar{C}_{REF}$  values are  $\sim 10.45 \text{ kg/m}^3$  and  $\sim 126.33 \text{ kg/m}^3$ , respectively. From these results, it becomes apparent that waves not only determine when sediment can become suspended and distributed by mean currents, but also the quantity and hence the rate of sediment transported by these currents (MATHEW, 1997).

The suspended sediment concentration throughout the depth profile varies over time. Equation 5.17 is a simple exponential model which provides a description of time-averaged sediment concentrations over rippled beds:

$$\bar{c}(z) = C_{REF} \exp\left(\frac{-z}{L_s}\right) \quad 5.17$$

where  $z$  is the vertical coordinate from the flat bed or ripple crest level, and  $L_s$  is the mixing length (NIELSON, 1992; GREEN and BLACK, 1999) approximated by:

$$L_s = 0.075 \frac{A_w \omega}{w_s} \eta \quad \text{for} \quad A_w \omega / w_s < 18 \quad 5.18$$

$$L_s = 0.4\eta \quad \text{for} \quad A_w \omega / w_s > 18 \quad 5.19$$

where  $\omega$  is the wave radian frequency ( $2\pi/T_s$ ) and  $w_s$  is the sediment settling speed, which was assumed to be 2.5 cm/s for sediments of  $D=0.18$  mm. Ripple height  $\eta$  was taken as 2 cm to be representative of the commonly observed lightly rippled bedforms.

The velocity profile in a steady, uniform turbulent boundary layer can be described by defining a height above the boundary layer at which mean velocity is zero, referred to as the roughness length. This may be expressed by the von Karman-Prandtl Equation (NIELSEN, 1992):

$$U(z) = \frac{U_*}{k} \ln\left(\frac{z}{z_o}\right) \quad 5.20$$

where  $k$  is von Karman's constant, which has a value of approximately 0.4. Rearranging this formula to solve for the friction velocity ( $U_*$ ) using mean current data measured 1 m above the bed ( $U_1$ ), gives:

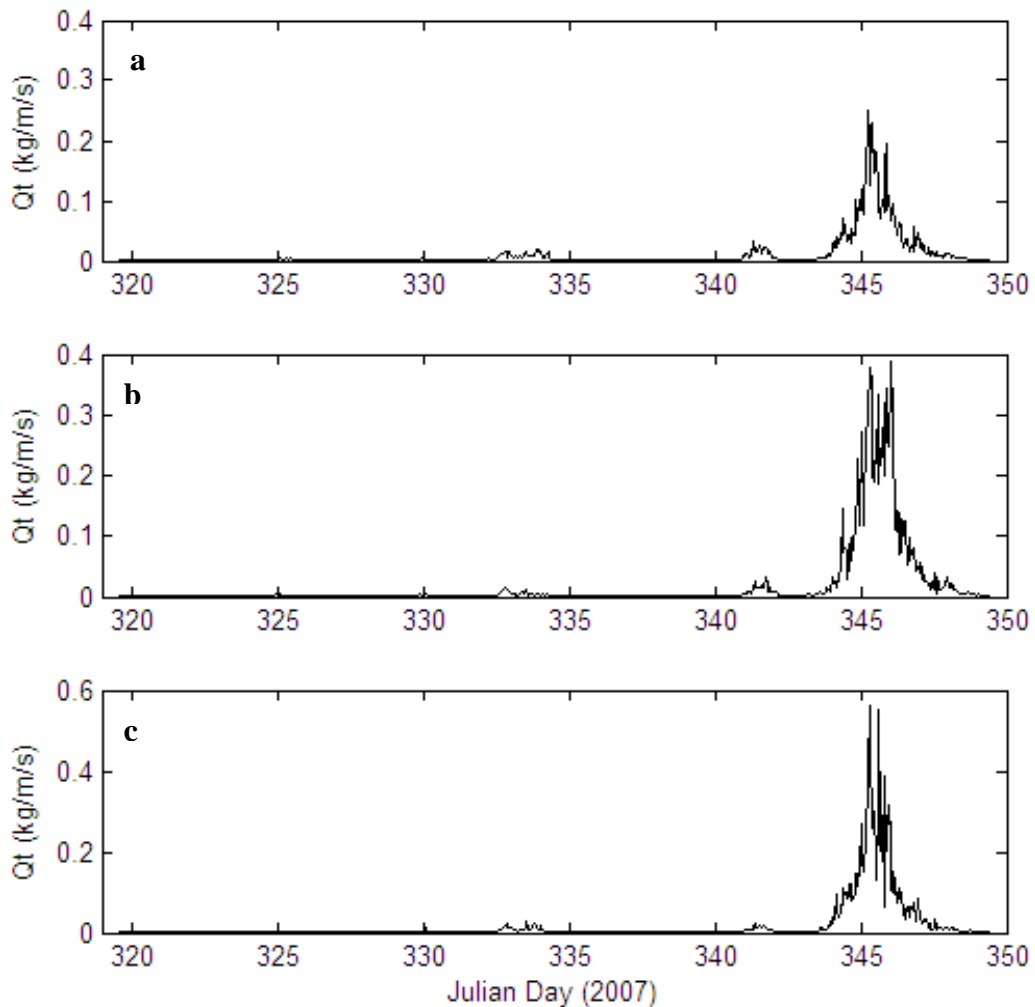
$$U_* = \frac{kU_1}{\ln\left(\frac{1}{z_o}\right)} \quad 5.21$$

Following the methodology of SAUNDERS (1999), vertical profiles of suspended sediment concentration and current velocity were calculated for each burst of wave data for both summer and winter deployment periods. Elevations between 0 and 2 m at 0.01 m intervals were used to define the vertical profiles. The sediment transport rate could then be calculated by combining sediment velocity distributions with suspended sediment concentration profiles. The sediment transport rate is usually in the form (NIELSON, 1992):

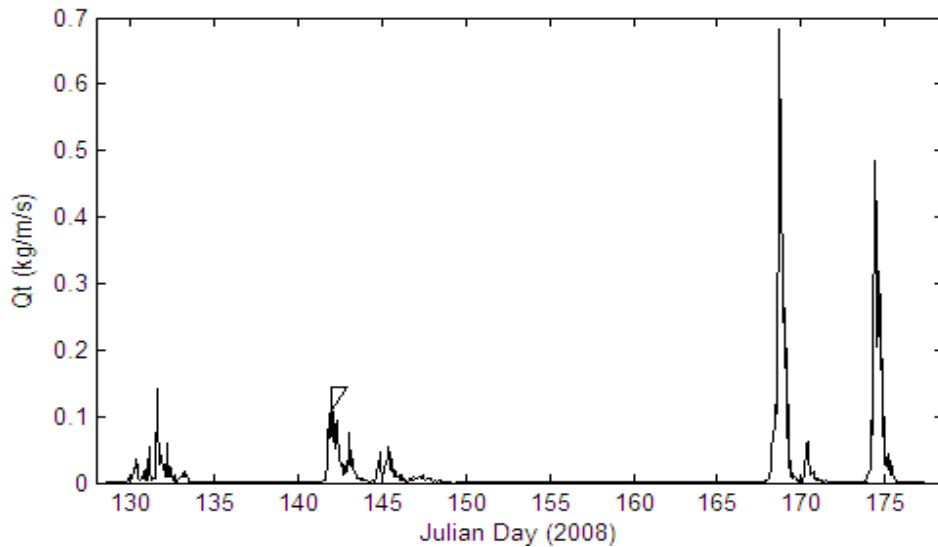
$$Q(t) = \int_0^h c(z,t)U(z,t)dz \quad 5.22$$

## 5.4.5 Results

Figures 5.26 and 5.27 show the time series of mass sediment flux per unit of sea bed, integrated over depths up to 2 m elevation above the bed for both deployment periods. Note that only the rate of sediment transport is being considered thus far. Direction of diabathic (onshore/offshore) sediment movement is not yet indicated. The nearshore sediment flux of both the summer and winter deployments are dominated by episodic events. Nearly 0.7 kg/m/s of suspended sediment is predicted to be transported during the storm event on June 17<sup>th</sup> (Julian day 169), when  $H_s$  exceeded 3 m. In contrast, a maximum of 0.25 kg/m/s of material was suspended within the boundary layer at the location of WAI1 during the summer



**Figure 5.26:** Suspended sediment flux integrated over time above the bed at a) WAI1, b) WAI2 and c) WAI3 during the summer deployment. The time series of  $Q(t)$  shows a distinct transport event between Julian days 344-347, although there is steady transport throughout the period.



**Figure 5.27:** Suspended sediment flux integrated over time above the bed at WAI3b (days 128 - 149) and WAI1b (days 149-177) during the winter deployment. The time series of  $Q(t)$  shows four distinct transport events, which dominate the overall sediment transport patterns during this period.

2007 deployment, indicative of more quiescent wave conditions and sheltering in the lee of the headland, as noted previously.

The direction of the mean currents measured 1 m above the seabed was then used to determine the frequency of shoreward/seaward movement of sediment at the location of each S4 instrument during the separate deployments. The onshore and offshore components of the sediment flux were calculated using the time series of mean current direction and depth integrated sediment flux  $Q(t)$ . Measured current directions at each instrument location were divided into quadrants to examine the direction of suspended sediment movement over both deployments periods. Onshore currents were defined as those which flowed towards 8-128°, and offshore currents were classified as having directions ranging between 188-308°. Suspended sediment flux per metre width of seabed was converted to gross mass flux onshore at each S4 location by obtaining the sum of  $Q(t)$  corresponding to periods of onshore currents over each deployment period. Likewise, rates of sediment flux offshore were determined by summing the  $Q(t)$  values which corresponded to periods of offshore currents. A daily rate of net sediment flux was then calculated, allowing comparison of rates during each period, before combining rates to provide an annual net sediment flux (Table 5.4).

**Table 5.4:** Predicted rates of diabathic suspended-sediment flux at 6 m depth off northern Waihi Beach. The summer deployment refers to the S4 data collected between 15/11/07-15/12/07. Overall, the entire winter deployment lasted from 07/05/08-25/06/08, although S4 WAI3b only recorded reliable data for the first 21 days; WAI1b collected data for the remaining 28 days.

Suspended sediment flux (m <sup>3</sup> /year)	WAI1/WAI1b		WAI2	WAI3/WAI3b	
	Summer Deployment	Winter deployment	Summer deployment	Summer deployment	Winter deployment
Onshore	0	44.5	37.7	52.9	92.1
Offshore	31.0	45.9	15.3	44.2	17.1
Net	-31.0	-1.4	+22.4	+8.7	+75.0

For the entire 30 day summer deployment, no onshore currents were recorded by WAI1. This is directly a result of the persistent seaward-flowing currents (~77% of the deployment) observed in the hydrodynamics analyses. Unsurprisingly, there was a net offshore flux of sediment at WAI1. This was repeated for WAI1b during the winter deployment, although the magnitude of offshore sediment transport was much smaller (Table 5.4). With the exception of WAI1/WAI1b, however, the results clearly demonstrate that shoreward transport dominates for a significant proportion of the time, with comparatively greater onshore flux experienced during each of the deployments at WAI2 and WAI3/WAI3b.

In an attempt to calculate nearshore diabathic transport rates required for the sediment budget in Chapter 7, the summer and winter daily rates of sediment flux were combined to provide an annual estimate of sediment flux. However, because there are a multitude of factors that may cause spatial variation in sediment transport in the nearshore zone, the sediment flux rates determined for each of the S4's were kept separate to enable greater transparency in sediment transport rates over the entire 4,500 m study area. Hence, annual flux rates calculated from information for each of the three current meters was allocated to an area 750 m either side of the S4 sites (1,500 m each). Suspended sediment fluxes were converted to volumetric rates, assuming the density of sands to be 2,650 kg/m<sup>3</sup>. Tables 5.5 shows the predicted annual sediment transport rates across the 6 m contour at northern Waihi Beach during the study period.

An enormous amount of spatial variation in sediment transport was observed between the three S4 locations (Table 5.5). As mentioned previously, offshore sediment transport dominates the far northern end of the beach, with a net offshore sediment flux of 6,099 m<sup>3</sup>/year (4.1 m<sup>3</sup>/m) along the 1500 m sector of beach for the combined WAI1/WAIb S4 data. The remainder of the study site displays greater magnitudes of onshore sediment transport. The largest component of net sediment flux was calculated at WAI3/WAI3b (13,261 m<sup>3</sup>/year or 8.8 m<sup>3</sup>/m). This section of the coastline is typically associated with higher wave energy, and thus greater magnitudes of sediment transport are expected. Along the entire 4.5 km length of northern Waihi Beach, an estimated 11,844 m<sup>3</sup>/year or 2.6 m<sup>3</sup>/m net sediment flux onshore is predicted. This information will be included in sediment budget calculations for the northern Waihi Beach littoral cell in Chapter 7.

**Table 5.5:** Estimates of diabathic transport along the 6 m contour within the northern Waihi Beach littoral cell. Each rate assumes a contour length of 1,500 m. Note the wide variation in sediment transport rate within the 4.5 km study area, with the greatest magnitude of onshore sediment transport observed at central Waihi Beach (WAI3/WAI3b). Offshore sediment flux dominates at the northern end where rip currents are a regular feature.

	WAI1/WAI1b	WAI2	WAI3/WAI3b
Onshore (m <sup>3</sup> /year)	7,841	7,789	22,765
Offshore (m <sup>3</sup> /year)	13,940	3,161	9,504
Net (m <sup>3</sup> /year)	-6,099	+4,682	+13,261

## 5.5 SUMMARY

Monochromatic statistical analysis was employed to examine the offshore wave climate at northern Waihi Beach during summer 2007 and autumn/winter 2008.

- Mean significant wave heights were slightly higher over the summer deployment ( $H_s=1.09\text{m} \pm 0.41 \text{ m}$ ) compared to the winter deployment ( $H_s=0.95\text{m} \pm 0.48 \text{ m}$ ), although wave events were more variable in frequency and duration in winter than over summer.
- Measured wave periods were similar over both summer and winter deployments, and indicate that both locally generated sea waves and



distantly generated swell exist. Storm waves ( $H_s > 2$  m) measured during both deployments nearly always exceeded the line of critical wave steepness distinguishing sea and swell waves, suggesting that larger waves were generated locally from storm systems within the Bay of Plenty.

- $H_s$  recorded by the northernmost S4 were consistently smaller than at both the other S4 locations, believed to be a result of the northernmost S4 being partly sheltered from the north to northwest by Rapatiotio Point.

Currents were measured in the nearshore to identify general trends in current speed and direction.

- The study area was dominated by two alongshore currents: weak southeasterly directed currents resulting from offshore winds, and stronger more persistent northwesterly flowing currents derived from strong onshore winds. This trend was apparent at all S4 locations except WAI1 during the summer deployment, where instead strong offshore-directed currents were more persistent. It is believed that the limited distribution of current directions recorded at WAI1 is likely to be a result of the sheltering effect caused by Rapatiotio Point.
- Both deployments displayed a great amount of variation in current speed. In general, as the wave height increased there was a corresponding increase in current velocity that also displayed great temporal variability, indicating that these currents are wave-generated.

Wind and current records were examined to determine the influence of wind on wave patterns and current generation in the study area.

- A comparison between wave heights and wind direction for both S4 deployments shows that the larger wave events are generally associated with strong onshore winds (east to northeasterly). This is especially apparent during storm events where the effects of stronger onshore winds on the wave spectra are more pronounced. Offshore winds on the other hand produced prolonged calm wave conditions.

- Analysis of wind and current records provides strong evidence that the near-bed current direction is highly related to wind direction. Strong alongshore currents associated with winds from the east to east-southeast, and weaker onshore currents related to winds from southwest, were the principal events that could be distinguished from the data. Wind speed appeared to have an almost immediate effect on current magnitude.

Wave and current interactions and their resulting impact on sediment movement were examined to identify the conditions required for sediment mobility and incipient motion. Diabathic sediment transport rates offshore northern Waihi Beach were subsequently evaluated.

- It was demonstrated that sediments at 3.5-6 m water depth off northern Waihi Beach were constantly agitated by waves at each of the instrument locations for both deployments. Current velocities alone were generally incapable of inducing incipient motion in  $\leq 6$  m water depth, with threshold conditions only exceeded at the S4 sites less than 6% of the deployment period. Hence, sediment transport was found to be reliant on the ability of waves to initiate and maintain particle entrainment, before mean currents are able to transport and distribute sediments in the nearshore.
- The near-bed suspended sediment concentration was found to be governed by wave height; increasing wave height significantly increases the concentration of suspended load. Analyses suggests that the wave sheltering influence of Rapatiotio Point shielding wave heights and hence wave orbital velocities is the primary cause of the smaller magnitudes of suspended sediment flux at the location of WAI1 in the lee of the headland.
- Net fluxes at all S4 sites were directed onshore, with the exception of WAI1 during the summer deployment where persistent seaward-flowing currents transported sediment offshore. Spatial variation in volumetric rates of sediment transported was observed along the beach, ranging from 6,099 m<sup>3</sup>/year lost offshore in the north to 13,261 m<sup>3</sup>/year moving onshore in the south. Combined sediment transport rates over both deployments provided an estimated net onshore flux of 11,844 m<sup>3</sup>/year or 2.6 m<sup>3</sup>/m.

# CHAPTER SIX: WAVE ENERGY FOCUSING AND NEARSHORE LITTORAL DRIFT

---

## 6.0 INTRODUCTION

Swell waves traversing the inner shelf and shoreface undergo shoaling and refraction processes around seafloor topographic highs, such as offshore reefs or transverse sand ridges. Wave refraction over such bathymetric irregularities may result in the focusing of wave energy onto specific zones at the shore. HEALY (1987) showed that sectors of beach subject to wave convergence and concentration of energy exhibited localised higher breaking waves, resulting in enhanced wave run-up, set-up and surge, causing preferential erosion of the dunes in these areas during episodic storm events. As a result, shallow embayments are carved in the frontal dune line.

Previous numerical simulations of storm wave refraction undertaken at Waihi Beach (HEALY, 1987; HOBAN, 1993; BEAMSLEY, 1996; STEPHENS, 1996) have indicated that dune embayments are zones of wave focusing, especially in storms. The complex and irregular bathymetry offshore Waihi Beach, as detailed in the morphology investigation in Chapter 3, immediately suggests that these features could significantly modify wave behaviour and have some influence on the focusing of waves onto Waihi Beach. In addition, because longshore currents are dependent on the angle of the waves breaking relative to the shoreline (KOMAR, 1998), local variation in littoral drift gradients may also result from the wave energy focusing caused by wave refraction.

This chapter investigates the influence of wave refraction and convergence on the distribution of wave energy along the Waihi Beach shoreline. Several wave scenarios are simulated using the numerical wave refraction model WBEND, in an attempt to identify the conditions which may be responsible for promoting wave energy focusing along sections of the coast. Particular emphasis is put on the influences of Mayor Island 36 km offshore, Steel's Reef 4 km offshore, and the large shore-normal sand ridges discussed in Chapter 3 on wave behaviour at

the coastline. Investigation of potential littoral drift directions and rates within the vicinity of northern Waihi Beach over short-term and longer-term scales using WBEND are also included. Following evaluation of littoral transport within the study area, an assessment of the potential sheltering induced by Rapatiotio Point is undertaken.

## 6.1 WAVE REFRACTION MODELLING

### 6.1.1 Introduction

Wave refraction, shoaling and frictional dissipation at northern Waihi Beach were simulated using the numerical wave shoaling and refraction model WBEND, developed by BLACK and ROSENBERG (1992). The objective was to examine the influence of wave refraction and convergence on the distribution of wave energy along the coast, and to identify the sea conditions which may promote wave focusing at particular sections along Waihi Beach. The model is suitable for general application to irregular bathymetry and variable wave conditions, and has been used successfully in recent wave studies at Raglan (HUTT, 1997), West End Ohope Beach (SAUNDERS, 1999), Gisborne (DUNN, 2001), and Pukehina (EASTON, 2002).

It is important to note that a model is never a substitute for physical measurements, but it is considered to be a powerful tool in scientific research as it may be the only technique available to solve certain problems. Thus, numerical models can be used to simulate conditions that are unable to be measured and to understand complex physical processes.

#### 6.1.1.1 Wave Refraction Theory

Upon entering shallow water, waves are subject to refraction, in which the direction of their propagation changes with decreasing water depth in such a way

that the crests tend to parallel the depth contours (KOMAR, 1998). This develops the final distribution of energies and the generation of longshore currents. The change in direction caused by refraction is related to the change in the wave celerity at various depths described by Snell's law:

$$\frac{\sin \alpha_1}{C_1} = \frac{\sin \alpha_2}{C_2} = \text{constant} \quad 6.1$$

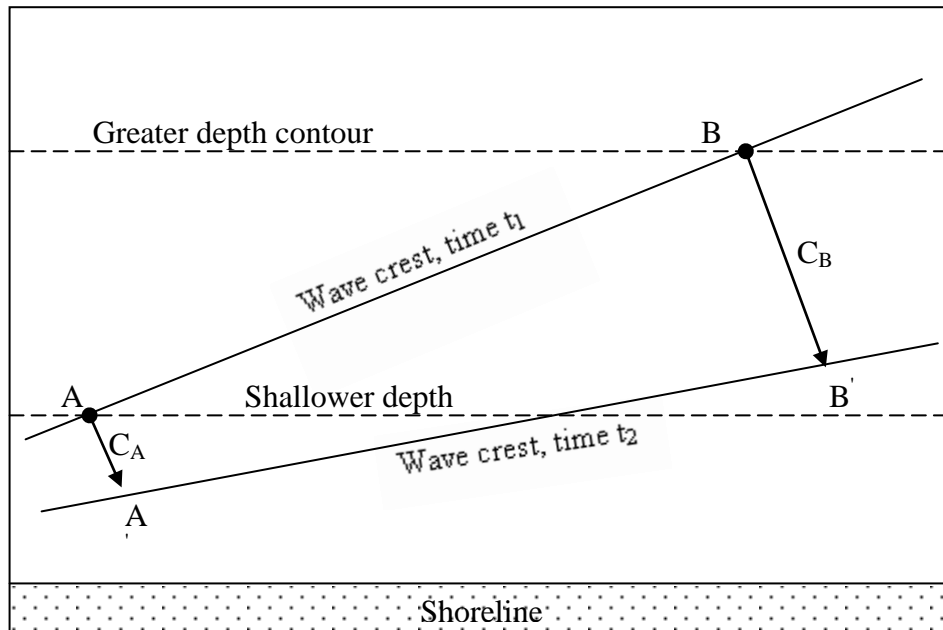
where  $\alpha_1$  and  $\alpha_2$  are angles between adjacent wave crests and the respective bottom contours, while  $C_1$  and  $C_2$  are the wave celerities at the two depths. As waves propagate toward the shore the wavelength decreases as the depth decreases. Hence, a wave crest in deep water will move a greater distance than the same wave crest in shallower water. This refraction of waves results from their velocity dependence on the water depth once they enter shallow water, according to linear wave theory:

$$C = \sqrt{gh} \quad 6.2$$

where  $g$  is acceleration due to gravity and  $h$  is water depth. This relationship predicts that the lower the depth the slower the rate of wave advance, resulting in the wave direction turning toward regions of shallow water and away from regions of deep water (Figure 6.1). The phenomenon explains why waves never hit the shoreline at an angle. Whichever direction the waves travel in deep water, they always refract towards shore-normal as they enter the shallower water near the beach.

#### 6.1.1.2 Wave Energy Focusing

An important consequence of wave refraction is that the wave energy becomes unevenly distributed along the shoreline, concentrated or focussed along some parts and greatly reduced in others. The importance of wave energy focusing along beaches is that it modifies wave characteristics, in particular wave height.

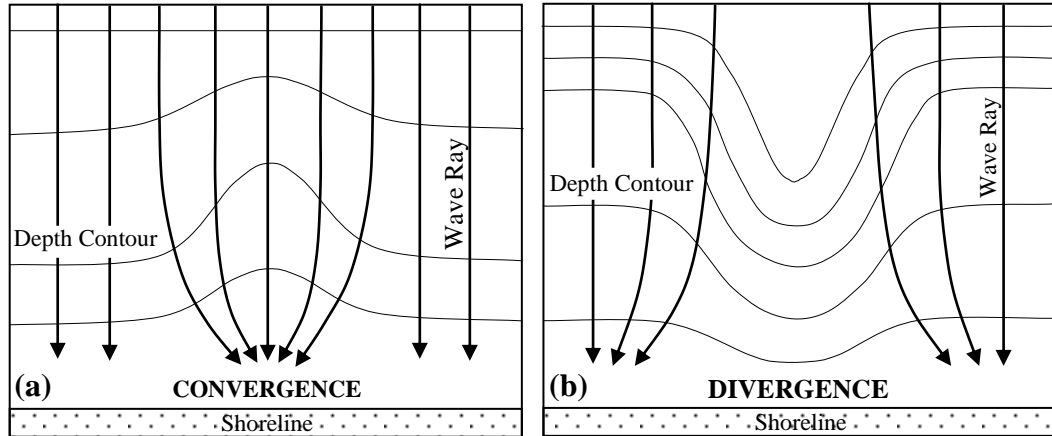


**Figure 6.1:** Wave refraction occurs due to faster movement of waves in deep water than in shallower water. During a certain time interval, the wave crest at point B in deeper water moves farther than the crest at point A in shallower water, causing the wave crest to rotate and become more nearly parallel to the shore. Source: KOMAR (1998).

According to linear wave theory, wave energy ( $E$ ) is directly related to wave height ( $H$ ), as shown in Equation 6.3:

$$E = \frac{1}{8} \rho g H^2 \quad 6.3$$

where  $\rho$  is the density of water. At any particular place local variations in topography can cause refraction, resulting in either a spreading out or convergence of the wave energy and hence greater, or lesser, wave heights in that locality (DRAPER, 1966b). Refraction of waves may lead to convergence of the wave rays shoreward of a seafloor topographic high, in which case energy along the wave front becomes concentrated resulting in localised greater wave heights (Figure 6.2a). Away from zones of wave energy concentration refraction will cause the wave rays to spread out, dispersing the wave energy so that wave heights are reduced at the shoreline (Figure 6.2b). The reason for this energy spreading is that the energy flux between adjacent rays is constant, and spreading due to refraction requires that the same amount of energy flux be spread out over a



**Figure 6.2:** (a) The convergence or focusing of wave rays such as over a seafloor topographic high. (b) The divergence of wave rays such as over a topographic depression. Source: KOMAR (1998).

greater length of wave crest (KOMAR, 1998). This change in energy is indicated by a refraction coefficient ( $K_r$ ), defined as:

$$K_r = \sqrt{\frac{s_\infty}{s}} \quad 6.4$$

where  $s_\infty$  is the spacing between wave rays in deep water and  $s$  is the spacing later in the shoaling waves. Using the refraction coefficient it is possible to evaluate the change in wave height of a shoaling wave undergoing refraction by Equation 6.5:

$$\frac{H}{H_\infty} = K_r \sqrt{\frac{C_\infty}{2nC}} \quad 6.5$$

where  $H$  is the wave height. The result of wave refraction may be localised zones of higher wave energy concentrated or focussed at the coastline. This feature of enhanced wave heights is well-known at headlands, but it is not often recognised along sandy beach coastlines.

Sectors of beach subject to wave focusing exhibit localised higher breaking waves, resulting in greater wave set-up, run-up, and surge and are thus more erosion prone than adjacent regions (HEALY, 1987). Enhanced water level setup as a result of wave convergence and concentration of energy at the shoreline may

cause particular sectors of the frontal dune to be over-washed or eroded preferentially, especially during storm events. These zones of accelerated dune erosion create shallow “arcuate duneline embayments” which are carved into the dune face (STEPHENS *et al.*, 1999). Numerical simulation of storm wave refraction undertaken at a number of New Zealand beaches, including Waihi Beach, show clearly that the embayments are zones of wave energy focusing (HEALY, 1987; STEPHENS, 1996). Similar effects have been reported along the coast of southern Brazil (SPERANSKI and CALLIARI, 2001).

## 6.1.2 Numerical Wave Propagation Model WBEND

### 6.1.2.1 Introduction

WBEND is a 2-dimensional wave propagation model for monochromatic waves or a wave spectrum over variable topography for refraction and shoreline longshore sediment transport studies. The model applies an iterative finite-difference solution to calculate wave height in the two horizontal dimensions using the energy conservation equation, given by:

$$\frac{\partial}{\partial x}(F \cos \theta) + \frac{\partial}{\partial y}(F \sin \theta) = -F_D \quad 6.6$$

where  $x$  and  $y$  are orthogonal co-ordinates,  $\theta$  is the wave angle and  $F_D$  is a combination of the bed friction ( $F_f$ ) and wave breaking ( $F_b$ ) dissipation terms.  $F$  is the wave power, which for Airy waves is:

$$F = EC_g = \frac{1}{8} \rho g H^2 C_g \quad 6.7$$

where  $E$  is the wave energy,  $C_g$  is the group speed,  $\rho$  is the fluid density,  $g$  is gravitational acceleration and  $H$  is the wave height.

For monochromatic cases, the wave-energy frictional dissipation term ( $F_D$ ) is given by:



$$F_D = \frac{\rho C_f}{6\pi} \left( \frac{H_\omega}{\sinh(kh)} \right)^3 \quad 6.8$$

where  $C_f$  is the friction coefficient,  $\omega$  is the radial frequency,  $k$  is the wave number and  $h$  is the water depth.

Wave angles are obtained from the equation for conservation of wave number:

$$\frac{\partial}{\partial x} (|k| \sin \theta) - \frac{\partial}{\partial x} (|k| \cos \theta) = 0 \quad 6.9$$

WBEND solves Equations 6.6 and 6.9 for wave power and wave angle respectively using a shoreward marching iterative scheme (BLACK and ROSENBERG, 1992).

For this study, WBEND was applied for monochromatic waves, with data obtained from the EBOP Pukehina wave buoy, which is deployed 13 km directly offshore from Pukehina and 6 km southeast of Motunau (Plate) Island (Figure 6.3), in 60 to 62 m water depth (Iremonger, *pers comm.* 2008). Wave information obtained during the S4 winter deployment (07/05/08 – 25/06/08) by WAI1b and WAI3b were utilised for both model calibration and the specific model scenarios. Details on S4 deployments and the retrieval and processing of wave data are described in Chapter 5.

#### 6.1.2.2 Model Inputs and Outputs

WBEND requires an information file, a wave boundary or spectrum file and a bathymetry file. The information file controls the model by providing the input data and output file names. It contains the main characteristics of the site including number of grid cells and sizes, friction coefficient and eddy viscosity.

There are three different types of wave boundary file that can be used:

1. Probability or time series files;

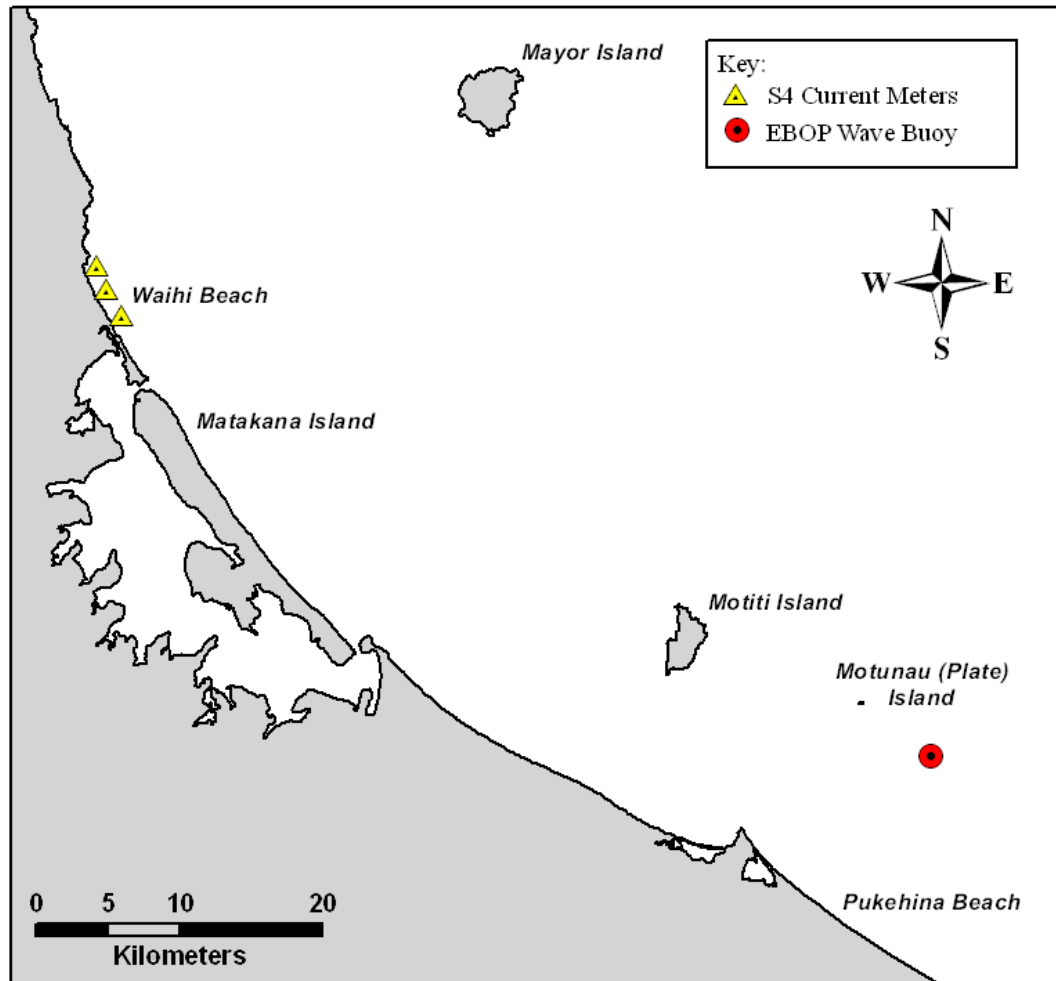


Figure 6.3: Location map showing the position of EBOP’s Pukehina wave buoy in relation to Waihi Beach and the S4 current meters deployed in the present study.

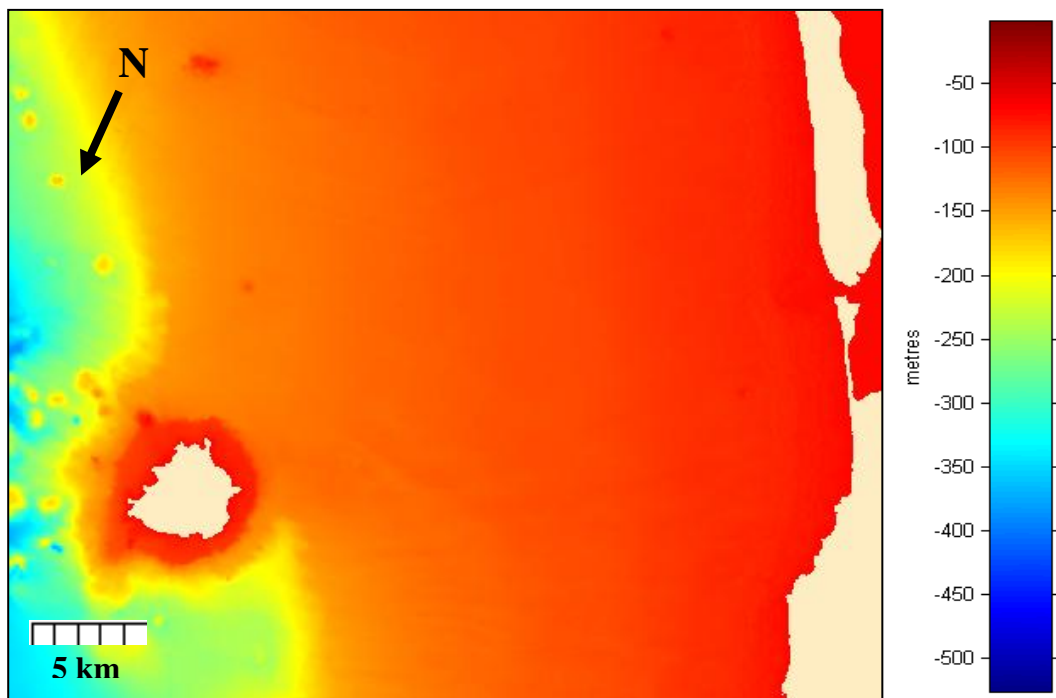
1. Spectrum files; or
2. Sediment transport contour files.

Monochromatic wave probability files were used as the boundary file type in the present study. The boundary file contains a time series of wave conditions, including six possible variables: probability of occurrence, wave height, wave period, wave angle, bed friction and tidal elevation.

Following the method of SAUNDERS (1999), probability was given by  $1/n$ , where  $n$  is the total number of bursts for a given period. For specific wave scenarios, probability was set to 1. Significant wave height, period and direction statistics obtained from zero down-crossing analysis were used as input to the model. The height, period and angle are specified in metres, seconds and degrees respectively.

Initially, a constant friction was used. Tide height was set to zero for all model simulations.

A bathymetric grid was created in ArcGIS using data acquired by digitised soundings from the R.N.Z.N. 1960 “Lachlan” Survey fairsheets (data supplied by Carol Kohl, LINZ). The digitised bathymetry spanned a rectangular area from north of Waihi Beach, south to the centre of Matakana Island and seawards to about the 300 m contour (Figure 6.4). The model assumes the shoreline is positioned on the eastern boundary of the grid. Therefore, using the software package SURFER32<sup>‡</sup>, the grid was rotated by 205° to align the shoreline and bathymetric contours with the open water boundary. Likewise, incoming wave directions used in the boundary files were also rotated by 205° to ensure realistic model runs. SURFER was then used to convert the rotated data set from binary format file into a 50 x 50 m bathymetry file in ASCII format. All depth and height measurements are relative to Moturiki Datum (0.32 m below Mean Sea Level).



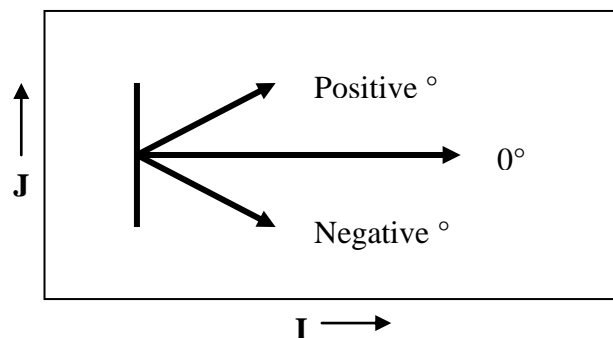
**Figure 6.4:** 50 m model grid of the Waihi Beach coastal sector generated and rotated 205° in SURFER. The offshore island to the east is Mayor Island, which is the major feature impacting upon nearshore waves at Waihi Beach.

<sup>‡</sup> SURFER32 (Version 6.04), software by Golden Software Inc, 1997.

### 6.1.2.3 Model Resolution

Originally a 100 m grid size was experimented with, but this was later reduced to 50 m in order to improve the accuracy of model results. The reduction in grid size unfortunately resulted in an increased computational time for model calibration and simulations. However, 50 m was determined the optimal grid size that retained a high enough model resolution and an acceptable model computational time.

SURFER ASCII files were subsequently converted into the format used by WBEND using the Fortran programme *TOBATH*. This programme converts grid cells into I (x-axis, positive to the east) and J (y-axis, positive north) coordinates, so that each cell is defined by an (I, J) coordinate associated with the mid-point wave height, period and angle. The cell (1,1) is located at the bottom left corner of the grid and the maximum coordinate (Imax, Jmax) are at the top right corner. For wave refraction and sediment transport simulations, a grid size of 868 x 706 (I, J) was created. Wave angle is defined relative to the left or east of the grid and is positive anti-clockwise (Figure 6.5). The (I,J) coordinates of the three S4 instruments were denoted in the information file, so that time series data could be extracted from these positions to allow model calibration.



**Figure 6.5:** The model grid, positive I is to the east, positive J is to the north. Wave angle is defined relative to the east and is positive clockwise. Source: HUTT (1997).

The WBEND binary output file, *filename.out*, contains depths, heights, periods, and bottom orbital velocity over the entire grid for each event in the time series

file. WBEND output files were prepared and results presented in the Matlab graphical support programme *Plot3DD*<sup>§</sup>.

#### 6.1.2.4 Model Calibration

Models can only produce meaningful results after proper calibration based upon comparisons of measured field data against model outputs. Model calibration involves adjusting various empirical constants in the model equations until the model accurately predicts known wave measurements recorded at a specific site within the model grid. It is considered calibrated if it reproduces acceptably the measured data. To calibrate WBEND in the present study, two S4 current meters (WAI1b and WAI3b) were deployed offshore from Waihi Beach in approximately 6 m water depth between 07/05/08 and 25/06/08. Due to instrument failure and unsuitable conditions delaying instrument deployment (see Chapter 5), wave data were only recorded between 07/05/08 – 04/06/08 at WAI3b, and 28/05/08 – 25/06/08 at WAI1b. Model simulation periods of these same timeframes were compared to measured data at both locations in order to calibrate WBEND. An attempt was also made to validate the model by comparing calibrated model predictions with measured wave data obtained from three ADV's deployed within the breaking wave zone (~3.5-4 m) for a period of 23 hours on the 28<sup>th</sup> and 29<sup>th</sup> May 2008, and again on the 24<sup>th</sup> and 25<sup>th</sup> June 2008 (Figure 5.2). Unfortunately, due to the extremely low wave heights recorded by the ADV's (i.e. mean  $H_s=0.29$  m for June deployment), the model consistently over-predicted measured wave heights by as much as 0.8 m. This is believed to be partly due to a limitation of WBEND in that the frictional drag influence of bottom topography bedforms is not taken into account when using a steady state frictional coefficient. This issue is discussed in greater detail in the model calibration results (section 6.1.2.6)

The model was forced using the wave height, period and direction data collected from EBOP's Pukehina wave buoy between 07/05/08 – 25/06/08 at the model boundary. Initial model runs were undertaken with the friction coefficient (bed roughness) set to 0.01 as defined by WBEND as being suitable for open coast

---

<sup>§</sup> Plot3DD, GORMAN, R., NIWA.

beaches, and an eddy viscosity of  $10 \text{ m}^2\text{s}^{-1}$ . Calibration of wave height and direction at Waihi Beach involved adjusting the values of the bed roughness and eddy viscosity until the model accurately predicted measured wave data. Wave heights and directions from the grid cells in the model corresponding to the positions where the S4's were placed were extracted and evaluated using Root Mean Square Error (RMSE) to find the best model calibration.

Several calibration runs were undertaken altering the bed roughness and eddy viscosity over the entire model grid. Plots of the residual error between modelled and measured wave height and direction data may be obtained from Appendix III. The smallest error based off the RMSE between measured and predicted wave heights and directions was achieved when bed roughness and eddy viscosity were set to 0.01 and 20, respectively. Results from the final model calibration for WAI1 and WAI3 are illustrated in Figures 6.6 and 6.7.

#### 6.1.2.5 Model Performance Statistics and Skill

Model performance measures can be used following model calibration in order to determine how well a model simulates reality. However, to date there is no internationally recognised set of criteria or protocols for evaluating the performance of numerical modelling results (BRADY and SUTHERLAND, 2001). Presently, model simulations are typically compared with measured results, and in most cases some form of qualitative analysis is performed. This comparison is typically subjective, and the question of how good a model is needs to be defined in a more quantitative manner than the usual ranking (poor, good and excellent) that is normally applied (BRADY and SUTHERLAND, 2001; SUTHERLAND *et al.*, 2001).

SUTHERLAND *et al.* (2004) state that the performance of any model can be assessed by calculating its bias, accuracy and skill. The following statistical parameters are recommended by BRADY and SUTHERLAND (2001) as a basic set of appropriate model performance indicators (MPIs) for the modelling of wave height:

1. Bias between observation and prediction;
2. Root Mean Square Error (RMSE); and
3. Brier Skill Score (BSS).

These three MPI's are defined and used in the present study in order to compare their performance and to allow for discussion of their relative merits.

Bias is a measure of the difference in the central tendencies of the modelled and predicted data set and the true value of the parameter being estimated. For this study the difference between the mean values has been used, but often the median may be more appropriate. The basic equation for bias in the mean is:

$$Bias = \frac{1}{J} \sum_{j=1}^J (y_j - x_j) = \langle Y \rangle - \langle X \rangle \quad 6.10$$

where  $Y$  is a set of  $J$  forecasts or predictions, and  $X$  is a set of  $J$  observations. Bias is often referred to as reliability, in that an “unreliable” model is one which consistently over or under-predicts the observations (SUTHERLAND *et al.*, 2004).

Accuracy is a measure of the average size of the difference between a set of predictions and the corresponding observations, so even when there is no bias in a model it may still have a low accuracy (SUTHERLAND *et al.*, 2004). One of the most common measures of accuracy is the Root Mean Square Error (RMSE), given by:

$$RMSE = E^{1/2} = \left\langle (Y - X)^2 \right\rangle^{1/2} \quad 6.11$$

Values of RMSE are based on a scale of 0-1, with values close to zero representing very little error. It is important to note that the RMSE carries the assumption that all errors are in the model prediction and the data is error free (SUTHERLAND *et al.*, 2004). Of course this is not always the case in reality.

The Brier Skill Score (BSS) is a measure of skill. Skill scores are non-dimensional measures of the accuracy of a prediction relative to the accuracy of a baseline prediction, which can be an initial condition, an average value, random choice (from a possible range of outcomes) or a simple predictor (SUTHERLAND *et al.*, 2004). The BSS compares the mean square difference between the forecast and observation with the mean square difference between baseline prediction and observation: (VAN RIJN *et al.*, 2003; SUTHERLAND *et al.*, 2004)

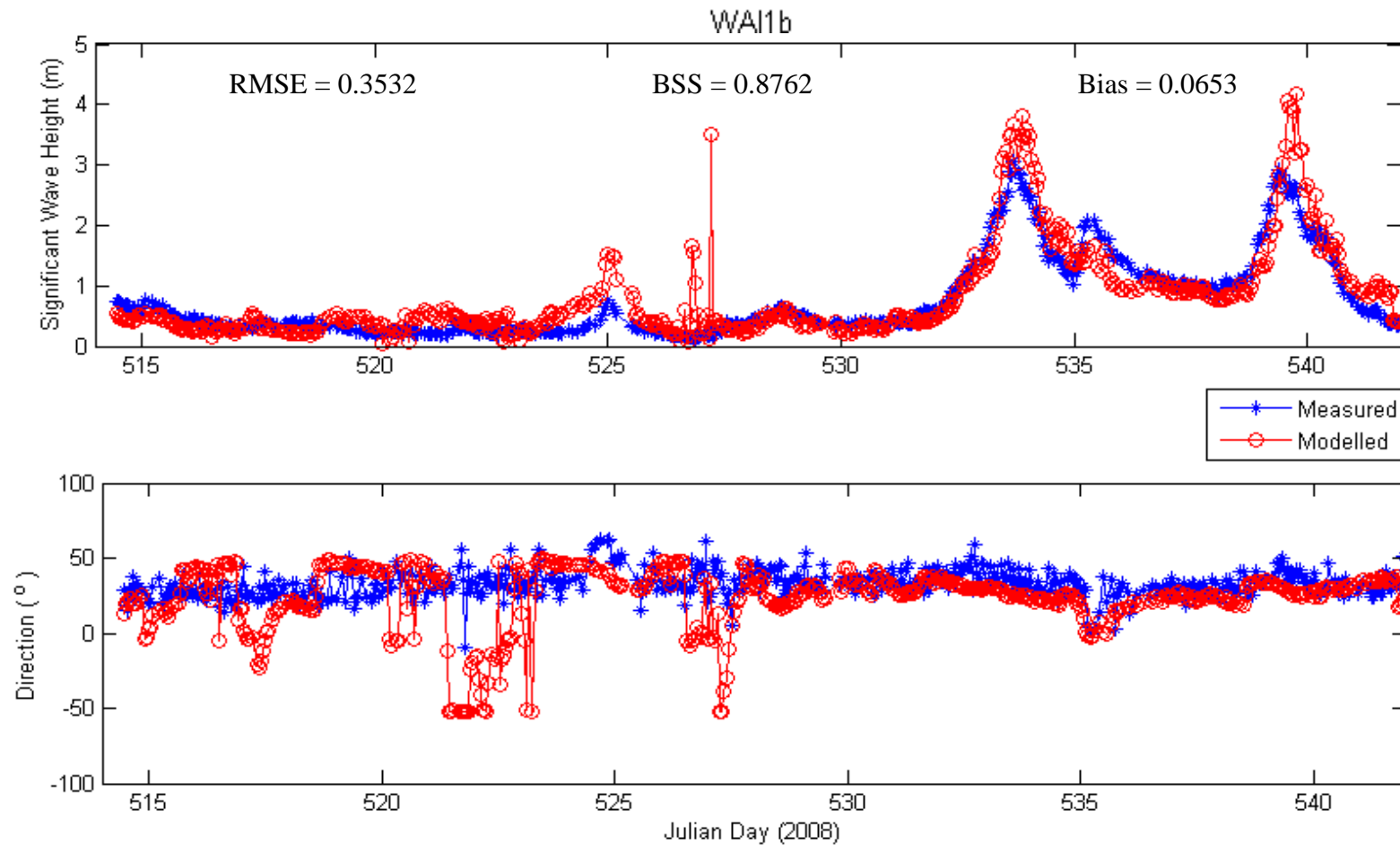
$$BSS = 1 - \frac{\langle (Y - X)^2 \rangle}{\langle (B - X)^2 \rangle} \quad 6.12$$

where  $B$  is the baseline prediction,  $X$  is set of observations and  $Y$  the final predictions. The BSS is also based on 0-1 performance criteria. However, unlike the RMSE, perfect agreement gives a score of 1 and zero indicates that the model is not predicting the results very well. Thus, any BSS higher than zero means that the modelling is more accurate than the baseline prediction, while a negative score represents a worse performance than the baseline prediction. One disadvantage with the BSS is that it can be extremely sensitive to small changes when the denominator is low, in common with other non-dimensional skill scores derived from the ratio of two numbers (VAN RIJN *et al.*, 2003; SUTHERLAND *et al.*, 2004).

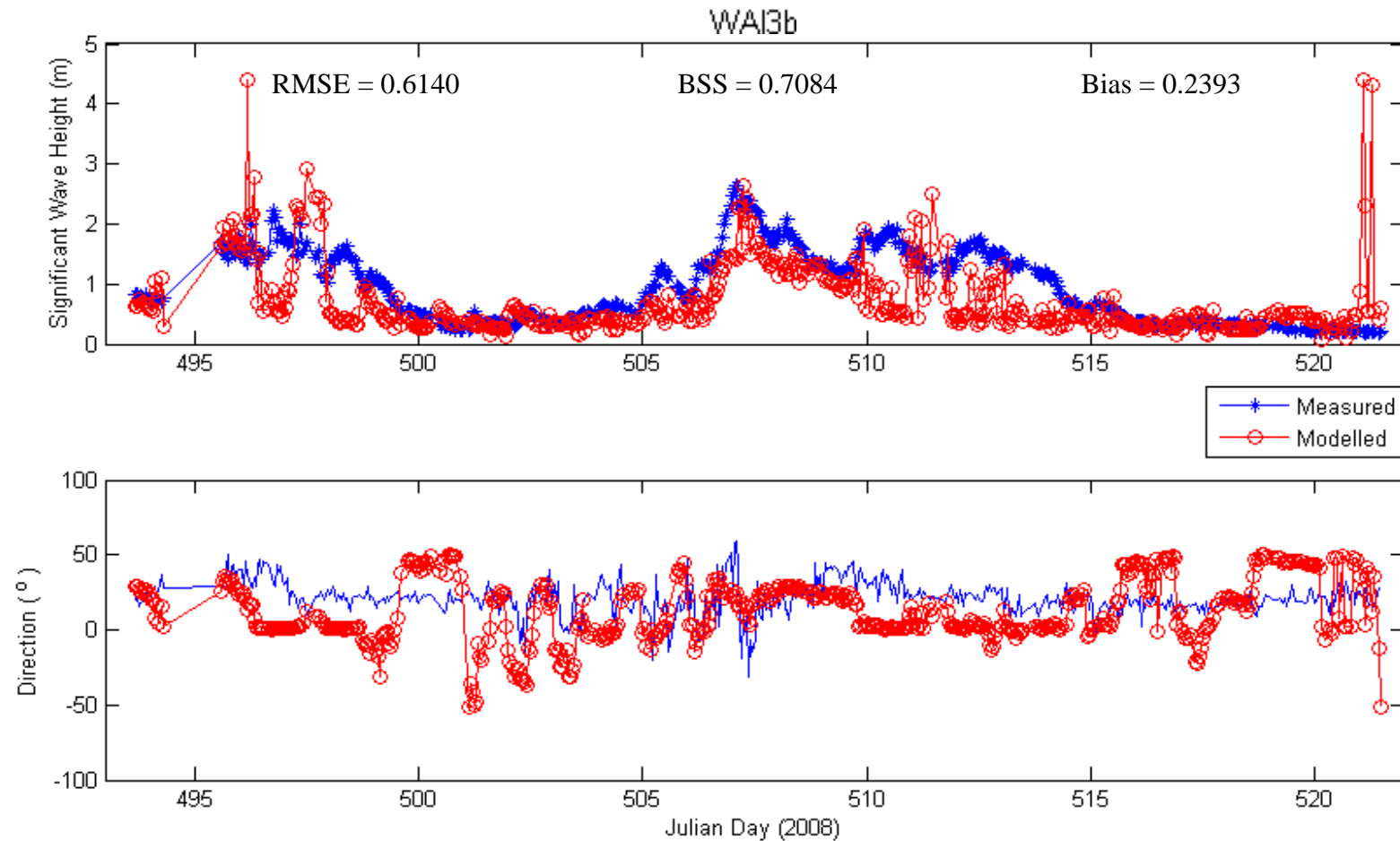
The BSS has already been applied to the modelling of coastal morphodynamics by BRADY and SUTHERLAND (2001), SUTHERLAND *et al.* (2001), SUTHERLAND *et al.* (2003) and VAN RIJN *et al.* (2003), all coming from the COAST3D project. SUTHERLAND *et al.* (2004) also described and applied a number of methods for assessing model performance to both hypothetical and real cases of coastal morphological modelling.

The proceeding results (Figures 6.6-6.7) demonstrate the calibration for the wave refraction modelling using WBEND. Bias, RMSE and BSS values for wave height calibrations are shown on each of the graphs to give an indication of how well the model performed.





**Figure 6.6:** Predicted model significant wave heights and direction against measured wave heights and direction at the S4 location WAI1b during the May/June 2008 deployment. Model prediction is shown in red and measured results are in blue. Final calibration was achieved using an eddy viscosity of 20 and a bottom friction of 0.01. Directions are relative to model grid (205° clockwise from true north).



**Figure 6.7:** Predicted model significant wave heights and direction against measured wave heights and direction at the S4 location WAI3b during the May/June 2008 deployment. Model prediction is shown in red and measured results are in blue. Final calibration was achieved using an eddy viscosity of 20 and a bottom friction of 0.01. Directions are relative to model grid (205° clockwise from true north).

#### 6.1.2.6 Calibration Results

Overall the model simulated measured wave heights reasonably well with only a few periods of deviation. It is apparent in both Figures 6.6 and 6.7 that the model outputs based on Pukehina wave buoy data slightly over-predicted wave heights during larger wave events. SAUNDERS (1999) noted a similar trend in modelled wave heights at West End Ohope Beach, and suggested that this may have been due to the frictional drag influence of bedforms not being taken into account with the steady state frictional coefficient. It has been established that frictional drag is governed by the size and overall geometry of sediment ripples created by wave-orbital motions (KOMAR, 1998). Therefore, bedforms that are generated by forcing waves are larger when the wave height increases, effectively dampening wave height. This effect provides a possible explanation for the slight over-predictions made by the model.

The directional calibration for the same data set was slightly poorer than that of the height calibration. Possible factors identified for causing directional discrepancies include:

1. The wave data used to force the model WBEND is derived from measurements obtained offshore Pukehina Beach, which is approximately 70 km southeast of Waihi Beach. Therefore, the wave parameters input into the model may not have been entirely representative of the wave characteristics present offshore Waihi Beach at that time. However, it is anticipated that any differences in wave behaviour at the two locations is likely to be relatively minor as both locations are subject to unlimited fetch from the vast Pacific Ocean.
2. Irregularities in the offshore bathymetry may have been amplified or minimised through hydrographic surveying errors, causing model simulations to inaccurately predict wave refraction and the subsequent zones of wave focusing and divergence near the shoreline.
3. Sheltering of WAI1b by Rapatiotio Point may mean that short period sea waves present offshore may not be as prominent in the nearshore. Hence

directional measurements offshore are not representative of the waves that reach the beach.

### *6.1.3 WBEND Scenarios*

Following calibration, WBEND was used to simulate a series of specific wave events using various combinations of wave height, period and direction captured during the S4 deployments. Specifically, the model was used to identify:

- i. The influence of Mayor Island and Steel's Reef on the focusing of wave energy along the coast;
- ii. The range of approaching directions that promote wave energy focusing at northern Waihi Beach;
- iii. Differences in refraction patterns between sea and swell waves, and;
- iv. What happens during extreme storm events.

Table 6.1 shows the various combinations of wave height, period and directions used in numerical simulations to investigate each of these specific aims.

Scenario 1 represents the average wave conditions at northern Waihi Beach as determined from the data collected during both summer and winter S4 deployments. 1.04 m and 6.99 s are the average mean significant wave height and average mean significant wave period respectively. The dominant wave direction at Waihi Beach was found to be from the east-northeast ( $62.5^\circ$  True), and was therefore used when determining the effect of varying wave heights and periods. Typical sea (6 s period) and swell (11 s period) waves are simulated in scenarios 2 and 3. For wave angle simulations (Scenarios 4-11), similar model runs were undertaken with the same height and period conditions but with the waves arriving from varying directions. Angles were varied by increments of  $10^\circ$  either side of the modal mean wave approach direction. Nine storm scenarios are simulated (Scenarios 12 to 20), applying the mean peak spectral period ( $T_p=9.35$  s) and the mean maximum height of the highest 10% of waves ( $H_{1/10} = 3.5$  m) for all the wave simulation angles.

**Table 6.1:** Different wave scenarios simulated in the WBEND model by using various combinations of wave height, wave period and wave approach angle.

Scenario	Wave Height (m)	Wave Period (s)	Wave Direction (True)	Model Direction
1	1.04	6.99	62.5°	22.5°
2	1.04	6	62.5°	22.5°
3	1.04	11	62.5°	22.5°
4	1.04	6.99	52.5°	32.5°
5	1.04	6.99	42.5°	42.5°
6	1.04	6.99	32.5°	52.5°
7	1.04	6.99	22.5°	62.5°
8	1.04	6.99	72.5°	12.5°
9	1.04	6.99	82.5°	2.5°
10	1.04	6.99	92.5°	-7.5°
11	3.5	6.99	102.5°	-17.5°
12	3.5	9.37	62.5°	22.5°
13	3.5	9.37	52.5°	32.5°
14	3.5	9.37	42.5°	42.5°
15	3.5	9.37	32.5°	52.5°
16	3.5	9.37	22.5°	62.5°
17	3.5	9.37	72.5°	12.5°
18	3.5	9.37	82.5°	2.5°
19	3.5	9.37	92.5°	-7.5°
20	3.5	9.37	102.5°	-17.5°

#### 6.1.4 Results

WBEND simulations of wave height, wave period, wave angle and storm scenarios are shown in Appendix IV. Summaries from each simulation are discussed in the following section.

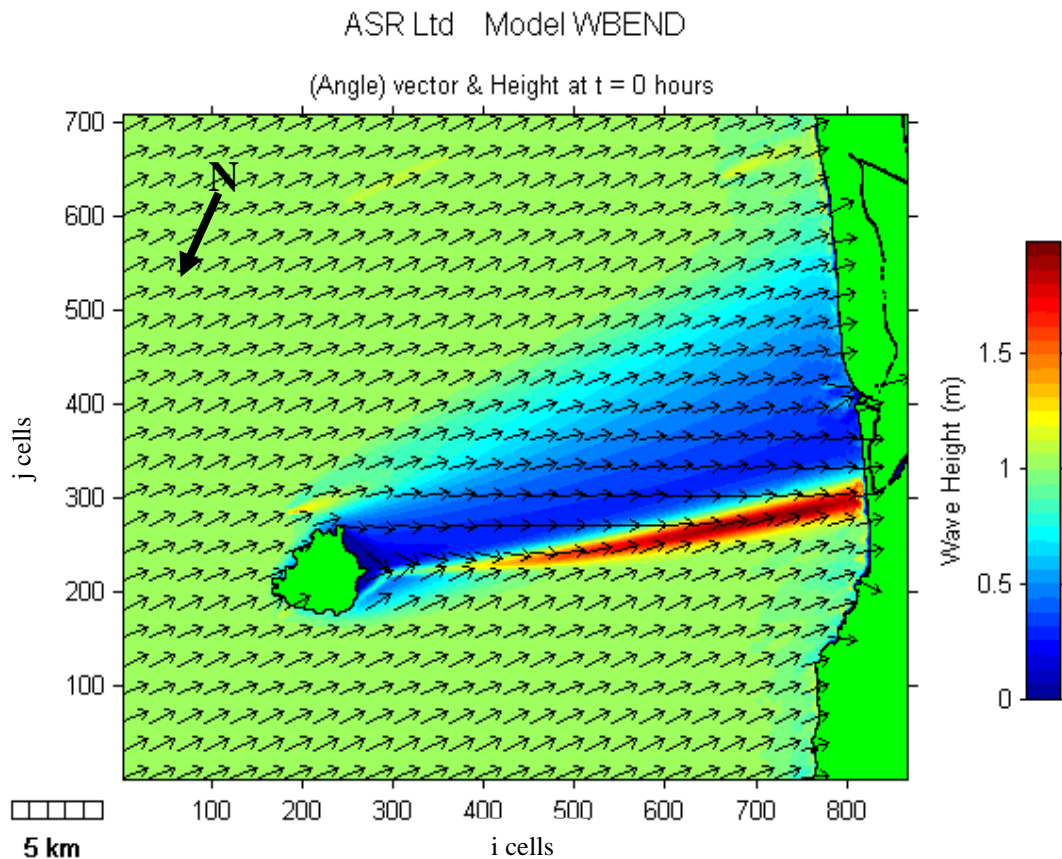
#### 6.1.5 Discussion

##### 6.1.5.1 Influence of Mayor Island and Steel’s Reef

Although previous wave refraction simulations at Waihi Beach have investigated the effect of Steel’s Reef on incoming waves, there has yet to be any detailed study on the wave refraction caused by Mayor Island. Mayor Island, located approximately 36 km offshore Waihi Beach, is the largest island in the Bay of Plenty and occurs in the lower left hand side of the Waihi Beach model grid

(Figure 6.4). MACKY *et al.* (1995) found that Mayor Island provided a significant wave sheltering effect for long period waves. It is therefore likely that significant wave refraction is occurring around Mayor Island by acting as a focal point for deepwater waves approaching the shelf. The shoals, reefs and small islands that surround Mayor Island may also have some effect. Similar impacts along other areas of the Bay of Plenty coastline outside the study area have been observed from other offshore anomalies (e.g. HAY, 1991; SPIERS, 2004). Figure 6.8 illustrates a scenario of average wave conditions as recorded from the directional current meter deployed offshore from northern Waihi Beach. Input values are: modal wave approach direction ( $62.5^\circ$  True), average mean significant wave height (1.04 m) and average mean significant wave period (10.64 s).

Figure 6.8 shows clearly that wave rays around the southern side of Mayor Island refract sharply towards the northwest, converging into those coming down the

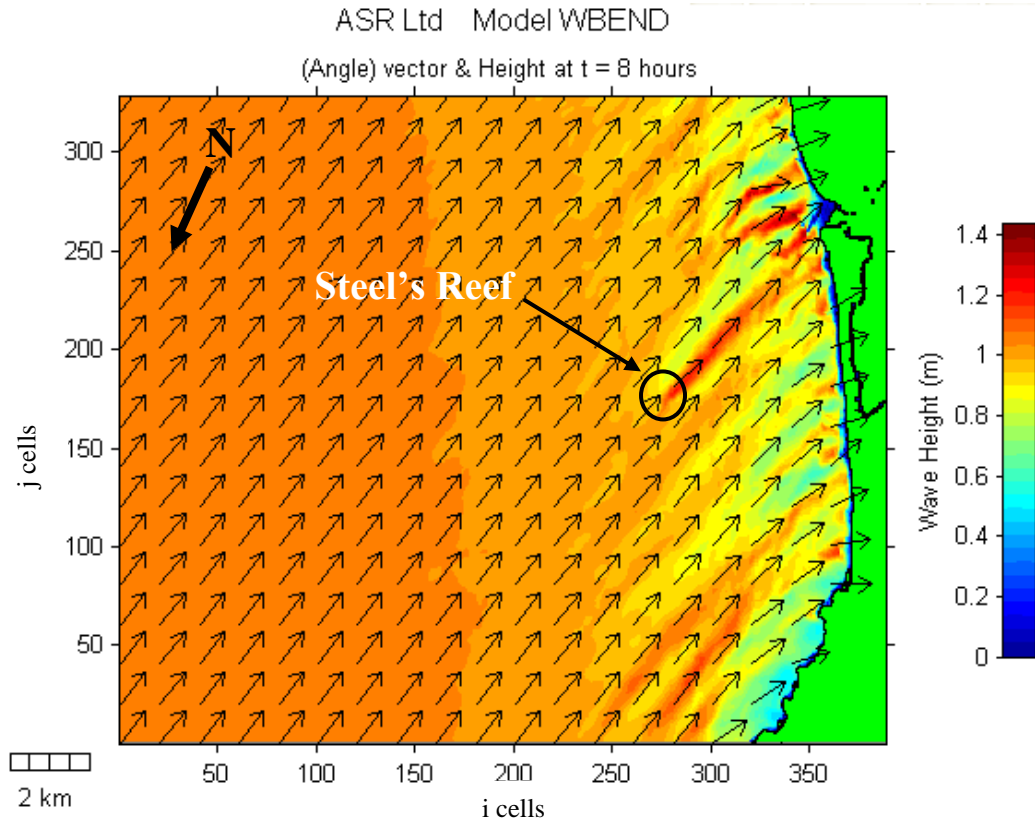


**Figure 6.8:** Model simulation using mean wave conditions (Scenario 1: 1.04 m, 6.99 s,  $62.5^\circ$  True) as recorded by the S4 current meters during the field deployment. Note the significant refraction influence of Mayor Island resulting in the strong, narrow concentration of high breakers impinging upon the shoreline. 1 grid cell = 50 m (i.e. 100 grid cells = 5 km).

northern side of the island. Through this strong refraction, Mayor Island effectively steers wave energy into a zone of convergence at the shore. It also acts to diverge wave energy and produce a “shadow” zone in its lee that is aligned parallel to the direction of wave advance. Under average wave conditions, waves progressing towards the coast from the modal wave approach direction ( $62.5^\circ$  True, ENE) refract around Mayor Island, producing a zone of wave convergence near Island View (located approximately j cell 300) (Figure 6.8). The model shows that this wave convergence will strongly concentrate a zone of high breakers ( $\sim 2$  m) upon the beach approximately 2 km wide. These findings imply that this area will likely be subject to higher energy levels than other sectors of the coastline in this region. This is also indicated by the results of the sediment textural analysis in Chapter 4, where it was found that grain sizes at Island View were coarser than elsewhere along northern Waihi Beach. With an increase in wave heights at the shoreline associated with wave focusing, wave set-up and wave run-up would also be expected to increase, thereby providing a mechanism for accelerated beach and dune erosion at Island View. A shadow zone of lower wave heights ( $\sim 0.4$ - $0.5$  m) due to wave divergence is predicted to stretch about 10 km southwards; an area which includes the southern end of Waihi Beach, the Katikati entrance to the Tauranga Harbour, and the very northern end of Matakana Island (Figure 6.8). The wave fronts south of Island View are relatively unchanged.

Areas of major refraction are also expected around Steel’s Reef, a stable rocky feature rising to 8 m water depth, located just beyond the 20 m depth contour approximately 4 km offshore southern Waihi Beach. As mentioned previously, as well as generating a strong narrow band of wave focusing at the coastline, wave divergence around Mayor Island also produces a wide ray of wave sheltering up 25 km long. The vast band of sheltering (illustrated by the blue in Figure 6.8) effectively “overshadows” or disguises any local bathymetry refraction influences closer to the shoreline, such as that of Steel’s Reef, and also the large shore normal sand ridges identified in the side-scan sonograph in Chapter 3. Therefore, a smaller bathymetry extending 388 x 328 grid cells was created by subsectioning the original larger grid, specifically for the purpose of assessing the influences of Steel’s Reef and the large sand ridges on the transformation of

approaching swell. Figure 6.9 shows an example of a simulation over the smaller bathymetric grid applying the same mean wave height and period parameters used to create Figure 6.8, but with a north-northeasterly ( $22.5^\circ$  True) wave approach. The location of Steel's Reef can be identified in Figure 6.9 by the increase in wave height as they travel over the reef.



**Figure 6.9:** Model simulation for a 1.04 m wave approaching from the NNE (Scenario 7). The location of Steel's Reef is shown. Note the increase in wave height as the wave progresses over the reef, and the resulting band of wave energy focusing at the southern end of Waihi Beach, which will likely be influencing accelerated beach and dune erosion. 1 grid cell = 50 m (i.e. 100 grid cells = 5 km).

Figure 6.9 clearly illustrates the narrow zone of higher waves in the lee of Steel's Reef, which is particularly evident for swell approaching from the northeast and east-northeast (Appendix IV: Scenarios 5, 6 and 7). The subsequent wave convergence in the lee of the reef causes a zone of high breakers to concentrate upon the shoreline at the southern end of Waihi Beach, which may contribute towards accelerated beach and dune erosion there. These findings complement the results of STEPHENS (1996), who also concluded that Steel's Reef provides a



means of focusing large waves up to 5000 m along the southern half of Waihi Beach, irrespective of the existing topography fronting the reef. STEPHENS (1997) suggests that refraction around Steel's Reef likely plays an important role in the formation of the arcuate duneline embayments at southern Waihi Beach, by focusing large storm waves on a particular sector of the beach depending upon the approaching direction of the waves. HOBAN (1993) also showed that wave refraction focused wave energy into the centre of the arcuate duneline embayments, and noted that the focusing of wave energy corresponded to greater magnitudes of beach change. STEPHENS (1996) points out that if the wave spectrum consists of multiple wave approach angles, or more than one wave period, then wave focusing may occur at more than one location.

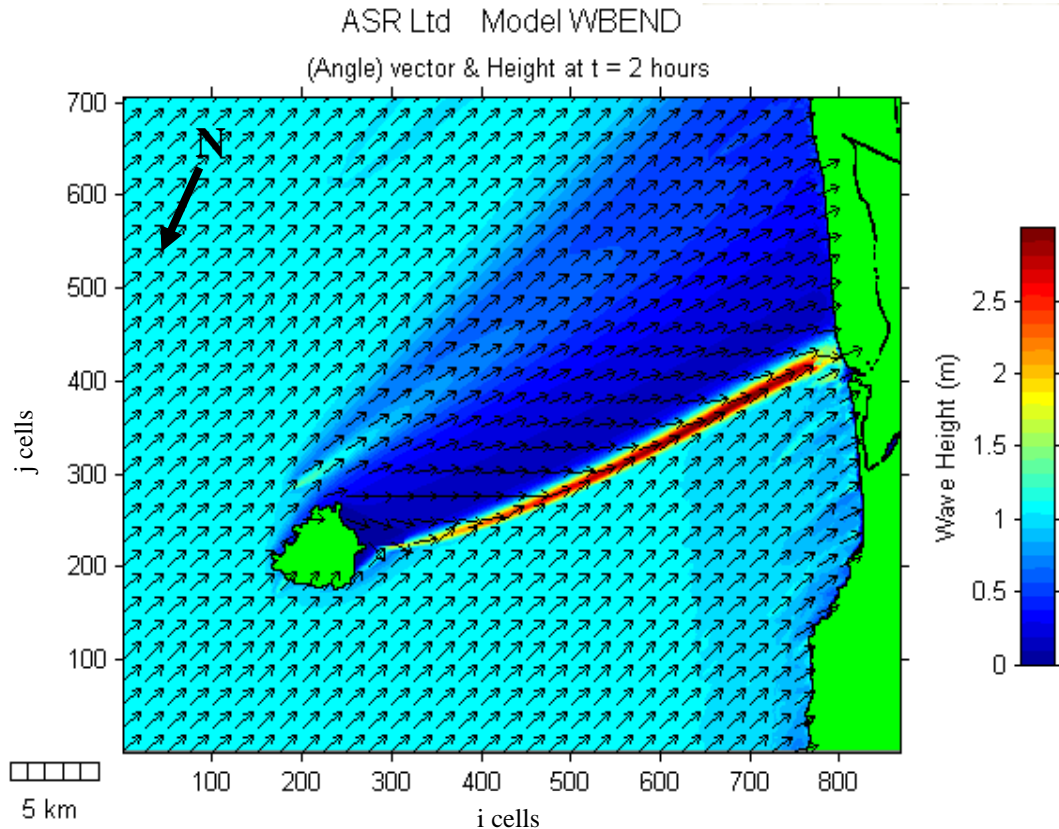
#### 6.1.5.2 Wave Direction Scenarios

From wave direction scenarios, the position of the zone of wave energy focusing associated with convergence around Mayor Island can be seen to vary alongshore with differing deep-water wave approach direction. Active wave focusing at Waihi Beach occurs with waves propagating onto the beach from 52°-83° True (Scenarios 1, 4, 8 and 9, Appendix IV). Particular areas of increased wave heights were concentrated at benchmarks CCS49 and CCS52 when waves were approaching from the east-northeast (62.5° and 72.5° respectively). Hence, these locations may be particularly prone to frontal dune erosion.

When the waves start arriving with more of a northerly component, the principal zone of convergence moves northwards, accordingly (Figure 6.10). The model also shows that a greater swath of the coastline is exposed to changes in wave heights. Although the width of the zone of wave focusing does not change much with varying wave approach direction, wave fronts arriving from the northeast to north-northeast produce a larger wave shadowing zone that may affect between 20 and 25 km of beach along this stretch of coastline (Figure 6.10).

By varying wave approach to the north-northeast, the predicted wave heights at the shoreline of northern Waihi Beach decreases, possibly due to a sheltering effect created by Rapatiotio Point. A zone of reduced wave heights about 1 km

wide in the lee of Rapatiotio Point can be seen in Figure 6.9, providing further evidence of wave sheltering by the headland at the far northern end of the beach. The model predicts an increase in wave heights along Waihi Beach associated with swells from the east (Scenario 10, Appendix IV).



**Figure 6.10:** Model simulation for a 1.04 m wave approaching from the NE (Scenario 5) illustrating the wide swath of wave sheltering extending south along Matakana Island and beyond the model grid boundary. 1 grid cell = 50 m (i.e. 100 grid cells = 5 km).

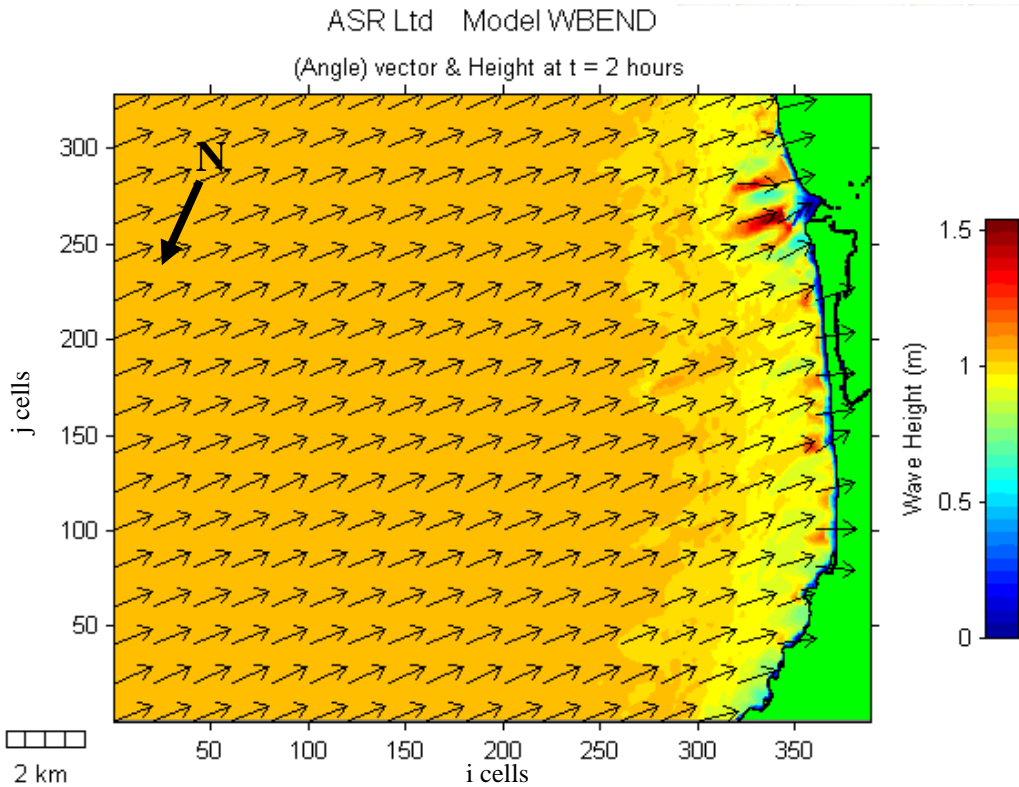
### 6.1.5.3 Wave Period Scenarios

The depth at which refraction commences is dependent upon the period of the wave. In deep water, wave period is directly related to wavelength:  $L = 1.56 T^2$ . Longer period waves have longer wavelengths, and hence begin to interact with the seafloor at greater depths than a shorter period wave (KOMAR, 1998). Consequently, long period (swell) waves are more affected by irregular bathymetry resulting in greater potential for refraction than short period (sea) waves (SHAND *et al.*, 2005).

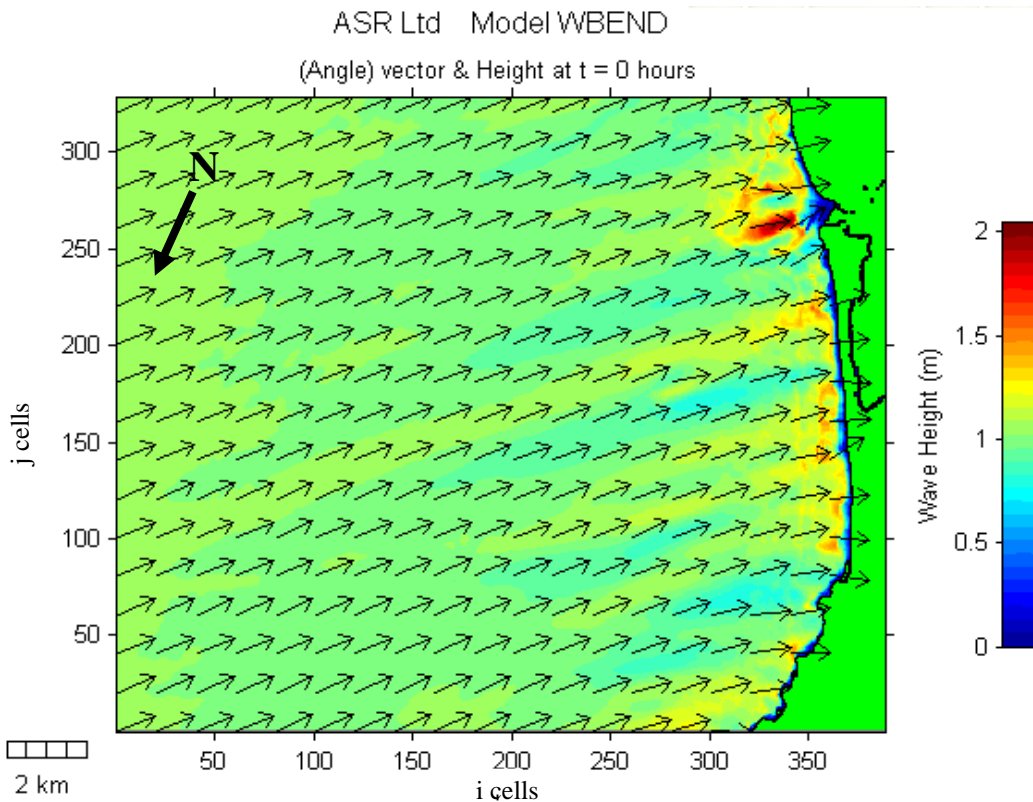
Figure 6.11 illustrates a simulation of a sea wave (6 s) and Figure 6.12 a long period swell wave (11 s), both scenarios approaching from the northeast. At Waihi Beach, the model predicts that longer period swell wave vectors will refract, tending shore-normal to align parallel to the coastline earlier than shorter period waves, which maintain the original approach angle input into the model until the wave reaches much shallower water depths. This is related to longer period waves feeling the bottom at greater depths and having more of a chance to align their crests with the bathymetric contours. More intensive wave refraction and focusing can be seen occurring at the far northern end of Waihi Beach and particularly around Rapatiotio Point. This is believed to be due to the differences in offshore gradient, as the beach and nearshore zone is steeper towards the south compared to the wide shallow nearshore zone off northern Waihi Beach (HEALY *et al.*, 1977; HUME and HICKS, 1993). This means that at the southern end of the beach, longer period waves have less time to align with the beach.

In addition to the angular changes in wave direction, changes in wave height along the Waihi Beach shoreline were observed associated with changes in wave period. Comparing the swell wave simulation (Figure 6.12) to that of the sea wave (Figure 6.11) reveals that wave refraction is intensified under longer period swell, resulting in greater wave focusing and hence larger wave heights at the shoreline, with an approximate wave height difference of 0.4 m between the two scenarios. From Figure 6.12, it is also clear that longer period waves are more affected by the large shore-normal sand ridges between depths of 15 to 30 m, so that variation in wave height alongshore is amplified. BEAMSLEY (1996) also found that for longer period waves the wave train is refracted more strongly by the shoreface topography, stating that “wave height distributions at the shoreline begin to mirror the topographic features”.

As Figure 6.12 illustrates, the large sand ridges which characterise the Waihi Beach shoreface play an important controlling role on the longshore wave height variability at the shoreline. These spatial gradients in wave height are expected to cause local erosion or accretion. Wave refraction analysis by BEAMSLEY (1996) found that zones of enhanced breaker wave heights consequently had the same



**Figure 6.11:** Sea wave (6 s period) simulation (Scenario 2), for a 1.04 m wave approaching Waihi Beach from the NE. The wave train maintains its northeasterly approach right up until very shallow water depths are reached. 1 grid cell = 50 m (i.e. 50 grid cells = 2.5 km).



**Figure 6.12:** Swell wave (11 s) simulation (Scenario 3), for a 1.04 m wave approaching Waihi Beach from the NE. The swell wave shoals in deeper water due to wave refraction being intensified, and so reaches a greater wave height further offshore. Consequently there is an increase in wave heights at the shoreline. 1 grid cell = 50 m (i.e. 50 grid cells = 2.5 km).

length scale as the large arcuate duneline embayments present along the Waihi Beach shoreline. The formation of these dune embayments has been previously linked to zones of wave convergence caused by wave refraction over the offshore sand ridges (HOBAN, 1993; STEPHENS, 1996).

The greater alongshore variation in breaking wave heights, directly related to wave refraction over the sand ridges on the shoreface, may subsequently influence nearshore circulation patterns by generating longshore currents flowing from positions of higher to lower wave height. Longshore currents which move towards each other in the surf zone may then turn seawards at the convergence and move offshore as fast flowing rip currents. The hydrodynamics analysis in Chapter 5 has already revealed the existence of strong seaward flowing currents at northern Waihi Beach, of which may possibly have been rip currents.

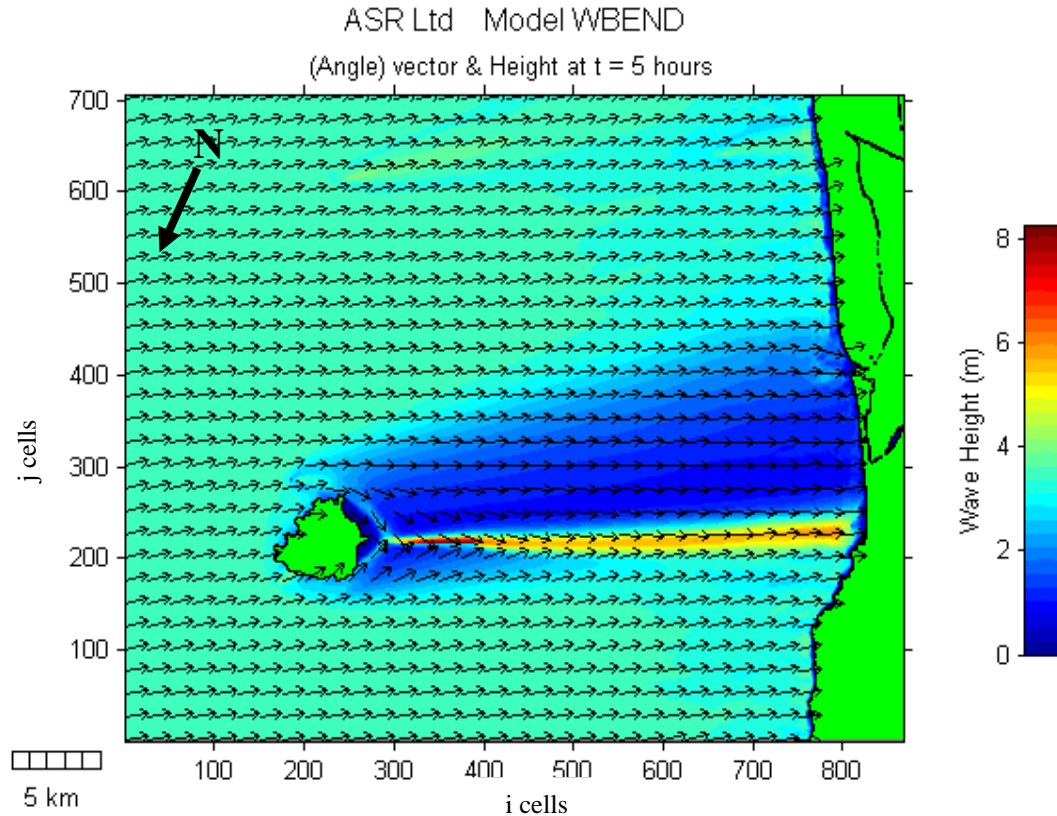
It is also apparent that the refraction influence of Mayor Island is more dominant under long period swell waves, with a much greater magnitude of wave rays bending around the southern side of the island, enabling an even larger modifying effect on wave behaviour. The result is a shift in the position of the zone of wave focusing and their associated larger wave heights approximately 3 km further north of Island View, near the sensitive areas of Two Mile Creek and the seawall at the southern end of Shaw Road. Because long period swell waves are found to be associated with enhanced wave heights at the shore, the modelling results therefore imply that the area of beach fronting the seawall and around the creek are highly prone to enhanced beach erosion when subject to swell from distantly generated storms. This outcome is supported by field observations in the present study, and those of previous studies (e.g. HARRAY, 1977; STEPHENS, 1996), of a very narrow beach profile and chronic sediment deficit at that location.

#### 6.1.5.4 Storm Wave Scenarios

Simulating a storm event using typical storm wave characteristics as measured during the field deployment may help to identify sectors of coast along northern Waihi Beach which are prone to considerable beach and frontal dune erosion. As expected, results obtained showed wave heights within the regions of wave energy

focusing to increase. This is because wave energy dissipation is not as effective with greater wave heights under storm conditions, as it is with smaller waves. Wave heights at the shoreline are also predicted to become progressively larger as waves become more northerly in their approach. Scenario 17 (Figure 6.13) depicts a wave approach from the east-northeast direction, illustrating active wave energy focusing near the surf club at northern Waihi Beach under modal wave approach conditions. A wide swath of wave sheltering is predicted to extend south to the northern end of Matakana Island. Adjusting the wave approach direction for storm simulations (Scenarios 11-20) illustrates generally similar trends to that of the wave direction scenarios, with the zone of wave focusing and associated increased wave heights moving further north or south with increasing or decreasing input wave angle, respectively.

Interestingly though, the last four storm simulations (wave directions of 72.5°-102.5° True) display only a very minor difference in the position and magnitude of the zone of active wave focusing produced by the convergence around Mayor



**Figure 6.13:** Model simulation of a typical storm wave scenario approaching Waihi Beach from the ENE (Scenario 17: 3.5 m, 9.5 s, 72.5° True), illustrating active wave focusing near the surf club at the very northern end of Waihi Beach. 1 grid cell = 50 m (i.e. 100 grid cells = 5 km).

Island. Rather, it is the wide band of wave sheltering which progresses further north with an increasingly northerly approach angle, while the zone of wave focusing remains relatively stationary around the very northern end of Waihi Beach and Rapatiotio Point (Scenarios 17-20, Appendix IV). It is not entirely certain what is causing this effect, although it is believed to be associated with the fact that waves naturally refract and bend towards headlands due to the offshore shoal area associated with the headland (KOMAR, 1998). The wave energy is therefore concentrated on and around the headland, resulting in subsequently larger wave heights due to the enhanced wave energy. The implication of this wave convergence being fixed on northern Waihi Beach over a wide range of wave approach angles is that it provides greater opportunity for enhanced wave heights at that location and, consequently, accelerated beach and dune erosion.

## 6.2 NEARSHORE LITTORAL DRIFT MODELLING AND SEDIMENT TRANSPORT BY WAVES

### 6.2.1 Method

By employing the breaking wave energy flux method outlined by KOMAR (1998), the numerical model WBEND was used to calculate nearshore littoral drift rates along northern Waihi Beach. WBEND has been previously used to estimate littoral drift rates based upon long-term wind and wave records at Mangawhai-Pakiri (BLACK *et al.*, 1998), West End Ohope (SAUNDERS, 1999), and Pukehina (EASTON, 2001).

This method is based on the assumption that the longshore transport rate ( $Q_l$ ) depends upon the longshore component of energy within the surf zone. Wave energy flux or power is evaluated at the breaker zone by:

$$P_{ls} = (ECn)_b \sin \alpha_b \cos \alpha_b \quad 6.13$$

where  $n$  is the wave number ( $1/2$  in deep water and 1 in shallow water),  $\alpha_b$  is the angle of the wave crest at breaking, and inclusion and multiplication by  $\cos$  and  $\sin$  terms yields the longshore component of wave power. The wave energy ( $E$ ), calculated at breaking depth (denoted by  $h_b$ ), is given as:

$$E = \frac{1}{8} \rho g H_b^2 \quad 6.14$$

The wave celerity ( $C$ ) can be approximated by:

$$C = \frac{gT}{2\pi} \tanh\left(\frac{2\pi h}{L}\right) \quad 6.15$$

The root mean square of the wave height at breaking ( $H_b$ ) was approximated using the ratio of water depth ( $h_b$ ) and wave gamma (taken as 0.78) ( $h_b = H_b/0.78$ ).

The volume of sediment transported is given by the CERC formula:

$$Q_l = \frac{I_l}{(\rho_s - \rho) g a'} \quad 6.16$$

where  $a'$  is the sediment porosity, given as 0.6 according to KOMAR (1998), and  $I_l$  is the immersed-weight transport rate which is empirically related to the longshore component of wave power:

$$I_l = K P_l \quad 6.17$$

where  $K$  is a coefficient taken to be 0.77 following KOMAR and INMAN (1970).

WBEND was used to make precise estimates of net littoral drift direction and sediment transport rates at northern Waihi Beach. Wave information used to generate outcomes were the mean significant wave height (1.04 m) and average mean significant wave period (6.99 s) over the combined summer (15/11/07 – 15/12/07) and winter (07/05/08 – 25/06/08) deployments at Waihi Beach. To



enable coverage of spatial variation in littoral drift rates, the coastline was divided into 5 sites as represented by the profile benchmarks (Figure 3.1). It must be stressed that directions and rates of littoral drift produced by WBEND are only relevant to data entered into the model.

## 6.2.2 Results

### 6.2.2.1 Littoral Drift during the Study Period

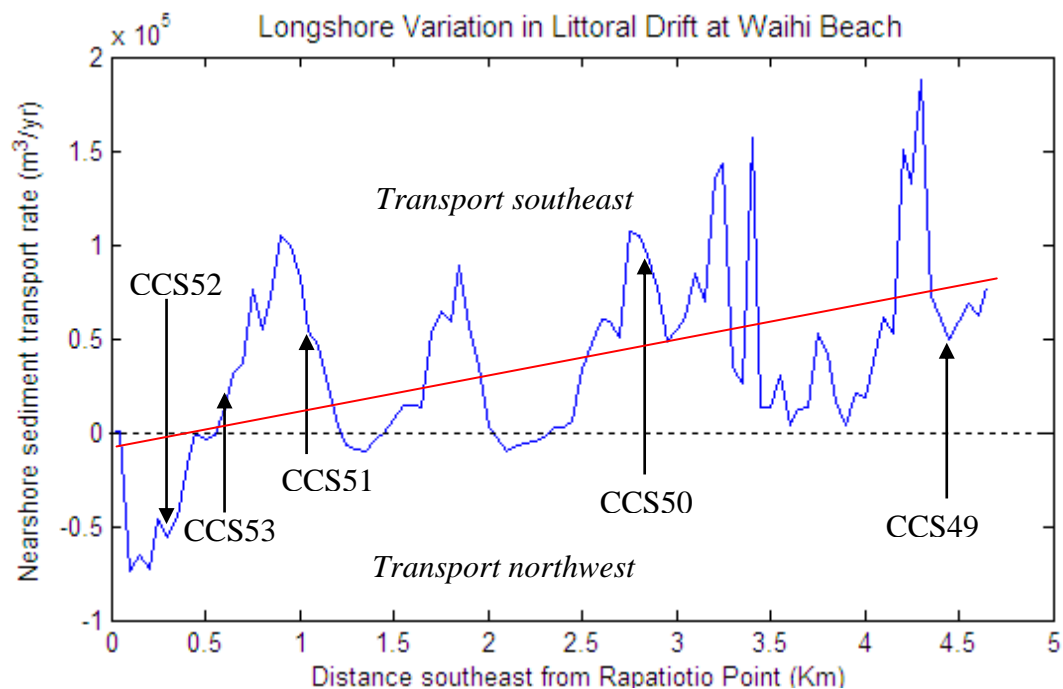
Longshore variation in nearshore transport rates ( $\text{m}^3/\text{yr}$ ) along northern Waihi Beach were examined over the study period. Table 6.2 compares estimates of littoral drift rates at the 5 benchmark locations along northern Waihi Beach. Results indicate a net northwesterly drift at benchmark CCS52, with a net southeasterly drift predicted at all other benchmarks locations towards the south. The northwesterly-directed drift predicted at the far northern end of Waihi Beach is likely to be influenced by the presence of Rapatiotio Point and the rocky Coromandel coastline, which effectively shelter the beach from waves originating from the north to northwest.

Predicted nearshore sediment transport rates vary along northern Waihi Beach (Table 6.2). The magnitude of the southeasterly littoral drift is greatest at Profile CCS49 in the centre of Waihi Beach. The average net sediment transport rate for the entire model grid is  $51,670 \text{ m}^3/\text{year}$ . This figure is consistent with values estimated for the Bay of Plenty coastline, which range from  $50,000 \text{ m}^3$  to  $100,000 \text{ m}^3$  of sediment per year (HEALY, 1980; BOPRC, 1991; HEALY *et al.*, 1991; HUME and HERDENDORF, 1992).

**Table 6.2:** Net littoral drift volumes at five profiles along northern Waihi Beach simulated using the wave refraction model WBEND. Estimates are based on 80 days of wave data collected over two deployments at Waihi Beach during 2007/2008. The breaking wave formulae was used to calculate transport volumes, with a negative value indicating a net northwesterly drift and a positive value a net southeasterly drift.

Littoral Drift Rate	Profile CCS52	Profile CCS53	Profile CCS51	Profile CCS50	Profile CCS49
$\text{m}^3/\text{day}$	-161	40	155	133	212
$\text{m}^3/\text{year}$	-58,597	17,655	56,470	79,418	46,210

Figure 6.14 illustrates the predicted net annual littoral drift rates within the modelled region derived from WBEND sediment transport simulations. The net northwesterly drift near Rapatiotio Point at the far northern end of the beach is evident. The location of the reversal in drift direction to southeasterly can be identified approximately 500 m south of Rapatiotio Point, almost exactly in the centre of CCS52 and CCS53. This implies that the anticipated wave sheltering effect caused by Rapatiotio Point is only impacting on the area of beach up to 500 m south from the headland. Beyond that location, nearshore littoral drift direction does not appear to be influenced by the headland. Littoral drift tends to become stronger as it switches to predominantly southeasterly towards the southern end of the study area. On the whole, the output results indicate that overall nearshore littoral drift along northern Waihi Beach is in a southeasterly direction. The nearshore sediment transport rate exiting the study region from the southeastern boundary (CCS49) was predicted by WBEND to be 46,210 m<sup>3</sup>/year or 10.3 m<sup>3</sup>/m. A regression analysis was also carried out in order to define a littoral drift gradient between benchmarks CCS52 and CCS49 (Figure 6.14).



**Figure 6.14:** Spatial variation in nearshore sediment transport estimates (m<sup>3</sup>/year) along the northern sector of Waihi Beach over the study period. Annual rates have been extrapolated from 80 days of wave data collected offshore Waihi Beach during 2007/2008. Net littoral drift is to the northwest at the far northern end, becoming southeasterly towards the south. Regression analysis illustrates a positive relationship, and hence could be expected to have a tendency towards erosion.

Outcomes of the regression analysis for sediment transport rate data along northern Waihi Beach illustrates a greater potential for net southeasterly sediment transport at CCS49 compared to CCS52. The implication of the littoral drift gradient is that  $\sim 75,000 \text{ m}^3/\text{year}$  or  $\sim 17 \text{ m}^3/\text{m}$  of sediment would be expected to be lost from the littoral sediment budget. This tendency implies a long-term sediment deficit for northern Waihi Beach.

The predicted littoral drift direction and rates of sediment transport from WBEND simulations is in agreement with previous conclusions that net movement at Waihi Beach is small and southeasterly (e.g. HEALY *et al.*, 1977; HARRAY and HEALY, 1978; HEALY, 1980). HEALY *et al.*, (1977) and HARRAY and HEALY (1978) have listed several environmental and geomorphic indicators which show that net littoral drift at Waihi Beach is towards the southeast. These include:

1. Central and southern sectors of Waihi Beach are characterised by significantly higher dunes than at the northern end, indicating greater sediment accumulation towards the south;
2. The orientation of the Bowentown Bar and the main channel of the Katikati Entrance to the Tauranga Harbour are deflected south of shore-normal, indicative of major sediment flux from the north;
3. 12 months of daily wind data collected from benchmark CCS50 revealed offshore and onshore wind resultants directed  $54^\circ$  and  $12^\circ$  south of shore-normal respectively, thereby generating southerly components of wave-generated littoral drift in the breaking wave zone.
4. Daily wave monitoring over the same 12 month period also revealed a wave resultant directed  $4^\circ$  south of shore-normal, again implying a tendency for southeasterly directed littoral drift.

It is essential to note that in comparison with previous short-term studies at Waihi Beach (e.g. HARRAY, 1977; HOBAN, 1993), the wave climate captured during the 2007/2008 S4 deployments in the present study was relatively energetic due to episodic storm activity. Because calculated annual drift rates have been extrapolated from only 80 days of S4 wave data, the few major storm events recorded, particularly during winter 2008, will have considerable influence on the

magnitude of littoral drift estimates. The confidence in these predictions would improve if a longer-term record of wave climate was available. It is also important to acknowledge that the rates of sediment transport calculated above are entirely dependent upon the available sediment supply, which must be accurately assessed.

#### 6.2.2.2 Longer-Term Littoral Drift

In order to investigate longer-term littoral drift trends at northern Waihi Beach, a five year record of instrumental wave data from 2003-2008 collected by EBOP's Pukehina wave buoy (Iremonger, *pers comm.* 2008) was used. The instrument is located 13 km directly offshore from Pukehina in 60 to 62 m water depth. It has been shown from model calibration (section 6.1.2.4 *Model Calibration*) that the Pukehina wave buoy data predicted measured nearshore wave heights at the study area with reasonable accuracy, and has thus been deemed suitable for determining long-term littoral drift direction and transport rates at northern Waihi Beach.

Long-term drift directions determined using the record of wave data from offshore Pukehina exhibited a similar pattern to those experienced during the study period (Table 6.3). As with the short-term results net drift tended to be northwesterly at the far north, although at comparatively slower drift rates (~9,000-28,000 m<sup>3</sup>/year), which again reflects the oscillatory nature of the drift at northern Waihi Beach. For the remainder of the beach littoral drift was generally southeasterly, as with the predicted littoral drift during the deployment period, with relatively uniform drift rates between years. Much smaller quantities of sediment were predicted to be leaving northern Waihi Beach via the littoral drift based upon the longer-term wave record, confirming that the energetic winter deployment certainly influenced predicted drift rates based upon the short-term wave data of the present study.

Interestingly the model output based upon the 2008 data, which consists of only six months of wave information, indicated a much more persistent northwesterly drift than the other years (Table 6.3). Upon examination of wave approach directions over the full wave buoy data set, it was observed that between January

**Table 6.3:** Annual littoral drift volumes at five profiles along northern Waihi Beach predicted from the wave data collected offshore Pukehina Beach between 2003-2008 (Source: S. Iremonger, EBOP, *pers comm.* 2008). The breaking wave formulae was used to calculate transport volumes, with a negative value indicating a net northwesterly drift and a positive value a net southeasterly drift. Annual drift rates tend to be much lower than those extrapolated from the wave data measured offshore northern Waihi Beach during 2007/2008.

Littoral Drift Rate m <sup>3</sup> /year	Profile CCS52	Profile CCS51	Profile CCS53	Profile CCS50	Profile CCS49
23/09/03-31/12/03	-11,171	21,771	2,038	20,560	11,200
01/01/04-31/12/04	-14,742	20,259	2,007	19,135	10,869
01/01/05-31/12/05	-28,334	39,638	23,457	58,063	14,544
01/01/06-31/12/06	-14,243	20,484	2,013	19,399	10,982
01/01/07-31/12/07	-9,395	38,655	1,790	48,631	9,455
01/01/08-30/06/08	-15,951	-7,887	1,297	-23,308	3,123

and June of 2008 the proportion of waves approaching from the southeast was much greater than any of the year-long data sets. The persistence of northwesterly approaching waves and resulting higher magnitude of northwesterly littoral drift may also explain why the model predicted a much smaller rate of littoral drift being lost from the southeastern boundary (CCS49) compared to the year-long records. This further demonstrates that short-term wave records may not provide accurate predictions of the annual drift rate in the Bay of Plenty due to the episodic wave climate.

### 6.2.3 Discussion of Littoral Drift Estimates

Oscillating longshore littoral drift was predicted at northern Waihi Beach by the numerical wave model WBEND using the short-term wave data from the S4 deployments in the present study, but also using the longer 5 year record of Pukehina wave buoy data. The location of the diverging drift was positioned approximately 500 m southeast of Rapatiotio Point. Implications of a diverging longshore current at this location indicate that an accumulation of sediment would be expected against the headland if there was a net drift to the northwest in this region. However, as the far northern end of Waihi Beach is characterised by a relatively flat beach profile typically lacking a well formed berm, no such surplus of sand exists against the headland nor within the offshore bar. The presence of a diverging littoral drift between CCS52 and CCS53 would also imply exceptional local sediment starvation at that location, which also is not apparent. Hence, there

is insubstantial geomorphic evidence to support the prediction of a diverging longshore current along this part of the beach.

The northwesterly directed littoral drift predicted at CCS52 by WBEND simulations also raises the question of the potential for sediment from northern Waihi Beach to be transported northwards of Rapatiotio Point to Orokawa Bay and beyond. However, previous mineralogical and sedimentological studies have revealed that beach sediments at Orokawa Bay to the north of Waihi Beach are distinctly different (SCHOFFIELD, 1970; HARRAY and HEALY, 1978), and therefore no observable sediment exchange occurs between the two beaches.

Despite the controversial northwesterly directed currents predicted at the far northern end of the beach, an overall net southeastwards littoral drift was predicted along northern Waihi Beach. This is in agreement with the collective geomorphic evidence mentioned previously, with a resulting net loss of sands alongshore from the Waihi Beach coastal sector. From numerical sediment transport modelling, it is estimated that 46,210 m<sup>3</sup>/year or ~10.3 m<sup>3</sup>/m of sediment is removed from the beach-nearshore sediment budget via littoral drift. Implications of this, combined with wave energy focusing outcomes, demonstrate a potential long-term sediment deficit along northern Waihi Beach. As previously mentioned, interpolation of annual drift from 80 days of wave data is questionable, as it does not account for storm events that may occur outside of the sampled timeframe, and may not represent the long-term wave climate. It must therefore be stressed that estimates of littoral drift rates are only for the 2007/2008 deployment period.

### 6.3 SUMMARY

Calibration of the model WBEND was performed using monochromatic wave statistics measured during the field study (Chapter 5) so output data matched data collected simultaneously at Waihi Beach:

- Relatively good wave height calibration was achieved using a constant friction and eddy viscosity of 0.01 and 20 respectively. It was observed, however, that the Pukehina wave buoy data slightly over-predicted measured wave heights during larger wave events, resulting in increased bias.
- The slightly poorer wave directional calibration for the same data set was attributed to the possibility that wave parameters obtained from Pukehina may not have been entirely representative of the wave climate offshore Waihi Beach, hydrographic surveying errors, and/or wave sheltering by Rapatiotio Point which meant that directional measurements offshore are not representative of the waves that actually reach the beach.

Following model calibration, several wave scenarios were simulated to investigate the patterns of breaking wave along the Waihi Beach shoreline. The results obtained indicate that:

- Wave refraction around Mayor Island effectively concentrates wave energy into a defined zone approximately 2 km wide. The subsequent concentration of wave energy produces the highest breakers that impinge upon the beach, which may contribute towards accelerated beach and dune erosion at northern Waihi Beach. Refraction around Steel's Reef also appears responsible for focusing wave energy at the southern end of Waihi Beach, particularly for swell approaching from the northeast and east-northeast.
- The zone of wave energy focusing associated with convergence around Mayor Island was observed to vary alongshore with differing deep-water wave approach direction. Varying wave approach to the north-northeast resulted in reduced wave heights at the shoreline and particularly in the lee of Rapatiotio Point, believed to be due to a wave sheltering effect created by the headland. The model predicted an increase in wave heights along the beach associated with easterly swells.
- Wave refraction was intensified under longer period swell. Consequently, swell waves were refracted more strongly by the large offshore sand ridges, which were found to play an important controlling role on the

longshore wave height variability at the shoreline. Thus, as deep-water wave period was increased, the result was greater wave focusing and hence greater variability in the wave heights predicted along the Waihi Beach shoreline.

Estimates of annual littoral drift during the study period were also calculated from the model WBEND, with approximately 80 days of wave data extrapolated to provide annual rates of sediment transport.

- Oscillating littoral drift was predicted along northern Waihi Beach by WBEND simulations, with a net northwesterly drift at the far northern end and a net southeasterly drift towards the south. Reversal of drift directions occurred approximately 500 m south of Rapatitio Point. However, there is insubstantial geomorphic evidence to support diverging littoral drift along northern Waihi Beach.
- The northwesterly-directed drift predicted at the far northern end of Waihi Beach is likely to be influenced by the presence of Rapatitio Point, which effectively shelters the beach from waves originating from the north to northwest.
- An overall net southeasterly drift was indicated along northern Waihi Beach, with an estimated 46,210 m<sup>3</sup>/year or 10.3 m<sup>3</sup>/m of sediment predicted to be removed from the sediment budget via the littoral drift. The energetic winter deployment will likely have had a considerable influence on the magnitude of estimates of annual drift rates at northern Waihi Beach. Similar drift patterns were observed using the longer-term wave record from offshore Pukehina Beach. Estimate discrepancies in drift rates with predictions based on wave data from the present study were attributed to the shorter length of the Waihi Beach wave record, reflecting the episodic nature of the Bay of Plenty wave climate.



# CHAPTER SEVEN: SEDIMENT BUDGET FOR NORTHERN WAIHI BEACH

---

## 7.0 INTRODUCTION

Beach sand is in a constant state of flux, moving on, off and alongshore under the influence of waves and currents. Sand is transported to beaches from a variety of sources, including rivers, sea cliffs, dunes, updrift beaches and possibly offshore sources. Sand generally remains at a given location on a beach for only a short time before it is entrained and moved on as littoral drift. A coastal sediment budget is an attempt to quantify changes in the onshore sand volume along a stretch of coast by applying the principle of conservation of mass (KOMAR, 1998; PATSCH and GRIGGS, 2006). In order to develop a sediment budget, quantitative estimates must be made of the rate of sediment input, transport, storage, and sand losses for an area of coastline. A sediment budget may be used to identify the extent of erosion or accretion occurring along a specific coastal sector (KOMAR, 1996; 1998) and provide insight into the stability of the beach or particular stretch of coast.

in order to provide an overview of the rates of the processes influencing beach state, an integrated coastal sediment budget was developed for the northern Waihi Beach littoral cell using information collected throughout 2007/2008. In this chapter, the concept of a sediment budget is reviewed, before outlining previous sediment budget applications along the Bay of Plenty coast. Estimates of littoral drift and nearshore diabathic transport rates during the study period are revisited, and sediment sources, sinks and transfers are identified and incorporated within a sediment budget for northern Waihi Beach. The sediment budget has been constructed to represent short-term conditions, with subsequent results related to existing conditions at the site during the study period (the year beginning November 2007).

## 7.1 THE SEDIMENT BUDGET CONCEPT

A sediment budget is simply an accounting of the sand entering, leaving, or contained within defined boundaries over a given period of time (PATSCHE and GRIGGS, 2008). The Shore Protection Manual (1984, p.4-113) defines a beach sediment budget as “a sediment transport volume balance for a selected segment of the coast...based on quantification of sediment transportation, erosion, and deposition for a given control volume”. A sediment budget comprises sediment inputs, transport pathways and outputs, and can take the form of positive sediment budgets (i.e. where net accretion of sediment occurs, inputs > outputs), equilibrium sediment budgets (inputs = outputs), and negative sediment budgets (inputs < outputs) (COOPER *et al.*, 2001). Usually the sediment quantities are listed according to the sources, sinks, and transporting processes causing the additions and subtractions.

Sediment sources can be considered as “inputs” to the littoral system and can be provided by a number of mechanisms. Sediment sources are vital to the sustainability of sediment circulation, and can be derived from eroding cliffs, erosion of the beach, fluvial input, supply from dune stores and beach renourishment. Sediment sinks and stores can be considered as “outputs” from the littoral system, and include losses to submarine canyons, tidal inlets or geomorphological barriers, accretion of the beach, or dredging and mining of the beach or nearshore. Sediment transport pathways can be considered as “throughputs” within the littoral system, and are primarily littoral drift, diabathic (onshore/offshore) transport, aeolian transport, and natural or artificial bypassing of tidal inlets.

The main challenge in developing a littoral sediment budget is quantitatively assessing all sources and sinks to a reasonable degree of accuracy. The difference between the total volume of sand provided by all sand sources and the volume lost to all sinks within a particular littoral cell will equal the change in sand volume or storage occurring within that region (ROSATI and KRAUS, 1999; PATSCHE and

GRIGGS, 2006), and is reflected in beach accretion or erosion. The sediment budget equation can be expressed as: (ROSATI and KRAUS, 1999; ROSATI, 2005)

$$\sum Q_{source} - \sum Q_{sink} - \sum \Delta V + P - R = residual \quad 7.1$$

where all terms are expressed as a volume or as a volumetric change rate:  $Q_{source}$  and  $Q_{sink}$  are the sources and sinks, respectively,  $\Delta V$  is the net change in volume within the cell,  $P$  and  $R$  are the amounts of material placed in and removed from the cell, respectively, and *residual* represents the degree to which the cell is balanced. For a balanced cell, the residual is zero.

Prior to development and quantification of a sediment budget for a littoral cell, the cell boundaries need to be accurately delineated. Littoral cells are defined as units within which coastal processes and morphological features are approximately self-confined, but characteristics of sediment throughput are exhibited (COOPER *et al.*, 2001). These cells are geographically bounded by specific physical features that act as barriers to longshore sediment transport, and contain additional features that either provide or remove sand from the cell (PATSCHE and GRIGGS, 2006). Ideally, each cell should exist independently from one another, with little or no sediment transport occurring between cells (BEST and GRIGGS, 1991; PATSCHE and GRIGGS, 2006). However, there can still be a thin “rolling carpet” of grains over the inner shelf-beach profile.

### 7.1.1 Previous Application of Sediment Budgets in the Bay of Plenty

To date there have been very few applications of detailed sediment budgets to beaches along the Bay of Plenty coastline, mainly due to a lack of adequate data. Most investigations have primarily focused on identifying sedimentary processes, but fail to provide a complete assessment of volumes of the sediment exchanged within a defined study area. Another major problem when applying a sediment budget in the Bay of Plenty is that the region consists of a series of ‘leaky’ littoral cells, where there is partial sediment by-passing around major harbour entrances and rocky headlands (HEALY, 1980). This has implications in defining littoral cell boundaries. According to HEALY (1980), further complications exist with regions

of diverging and converging drift along the Bay of Plenty coastline. HEALY (1980) further suggests that secondary drift patterns may oppose the long-term net littoral drift towards the southeast. Consequently, a large amount of uncertainty is involved in delineation of littoral cells, and is therefore an important consideration in sediment budget estimates within the Bay of Plenty.

PHIZACKLEA (1993) calculated a sediment budget for the Pukehina-Matata coastal sector in order to assess the effects of sand mining at Otamarakau Beach. With boundaries defined at Town Point in the north and the Tarawera River in the south, PHIZACKLEA (1993) estimated that a deficit of 90,570 m<sup>3</sup> was apparent along the Pukehina-Matata coastline between 1989 and 1993. He further concluded that a longer-term sediment budget between 1978 and 1993 indicated a sediment surplus of 218,560 m<sup>3</sup> within the entire beach system.

EASTON (2002) also compiled an integrated sediment budget for the Pukehina coastal sector in order to identify the major components which are significant to the enhanced frontal dune erosion at Pukehina Beach. His results illustrated that the Pukehina coastal sector receives a net erosion rate of approximately 4,383 m<sup>3</sup>/year. A deficit of approximately 7,000 m<sup>3</sup>/m was regarded as a major contributor to the long-term erosion problem occurring at Pukehina Beach. EASTON (2002) concluded that overall the volume change calculated at Pukehina Beach is reasonably small, and admits that with an associated error of ±27,429 m<sup>3</sup>/year erosion rates could be larger than the calculated rate of retreat.

FOSTER *et al.* (1994) utilised the diabathic transfer component of a sediment budget to assess volumetric changes of beach and nearshore profiles during 1990-1991, to investigate the effects of artificial beach renourishment at Mount Maunganui. They concluded that most of a total volume of 93,600 m<sup>3</sup> of sediment added to the nearshore profile between 4-7 m water depth (relative to MSL) could be subsequently accounted for onshore, renourishing the swash zone and beach face along Mount Maunganui Beach. SPIERS (2004) also applied the diabathic transfer component of a sediment budget to determine the fate of, and account for, the sandy material dumped in the nearshore zone off Mount Maunganui Beach.

An integrated sediment budget was undertaken by SAUNDERS (1999) at West End Ohope Beach in an attempt to offer an explanation for the initiation of shoreline erosion and provide an avenue for remedial action. SAUNDERS (1999) concluded that approximately 28,000 m<sup>3</sup>/year of material was unaccounted for by the sediment budget for West End Ohope, equating to a loss of around 8.1 m<sup>3</sup>/m of sand for the year commencing December 1997.

## 7.2 THE NORTHERN WAIHI BEACH LITTORAL CELL

Littoral cells define the boundaries for each sediment budget calculation and denote the existence of a complete self-contained sediment budget within its boundaries (DOLAN *et al.*, 1987). Cells are defined by geologic controls, available data resolution, coastal structures, knowledge of the site, and to isolate known quantities or the quantity of interest (ROSATI, 2005). For the purpose of this investigation, the stretch of coast between Rapatiotio Point in the north and Island View, located approximately 4.5 km southeast, is recognised as a littoral cell for northern Waihi Beach.

Using data from HARRAY (1977), HEALY *et al.* (1977) showed that substantial beach sediment was not being supplied to Waihi Beach from the north. Thus, Rapatiotio Point creates a significant barrier to the littoral drift and therefore represents the northern boundary of the littoral cell. Sedimentary processes associated with the southern end of Waihi Beach and the Katikati entrance to the Tauranga Harbour have not been investigated in this study, and are therefore excluded from the sediment budget. A littoral cell containing the entire length of Waihi Beach would require extrapolation of data measurements taken at the northern end of the beach, increasing uncertainty of sediment transport estimates. Island View was therefore selected as the southern boundary of the northern Waihi Beach littoral sector.

The landward boundary of the littoral cell is essentially taken from a line on the beach which marks the limit of sediment interaction between land and the sea.

DOLAN *et al.* (1987) recommend that the closure depth be used to define the seaward boundary for sediment budget analysis, as this is the minimum water depth at which no measurable or significant morphological changes to the profile occur from year to year.

### 7.2.1 Depth of Closure

The depth of closure is the minimum water depth beyond which sand level changes between seasonal profile surveys become unmeasurable or insignificant (HALLERMEIER, 1978; NIELSON, 1992). Shoreward, the subtidal beach profile varies in an envelope of change, but beyond the closure depth it is difficult to detect any morphology change. To determine the offshore limits of sediment transport under waves at northern Waihi Beach, the method of HALLERMEIER (1981a; 1981b) was adopted.

HALLERMEIER (1981a; 1981b) defined two limits (the landward and seaward limits) to an area he called the *shoal zone*, between the littoral and inner shelf zones. In the shoal zone, surface waves are likely to cause little sand transport; “waves have neither strong nor negligible effects on the sand bed” (HALLERMEIER, 1978; 1981a). Hallermeier’s inner limit (HIL) refers to the seaward limit of sand transport due to extreme surf related processes ( $d_1$ ) (HALLERMEIER, 1981a). The Hallermeier outer limit (HOL) defines the seaward limit for significant offshore and onshore movement of sediment ( $d_i$ ) and is due to sand transport outside the surf zone by average waves (HALLERMEIER, 1981a). Average waves are defined as those with the median annual significant wave height, and corresponding wave period (HILTON and HESP, 1996). Hallermeier’s inner and outer limits can be approximated by (HALLERMEIER, 1981a):

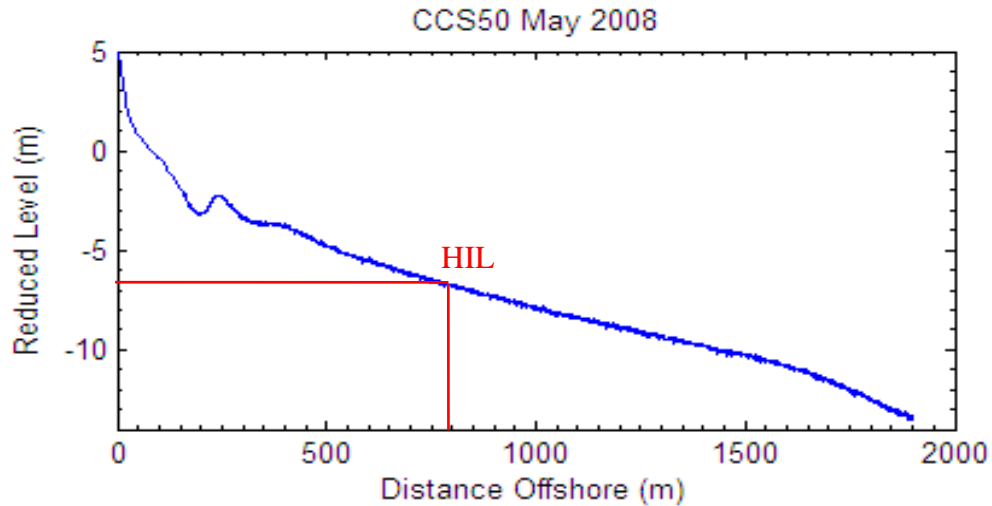
$$d_1 = 2H_s + 11\sigma \quad 7.2$$

$$d_i = (H_s - 0.3\sigma)T_s \sqrt{\left(\frac{g}{5000D}\right)} \quad 7.3$$

where  $H_s$  is the annual mean significant wave height (m),  $\sigma$  is the standard deviation of the annual significant wave height (m),  $T_s$  is the annual mean significant wave period (s) and  $D$  is the mean grain size diameter (m). These equations typically require definition by at least one year's daily wave data (HALLERMEIER, 1981a). Unfortunately, a wave record of this length was unattainable for the monitoring period at northern Waihi Beach. Following the same assumption made by SAUNDERS (1999), waves measured over the 80 days during summer 2007 and winter 2008 periods at the three S4 locations were assumed to be representative of the annual wave conditions. While this approach is not completely ideal for calculating the Hallermeier limits, these provide the best available data.

For northern Waihi Beach  $H_s$  was taken as 1.04 m  $\pm$ 0.43 m and  $T_s$  was calculated as 6.99 s. Mean grain diameter was averaged from offshore sediment samples collected between depths of 6 to 30 m (Chapter 4), giving  $D = 0.26 \times 10^{-3}$  m. These measurements provided Hallermeier limits of HIL = 6.8 m and HOL = 17.5 m (Figure 7.1). These depths correspond to distances of approximately 800 m and 2,400 m offshore Waihi Beach from benchmark CCS50 respectively. These findings compare well with previous investigations of the closure depth on the Western Bay of Plenty inner shelf. FOSTER (1991), HEALY (1993), HUME and HICKS (1993), DE LANGE and HEALY (1994) and SPIERS (2004) estimated HIL of 5.5-6.6 and HOL of 9-25.1. The short-term nature of the wave record used for the Hallermeier estimates is a cause for concern, and confidence in these results would improve if a longer-term record of wave climate for northern Waihi Beach was available. However, the values determined are still likely to provide a reasonable indication of the limits of nearshore sediment transport under waves.

In order to investigate the offshore limits of sediment transport using longer-term data, the Hallermeier limits were recalculated using Pukehina wave buoy data from the last 5 years ( $H_s = 1.00$  m  $\pm$ 0.61;  $T_s = 6.45$  s) to give HIL of 9.37 m and HOL of 14.16 m (Iremonger, *pers comm.* 2008). The inner limit of 9.37 m is greater than that estimated using wave data from the present study and many other estimates of HIL in the Western Bay of Plenty. Applying this value for Waihi



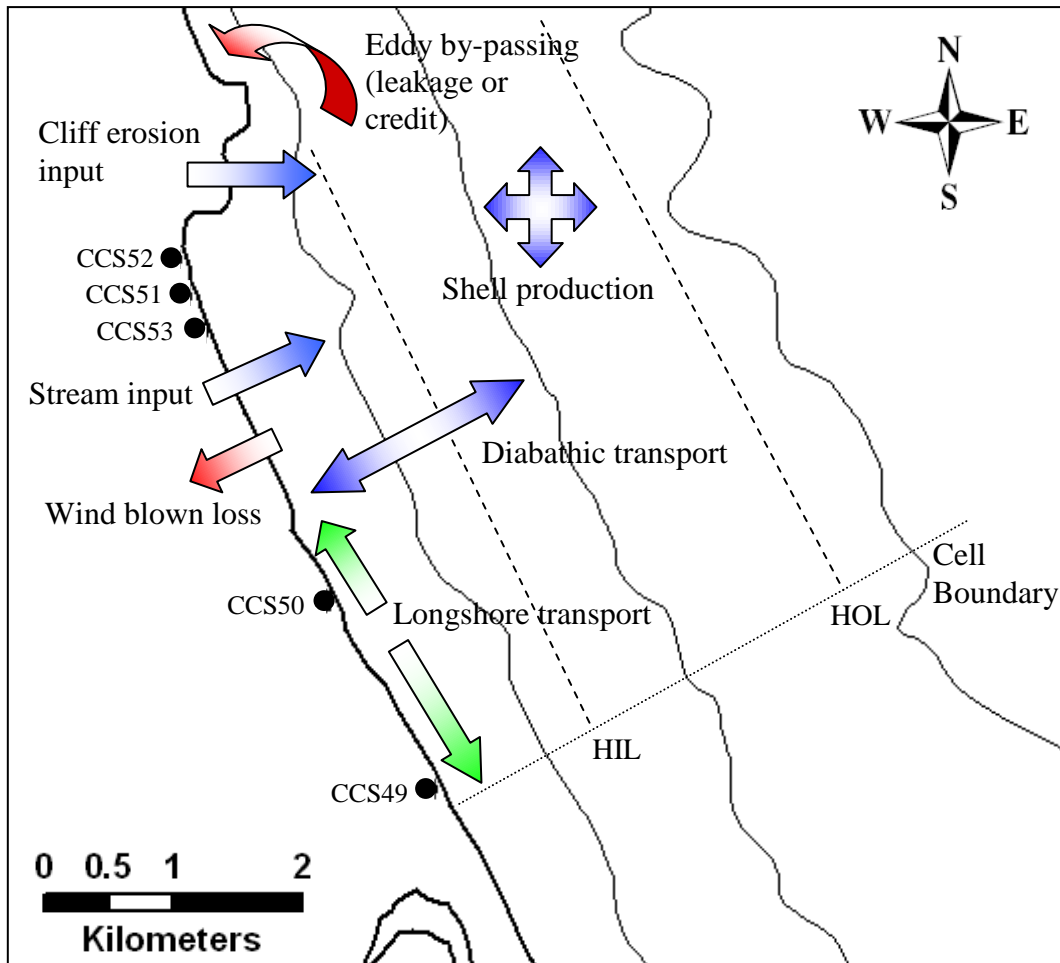
**Figure 7.1:** Benchmark CCS50 offshore profile near the Waihi Beach Surf Club with the Hallermeier inner limit (HIL) superimposed.

Beach, HIL corresponds to a distance of around 1,300 m from the shore, indicating a much wider surf zone of active onshore-offshore and longshore transport than that determined using the 80 days of S4 wave data from the current study. It is believed that the wave characteristics obtained from the Pukehina wave buoy used for these estimates are not unusually high for the Bay of Plenty coast. Rather, the larger HIL is likely due to the higher standard deviation associated with the huge amount of variation captured over the five years of data collection, as opposed to only a few months in the present study.

The depth of closure calculated for the data collected during the present study was used to define the seaward boundary of the northern Waihi Beach littoral cell. For the purpose of the study, the outer limit (HOL) was considered more appropriate as the closure depth as it represents the maximum offshore extent of sediment transport, compared to the inner limit (HIL) which is more concerned with surf zone processes. Thus, 17.5 m was deemed suitable to define the seaward littoral cell boundary.

Figure 7.2 illustrates a schematic of the northern Waihi Beach littoral sub-cell. Possible sediment transport pathways are indicated, which are to be quantified and compared against changes in the sediment storage on the beach.





**Figure 7.2:** Schematic of the northern Waihi Beach littoral sector. Beach profile benchmarks used during this study are shown. Possible sediment transport pathways are specified, which are to be evaluated and compared against changes in the sand storage on the beach.

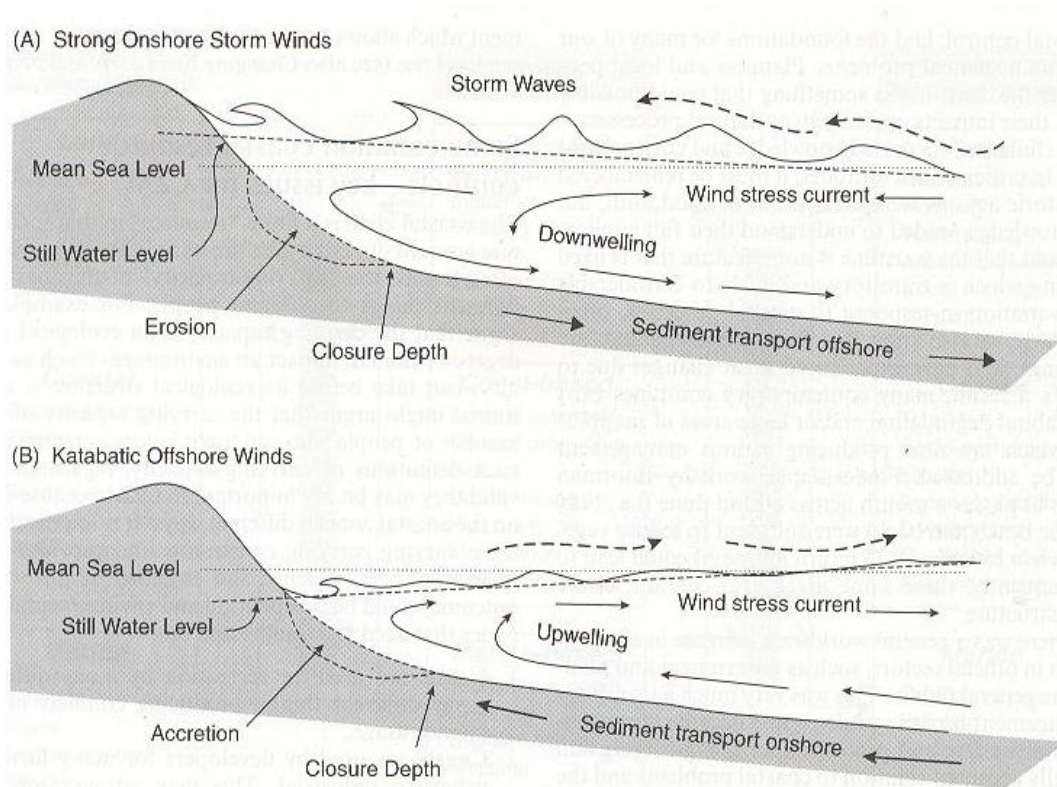
### 7.3 DIABATHIC TRANSPORT AT NORTHERN WAIHI BEACH

Quantifying the potential diabathic (cross-shore) movement of sand within the dune-beach-nearshore system is often regarded as the most challenging and poorly evaluated sediment budget element (PATSCHE and GRIGGS, 2006). A comparison of sediment composition between beach and offshore sand is often used as evidence for a net onshore or offshore transport (KOMAR, 1996; PATSCHE and GRIGGS, 2006). However, the similarity in composition only indicates that an exchange has taken place. It rarely indicates direction of transport or volumes of sand moved, which are necessary for development of a littoral sediment budget.

According to VINCENT *et al.* (1983), diabathic exchanges of sediments between the beach and offshore are fundamental to the episodic changes in beach and surf zone sediment storage, as well as to long-term erosional or accretional trends. WRIGHT *et al.* (1991) found that applied wind stress produces a slope on the sea surface that can induce significant bottom circulation in the opposing direction to the wind (WRIGHT, 1995). During large storm events, sand may be either transported offshore or onshore depending on wind stress and wave steepness driving upwelling or downwelling circulation. Thus, diabathic transport can result in either a net gain or loss for the beach. Figure 7.3 illustrates how wave steepness and wind direction can modify diabathic transfer.

Diabathic transport offshore is induced by high wave steepness and associated onshore winds. This combination of wind and wave conditions causes increased water elevation at the coast. The set-up of water level increases pressure differences at the shore, driving offshore bottom currents towards the zone of lower pressure. The downwelling current may subsequently entrain beach sediment and transport it offshore (Figure 7.3a). Conversely, low wave steepness is associated with larger wave orbital motions, which can penetrate deeper into the water column than steeper waves and associated smaller wave orbital motion. If sediment becomes entrained by interaction of the orbital motion with the seabed, there may consequently be onshore sediment transport via an upwelling current, which is initiated by offshore winds forcing surface water offshore (Figure 7.3b).

Using a combination of hydrodynamic and sedimentological data from field investigations, predicted diabathic transport rates were derived using an approach that required waves to initiate movement of sediments in the nearshore, before enabling wind-generated near-bed currents to transport and distribute sediments (section 5.4.5 *Calculation of Diabathic Sediment Transport Rates*). Diabathic sediment flux was calculated in 6 m water depth offshore Waihi Beach, for both summer and winter deployment periods. Combining the two rates of the separate deployments provided a net estimate of ~11,800 m<sup>3</sup>/year, or 2.6 m<sup>3</sup>/m of material available within the 4.5 km northern Waihi Beach littoral cell.



**Figure 7.3:** a) Showing the effect of an onshore wind producing an elevated still water level. The induced downwelling current facilitates diabathic transport of sediment offshore. b) Showing the effect of an offshore wind producing a reduced still water level. The induced upwelling current facilitates diabathic transport onshore. Source: SCHWARTZ (2005).

#### 7.4 SEDIMENT INPUTS INTO NORTHERN WAIHI BEACH (CREDITS)

Annual rates of diabathic onshore sediment transport were calculated for the 6 m contour along northern Waihi Beach. Gross onshore movement was estimated to be approximately 38,400 m<sup>3</sup>/year or 8.5 m<sup>3</sup>/m over the study period.

Two small streams discharge along Waihi Beach: Two Mile Creek and Three Mile Creek. They were cut in the 1930's to drain the backshore area and enable further residential development. Because the streams drain swamps, they are not expected to contribute significant quantities of sediment to the beach (HARRAY, 1977). Hence, fluvial input into the northern Waihi Beach littoral cell is assumed to be negligible and is not included in the sediment budget formulation.

When eroded, Rapatiotio Point may also contribute sand to northern Waihi Beach. Coastal cliffs that consist of materials such as sandstone or granite that break down into sand-sized grains will contribute directly to the beaches. Fine-grained rocks that consist of silt and clay, on the other hand, will not contribute significantly to beaches (PATSCHE and GRIGGS, 2006). The cliff material within Rapatiotio Point comprises of igneous rocks of late Miocene early Pliocene age, overlain by late Quaternary tephra.

Although no conformational evidence has been obtained in the present study to confirm actual cliff erosion rates, it is anticipated that the contribution of sand relative to other sediment inputs at northern Waihi Beach is comparatively small. Using GPS, MOON and DE LANGE (2005) measured the widths of shore platforms associated with Waitemata Group sedimentary rocks to assess long-term erosion rates at two sites: the North Shore of Auckland and the Tawharanui Peninsula, North Auckland. The main geological units present at the North Shore are tuffaceous grit (Parnell Grit) and a flysch sequence of alternating sandstone and mudstone beds. The Tawharanui Peninsula consists almost entirely of flysch sequences with dominant massive sandstone units (1–2 m thick) (MOON and DE LANGE, 2005). MOON and DE LANGE (2005) estimated a mean long-term cliff recession rate of  $8.0 \pm 0.3$  mm/y. Rates of coastal cliff retreat in the vicinity of Pukehina Redoubt in the Bay of Plenty have been estimated by PHIZACKLEA (1993) to be retreating at a rate of 5.49 mm/year, or  $30 \text{ m}^3/\text{year}$ . However, as EASTON (2001) points out, this estimate is conflicting and likely to be incorrect as it is based on erosion rates determined for the Waitemata formation, which comprises of a very different structural lithology (MOON and DE LANGE, 2005). EASTON (2001) estimated the rate of erosion of the Okurei cliffs at Pukehina by measuring the distance of cliff erosion between aerial photographs taken in 1943, 1981 and 1993. EASTON (2001) found the rate of cliff retreat to be relatively constant between 1993 and 1943, and estimated that erosion from the entire coastal cliff length contributed approximately  $59 \text{ m}^3/\text{year}$  at a rate of 9.33 mm/year.

The geology of Okurei Point is comparable to that of Rapatiotio Point, comprised of mid-Pleistocene fluvial volcanoclastic silts, sands, gravels and conglomerates

covered by late Quaternary tephras and palaeosols (WEHRMANN, 2000). In order to make a qualitative assessment of the rate of cliff retreat, the cliff erosion rate defined by EASTON (2001) was selected to provide the potential contribution of sediment to northern Waihi Beach from coastal cliff erosion. Assuming the length of the Rapatiotio Point cliff within the northern Waihi Beach littoral cell to be 980 m, and an average height of 6.5 m for the actively eroding cliff face, the rate of cliff retreat was estimated as  $60 \text{ m}^3/\text{year}$ .

An estimate of the biogenic inputs supplied to northern Waihi Beach was approximated from investigations on the Pakiri coast by HILTON (1990). HILTON (1990) showed that modern biogenic production of shell had the potential to significantly contribute to the bulk of the sediments in the Pakiri Beach nearshore-inner shelf environment. This shell material derives from molluscs growing mostly at the base of the shoreface in 20-25 m water depth, which break down to gravel and sand-sized fragments. The side-scan sonar survey and subsequent underwater video analysis and grab sampling offshore northern Waihi Beach during the field study detected large quantities of shell material, particularly in the troughs of megaripple facies. An extensive side-scan survey by BEAMSLEY (1996) has shown Sand Dollars (*Fellaster zelandica*) to be abundant in water depths less than 15 m off northern Waihi Beach. He also noted areas of densely packed Horse Mussels (*Atrina zelandica*) and Ostrich Foot Whelks (*Stuthuolaria papulosa*) in the nearshore, usually about 10-80 m in size (HUME *et al.*, 1995). These observations, combined with those of the present study, imply that shells and biological features are an important component of the beach sediment within northern Waihi Beach.

The nearshore area within the northern Waihi Beach littoral cell was taken to be 4,500 m alongshore by 2,400 m cross-shore out to the HOL, producing a seabed area of  $1.08 \times 10^7 \text{ m}^2$ . According to HILTON (1990), the average concentration of shell material over Pakiri Bay was  $97 \text{ g/m}^2$ . By applying this concentration to the present study, and assuming a whole shell density of  $1,770 \text{ kg/m}^3$  (CRC, 1978), approximately  $590 \text{ m}^3$  of shell is predicted to be added to the northern Waihi Beach nearshore zone each year.

## 7.5 SEDIMENT LOSS FROM NORTHERN WAIHI BEACH (DEBITS)

Gross diabathic offshore sediment transport from the 6 m contour along northern Waihi Beach was estimated to be approximately 26,600 m<sup>3</sup>/year or 5.9 m<sup>3</sup>/m during the study period.

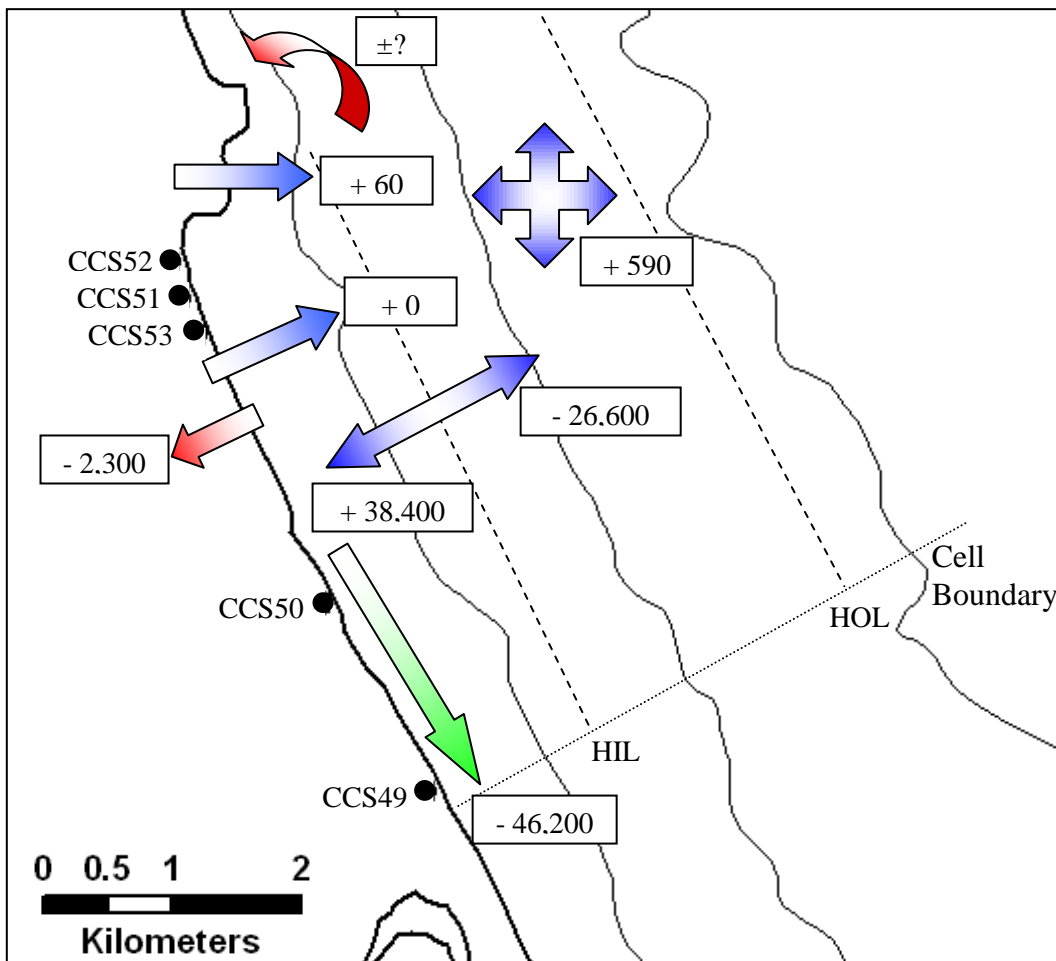
Aeolian sediment transport across beaches is characteristically complex. Sediment flux at any point across a sandy surface is dependent on wind stress, grain size, and available sand supply, as well as a host of other complicating factors such as moisture content of the sand surface, grain size sorting, bed roughness, beach slope and vegetation cover (BAUER *et al.*, *in press*). Hence, effective losses from the beach to the dune systems during the study period are difficult to evaluate, and it is likely that sand transported by winds returns to the beach when storm waves erode the frontal dunes. It is anticipated that aeolian sediment loss by wind processes will only be a very small component of the sediment budget at northern Waihi Beach, as most of the dunes are covered in vegetation which helps to trap wind-blown sands during periods of onshore winds.

From 20 years of beach profile data, HUME *et al.* (2000) approximated a net loss of sand to the foredunes from aeolian processes to be approximately 20,000 m<sup>3</sup>/year within the Pakiri embayment. A similar approach was taken by SAUNDERS (1999) for West End Ohope Beach. From a years worth of beach and dune profile data, SAUNDERS (1999) estimated a net loss of sand by wind transport of approximately 6,800 m<sup>3</sup>/year. Following a similar method to that of HUME *et al.* (2000) and SAUNDERS (1999), the volume of sand accumulated in the foredune area between the landward and seaward benchmarks at profile CCS49 was calculated. Between the collected winter and summer profiles, a volume of 1.9 m<sup>3</sup>/m of sand accumulated in the foredune area, providing an estimated total loss of ~2,300 m<sup>3</sup>/year of sand from the northern Waihi Beach littoral cell. Although the influences of the complicating factors mentioned above are neglected, this value gives a simple prediction for the aeolian transport at Waihi Beach.

From sediment transport rate calculations obtained in Chapter 6, sediment loss due to net sediment being transported out of the northern Waihi Beach littoral cell using the numerical model WBEND was estimated to be 46,200 m<sup>3</sup>/year, or 10.3 m<sup>3</sup>/m. However, as previously mentioned, the interpolation of annual drift rates from only 80 days of field data is dubious. Net drift rates calculated from the collected field data may overestimate annual drift magnitudes, as the study period contained several episodic storm events. Further, the short-term wave record does not account for storm events that may occur outside of the sampled timeframe, and therefore may not represent the long-term wave climate. Hence, the calculated annual net littoral drift rate should be regarded with caution.

## 7.6 INTEGRATED SEDIMENT BUDGET BALANCE

Figure 7.4 represents an integrated sediment budget for northern Waihi Beach.



**Figure 7.4:** Net annual credits and debits to the sediment budget along the northern Waihi Beach littoral cell. Units are in  $\text{m}^3/\text{year}$ .

**Inputs – Outputs = Net Erosion/Accretion Rate**

$$60 + 590 + 38,400 - 2,300 - 46,200 - 26,600 = -36,050 \text{ m}^3/\text{year}$$

According to this sediment budget, approximately  $36,000 \text{ m}^3/\text{year}$  of sediment was lost from the northern Waihi Beach littoral cell. This equates to a loss of around  $8 \text{ m}^3/\text{m}$  of sand for the year commencing November 2007.



### *7.6.1 Discussion of the Sediment Budget Outcome*

The integrated sediment budget indicates that sediment losses within the northern Waihi Beach littoral system are exceeding supply, resulting in an overall annual budget deficit of 36,000 m<sup>3</sup>/year or 8 m<sup>3</sup>/m. Through a combination of geomorphic, sedimentological and hydrodynamic evidence, the negative sediment budget has been related to the physical processes influencing erosion at northern Waihi Beach. The major contributor to the net erosion rate can be identified as the large magnitude of sand exiting the system in the littoral drift far exceeding available supply to the beach from diabathic movement of sediment onshore. Erosion along certain sectors of the Waihi Beach coastline was previously shown to be enhanced by wave energy focusing from numerical wave refraction simulations (Chapter 6).

The sediment budget developed for northern Waihi Beach was based upon 80 of collected field data, and hence only represents short-term conditions. However, when planning a large engineering, restoration or nourishment project or other alteration to the coast, it is best to construct a long-term sand budget that includes historic and present conditions. Many assumptions and errors involved in the data analysis and interpretation of the sediment budget could be reduced with a budget which spans a greater length of time, and averages out year-to-year variations in the components. Yet despite the temporal constraint limiting the application of data collected during this study, the conceptual model of hypothesised sediment transport pathways (Figure 7.4) still provides a good indication of the complexity of the erosion problem and has helped to identify and quantify the fundamental processes contributing towards erosion at northern Waihi Beach.

## **7.7 SUMMARY**

In an effort to better understand the processes affecting the beach morphology, the concept of a littoral sediment budget has been applied to identify and quantify additions and losses of sand that influence beach width at northern Waihi Beach.

- Hallermeier (1981a) limits were used to calculate the depth of closure at northern Waihi Beach using all wave data collected at the three S4 locations throughout both deployment periods. An inner limit of 6.8 m and an outer limit of 17.5 m were determined. Using five years of wave data collected by the Pukehina wave buoy since September 2003 provided similar inner and outer limits of 9.37 m and 14.16 m respectively. The HIL of 17.5 m determined from data of the current study was selected to represent the seaward boundary of the northern Waihi Beach littoral cell.
- Due to the small net diabathic exchange ( $8.5 \text{ m}^3/\text{m}$  onshore and  $5.9 \text{ m}^3/\text{m}$  offshore), the removal of sands by net southeastward littoral drift ( $\sim 10.3 \text{ m}^3/\text{m}$ ) during the study period was the largest net sediment transfer within the cell, so that there was an overall tendency for sands to be transported alongshore out of the cell rather than offshore.
- Approximately  $115,000 \text{ m}^3/\text{year}$  of sediment was estimated to be moving through the defined northern Waihi Beach littoral cell during the study period. The derived sediment budget produced a net deficit of sediment of approximately  $36,000 \text{ m}^3/\text{year}$  or  $8 \text{ m}^3/\text{m}$  during the year commencing November 2007.

# CHAPTER EIGHT: SUMMARY, CONCLUSIONS AND RECOMMENDATIONS

---

## 8.0 INTRODUCTION

During the past 60 years northern Waihi Beach has undergone episodes of exceptional erosion. This has led to increased vulnerability to the joint coastal hazards of duneline retreat and storm surge inundation. A rock seawall was constructed in the 1960s in an attempt to protect coastal property at risk from coastal erosion and flooding hazards, however, it has failed to prevent further erosion. This study aimed to investigate the sedimentary morphodynamics at northern Waihi Beach, in order to identify and evaluate the fundamental coastal processes influencing beach erosion. In this chapter, the key findings of the study are outlined and the implications for erosion and sedimentation at northern Waihi Beach are discussed. Recommendations for future research in the area are also provided.

## 8.1 SUMMARY OF KEY FINDINGS

### *8.1.1 Environmental Setting and Processes Influencing Erosion*

Local geology, geomorphology, wind, wave and current climates, tropical cyclones and storm surge were examined to identify the major processes which may influence coastal erosion and sedimentation at northern Waihi Beach.

Waihi Beach is a long straight barrier beach, varying from a wide gently sloping beach in the north where there is very little dune present, to a steep short beach with a pronounced dune in the south. Offshore Waihi Beach is characterised by a reasonably flat intertidal and subtidal system. The major morphological units which comprise the nearshore seabed at Waihi Beach are the upper shoreface, of which longshore bar-trough topography is evident; a convex-up lower shoreface, and a gentle inner continental shelf punctuated by Steel's Reef 4 km offshore.

Waihi Beach has been identified as a closed sedimentary system, receiving little sediment from littoral drift or rivers. The main source of sediment exchange is from offshore exchange with the continental shelf. The Waihi Beach mineral assemblage ultimately derives from the erosion of the Quaternary tephra deposits of the Taupo Volcanic Zone, which have been transported to the coast by rivers. Sediments commonly comprise of plagioclase feldspar, quartz, volcanic glass and rock and shell fragments. Of less abundance are the heavy minerals hypersthene, hornblende, cummingtonite, augite and other opaque minerals.

Wind climate within the Bay of Plenty is a critical parameter of coastal erosion and accretion patterns within the region. Local topography influences wind direction and speeds at Waihi Beach, with surrounding mountain ranges providing a sheltering effect from predominant westerly winds. The region is however exposed to infrequent gales mostly from the northeast or southwest.

Relatively low wave energy characterises Waihi Beach for the majority of the year, with wave heights typically less than 1 m. However, the beach is susceptible to large wave forces ( $H_s > 2$  m) and elevated water levels during high north to northeasterly winds. Wave behaviour at Waihi Beach is modified by the refraction influences of Mayor Island and adjacent reefs. Inner shelf currents are weak and flow predominantly shore parallel, alternating between a southerly-directed current during prevailing calm offshore winds, and northerly-directed flow derived from passing low pressure systems producing strong onshore winds. Only the northwards flowing currents are considered strong enough to transport shelf sediments.

### *8.1.2 Beach and Nearshore Morphology*

Dune and sub-aerial beach profiling was undertaken along northern Waihi Beach in conjunction with hydrographic surveying to assess the characteristics and behaviour of the beach and nearshore morphology. Beach profiles revealed a low angle with a wide high tide beach and typically no berm feature present. The beach becomes increasingly narrower and steeper towards the southeast, with

wide gently sloping gradients characteristic of profiles in the north. Profiles also indicated a greater sediment accumulation and availability for building dunes towards the southern end of the beach. Measured summer profile elevations were typically higher than the subsequent winter profiles, with beach levels fluctuating up to 1-1.5 m between seasons.

Typically, the nearshore zone at Waihi Beach is comprised of a well-defined offshore bar approximately 250 m from the shoreline with an associated alongshore trough. Often, a poorly defined secondary bar also exists. Seaward of these features is a characteristically flat nearshore with a gently sloping seabed gradient consistently around 1:200 out to about 1400 m offshore, beyond which the slope becomes mildly convex seaward. The presence of longshore bars, in conjunction with the observed decrease in beach profile elevation from summer beach profiles, implies that sediment has been removed from the beach face and berm during a period of erosion prior to winter profiling. The eroded sediment has subsequently shifted offshore and been deposited to form the nearshore bar.

The distribution of sediment textures and bedforms on the inner shelf were mapped using side-scan sonar, offshore sediment grab sampling, SCUBA diver and video observations. The shallow inshore zone was found to be characterised by fine featureless sand. SCUBA ground truthing revealed the presence of small wave generated ripples which were indistinguishable on the side-scan record. Seaward of about 15 m depth, the featureless topography is interrupted by large shore-normal sand ridges ( $\eta=0.4-2.5$  m,  $\lambda=300-1400$  m) dominated by shore parallel coarse megaripples ( $\eta=0.1-0.14$  m,  $\lambda=0.5-1.5$  m). Sharp, well-defined southeastern boundaries with an abrupt transition in bottom topography from coarse megaripples to fine featureless sand are characteristic of the shore-normal elongated megaripple features. The asymmetrical nature of the shore-normal sand ridges (oriented northeast to southwest) also implies a net northwesterly directed alongshore sediment transport.

### 8.1.3 Sediment Characteristics

Textural analyses of beach and nearshore sediments was undertaken to identify grain size distributions and to evaluate the physical processes influencing sediment transport and deposition at northern Waihi Beach. Beach and dune sediments at northern Waihi Beach consist of moderately well to well sorted fine sands, becoming marginally coarser towards the southern end of the study area where higher energy conditions and a steeper beach slope prevail. This trend was shown by wave refraction modelling to be associated with a zone of wave energy focusing in central Waihi Beach (Island View), causing finer sediments to be preferentially eroded and transported offshore. The slight inferred fining in grain size that occurs towards the northern end of Waihi Beach is possibly a result of lower wave energy at the shore when subject to swell and sea waves from the north to northwest, due to sheltering in the lee of Rapitiotio Point.

A more definite variation in sediment size was observed in offshore sediments. Measured grain sizes in the northern Waihi Beach nearshore vary from fine (2.74  $\emptyset$ ) to coarse sands (0.71  $\emptyset$ ), showing a seaward-coarsening progression. The observed coarsening and deterioration in sediment sorting seaward of ~20 m water depth offshore Waihi Beach are associated with the presence of coarse megarippled features identified in the side-scan sonar survey.

Three sediment transport models were applied to measured textural characteristics from beach face samples along northern Waihi Beach. Model results suggest that littoral drift is bi-directional along northern Waihi Beach, with converging longshore currents at CCS50 and CCS51. The likelihood of such an occurrence is doubtful as there is no evidence to support sediment accumulation at either of these locations, as would be expected with converging longshore drift. However, in spite of alternating littoral drift patterns predicted along northern Waihi Beach, overall net sediment transport determined by the models favoured a southeasterly littoral drift from Rapitiotio Point to Island View. This is in good agreement with environmental and geomorphic indicators of littoral drift direction previously identified by HEALY *et al.*, (1977) and HARRAY and HEALY (1978).

#### *8.1.4 Nearshore Hydrodynamics and Sediment Transport*

Directional current meters were deployed offshore from Waihi Beach in 6 m water depth, recording wave and current information 1 m above the bed. Results indicated that the S4 instrument at the far northern end of the beach recorded smaller wave heights than simultaneously collected data at central and southern localities along the study area. The observed differences may be explained by the positioning of the northernmost S4 in the lee of Rapatiotio Point and the apparent wave sheltering effect from north to northwesterly swell.

The study area was dominated by two alongshore currents: weak southeasterly directed currents resulting from offshore winds, and stronger more persistent northwesterly flowing currents derived from strong onshore winds. Currents typically ranged from 5-10 cm/s, with maximum (seaward flowing) currents of around 20 cm/s possibly indicative of rip currents at the far northern end of the beach. It is believed that sheltering by Rapatiotio Point is controlling the very limited distribution of current directions recorded at the northern extent of the beach in the lee of the headland.

Conditions required to initiate sediment transport in the nearshore zone were examined. Threshold conditions under waves were continually exceeded throughout the deployment period. However, threshold conditions for sediment entrainment by currents alone were exceeded less than 6% of the entire deployment period. Hence, results suggest that transport of sediment by mean currents in 6 m water depth or less at Waihi Beach is reliant on the ability of stronger wave orbitals to initiate particle entrainment.

Diabathic transport rates were evaluated along the 6 m contour offshore northern Waihi Beach from three sites where wave, current and sediment data were collected during the field study. A net offshore sediment flux of 6,099 m<sup>3</sup>/year or 4.1 m<sup>3</sup>/m was observed at the far northern end of the beach, associated with persistent rip currents. Analysis also suggested that the wave sheltering influence of Rapatiotio Point shielded wave heights and hence wave orbital velocities, resulting in smaller magnitudes of suspended sediment flux in the lee of the

headland. Over the entire study area, an estimated 11,844 m<sup>3</sup>/year or 2.6 m<sup>3</sup>/m net sediment flux onshore is predicted.

#### *8.1.5 Wave Energy Focusing and Nearshore Littoral Drift*

The numerical wave refraction model WBEND was used to simulate a range of wave conditions at northern Waihi Beach. Calibration errors were minimised using a friction coefficient of 0.01 and eddy viscosity of 20 m<sup>2</sup>/s. The zone of wave energy focusing associated with convergence around Mayor Island was observed to shift alongshore with differing deep-water wave approach direction. However, the persistent wave conditions experienced at northern Waihi Beach during the study period showed that wave refraction and focusing was likely to contribute towards accelerated beach erosion at Island View. Refraction around Steel's Reef also appears responsible for focusing of wave energy at the central and southern end of Waihi Beach.

Nearshore wave heights and hence wave focusing at northern Waihi Beach was found to be maximised by swell waves, particularly those approaching from the east. Varying wave approach to the north-northeast resulted in reduced wave heights at the shoreline and particularly in the lee of Rapatitio Point, believed to be due to the wave sheltering effect created by the headland. The large offshore sand ridges were found to play an important controlling role on the longshore wave height variability at the shoreline, which has been previously linked to the formation of large arcuate duneline embayments at Waihi Beach.

Oscillating longshore littoral drift was predicted along northern Waihi Beach by WBEND simulations, with a net northwesterly drift at the far northern end and a stronger net southeasterly drift towards the south. The location of the divergence was positioned ~500 m south of Rapatitio Point. Implications of this indicate that an accumulation of sediments would be expected against the headland, a feature which was not observed. The northwesterly-directed drift predicted at the far northern end of Waihi Beach is likely to be influenced by the sheltering influence of Rapatitio Point from waves approaching from the north to northwest. Restricted sediment transport near Rapatitio Point is also likely to be a result of



the headlands sheltering influence. Model simulations indicated an overall net southeasterly nearshore littoral drift. Predicted nearshore sediment transport rates varied between 17,655 and 79,418 m<sup>3</sup>/year, with approximately 46,200 m<sup>3</sup>/year or 10.3 m<sup>3</sup>/m estimated to be exiting the study region from the southeastern boundary. Implications of this, combined with wave focusing outcomes, demonstrate a potential long-term sediment deficit along northern Waihi Beach.

Longer-term littoral drift trends at Waihi Beach were examined using a five year record of instrumental wave data collected offshore Pukehina Beach by EBOP between 2003-2008. Long-term drift directions exhibited a similar pattern to those experienced during the shorter study period. Predictions of net annual drift rates varied between 297-58,000 m<sup>3</sup>/year. The difference between these annual rates and those extrapolated from the wave data of the present study were attributed to the shorter length of the 2007/2008 Waihi Beach wave record, reflecting the episodic nature of the Bay of Plenty wave climate.

#### *8.1.6 Northern Waihi Beach Integrated Sediment Budget*

An integrated sediment budget was undertaken in order to provide an overview of the rates of processes influencing beach state at northern Waihi Beach. Sediment sources, sinks and transfers were quantified and evaluated from field data collected between 2007 and 2008. Alongshore littoral cell boundaries were tentatively delineated at the northwestern edge of Rapatiotio Point and Island View, with the seaward boundary defined by the closure depth (17.5 m), to permit accurate assessment of sediment exchanges at northern Waihi Beach.

Outcomes of the sediment budget illustrated a net erosion rate of approximately 36,000 m<sup>3</sup>/year or -8 m<sup>3</sup>/m per year for the northern Waihi Beach littoral cell. The largest net transfer within the cell identified during the study period was nearshore littoral drift. The net southeastwards sediment transport out of the coastal sector was estimated at approximately 46,200 m<sup>3</sup>/year, compared to diabathic onshore and offshore sediment transport rates of 38,400 m<sup>3</sup>/year and 26,600 m<sup>3</sup>/year respectively. These results demonstrate an overall tendency for sands to be transported alongshore out of the cell rather than offshore.

## 8.2 RECOMMENDATIONS AND SUGGESTIONS FOR FUTURE RESEARCH AT WAIHI BEACH

This study investigated the sedimentary and coastal processes influencing erosion at northern Waihi Beach. Certain aspects are recommended to be researched further to enable an improved understanding of the coastal erosion problem at northern Waihi Beach. Areas requiring further characterisation include:

- Evaluation of the volume of sediment present offshore northern Waihi Beach, using sub-bottom seismic profiling and/or stratigraphic coring techniques. The outcome should help to identify and evaluate any structural controls that may influence erosion at northern Waihi Beach, and assist identification of potential remedial solutions.
- Frequent and regular beach and nearshore profiles undertaken at sites every 500 m along Waihi Beach, providing rates of volumetric change over time.
- Investigation of ocean-atmosphere interactions, such as the El Nino Southern Oscillation (ENSO) and Inter-decadal Pacific Oscillation (IPO), in order to identify whether climatic processes influence the state of the calculated sediment budget for northern Waihi Beach by altering wind and wave climates.

## REFERENCES

---

- ABRAHAMSON, L., 1987. Aspects of late Quaternary stratigraphy and evolution of some coastal embayments on the east Coromandel Peninsula, New Zealand. Unpublished MSc thesis, Department of Earth Sciences, University of Waikato. 250p.
- BARNHARDT, W.A., KELLEY, J.T., DICKSON, S.M. and BELKNAP, D.F., 1998. Mapping the Gulf of Maine with side-scan sonar: A new bottom-type classification for complex seafloors. *Journal of Coastal Research*, 14(2): 646–659.
- BAUER, B.O., DAVIDSON-ARNOTT, R.G.D., HESP, P.A., NAMIKAS, S.L., OLLERHEAD, J. and WALKER, I.J. (*in press*). Aeolian sediment transport on a beach: Surface moisture, wind fetch, and mean transport. *Geomorphology*, 2008. 11p.
- BEAMSLEY, B.J., 1996. Shoreface wave height reinforcement and frictional dissipation off Waihi Beach, with emphasis on sea bed characteristics and numerical modelling. Unpublished MSc thesis, Department of Earth Sciences, University of Waikato. 125p.
- BEHESHTI, A.A. and ATAIE-ASHTIANI, B., 2008. Analysis of threshold and incipient conditions for sediment movement. *Coastal Engineering*, 55: 423–430.
- BELL, R.G. and GORING, D.G., 2003. Coastal Hazards. *Tephra*, 20 (June): 21–26.
- BEST, T.C. and GRIGGS, G.B., 1991. The Santa Cruz littoral cell: difficulties with defining a sediment budget. *Coastal Sediments '91*, American Society of Civil Engineers (A.S.C.E.): 2262–2276.
- BLACK, K.P., 1983. Sediment Transport and Tidal Inlet Hydraulics. Unpublished D.Phil thesis, Department of Earth Sciences, University of Waikato. 331p.
- BLACK, K.P. and HEALY, T.R., 1983. Northland Forestry Port Marsden Point, side scan survey. Unpublished report prepared for the Northland Harbour Board. 88p.
- BLACK, K.P. and ROSENBERG, M.A., 1992. Semi-empirical treatment of wave transformation outside and inside the breaker line. *Coastal Engineering*, 16: 313–345.
- BLACK, K.P., OLDMAN, J.W. and HUME, T.M., 1998. Mangawhai-Pakiri Sand Study. Module 5: Technical Report. Numerical Modelling. Prepared for the working party, ARC Environment, Auckland Regional Council. 66p.
- BOHLING, B. (*in press*). Measurements of threshold values for incipient motion of sediment particles with two different erosion devices. Submitted to *Journal of Marine Systems*, 2008. 6p.

- BOPRC, 1991. BOP Council Overview Report. Prepared by Stephen Park. Bay of Plenty Regional Council Technical Publication No. 3. 98p.
- BRADSHAW, B.E., 1991. Nearshore and inner shelf sedimentation on the east Coromandel coast, New Zealand. Unpublished D.Phil thesis, Department of Earth Sciences, University of Waikato. 565p.
- BRADSHAW, B.E., HEALY, T.R., DELL P.M. and BOLSTAD, W.M., 1991. Inner shelf dynamics on a storm-dominated coast, East Coromandel, New Zealand. *Journal of Coastal Research*, 7(1): 11–30.
- BRADSHAW, B.E., HEALY, T.R., NELSON, C.S., DELL P.M. and DE LANGE, W.P., 1994. Holocene sediment lithofacies and dispersal systems on a storm-dominated, back-arc shelf margin: the east Coromandel coast, New Zealand. *Marine Geology*, 119(1-2): 75–98.
- BRADY, A.J. and SUTHERLAND, J., 2001. COSMOS modeling of COAST3D Egmond main experiment. *HR Wallingford Report TR 115*.
- BRUGMANS, J., VAN DIJK, R., VAN DER LANS, J., LOEFFEN, R. and WAGNER, J., 2003. Waihi Beach to the future: an objective review. TUDelft, The Netherlands. Department of Earth Sciences, University of Waikato. October 2003. 104p.
- COOPER, N.J., HOOKE, J.M. and BRAY, M.J., 2001. Predicting coastal evolution using a sediment budget approach: a case study from southern England. *Ocean and Coastal Management*, 44: 711–728.
- CRC, 1978. Handbook of chemistry and physics. Published by the Chemical Rubber Co., Cleveland, Ohio.
- DAVIS, R.A. and HAYES, M.O., 1984. What is a wave dominated coast? *Marine Geology*, 60: 313–329.
- DEAN, R.G. and DALRYMPLE, R.A., 2004. *Coastal processes: With engineering applications*. Cambridge University Press, Cambridge, U.K. 475p.
- DE LANGE, W.P., 1990. Preliminary assessment of the offshore wave climate at Tauranga. *Proceedings of the 2<sup>nd</sup> symposium of the New Zealand Ocean Wave Society*: 39–41.
- DE LANGE, W.P., 1991. Wave climate for No. 1 Reach, Port of Tauranga, Tauranga Harbour. Marine Geosciences Group, University of Waikato. pp.1–18.
- DE LANGE, W.P., 2000. Interdecadal Pacific Oscillation (IPO): a mechanism for forcing decadal scale coastal change on the northeast coast of New Zealand? *Journal of Coastal Research*, Special Issue 34: 657–664.
- DE LANGE, W.P. and GIBB, J.G., 2000. Seasonal, interannual, and decadal variability of storm surges at Tauranga, New Zealand. *New Zealand Journal of Marine and Freshwater Research*, 34: 419–434.

- DE LANGE, W.P. and HEALY, T.R., 1994. Assessing the stability of inner shelf dredge spoil mounds using spreadsheet applications on personal computers. *Journal of coastal Research*, 10: 946–958.
- DE LANGE, W.P., HEALY, T.R. and DARLAN, Y., 1997. Reproducibility of sieve and settling tube textural determinations for sand-sized beach sediment. *Journal of Coastal Research*, 13(1): 73–80.
- DELL, P.M., HEALY, T.R. and NELSON, C.S., 1985. A preliminary investigation of the sediments on the eastern Coromandel inner shelf and implications for across-shelf sediment transport. 489–449.
- DOLAN, T.J., CASTENS, P.G., SONU, C.J. and EGENSE, A.K., 1987. Review of sediment budget morphology: Oceanside littoral cell, California. *Coastal Sediments '87*. A.S.C.E. 1289–1304.
- DRAPER, L., 1966a. The analysis and presentation of wave data: a plea for uniformity. In *Proceedings of the 10<sup>th</sup> International Conference on Coastal Engineering*, Tokyo. A.S.C.E. 1–11.
- DRAPER, L., 1966b. Waves at Sekondi, Ghana. In *Proceedings of the 10<sup>th</sup> International Conference on Coastal Engineering*, Tokyo. A.S.C.E. 12–17.
- DUNN, A.S., 2001. Coastal erosion at Wainui Beach, Gisborne. Unpublished MSc thesis, Department of Earth Sciences, University of Waikato. 244p.
- DYER, K.R., 1986. *Coastal and Estuarine Sediment Dynamics*. J. Wiley & Sons, Chichester. 342p.
- EASTON, H.R., 2002. Coastal erosion and sedimentation of Pukehina Beach and Waihi Estuary. Unpublished MSc thesis, Department of Earth Sciences, University of Waikato. 250p.
- FOLK, R.L., 1968. *Petrology of sedimentary rocks*. Hemphill Publication Co, Austin, Texas. 170p.
- FOSTER, G.A., 1991. Beach nourishment from a nearshore dredge spoil dump at Mount Maunganui Beach. Unpublished MSc thesis, Department of Earth Sciences, University of Waikato. 156p.
- FOSTER, G.A., HEALY, T.R. and DE LANGE, W.P., 1994. Sediment budget and equilibrium profiles applied to renourishment of an ebb tidal delta adjacent beach, Mt Maunganui, New Zealand. *Journal of Coastal Research*, 10(3): 346–575.
- FULTON, V.G., 1991. Beach morphology on the Eastern Coromandel Peninsula. Unpublished MSc thesis, Department of Earth Sciences, University of Waikato. 174p.

- GIBB, J.G., 1996. Assessment of the effects of the Waihi Beach seawalls. C.R. 96/5 Report prepared for the Western Bay of Plenty District Council, Tauranga. August 1996: 43p. + Appendices.
- GIBB, J.G., 1997. Strategic options of sustainable management of the coastal interface along Waihi Beach, Western Bay of Plenty District. C.R. 97/1 Report prepared for the Western Bay of Plenty District Council, Tauranga, Tonkin & Taylor. May 1997. 108p. + Appendices.
- GREEN, M.O., 1999. Test of sediment initial-motion theories using irregular wave field data. *Sedimentology*, 46(3): 427–441.
- GREEN, M.O. and BLACK, K.P., 1999. Suspended sediment concentration under waves: field observations and critical analyses of two predictive models. *Coastal Engineering*, 38(3): 115–141.
- HALLERMEIER, R.J., 1978. Uses for a calculated depth limit to beach erosion. In *Proceedings of the 16<sup>th</sup> Coastal Engineering Conference*, Hamburg. Volume 1, A.S.C.E. 1493–1512.
- HALLERMEIER, R.J., 1981a. A profile zonation for seasonal sand beaches from wave climate. *Coastal Engineering*, 4: 253–277.
- HALLERMEIER, R.J., 1981b. Seaward limit of sand transported by waves: an annual zonation for seasonal profiles. *Coastal Engineering Technical Aid*: 7–18.
- HANLEN, H., 1999. *The Why, How, When and Where of the Waihi Beach Story: Its Politics, Places and People*. 96p.
- HARMS, C., 1989. Dredge spoil dispersion from an inner shelf dump-mound. Unpublished MPhil thesis, Department of Earth Sciences, University of Waikato. 177p.
- HARRAY, K.G., 1977. Beach Erosion and Sediments at Waihi Beach. Unpublished MSc thesis, Department of Earth Sciences, University of Waikato. 91p.
- HARRAY, K.G. and HEALY, T.R., 1978. Beach erosion at Waihi Beach, Bay of Plenty, New Zealand. *New Zealand Journal of Marine and Freshwater Research*, 12(2): 99–107.
- HARRIS, T.F., 1985. *North Cape to East Cape: aspects of the physical oceanography*, Auckland University Press, Auckland. 178p.
- HARRIS, T.F., HUGHS, T.S. and VALENTINE, E.M., 1983. Deepwater waves of Hicks Bay and the northeast coast, North Island. *Water and Soil Miscellaneous Publications*, 56. 86p.
- HAY, D.N., 1991. Storm and oceanographic databases for the Western Bay of Plenty. Unpublished MSc thesis, Department of Earth Sciences, University of Waikato. 209p.

- HEALY, T.R., 1980. Erosion and sediment drift along the Bay of Plenty coast. *Soil and Water*. August 1980. 12–15.
- HEALY, T.R., 1985. *Field collection programme and morphological study, Tauranga Harbour study, Parts II and V*. A report to the Bay of Plenty Harbour Board, 25p.
- HEALY, T.R., 1987. The importance of wave focusing in the coastal erosion and sedimentation process. In *Coastal Sediments '87*. A.S.C.E. 1472–1485.
- HEALY, T.R., 1993. Coastal erosion, setback determination, and recommendations for management of the Waihi-Bowentown and Pukehina beach and dunes. A report to the Western Bay of Plenty District Council. September, 1993. 55p. + Appendices.
- HEALY, T.R., 1997. Peer review of the report entitled “Strategic options of sustainable management of the coastal interface along Waihi Beach, Western Bay of Plenty District”. 28p.
- HEALY, T.R., 2007. Geomorphic and sedimentologic evidence for net littoral drift – A review. In *Coastal Sediments '07*. A.S.C.E. 165–178.
- HEALY, T.R. and DELL, P.M., 1982. Coromandel Coastal Survey, Volume 2: Beach and sediment textural data. Hauraki Catchment Board. Report number 115. 33p.
- HEALY, T.R., DELL, P.M. and WILLOUGHBY, A.J., 1981. Coromandel Coastal Survey, Volume 1: Basic survey data. Hauraki Catchment Board. University of Waikato. 233p.
- HEALY, T.R., HARRAY, K.G. and RICHMOND, B., 1977. *The Bay of Plenty coastal erosion survey*. Occasional report 3, Department of Earth Sciences, University of Waikato. 64p.
- HEALY, T.R., MCCABE, B. and THOMPSON, G., 1991. Port of Tauranga Ltd environmental impact assessment: channel deepening and widening dredging programme 1991-1992, May 1991. 122p.
- HEALY, T.R., NICHOL, S., HUME, T., IMMENGA, D. and MATHEW, J., 1996. The Mangawhai-Pakiri sand study. Module 2: Technical Report. Marine Sands. Prepared for the working party, ARC Environment, Auckland Regional Council. 111p.
- HEATH, R.A., 1979. Significance of storm surges on the New Zealand coast. *New Zealand Journal of Geology and Geophysics*, 22(2): 259–266.
- HICKS, D.M. and HUME, T.M., 1996. Morphology and size of ebb-tidal deltas at natural inlets on open-sea and pocket-bay coasts. *Journal of Coastal Research*, 12(1): 47–63.

- HICKS, D.M. and HUME, T.M., 1997. Determining sand volumes and bathymetric change on an ebb-tidal delta. *Journal of Coastal Research*, 13(2): 407–416.
- HILTON, M.J., 1990. Processes of sedimentation on the shoreface and continental shelf and the development of sand facies, Pakiri, New Zealand. Unpublished PhD thesis, University of Auckland. 352p.
- HILTON, M.J. and HESP, P., 1996. Determining the limits of beach-nearshore sand systems and the impact of coastal sand mining. *Journal of Coastal Research*, 12, 496–519.
- HOBAN, M.J., 1993. Processes, morphology, and change on a storm-driven multiple barred beach system, Waihi Beach, New Zealand. Unpublished MA Thesis, Department of Geography, University of Auckland. 147p.
- HUANG, J.D., JACKSON, D.W.T. and COOPER, J.A.G., 2002. Morphological monitoring of a high energy beach system using GPS and total station techniques, Runkerry, Co. Antrim, Northern Ireland. *Journal of Coastal Research*, Special Issue 36: 390–398.
- HUME, T.M. and HERDENDORF, C.E., 1992. Factors controlling inlet characteristics on low drift coasts. *Journal of Coastal Research*, 8: 355–375.
- HUME, T.M. and HICKS, D.M., 1993. Shelf morphology and processes near an ebb tidal delta, Katikati Inlet, New Zealand. In *Proceedings of the 11th Australasian Conference on Coastal and Ocean Engineering*, Australia: 671–676.
- HUME, T.M., OLDMAN, J.W. and BLACK, K.P., 2000. Sediment facies and pathways of sand transport about a large deep water headland, Cape Rodney, New Zealand. *New Zealand Journal of Marine and Freshwater Research*, 34: 695–717.
- HUME, T.M., BEAMSLEY, B.E., GREEN, M.O., DE LANGE, W.P. and HICKS, D.M., 1995: Influence of seabed topography and roughness on longshore wave processes. In *Proceedings of the International Conference on Coastal Research in terms of Large Scale Experiments*: 975–986.
- HUME, T.M., BELL, R.G., BLACK, K.P., HEALY, T.R. and NICHOL, S.L., 2000. Mangawhai-Pakiri Sand Study. Module 6: Technical Report. Final Report. Sand movement and storage and nearshore sand extraction in the Mangawhai-Pakiri embayment. Prepared for the working party, ARC Environment, Auckland Regional Council. 55p + Figures.
- HURN, J., 1993. Differential GPS Explained: An expose of the surprisingly simple principles behind today's most advanced positioning technology. Booklet for Trimble Navigation Ltd. 55p.
- HUTT, J., 1997. Bathymetry and wave parameters defining the surfing quality of five adjacent reefs. Unpublished MSc thesis, Department of Earth Sciences, University of Waikato. 170p.



- INTEROCEAN SYSTEMS INC., 1996. Users Manual – S4 Application Wave Software (WAVE). Version 3.0.
- IREMONGER, S., 2007. NERMN Beach Profile Monitoring. Environment Bay of Plenty. Environmental Publication 2007/08. 178p.
- KLEIN ASSOCIATES INC, 2008. Side scan sonar operation tips. [http://www.1-3klein.com/operator\\_tips/optips/geometry.html](http://www.1-3klein.com/operator_tips/optips/geometry.html).
- KOMAR, P.D., 1976. *Beach Processes and Sedimentation*. 1<sup>st</sup> Edition. Prentice Hall, New Jersey, U.S.A. 429p.
- KOMAR, P.D., 1996. The budget of littoral sediments. Concepts and applications. *Shore and Beach*, 64: 18–26.
- KOMAR, P.D., 1998. *Beach processes and sedimentation*. 2<sup>nd</sup> Edition. Prentice-Hall, New Jersey, USA. 544p.
- KOMAR, P.D. and INMAN, D.L., 1970. Longshore sand transport on beaches. *Journal of Geophysical Research*, 75(30): 5914–5927.
- KOMAR, P.D. and MILLER, M.C., 1975. On the comparison between the threshold of sediment motion under waves and unidirectional currents with a discussion of the practical evaluation of the threshold. *Journal of Sedimentary Petrology*, 45(4): 362–367.
- KRUGER, J.C. and HEALY, T.R., 2006. Mapping the morphology of a dredged ebb tidal delta, Tauranga Harbour, New Zealand. *Journal of Coastal Research*, 22(3): 720–727.
- LARSEN, R., MORANG, A. and GORMAN, L., 1997. Monitoring the coastal environment; Part 2: Sediment sampling and geotechnical methods. *Journal of Coastal Research*, 13(2): 308–330.
- LEEDER, M.R., 1982. *Sedimentology: Process and Product*. George Allen and Unwin Ltd., London. 344p.
- LONGDILL, P.C., 2004. Site characterisation and assessment of sediments for beach renourishment. Unpublished MSc thesis, Department of Earth Sciences, University of Waikato. 302p.
- MACKY, G.H., LATIMER, G.J. and SMITH, R.K., 1995. Wave climate of the western Bay of Plenty, New Zealand, 1991–93. *New Zealand Journal of Marine and Freshwater Research*, 25: 311–327.
- MASSELINK, G., 1992. Longshore Variation of Grain Size Distribution along the Coast of the Rhône Delta, Southern France: A Test of the "McLaren Model". *Journal of Coastal Research*, 8(2): 286–291.

- MATHEW, J. 1997. Morphological changes of tidal deltas and an inner shelf dump ground from large scale dredging and dumping, Tauranga, New Zealand. Unpublished PhD thesis, Department of Earth Sciences, University of Waikato. 351p.
- MCLAREN, P., 1981. An interpretation of trends in grain size measures. *Journal of Sedimentary Petrology*, 51(2): 611–624.
- MCLAREN, P. and BOWLES, D., 1985. The effects of sediment transport on grain-size distributions. *Journal of Sedimentary Petrology*, 55(4): 457–470.
- MILLER, M.C., MCCAVE, I.N. and KOMAR, P.D., 1977. Threshold of sediment motion under unidirectional currents. *Sedimentology* 24(4): 507–527.
- MILLER, J.E., HUGHES-CLARK, J. and PATERSON, J., 1997. How effectively have you covered your bottom? *The Hydrographic Journal*, 83: 3–10.
- MOON, V.G. and DE LANGE, W.P., 2005. Estimating long-term cliff recession rates from shore platform widths. *Engineering Geology*, 80: 292–301.
- MORANG, A., LARSON, R. and GORMAN, L., 1997. Monitoring the coastal environment, Part 3: geophysical and research methods. *Journal of Coastal Research*, 13(4): 1064–1085.
- NIEDORODA, A.W., SWIFT, D.J. and HOPKINS, T.S., 1985. The Shoreface. In DAVIS, R.A. JR. (Ed), *Coastal Sedimentary Environments*. New York, Springer-Verlag. 533–624.
- NIELSON, P., 1986. Suspended sediment concentration under waves. *Coastal Engineering*, 10: 23–31.
- NIELSON, P., 1992. *Coastal Bottom Boundary Layers and Sediment Transport*. Advanced Series on Ocean Engineering, Volume 4. World Scientific Publishing Ltd, Singapore. 324p.
- OPEN UNIVERSITY, 2002. *Waves, tides and shallow-water processes*. 2<sup>nd</sup> Edition. Butterworth Heinemann in association with the Open University, Milton Keynes, England. 227p.
- PATSCH, K. and GRIGGS, G., 2006. Littoral Cells, Sand Budgets, and Beaches: Understanding California's Shoreline. Institute of Marine Sciences. University of California, Santa Cruz. 40p.
- PATSCH, K. and GRIGGS, G., 2008. A sand budget for the Santa Barbara Littoral Cell, California. *Marine Geology*, 252: 50–61.
- PHIZACKLEA, D., 1993. Littoral sediment budget and beach morphodynamics, Pukehina Beach to Matata, Bay of Plenty. Unpublished MSc thesis, Department of Earth Sciences, University of Waikato. 322p.

- PICKRILL, R.A. and MITCHELL, J.S., 1979. Ocean wave characteristics around New Zealand. *New Zealand Journal of Marine and Freshwater Research*, 13(4): 501–520.
- PLANT, N.G. and GRIGGS, G.B., 1992. Interactions between nearshore processes and beach morphology near a seawall. *Journal of Coastal Research*, 8: 183–200.
- PUGH, D.T., 2004. *Changing sea levels: effects of tides, weather, and climate*. Cambridge University Press, 265p.
- QUALE, A.M., 1984. The climate and weather of the Bay of Plenty region. New Zealand Meteorological service, Ministry of Transport, Wellington. 56p.
- ROSATI, J.D., 2005. Concepts in Sediment Budgets. *Journal of Coastal Research*, 21(2): 307–322.
- ROSATI, J.D. and KRAUS, N.C., 1999. Formulation of sediment budgets at inlets. Coastal and Hydraulics Engineering Technical Note CHETN-IV-15, U.S. Army Engineer Research and Development Center, Vicksburg, MS.
- SAUNDERS, H.A., 1999. Coastal processes influencing beach erosion at West End Ohope. Unpublished MSc thesis, Department of Earth Sciences, University of Waikato. 229p.
- SCHOFFIELD, J.C., 1970. Coastal sands of Northland and Auckland. *New Zealand Journal of Geology and Geophysics*, 13: 767–824.
- SCHWARTZ, M.L., 2004. *Encyclopedia of Coastal Science*. Dordrecht, Kluwer Academic. 1211p.
- SHAND, T., SHAND, R., BAILEY, D. and ANDREWS, C., 2005. Wave deformation in the vicinity of a long ocean outfall at Wanganui, New Zealand. *Proceedings of the 17<sup>th</sup> Australasian Coastal and Ocean Engineering Conference*: 173–178.
- SHEPHERD, M.J., MCFADGEN, B.G., BETTS, H.D. and SUTTON, D.G., 1997. Formation, landforms, and palaeoenvironment of Matakana Island. Department of Conservation, Wellington. Science and Research Series 102. 99p.
- SILVESTER, R. and HSU, J.R.C., 1997. *Advanced Series on Ocean Engineering*, Volume 14. World Scientific Publishing Ltd, Singapore. 596p.
- SPERANSKI, N. and CALLIARI, L., 2001. Bathymetric lenses and localized coastal erosion in southern Brazil. *Journal of Coastal Research*, Special Issue 34: 209–215.
- SPIERS, K.C., 2005. Continued beach renourishment from dredge spoil disposal. Unpublished MSc thesis, Department of Earth Sciences, University of Waikato. 241p.

- STEELE, D.A., 1995. Possible interactions between groundwater, a seawall and coastal processes: impact on erosion at Waihi Beach, New Zealand. Unpublished MSc thesis, Department of Earth Sciences, University of Waikato. 106p.
- STEPHENS, S.A., 1996. Arcuate duneline embayments, intragravity signals and rip currents at Waihi Beach. Unpublished MSc thesis, Department of Earth Sciences, University of Waikato. 91p.
- STEPHENS, S.A., HEALY, T.R., BLACK, K.P. and DE LANGE, W.P., 1999. Arcuate duneline embayments, infragravity signals, rip currents, and wave refraction at Waihi Beach, New Zealand. *Journal of Coastal Research*, 15(3): 823–829.
- STURMAN, A. and TAPPER, N., 1996. *The weather and climate of Australia and New Zealand*. Oxford University Press, Melbourne. 476p.
- SUNAMURA, T. and HORIKAWA, K., 1971. A study on the prevailing direction of littoral drift along the Kashiwazaki coast, Japan. Annual report of the Engineering Research Institute. Faculty of Engineering, University of Tokyo 30: 21–28.
- SUNAMURA, T. and HORIKAWA, K., 1972. An improved method for inferring the direction of littoral drift from grain size properties of beach sands. Annual report of the Engineering Research Institute. Faculty of Engineering, University of Tokyo 31: 61–68.
- SUTHERLAND, J., HALL, L.J. and CHESHER, T.J., 2001. Evaluation of the coastal area model PISCES at Teignmouth (UK). *HR Wallingford Report TR125*.
- SUTHERLAND, J., PEET, A.H. and SOULSBY, R.L., 2004. Evaluating the performance of morphological models. *Coastal Engineering*, 51: 917–939.
- TONKIN & TAYLOR LTD, 2004. Waihi Beach Erosion Protection Works: Assessment of Environmental Effects. Job No. 20801 Report prepared for the Western Bay of Plenty District Council, Tauranga, Tonkin & Taylor. November 2004. 62p.
- TRENHAILE, A.S., 1997. *Coastal Dynamics and Landforms*. Clarendon Press, Oxford. 366p.
- USACE., 1984. *Shore Protection Manual*. 4<sup>th</sup> edition, Volume 2. U.S. Army Engineer Waterways Experiment Station, Coastal Engineering Research Center, U.S. Government Printing Office, Washington D.C.
- USACE, 2002. Coastal Engineering Manual. Engineer Manual 1110-2-1100, United States Army Corps of Engineers, Washington, DC. In 6 volumes.
- VAN LANCKER, V., LANCKNEUS, J., HEARN, S., HOEKSTRA, P., LEVOY, F., MILES, J., MOERKERKE, G., MONFORT, O. and WHITEHOUSE, R., 2004. Coastal and nearshore morphology, bedforms and sediment transport pathways at Teignmouth (UK). *Continental Shelf Research*, 24: 1171–1202.

- VAN RIJN, L.C., WALSTRA, D.J.R., GRASMEIJER, B., SUTHERLAND, J., PAN, S. and SIERRA, J.P., 2003. The predictability of cross-shore bed evolution of sandy beaches at the time scale of storms and seasons using process-based Profile models. *Coastal Engineering*, 47: 295–327.
- VINCENT, C.E. and DOWNING, A., 1994. Variability of suspended sand concentrations, transport and eddy diffusivity under non-breaking waves on the shoreface. *Continental Shelf Research*, 14: 233–250.
- VINCENT, C.E., YOUNG, R.A. and SWIFT, D.J.P., 1982. On the relationship between bedload and suspended sand transport on the inner shelf, Long Island, New York. *Journal of Geophysical Research*, 87(6): 4163–4170.
- VINCENT, C.E., YOUNG, R.A. and SWIFT, D.J.P., 1983. Sediment transport on the Long Island shoreface, North American Atlantic Shelf: Role of waves and currents in shoreface maintenance. *Continental Shelf Research*, 2: 163–181.
- WBOPDC, 2004. Waihi Beach Newsletter, December 2004. Western Bay of Plenty District Council, URL: <http://www.wbopdc.govt.nz>.
- WEHRMANN, H., 2000. Lahar deposits and tephrostratigraphy, Okurei Point, Bay of Plenty, New Zealand. Unpublished MSc thesis, Department of Earth Sciences, University of Waikato. 111p.
- WRIGHT, L.D., 1995. Morphodynamics of inner continental shelves. CRC Press, Boca Raton.
- YOU, Z, 2000. A simple model of sediment initiation under waves. *Coastal Engineering*, 41: 399–412.